2024-2025 California Current Ecosystem Status Report

A report of the NOAA California Current Integrated Ecosystem Assessment Team (CCIEA) to the Pacific Fishery Management Council, March 2025

Edited by: Andrew Leising, Mary Hunsicker, Nick Tolimieri, Greg Williams, Amanda Phillips, Lynn Dewitt & Christopher Dailey
Northwest and Southwest Fisheries Science Centers

With contributions from:
Kelly Andrews, Toby Auth, Tracie Barry, Jack Barth, Kirby Bartlett, Eric Bjorkstedt, Steven Bograd, Anna Bolm, Jerry Borchert, Brian Burke, Megan Cimino, Kelly Corbett, Jeff Cowen, Elizabeth Daly, Meredith Elliott, Blake Feist, Jerome Fiechter, John Field, Jennifer Fisher, Zachary Forster, Chris Free, Matt George, Thomas Good, Christina Grant, Correigh Greene, Chris Harvey, Elliott Hazen, Daniel Holland, Ali Hossain, Matthew Hunter, Lila Isé, Kym Jacobson, Michael Jacox, Jaime Jahncke, Mike Johns, Christy Juhasz, Isaac Kaplan, Stephen Kasperski, William Kennerly, Su Kim, Dan Lawson, Connor Lewis-Smith, Kirsten Lindquist, Jackie Lyndsay, Nate Mantua, Sharon Melin, Monique Messie, Rebecca Miller, Stephanie Moore, Cheryl Morgan, Barbara Muhling, Stuart Munsch, Shannon Murphy, Karma Norman, Rachael Orben, Julia Parrish, Scott Pearson, Stephen Pierce, Antonella Preti, Josiah Renfree, Travis Richards, Roxanne Robertson, Tanya Rogers, Jan Roletto, Dan Rudnick, Lauren Saez, Keith Sakuma, Jameal Samhouri, Jarrod Santora, Isaac Schroeder, Kayleigh Somers, Beckye Stanton, Kevin Stierhoff, William Sydeman, Andrew Thompson, Sarah Ann Thompson, Duy Truong, John Wallace, Amanda Warlick, Peter Warzybok, Brian Wells, Curt Whitmire, Jen Zamon, Samantha Zeman, Vanessa Zubkousky-White, Juan Zwolinski

Table of Contents

1. INTRODUCTION

The 2013 and 2022 Fishery Ecosystem Plans (FEPs) establish a process wherein NOAA provides the Pacific Fishery Management Council (Council) with a yearly update on the status of the California Current Ecosystem (CCE), as derived from environmental, biological, economic and social indicators. NOAA's California Current Integrated Ecosystem Assessment (CCIEA) team is responsible for this report. This is our 13th report, with prior reports in 2012 and 2014-2024.

New for this year's report, based on Council advisory body feedback, we have split the "Developing indicators of climate change and variability" appendix into two separate appendices: one concerning short-term forecasts (Appendix D), and one concerning long-term projections and climate variability (Appendix E). We have also removed some of the more static methodological descriptions from the main section of the report to a ESR Technical Documentation appendix (Appendix V; online version).

This report summarizes CCE status based on data and analyses that generally run through 2024 and some that extend into 2025. Highlights are summarized in Box 1.1. Appendices provide additional information or clarification, as requested by the Council and its committees and advisory bodies.

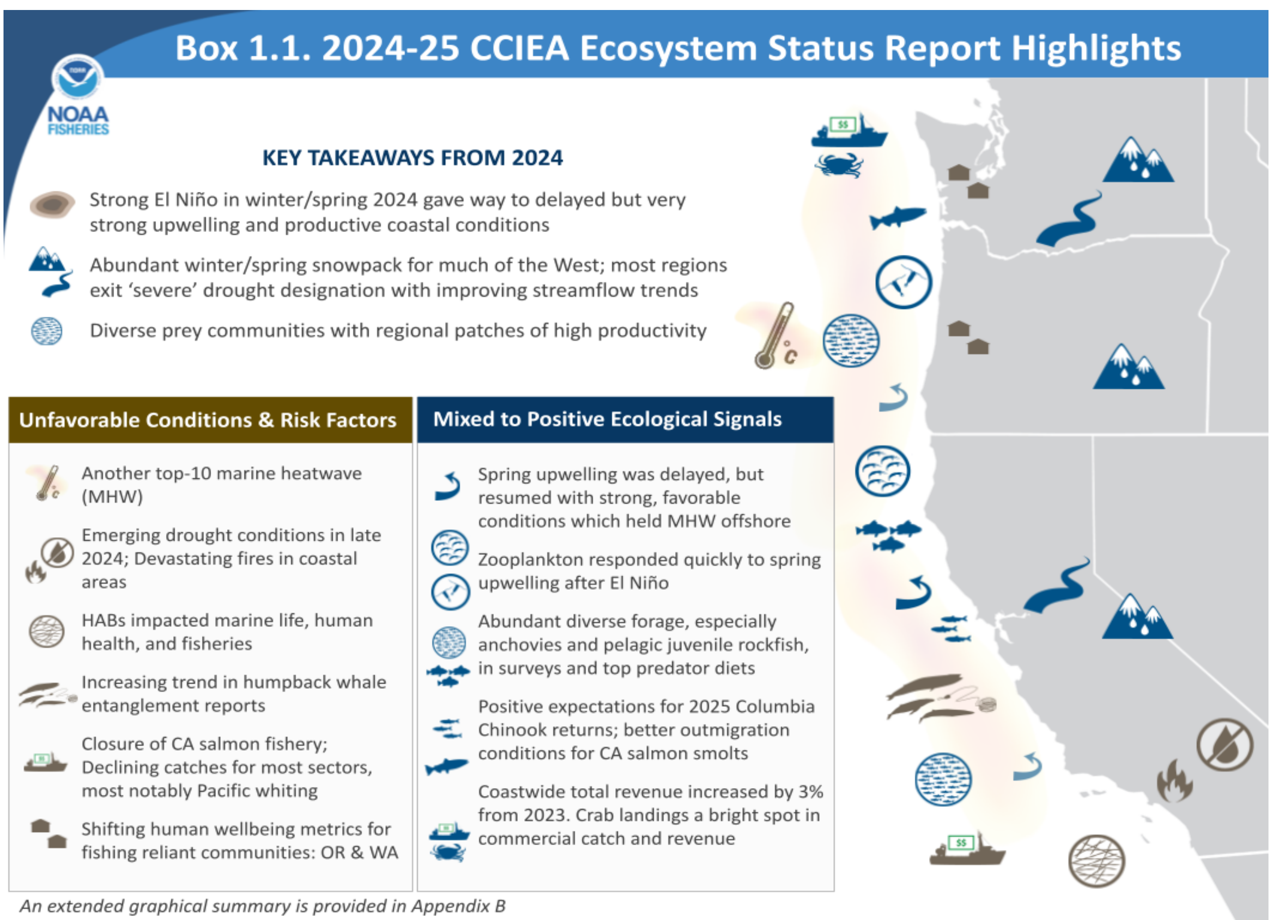

An extended graphical summary is provided in Appendix B

1.1 Sampling Locations

We refer to areas north of Cape Mendocino as the "Northern CCE," Cape Mendocino to Point Conception as the "Central CCE", and south of Point Conception as the "Southern CCE." Figure 1.1 shows sampling areas for most regional oceanographic data. Key oceanographic transects are the Newport Line off Oregon, the Trinidad Head Line off northern California, and CalCOFI lines further south, while shaded marine regions indicate sampling areas for most biological surveys. Sampling is complemented by basin-scale oceanographic observations and outputs from various models. Figure 1.1 also shows sampling areas for most biological indicators. The shaded terrestrial areas in Figure 1.1 represent freshwater ecoregions in the CCE, and are the basis for indicators for snowpack, flows, and stream temperatures.

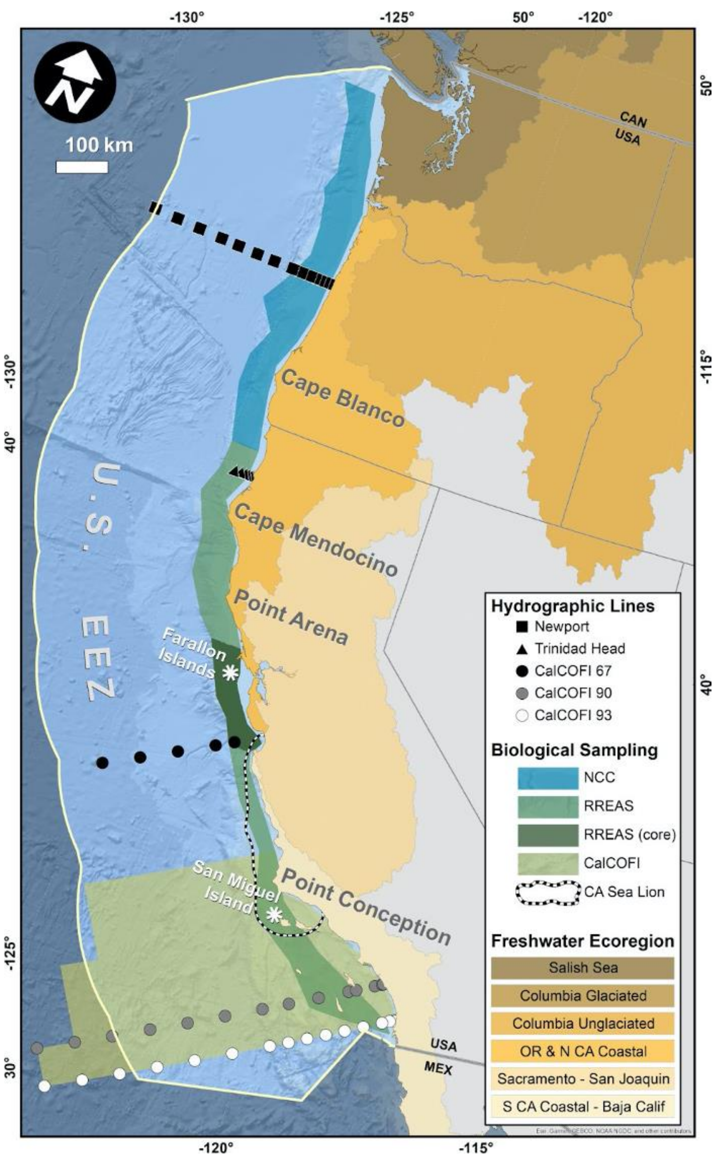

Figure 1.1: Map of most sampling efforts in the California Current Ecosystem (CCE) and U.S. west coast Exclusive Economic Zone (EEZ). Symbols indicate hydrographic line sampling stations for oceanographic data. Shaded ocean regions represent biological sampling areas

for the Northern CCE (NCC), which includes the Juvenile Salmon and Ocean Ecology Survey (JSOES); the Rockfish Recruitment and Ecosystem Assessment Survey (RREAS), including its Core Area; and the CalCOFI sampling region. The NCC and RREAS shaded areas, combined, also approximate the survey footprints for NOAA's coastwide CPS acoustic/trawl and groundfish bottom trawl surveys. Dashed black line approximates foraging area for adult female California sea lions from the San Miguel colony. Shaded terrestrial areas represent the six freshwater ecoregions in the CCE.

2. CLIMATE AND OCEAN DRIVERS

Key Message

The California Current during 2024 experienced a strong El Niño which caused widespread warmer than normal coastal ocean temperatures during winter/spring 2023-2024. The El Niño delayed the normal onset of spring upwelling by ~two weeks for the central region, after which the system rapidly transitioned to favorable upwelling conditions, although large marine heatwaves again impacted the system during the summer and fall. Bottom oxygen levels were mostly favorable. Snowpack was normal or above-normal at the start of the year, particularly in the south due to El Niño. Conditions moved back toward drought during the summer and fall; extreme drought in the southwest likely exacerbated conditions leading up to the Los Angeles wildfires. Streams were warm and flows were low as in past years, although at values close to median levels.

2.1 Basin-Scale Indicators

We use three indices to characterize large-scale physical ecosystem states in the North Pacific:

- The Oceanic Niño Index (ONI) describes the equatorial El Niño Southern Oscillation (ENSO). An ONI above 0.5°C indicates El Niño conditions, which often lead to lower primary production, weaker upwelling, poleward transport of equatorial waters and species, and more southerly storm tracks in the CCE. An ONI below -0.5°C means La Niña conditions, which influence atmospheric pressure conditions that lead to upwelling-favorable winds that drive productivity in the CCE.
- The Pacific Decadal Oscillation (PDO) describes North Pacific sea surface temperature (SST) anomalies that may persist for many years. Positive PDOs are associated with warmer SST and lower productivity in the CCE, while negative PDOs indicate cooler SST and are associated with higher productivity.
- The North Pacific Gyre Oscillation (NPGO), an index of sea surface height, indicates changes in circulation that affect source waters for the CCE. Positive NPGOs are associated with strong equatorward flow and higher salinity, nutrients, and chlorophyll-a. Negative NPGOs are associated with decreased subarctic source water and lower CCE productivity.

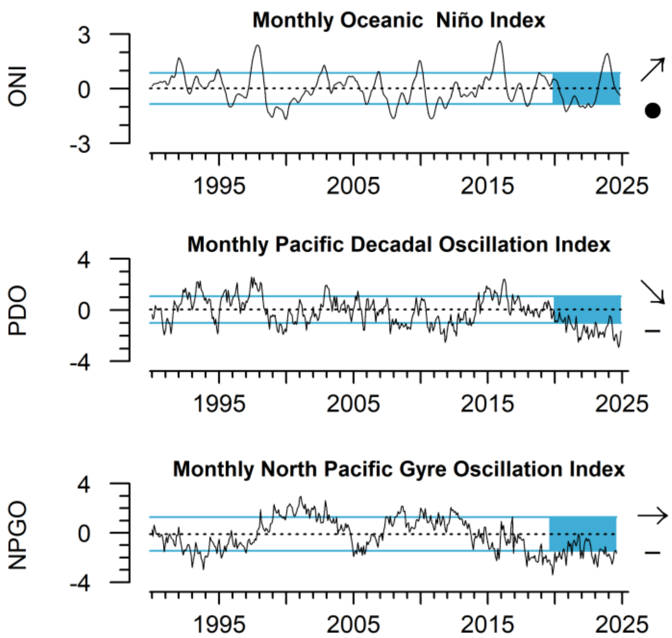

Figure 2.1: Monthly values of the Oceanic Niño Index (ONI), Pacific Decadal Oscillation (PDO), and North Pacific Gyre Oscillation (NPGO) from 1990 - 2024 relative to the mean (dashed line) ±1 s.d. (blue lines) from 1991-2020. The blue shaded area is the most recent 5 years of data. Arrows indicate if the recent 5-year trend is positive (⍰), neutral (→), or negative (⍰). Symbols indicate if the recent 5-year mean is above the upper blue line (+), within the blue lines (⍰), or below the lower blue line (−).

Basin-scale indices suggest average to below-average conditions for productivity in 2024. The ONI was positive during the beginning of the year and indicative of El Niño conditions, with a shift towards negative at the end of the year, whereas the PDO and NPGO were negative during the entire year (Fig. 2.1). Although the PDO remained negative for a 5th consecutive year (Fig. 2.1 top), it shifted towards more positive values during the early part of the year, in concert with the El Niño. After reaching relatively neutral values during parts of 2021 and 2022, the NPGO has remained negative since then (Fig. 2.1, bottom),indicating weaker than average general circulation. Seasonal values for all indices are in Appendix F.

The northeast Pacific continues to experience large marine heatwaves in surface waters. At the beginning of the year, the El Niño dominated the patterns in ocean temperatures (Fig. 2.2), until it subsided in mid April. Separate from the El Niño, another large marine heatwave developed in the far offshore region (>1000km) during late April, grew during the summer, and reached its maximum size (~6 million km^2) on September 3rd (Fig. 2.2). It was the 6th largest heatwave by area and the 5th longest in duration since monitoring began in 1982, although it is still ongoing (Fig. 2.2). Similar to 2023, this year's heatwave had several large intrusions into the coastal area (Fig. 2.2). These intrusions were related to fairly widespread relaxations in upwelling during the summer and fall (Fig. 2.4). Additional information on the 2024 marine heatwave is in Section F.2.

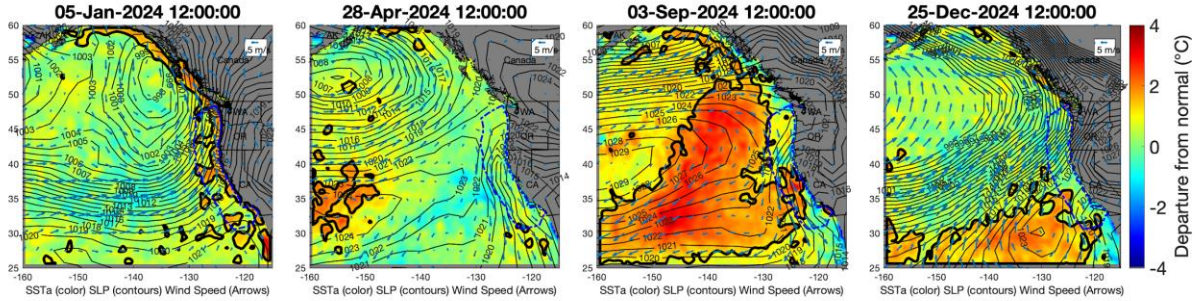

Figure 2.2: Progression of the 2024 marine heatwave in the northeast Pacific Ocean. Colors represent standardized SST anomalies. Heavy black lines denote regions that meet the criteria for a marine heatwave (see Appendix F.2). Gray contours represent sea level pressure (in hectoPascals) and arrows represent wind speed and direction.

Subsurface temperatures (>50 m depth) were warmer than normal for the winter and spring of 2024 due to the presence of El Niño, with a return to colder than normal temperatures during the summer. During the summer off of Oregon, temperatures in the upper 50 m were variable, with periods of cooler than normal waters reflecting active upwelling, and a brief period of warmer than average temperature coinciding with an intrusion of the large offshore marine heatwave (Fig. 2.3, top). In the south temperatures were mainly above average in surface waters throughout the summer but mostly localized to the upper 10 m, whereas deeper waters were cooler than normal (Fig. 2.3, bottom).

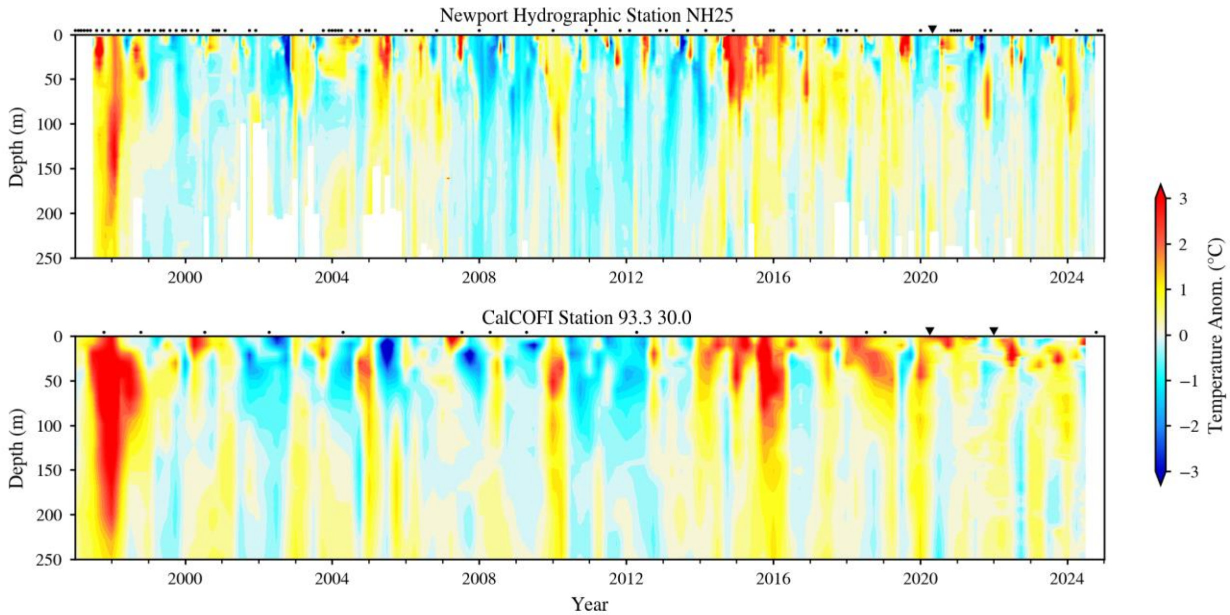

Figure 2.3: Time-depth temperature anomalies at Newport station NH25 and CalCOFI station 93.30, from 1997 through late 2024. Transect locations are in Fig. 1.1.

2.2 Upwelling and Habitat Compression

Upwelling is a major driver of coastal productivity in the CCE. It occurs when equatorward coastal winds force deep, cold, nutrient-rich water to the surface. The greatest upwelling in the CCE occurs off central California and typically peaks in June. Here, we present two upwelling indices: vertical flux of water (Coastal Upwelling Transport Index; CUTI) and of nitrate (Biologically Effective Upwelling Transport Index; BEUTI) (Jacox et al. 2018).

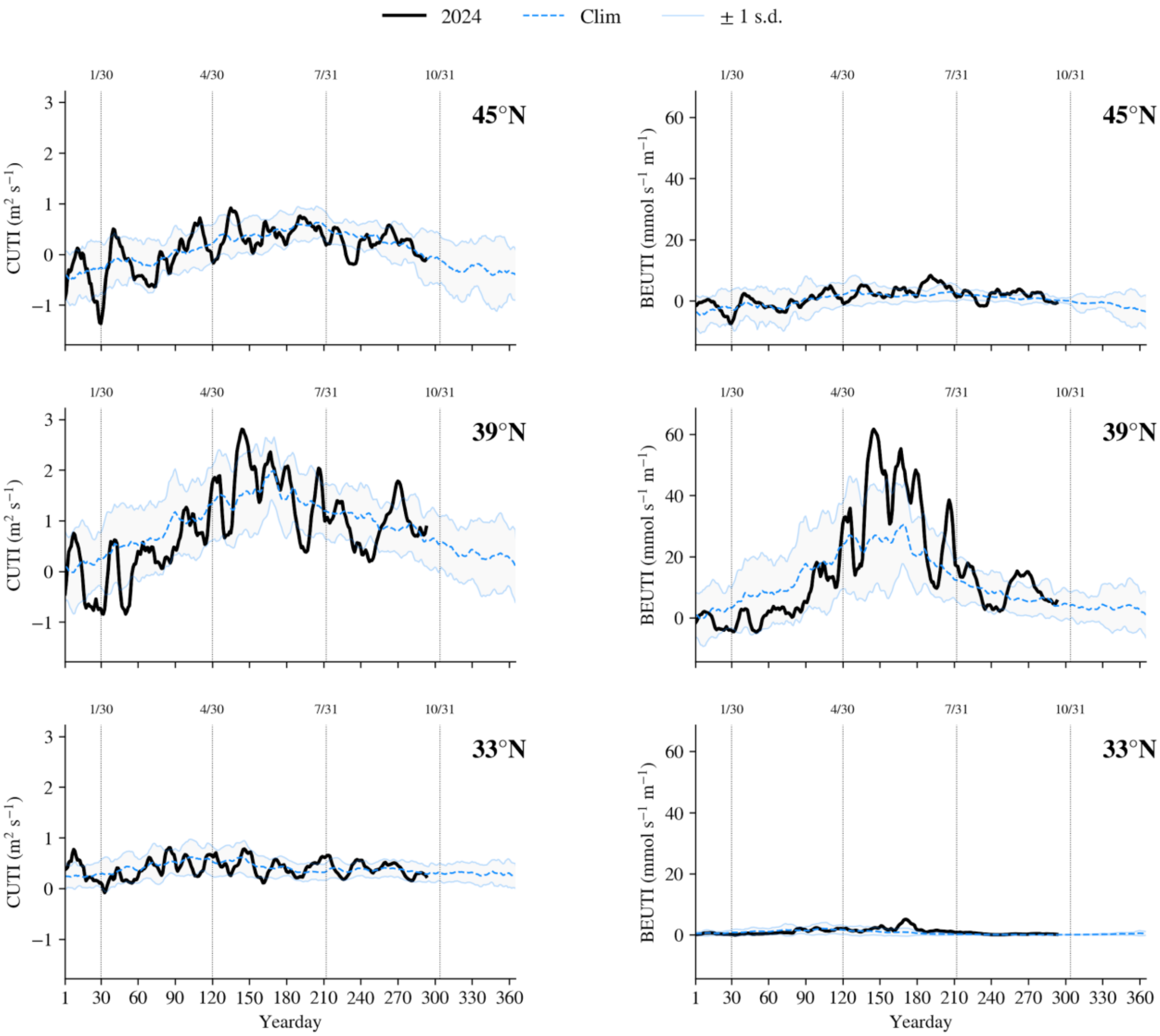

Figure 2.4: Daily estimates of vertical transport of water (CUTI, left) and nitrate (BEUTI, right) in 2024, relative to the 1988-2024 climatological average (blue dashed line) ±1 s.d. (shaded area), at latitudes 33°N (San Diego), 39°N (Pt. Arena), and 45°N (Newport).

Overall, 2024 saw varying levels of total cumulative upwelling with lower than average levels in the north, and average to above average in the central region and within the Southern California Bight (Fig. F6). The reduction in total upwelling was related to a delay in the upwelling season due to the influence of the El Niño. During the summer, particularly off Oregon, there were several periods of significant upwelling relaxation, or even downwelling (Fig. 2.4). Whereas off of northern California (~39°N Fig. 2.4), there was very strong upwelling after the spring delay, and an associated strong transport of nutrient rich waters to the surface (BEUTI index at 39°N Fig. 2.4). Despite the delay in upwelling, the strong upwelling and nutrient transport in central and northern California suggest favorable productivity in those regions during the summer of 2024.

Santora et al. (2020) developed the habitat compression index (HCI) to describe how much cool, productive water is available adjacent to the coast. HCI ranges from 0 (= complete coverage of warm offshore water in the region) to 1 (= cool water fully extending 150 km from the coast). During 2024, there was a decrease in HCI (less cool, productive water) during winter and spring due to El Niño, with a shift back to average values during summer and fall (Fig. 2.5, Appendix F.3).

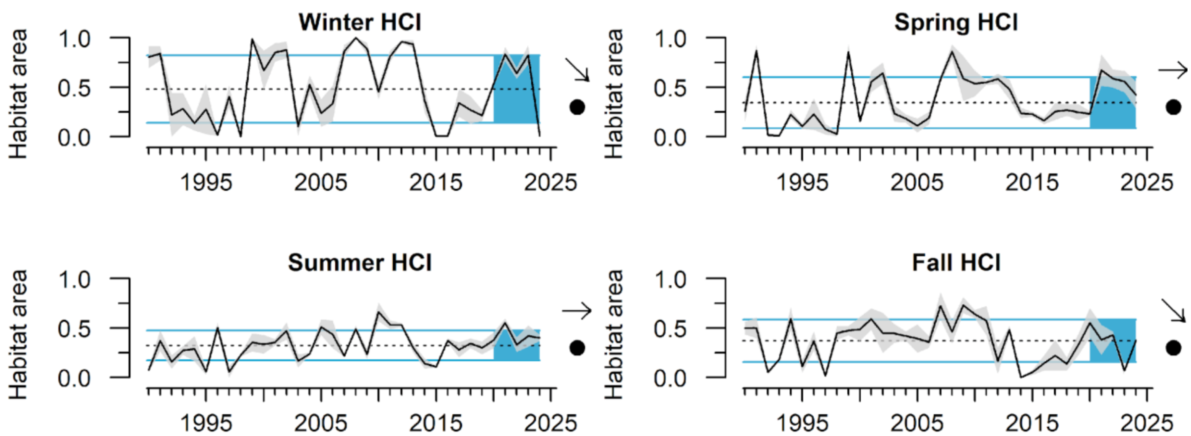

Figure 2.5: Mean habitat compression index (HCI) off central California in winter (Jan-Mar), spring (Apr-Jun), summer (Jul-Sep), and fall (Oct-Nov) for 1990 - 2024. Habitat area is the fraction of coastal habitat that is cooler than the threshold (higher values indicate less compression). Gray envelope indicates ±1 s.e. Lines, colors, and symbols are as in Fig. 2.1.

2.3 Hypoxia and Ocean Acidification

Dissolved oxygen (DO) is influenced by processes such as currents, upwelling, air-sea exchange, primary production, and respiration. Low DO (aka hypoxia, concentrations <1.4 ml DO/l) can compress habitat and cause stress or die-offs in sensitive species (Chan et al. 2008). During 2024, the timing of the hypoxic period was similar to most other years (Fig. 2.6). The nearshore station NH05 off Newport, Oregon only briefly experienced hypoxic conditions (Fig. 2.6), whereas the station off Washington (CE07) experienced a longer period of hypoxia. The offshore station NH25 off Newport, Oregon also did not experience as low oxygen levels this year as previous years (150 m Appendix F.4). Off southern California, CalCOFI DO data saw average or slightly above average DO levels at depths of 150 m during the entire year (Appendix F.4), noting that this region typically is well above hypoxic values at even these depths at all times.

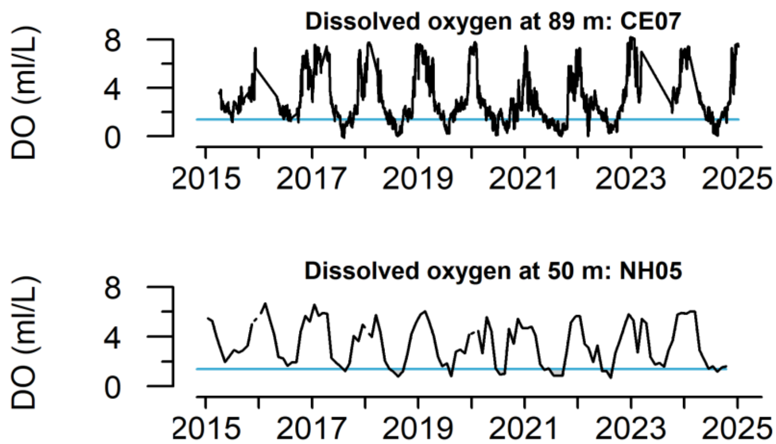

Figure 2.6: Near-bottom dissolved oxygen off Grays Harbor, WA (CE07) and Newport, OR (NH05), from 2015 - 2025. Blue lines indicate the hypoxia threshold (1.4 ml DO/L).

Ocean acidification, caused by increased anthropogenic CO_2, reduces pH and dissolved carbonate in seawater and is stressful to many marine species (Feely et al. 2008; Busch and McElhany 2016). At station NH05 off Newport, the saturation state levels for aragonite (a form of calcium carbonate) were above the reference threshold of 1.0 in winter, but decreased through spring and summer to <1.0 (Fig. 2.7), a level which is corrosive for many shell-forming organisms, and is a typical seasonal pattern at this station. During 2024, summer values were similar to 2023, but with a longer period of low values during the summer (see details in Appendix F.4).

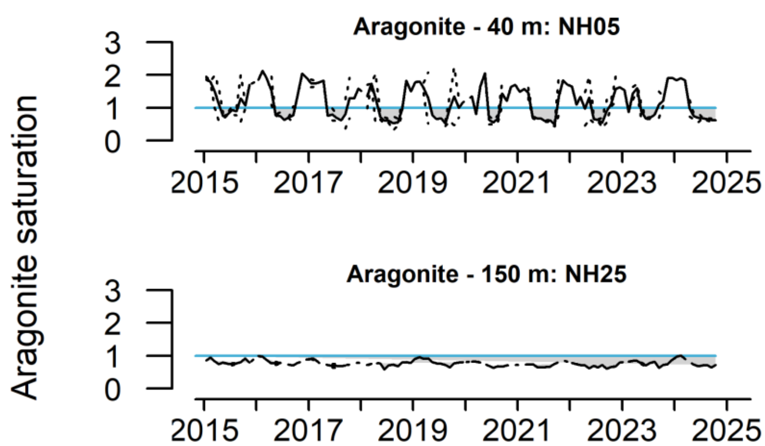

Figure 2.7: Aragonite saturation states off of Newport, OR from 2015 - 2024. Blue lines indicate a threshold for aragonite saturation state (1.0). Dotted lines indicate +/- 1.0 SE.

2.4 Snowpack and Hydrology

Snow-water equivalent (SWE) is the water content in snowpack, which supplies cool freshwater to streams in spring, summer and fall critical for salmon production (Appendix G, Appendix J.2). Winter storms in 2024 in California mountain ranges were less extreme than in 2023, but created good snowpack (median or better compared to 30-year median) as well as major flooding. Typical of an El Niño year, patterns of snowpack graded from high in southerly mountain ranges to lower in the northern and eastern ones (Fig. 2.8). Snowpack was lower and more variable in Oregon, Washington, and Idaho, and most snowpack monitoring sites north and east of Mt. Hood in Oregon exhibited below-median SWE.

Snowpack supported freshwater resources for much of the Pacific Coast, although a dry summer in the Pacific Northwest somewhat exacerbated water scarcity. By the end of the water year in September 2024, 55% of Washington, Oregon, and Idaho was experiencing at least moderate drought conditions (D1 or higher levels of the U.S. Drought Monitor index), while California levels were much lower at 11%, and down from a high of nearly 100% in 2022. Where water scarcity existed, it generally was not severe: over 95% of the Pacific west experienced moderate drought conditions (D1) or better.

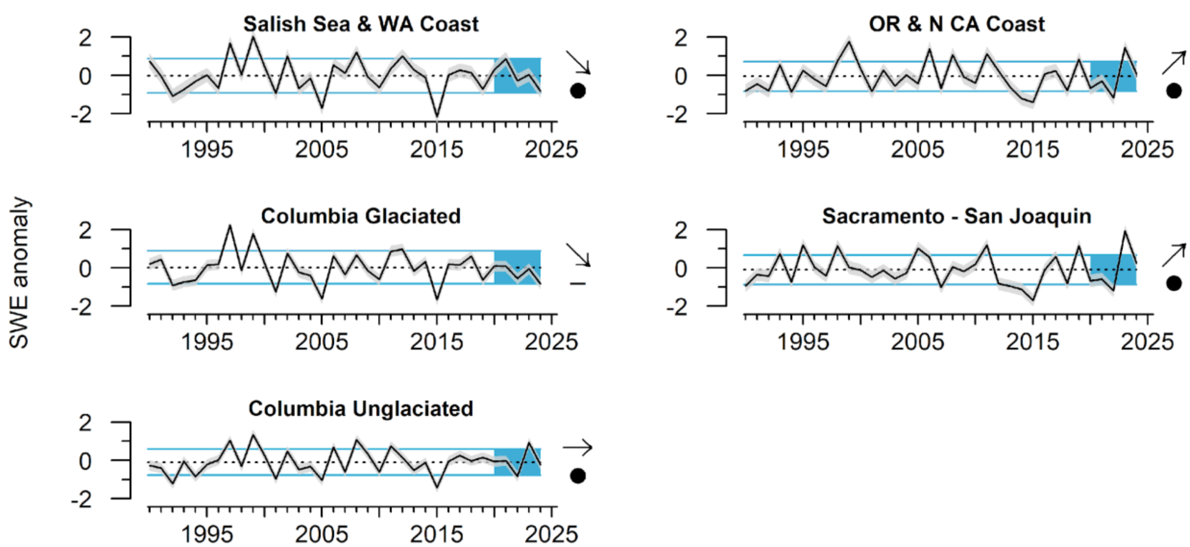

Figure 2.8: Anomalies of April 1st snow-water equivalent (SWE) in freshwater ecoregions of the CCE, 1990 - 2024. Error envelopes represent 95% credible

intervals. Lines, colors and symbols are as in Fig. 2.1. Ecoregions are mapped in Fig. 1.1.

As of February 2 2025, winter storms have created abundant snowpack in northern California and much of Oregon, but conditions in the Central and Southern Sierra Nevada of California are below median (Fig. G.1). Much of Washington and Idaho are experiencing median snowpack or worse. Winter precipitation outlooks suggest a pattern mimicking current snowpack, with drought conditions lessening in northern California and Southern Oregon and worsening in Washington, Idaho, and the southern Sierra Nevada. Water-year and longer outlooks suggest favorable drought conditions throughout the west, except in the northern Cascades and Idaho.

Across ecoregions, conditions within rivers were close to median levels in 2024. Maximum and minimum river flow patterns tended to follow spatial patterns in snowpack, with Columbia ecoregions slightly below average levels and California ecoregions above median levels (Fig. G.2 and Fig. G.3). Likewise, summer water temperatures were near average in all regions (Appendix G), although the onset of the warmest temperatures appeared earlier in the year.

Five-year status and trends for regional hydrology are shown in quad plots (Fig. 2.9), which indicate if conditions over the last five years were above or below average (y-axis), and had increasing or decreasing trends (x-axis). Overall, both maximum and minimum flows have shown evidence of widespread lows in their recent status and trends (Fig. 2.9). For both indicators, the 5-year average was below the long-term average for all but two ecoregions. Five-year trends suggested a latitudinal cline, with both flow indicators trending negative in the north and more positive in the south. Concomitant with patterns of summer low flows, recent average maximum August temperatures were above-average for all ecoregions. Five-year trends in water temperature showed an inverted pattern compared to low flows, with northern ecoregions trending upward but southern ecoregions trending downward. These patterns suggest average winter-spring freshwater salmon outmigration conditions but challenging summer conditions for adult upstream migrants or for stocks that live in freshwater during summer months.

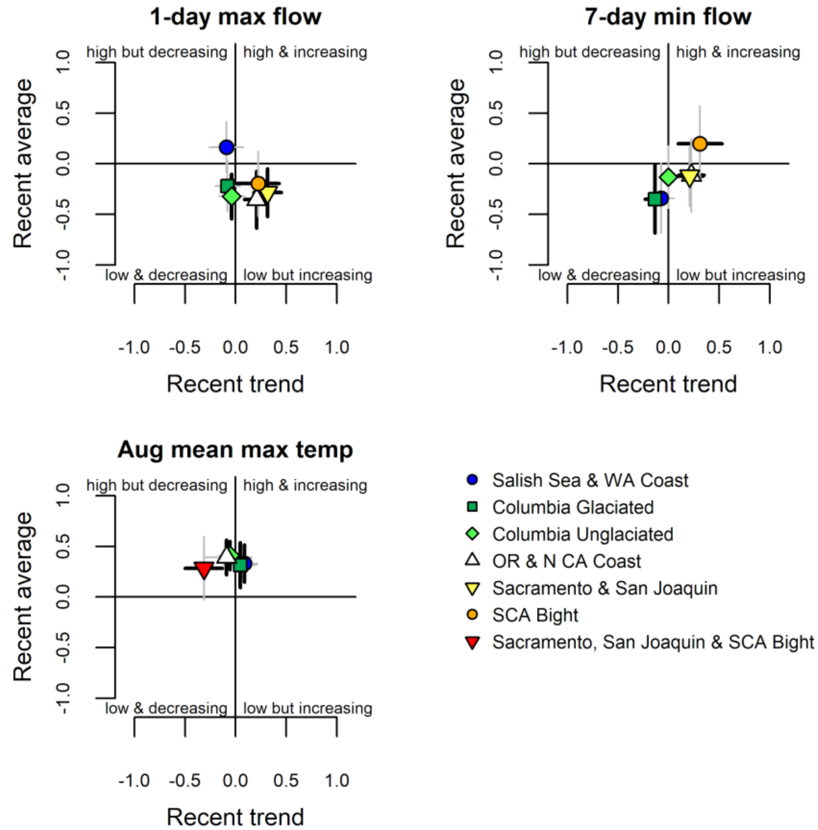

Figure 2.9: Recent (2019-2024) averages and trends in maximum and minimum flow in streams within six Chinook salmon ecoregions. Symbols for each ecoregion fall into quadrants based on recent average (high or low) and recent trend (increasing or decreasing) relative to long-term data (1980-present). Error bars represent 95% credible intervals. Heavy black error bars represent significant differences from zero. Ecoregions correspond to freshwater ecoregions (Fig. 1.1).

3. FOCAL COMPONENTS OF ECOLOGICAL INTEGRITY

Key Message

In early 2024, ecological indicators reflected less favorable conditions that are typically observed during El Niño events. However, strong spring upwelling ushered in cool, productive waters that supported mixed to good marine conditions throughout the remainder of the year. The forage community was diverse and productive. Anchovy and juvenile groundfishes remained abundant in the Central and Southern CCE and were an important prey source for top predators. Juvenile groundfishes continued to be abundant in the Northern CCE as well. Recent ocean conditions for Chinook salmon returning to the Columbia Basin indicate improving returns in 2025. Indicators for salmon in California suggest most adults returning *in 2025 and 2026 experienced improvements toward average conditions. Multiple harmful algal blooms impacted marine life, shellfish fisheries, and human health.*

3.1 Copepods and Krill

Copepod biomass anomalies represent variation in northern copepods (cold-water crustacean zooplankton rich in wax esters and fatty acids) and southern copepods (smaller species with lower fat content and nutritional quality). Northern copepods usually dominate the summer zooplankton community along the Newport Line off Oregon (Fig. 1.1), while southern copepods dominate in winter. Positive northern copepod anomalies generally correlate with stronger returns of Chinook salmon to Bonneville Dam and coho salmon to coastal Oregon (Peterson et al. 2014). Historically, northern copepods typically have been favored by La Niña and negative PDO conditions (Keister et al. 2011; Fisher et al. 2015).

Copepod indicators suggest average feeding conditions for pelagic fishes off central Oregon in 2024. Lipid-rich northern copepods were well below average along the Newport Hydrographic Line in winter and spring of 2024, reflecting El Niño conditions. However, biomass increased following the onset of spring upwelling, and the northern biomass anomaly was average compared to the 27-year time series through the remainder of 2024 (Fig. 3.1, top). Southern copepod biomass was above average in winter and spring (Fig. 3.1, bottom) and copepod species richness was high during this period due to increased numbers of sub-tropical copepods; typical under El Niño conditions. Southern copepods transitioned to negative biomass anomalies in early summer (Fig. 3.1, bottom).

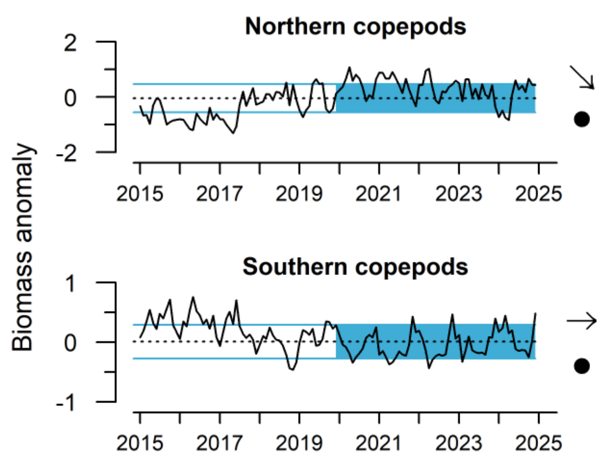

Figure 3.1: Monthly northern and southern copepod biomass anomalies from station NH05 off Newport, OR from 2015 - 2024. Full time series can be found here. Positive values indicate above-average biomass, and negative values indicate below-average biomass. Lines, colors, and symbols are as in Fig. 2.1.

Krill are among the most important prey groups in the CCE. North Pacific krill, *Euphausia pacifica,* is sampled year-round along the Trinidad Head Line off northern California (Fig. 1.1). Mean length of adults and total biomass of *E. pacifica* indicate productivity at the base of the food web, krill condition, and energy content for predators (Robertson and Bjorkstedt 2020). Krill length and biomass were below average in winter 2024. Following spring upwelling, krill length increased substantially and remained near or above average for most of the spring and summer (Fig. 3.2, top). Biomass of *E. pacifica* also increased and remained near-average throughout spring and summer (Fig. 3.2, bottom). Off central California, krill abundance was near average in 2024 and showed an increasing trend over the past five years (see Fig. 3.5, Fig. I.2). This is unusual as observations of krill are typically low in this region during El Niño events. Moderate abundances of krill were observed off Oregon as well (Section 3.2).

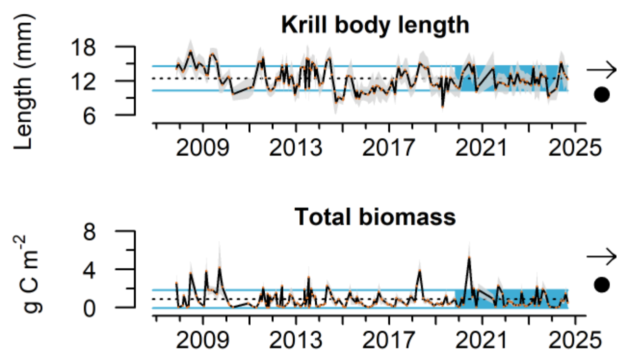

Figure 3.2: Monthly mean adult E. pacifica length (top) and total E. pacifica biomass (bottom) off Trinidad Head, CA, 2007 - 2024. Gray envelopes indicate ± 1.0 s.d. Lines, colors, and symbols are as in Fig. 2.1.

3.2 CPS and Regional Forage Availability

3.2.1 Coastwide Coastal Pelagic Species (CPS)

The NOAA CPS survey estimates CPS abundance and distribution from Cape Flattery to San Diego, and at times off Vancouver Island and Baja California. The central stock of anchovy reached ~2.75 million tons in 2021 and remained highly abundant through 2024 (Stierhoff et al. 2023a, Stierhoff et al., in prep). Jack mackerel and Pacific herring were the major components of the CPS community north of San Francisco Bay in 2024 (see Appendix H). The 2024 biomass estimates are preliminary and therefore not presented in this report (Stierhoff et al., in prep). Information on spatial distributions and other CPS data are in Appendix H.

3.2.2 Regional forage composition

The regional surveys that produce CCE forage data use different gears and survey designs, which makes regional comparisons difficult. In past reports, we developed cluster analysis methods to identify regional shifts in forage composition (Thompson et al. 2019). Those plots are shown here; see the caption of Figure 3.4 for how to interpret the plots.

Northern CCE: The JSOES survey off Washington and Oregon (Fig. 1.1) targets juvenile salmon in surface waters, and also samples surface-oriented fishes, squid, and jellies. The 2024 forage assemblage was similar to the previous year (Fig. 3.4) and was characterized by moderate abundances of 'young-of-year' (YOY) sablefish, pompano, sea nettle, and moon jelly. Juvenile salmon were also moderate in abundance, except for the high abundances of yearling coho salmon. Jellyfish abundance was moderate to high in 2024, and market squid decreased to the lowest abundance since 2013. Juvenile salmon time series are discussed further in Section 3.3, and data for the remaining species are in Appendix I.1. The northern portion of the RREAS survey (Fig. 1.1) observed high abundances of YOY rockfish and whitebait smelt, and krill were moderately abundant (data not shown). Further, during a Fishermen and Scientists roundtable in November 2024, Oregon fishermen noted the 'market basket' or high diversity of forage during the summer and early fall. From a predator's perspective, average to above average abundance of many forage species means prey availability was high.

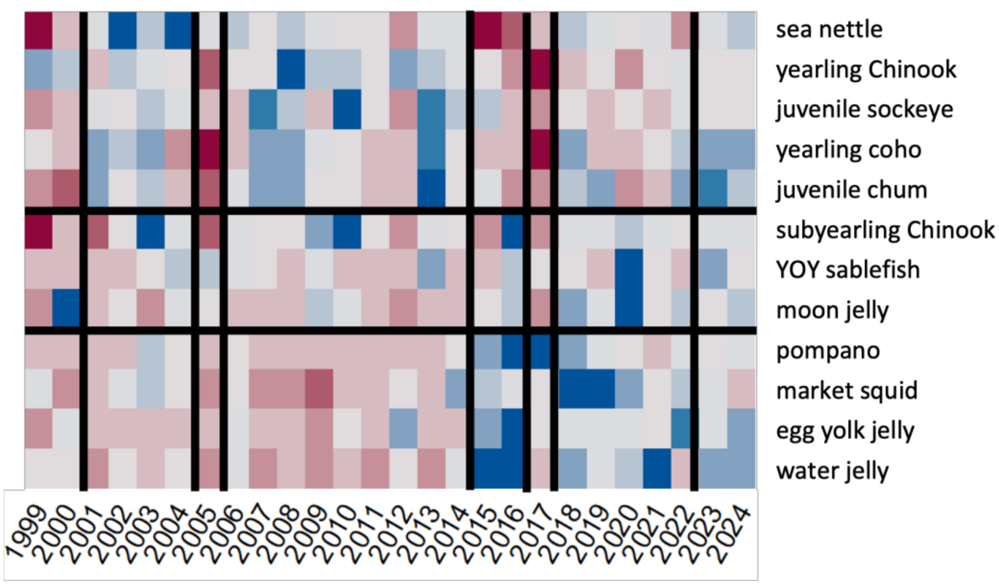

Figure 3.4: Cluster analysis of pelagic community indicators in the northern CCE, 1999-2024. Colors indicate relative catch per unit effort (blue = abundant, red = rare). Horizontal bars separate clusters of typically co-occurring species. Vertical bars demarcate breaks in assemblage structure between years.

Central CCE: Data presented in Fig. 3.5 are from the "Core Area" of the nearly coastwide RREAS survey (Fig. 1.1) that targets pelagic YOY rockfishes, and samples other pelagic species. The 2024 forage assemblage in this area, centered off Monterey Bay, was similar to 2021-23 (Fig. 3.5). YOY rockfishes, myctophids, and YOY pelagic fishes, including anchovy, sardine, and Pacific hake, were highly abundant in 2024. Notably, catches of YOY anchovy, YOY rockfishes, and myctophids were at their highest abundances relative to the past several years. Adult anchovy abundance decreased from recent years, though was still above the long-term average. Adult sardine and market squid also decreased in 2024 and were very low compared to past years. The abundances of krill, octopus, and YOY sanddabs were near-average in 2024. Time series of these catch data are in Appendix I.2.

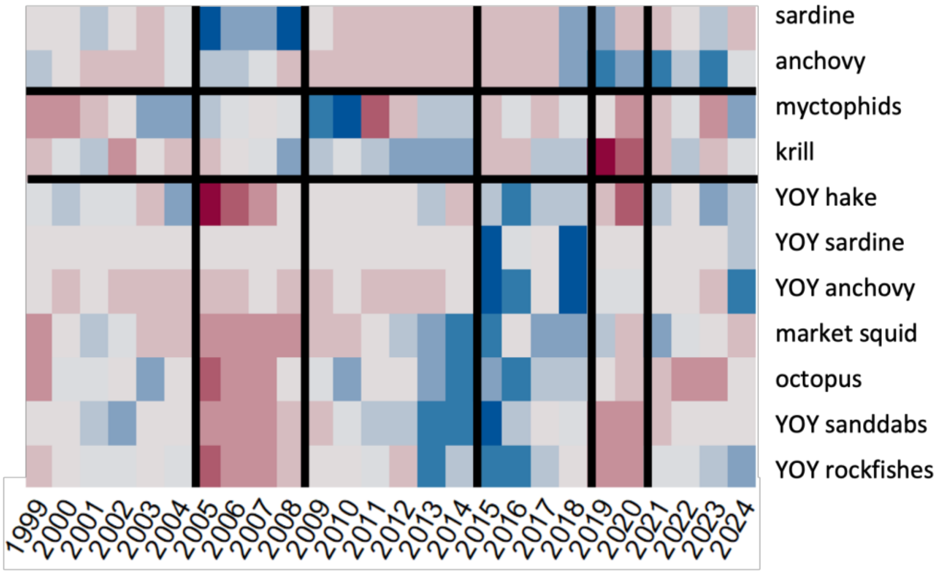

Figure 3.5: Cluster analysis of forage indicators in the Core Area of the central CCE, 1999-2024. See Figure 3.4 for how to interpret the plot.

Forage data for the Southern CCE come from spring CalCOFI larval fish surveys (Fig. 1.1). The ichthyoplankton assemblage in 2024 was similar to assemblages in 2017-23 (Fig. 3.6). In 2017, the abundances of larval rockfishes, larval anchovy, northern lampfish, and southern mesopelagics increased abruptly and remained elevated through 2024. Larval abundances of Pacific hake, Pacific mackerel and jack mackerel were also very high in 2024. Larval hake abundance in 2024 was the highest in the time series (Fig. I.4). Among larval flatfishes, sanddabs and slender sole abundances were near-average while English sole was low. Larval sardine and market squid abundances were also low in 2024. Time series of catches are available in Appendix I.3.

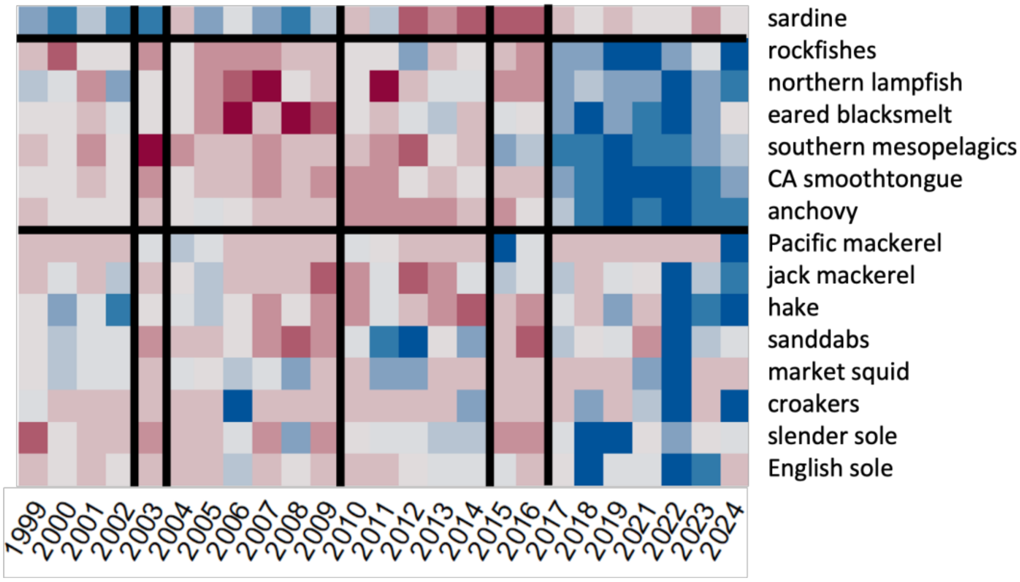

Figure 3.6: Cluster analysis of forage indicators in the Southern CCE, 1999-2024. See Figure 3.4 for how to interpret the plot. No data collected in 2020.

3.3 Salmon Indicators

Juvenile salmon abundance: Catches of juvenile coho and Chinook salmon from June surveys in the Northern CCE (Fig. 1.1) are indicators of salmon survival during their first few weeks at sea. Catch-per-unit-effort of juvenile subyearling Chinook salmon and juvenile yearling Chinook salmon in 2024 were once again close to time series averages. Catches of juvenile yearling coho salmon were above average for a second consecutive year and suggest an increasing five-year trend in their early marine survival (Fig. 3.7).

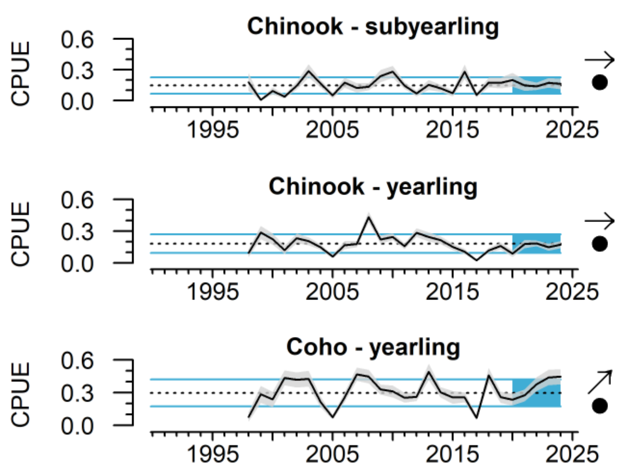

Figure 3.7: Catch per unit effort of juvenile salmon off Oregon and Washington in June, 1998 - 2024. Gray envelope indicates ±1 s.e. Lines, colors, and symbols are as in Fig. 2.1.

3.3.1 Stoplight tables

Long-term associations between oceanographic conditions, food web structure, and salmon productivity support qualitative outlooks of Chinook salmon returns to the Bonneville Dam and smolt-to-adult survival of Oregon Coast coho salmon (Burke et al. 2013; Peterson et al. 2014). The “stoplight table” (Figure 3.8) summarizes many indicators shown elsewhere in this report (PDO, ONI, SST, deep temperature, copepods, juvenile salmon catch) relevant to salmon returns.

In 2024, physical and biological indicators were mixed, suggesting poor to moderate ocean conditions for juvenile salmon. Early in the year, the strong El Niño combined with below average local physical and biological indicators (e.g. above-average temperatures and low larval fish biomass) indicate less favorable marine conditions for juvenile salmon in the northern CCE. However, some indicators, such as northern copepod biomass ratios and PDO phase, are consistent with productive conditions that are typically favorable for salmon (Figure 3.8).

Marine conditions in 2024 indicate average survival for coho salmon returning to this area in 2025. Chinook salmon spend two years or more in the ocean, therefore for their return to the Columbia Basin in 2025, we look to conditions in 2023; indicators that year reflect a mix of good and intermediate conditions. As further evidence, we used quantitative models that use the stoplight indicators in Figure 3.8 and spatial patterns of SST to predict Chinook salmon returns (see Appendix J.2). The predicted counts of Chinook salmon returning to the Snake and Upper Columbia rivers in 2025 are above the 10-year average. For smolts that went to sea in 2024 (most of which will return in 2026), the models consistently suggest lower adult returns than for salmon that went to sea in 2023 (returning in 2025) but the counts are still above the 10-year average. The mean rank of ecosystem indicators in the stoplight table suggest poorer ocean conditions in 2024 compared to 2023 (Figure 3.8). See Appendix J for more information.

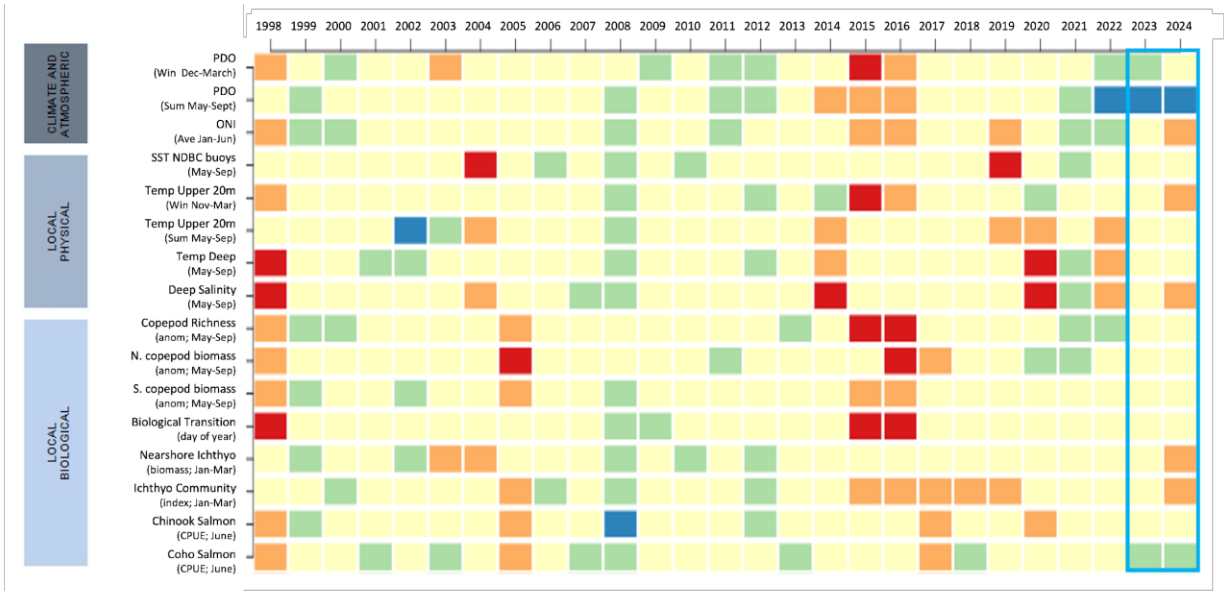

Figure 3.8: Stoplight table of conditions for smolt years 1998-2024 for coho salmon originating in coastal Oregon and Chinook salmon from the Columbia Basin. Colors represent a given year's indicator relative to the reference period (1998-2020). Blue: >2 s.d. above the mean; green: >1 s.d. above the mean; yellow: ±1 s.d. of the mean; orange: >1 s.d. below the mean; red: >2 s.d. below the mean. Chinook salmon from smolt year 2023 and coho salmon from smolt year 2024 (outlined in blue box) represent the dominant adult age classes returning in 2025.

The Council's Habitat Committee, Salmon Technical Team, and others including CCIEA scientists have developed a comprehensive stoplight table for Central Valley spring Chinook salmon, Sacramento River fall Chinook salmon, and Klamath River Fall Chinook salmon (Fig. 3.9). This table features indicators from throughout the stocks' life histories, spanning the 1983-2023 brood years (see also Appendix J.3). Indicators for the most recent brood years suggest improved habitat conditions for Central Valley spring Chinook and Sacramento River fall Chinook. Specifically, warm incubation temperatures, warm outmigration temperatures, and low outmigration flows were less prevalent for brood years 2022 and 2023 than for brood years 2020 and 2021. Additionally, sea surface temperatures and the North Pacific Index, which predict Klamath River Fall Chinook salmon returns, have been average or favorable for the past five brood years while outmigration and incubation temperatures have been variable and average to below average over the same period.

Indicators summarizing spawning, incubation, and outmigration conditions lead adult returns by two to three years, and efforts are underway to produce indicator-based outlooks two years in advance of adult returns (see Appendix J.3). These preliminary outlooks suggest moderate returns of Sacramento River Fall and Central Valley Spring Chinook in 2025 that are expected to increase in 2026. In contrast, Klamath River Fall

Chinook salmon indicator-based outlooks are consistent with low returns in 2025 and slight improvements in 2026. However, considerable uncertainty exists over how removal of the lower four Klamath River dams in 2024 might have affected adult recolonization, spawning, and juvenile productivity. The effects will be most clear starting in return year 2027.

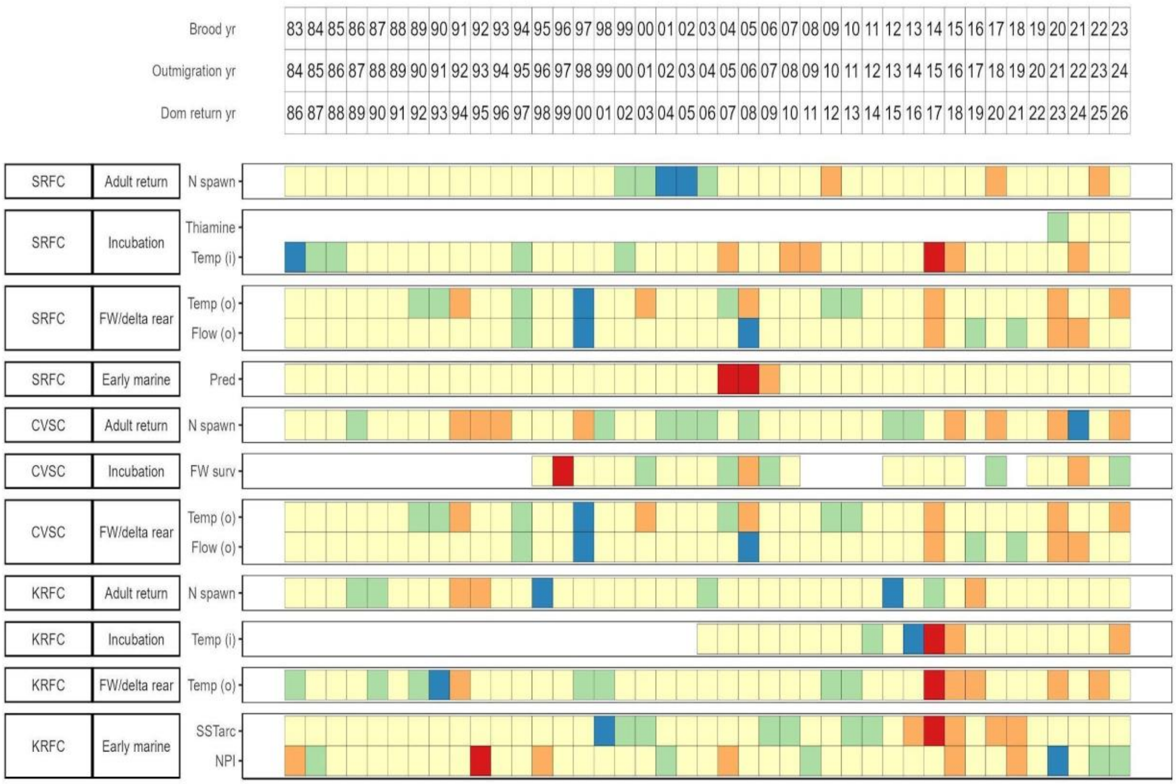

Figure 3.9: Stoplight charts of indicators key to the recruitment of Sacramento River fall Chinook salmon (SRFC), Central Valley spring Chinook salmon (CVSC), and Klamath River Fall Chinook salmon (KRFC) stocks. Rows are ordered by basin of origin, then life stage. Cooler colors for each cell represent hypothesized better habitat conditions. Colors represent the deviation from the overall mean for each indicator: ±1 standard deviation (s.d.) is yellow, between 1 and 2 s.d. from the mean is in orange (below the mean) and green (above the mean), more than 2 s.d. from the mean is represented by red (below the mean) and blue (above the mean). Thiamine color coding reflects health risks associated with egg thiamine concentrations based on fry survival and behavior studies on Chinook salmon.

3.4 Groundfish

3.4.1 Abundance and distribution of juvenile groundfish

Strong year classes can determine age structure and set stock size for marine fishes, and may also indicate favorable environmental conditions, increased future catches, and impending potential bycatch issues. Multiple surveys indicate that many juvenile groundfishes fared well in 2024. Juvenile rockfishes and hake were highly abundant in pelagic surveys (see Section 3.2.2) and coastwide abundances of juvenile sablefish and longspine thornyhead from the NOAA West Coast Bottom Trawl Survey were high as well (Fig. 3.10).

The abundance of juvenile sablefish has been high from 2021-2024 relative to the last 20+ years (Fig. 3.10). Longspine thornyhead also showed high juvenile abundance in recent years. Dover sole and shortspine thornyheads were generally at low abundance and did not show as much recent variation. Time series of juvenile abundance for additional groundfishes are presented in Figure K.1 (Appendix K.1).

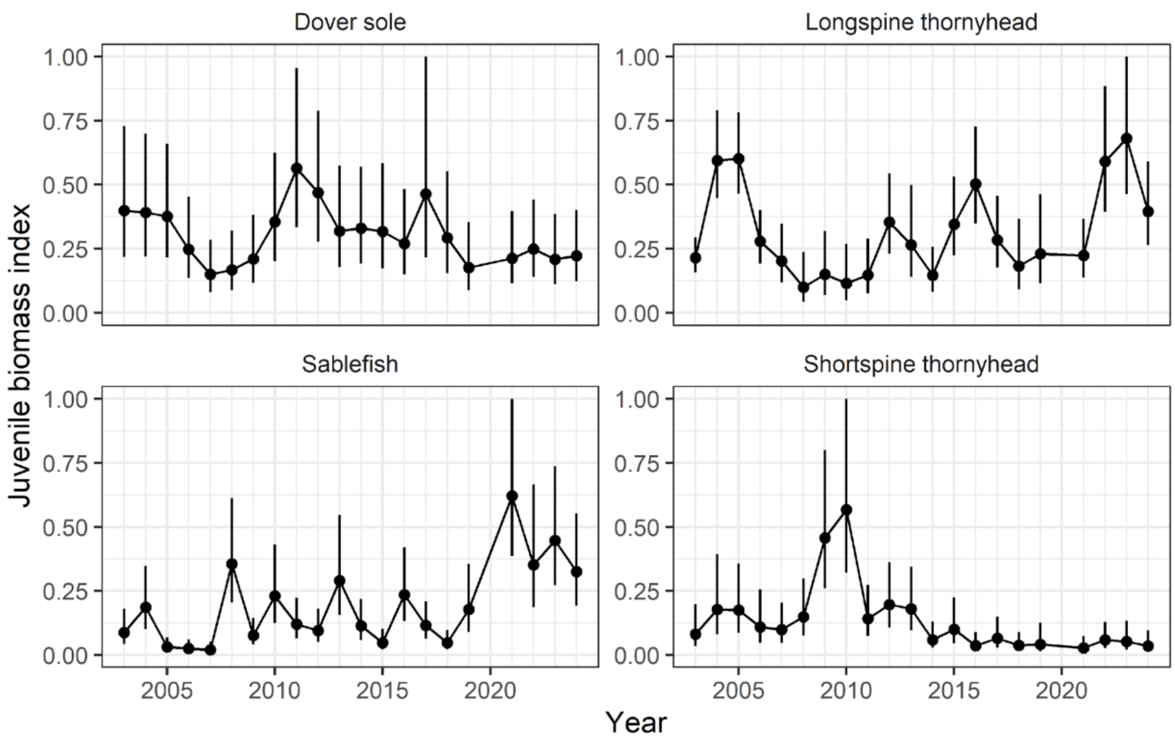

Figure 3.10: Coastwide indexes of abundance of juveniles of Dover sole, sablefish, longspine thornyhead, and shortspine thornyhead, based on data from the NOAA West Coast Groundfish Bottom Trawl Survey. Index is scaled to 0-1 by dividing CPUE by the max s.e.. Error bars indicate +/- 1 S.E..

We examined juvenile sablefish distribution through time to determine whether changes in abundance were associated with changes in distribution (Fig. 3.11). Juvenile sablefish had a higher probability of occurrence and were more abundant in shallower areas across all years. Since 2014, juvenile sablefish have been more abundant in the north, which may reflect overall better recruitment in this region. In years of exceptionally high juvenile sablefish abundance (e.g., 2021 in Fig. 3.10), recruitment has been coastwide. See Appendix K for more information. Long-term projections of the abundance and distribution of groundfish species under climate change and in relation to offshore wind energy development potential are included in Appendix E.

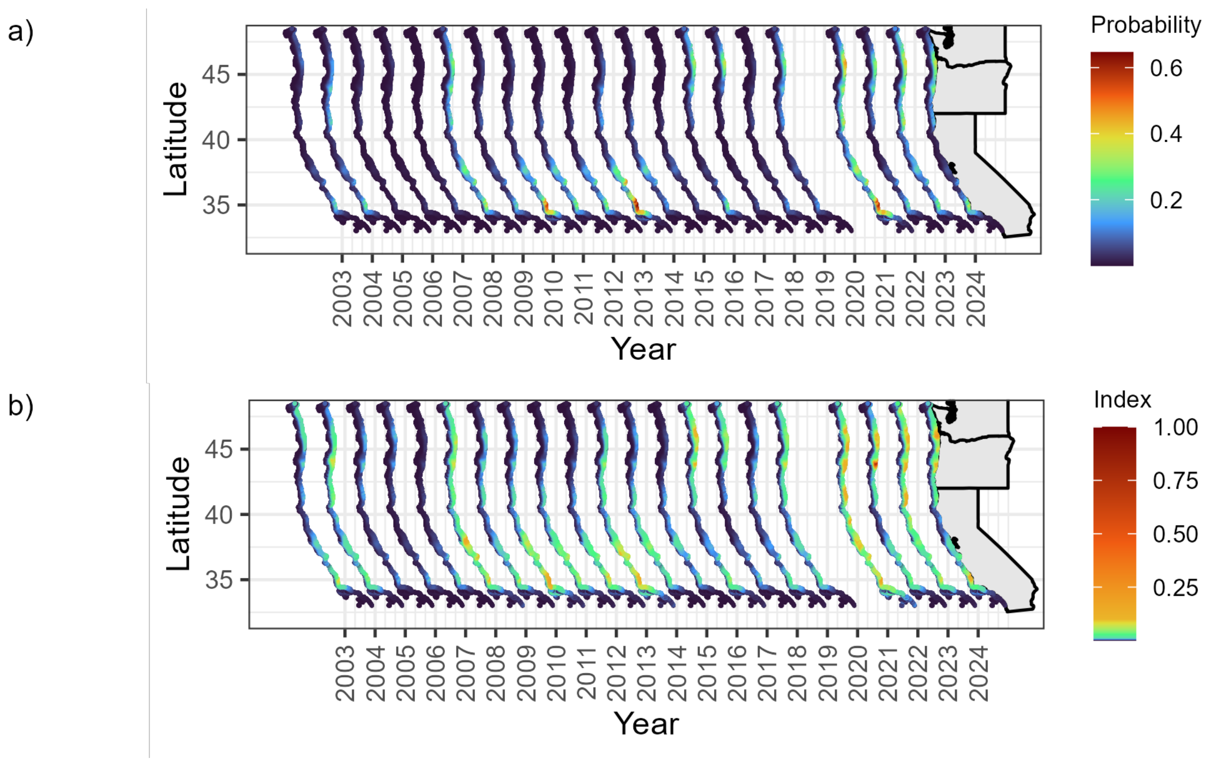

Figure 3.11: Distribution of juvenile sablefish along the West Coast. a) probability of occurrence, and b) index of abundance (scaled to 0-1). Results are from a species distribution model; details in Appendix K. Probability of occurrence was calculated from the presence/absence model, while the index of abundance is the estimate from the full species distribution model.

3.5 Highly Migratory Species (HMS)

3.5.1 Spawning stock biomass and recruitment

Recent ESRs have featured stock assessment-based biomass and recruitment estimates for several HMS stocks that occur in the CCE. Updates for this year are for Pacific bluefin tuna, skipjack tuna, and bigeye tuna. Pacific bluefin tuna spawning stock biomass estimates continue to increase, as they have since approximately 2010 (Appendix L). Skipjack tuna and bigeye tuna biomass has been largely stable since 2015. Recent recruitment estimates were around average for all species. Time series of biomass and recruitment estimates for all available HMS stocks through their most recent assessments are in Appendix L.

3.5.2 HMS diet

HMS are opportunistic predators and information on their diets complements forage surveys and provides direct measures of forage use by these predators. Analyses of stomach contents collected by commercial and recreational fishers in central and southern California indicate that HMS continue to prey on anchovy. Anchovy was the most important prey of swordfish, increasing from 13% in 2022 to 35% in 2023. Hake was also an important prey item for swordfish in 2023 and was above the long-term average for both swordfish and bluefin tuna for the third consecutive year. Consumption of Pacific sardine was near record high levels for albacore tuna (35%) in the Northern CCE and was above average for bluefin tuna diets in the southern region. Rockfish consumption was low for all three predators. Notably, consumption of “other” prey by bluefin tuna reached 64% and was mostly composed of pyrosomes and myctophids. This aligns with the high abundance of myctophids observed in the RREAS and CalCOFI surveys in recent years. These findings highlight the dynamic nature of HMS feeding behavior, which is influenced by factors such as prey availability and environmental conditions. See also Appendix L.

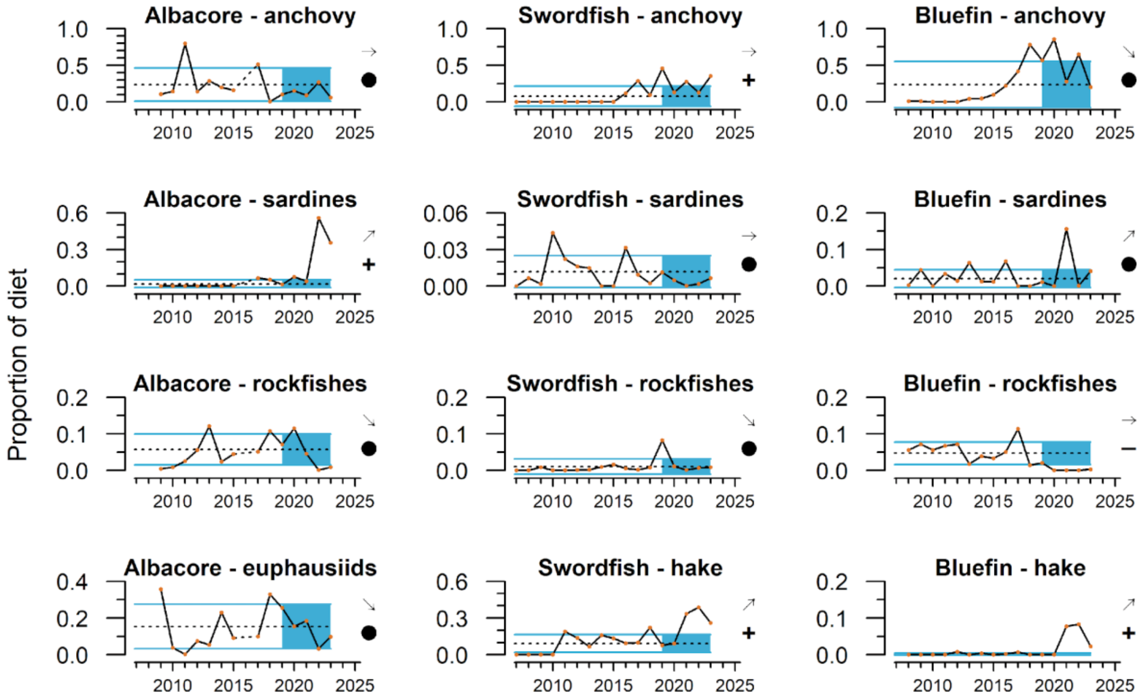

Figure 3.12: Diets of albacore tuna, swordfish, and bluefin tuna sampled from commercial and recreational fisheries in the CCE, 2008 - 2023. Data are proportional contributions of four key prey classes. Lines, colors, and symbols are as in Fig. 2.1.

3.6 Seabird Indicators

Seabird indicators (productivity, density, diet, and mortality) reflect population health and condition of seabirds, as well as links to lower trophic levels and other conditions in the CCE. The species we report on here and in Appendix M represent a breadth of foraging strategies, life histories, and spatial ranges.

3.6.1 Fledgling production and diet

In 2024, fledgling production decreased at seabird colonies on Yaquina Head, Oregon and Destruction Island, Washington relative to the previous year. Fledgling productivity declined to below average levels at all colonies except Brandt's cormorant, which continued to experience above average production (Fig. 3.13, Appendix M). Smelts continued to dominate the diets of rhinoceros auklets and common murres in the Northern CCE, and the proportion of juvenile rockfishes consumed by common murres has increased significantly in recent years (Appendix M).

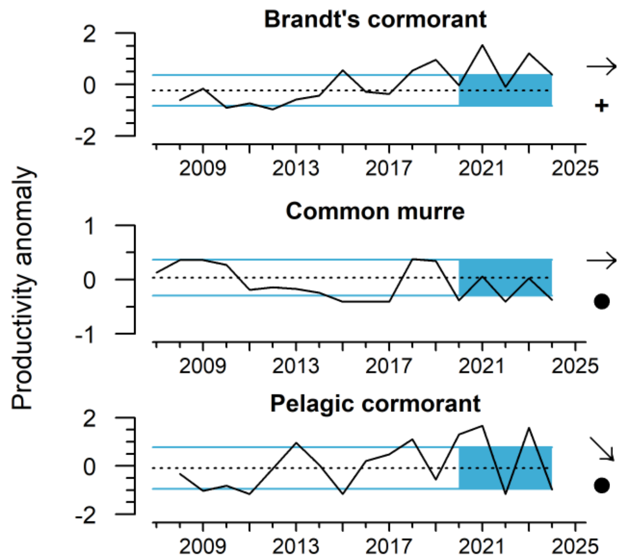

Figure 3.13: Standardized productivity anomalies for three seabird species breeding at Yaquina Head, OR through 2024. Data courtesy of R. Orben, Oregon State University. Lines, colors, and symbols are as in Fig. 2.1.

Seabird colonies on Southeast Farallon Island off central California experienced near average fledgling production in 2024, except for Brandt's cormorant, which declined to well below average (lowest in >10 years) (Fig. M.2). This low productivity in 2024 appears to be part of normal variability. Poor local conditions during winter and early spring likely limited prey resources and led to poor adult condition and later breeding. Pairs that bred early abandoned those attempts, while those that bred later experienced improved ocean conditions and prey abundance. Most piscivorous birds at Southeast Farallon Island relied more on juvenile rockfish and less on anchovy for the first time in several years. Brandt's cormorant diet showed reduced numbers of fish and a reduced reliance on northern anchovy, which has been associated with poor chick production (Fig. M.5, Appendix M).

3.6.2 Mortality

Significant mortalities of Cassin's auklet were reported on beaches in the Northern and Central regions of the CCE in early 2024 (Appendix M). There was also a die-off of brown pelicans on beaches of central and southern California in spring of 2024 that has been attributed to lower prey availability and greater intraspecific competition for food due to an increasing pelican population over the last several years.

3.7 Marine Mammals

3.7.1 Sea lion productivity

California sea lion pup counts and condition at San Miguel Island are positively correlated with seasonal prey availability in the Central and Southern CCE, and are high when energy-rich prey like sardines, anchovy or mackerel have high occurrence in adult female sea lion diets (Melin et al. 2012). Counts of live sea lion pups in July 2024 declined relative to recent years, though remained slightly above average (Fig. 3.14). The lower count indicates a reversal after several years of increases in pup births. This decline may be attributed to multiple factors, including winter El Niño conditions that are often associated with less food availability during early pregnancy, and significant harmful algal bloom activity that exposed California sea lions to the neurotoxin domoic acid and led to pup strandings (Appendix N). Pup condition indices of the 2024 cohort were not measured at the time of this writing; we will provide an update in the March 2025 presentation to the Council if data are available.

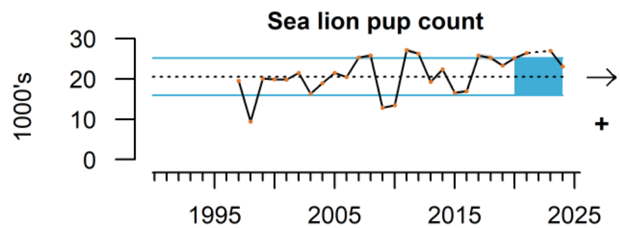

Figure 3.14: California sea lion pup counts on San Miguel Island for the 1997 - 2024 cohorts. Lines, colors, and symbols are as in Fig. 2.1; dashed line indicates years of missing data. Counts of live sea lion pups in 2024 were from images collected during a fixed-wing aerial survey.

3.7.2 Whale entanglements

Reports of whale entanglements along the West Coast increased in 2014 and high rates have continued over subsequent years. The dynamics of entanglement risk and reporting are complex, and are affected by shifts in ocean conditions and prey fields, changes in whale populations, changes in distribution and timing of fishing effort, and increased public awareness.

Based on preliminary data, West Coast entanglement reports were higher in 2024 than 2023, but below the peak years of 2015-2018 (Fig. 3.15). Humpback whales continued to be the most common species reported. Most reports were in California, although reports involved gear from all three West Coast states, including confirmed reports involving U.S. gear received from Mexico and Canada. Entanglement reports in 2024 involved a range of sources, including: commercial Dungeness crab gear; commercial spot prawn; commercial coonstripe shrimp; groundfish trawl; and unidentified gillnet fisheries. No entanglements in large mesh drift gillnet gear were confirmed in 2024.

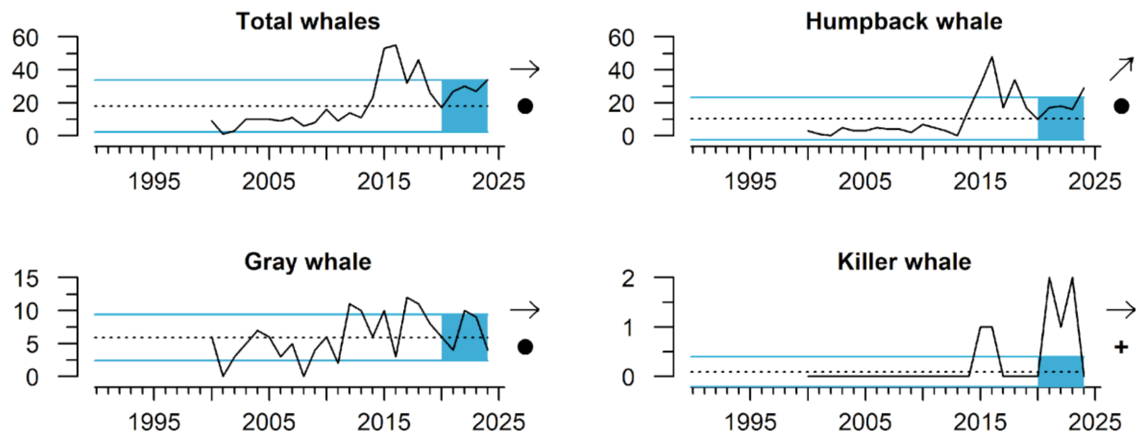

Figure 3.15: Numbers of reported entanglements for selected species (alive and dead) in fishing gear along the West Coast from 2000 - 2024. No killer whale entanglements have been associated with the endangered Southern Resident population. 2024 data are preliminary.

Multiple actions were taken in 2024 to reduce entanglement risk (see Appendix N). Despite action that reduced fishing effort in some crab fisheries, confirmed entanglement reports have remained elevated above pre-2014 baseline levels (Fig. 3.15). Additional factors continue to present obstacles to risk reduction, including growth of some whale populations, derelict gear, and nearshore whale foraging under habitat compressed ecosystem conditions. High abundances of anchovies near Monterey Bay have drawn whales closer to Monterey, an active coastal region with whale-watching tours, researchers, and more human activity. Late-summer and early-fall increases in habitat compression (Fig. 2.5) and a nearshore increase in adult anchovy (a main prey of humpback whales) both contributed to this aggregation. Habitat compression levels off California this past year were similar to those in 2015-2016, when reported humpback whale entanglements peaked. See Appendix N.2.

3.8 Harmful Algal Blooms (HABs)

Blooms of the diatom genus *Pseudo-nitzschia* can produce domoic acid, a toxin that can affect coastal food webs and lead to fishery closures. In 2024, such blooms occurred along the entire West Coast throughout much of the summer (Appendix O), but they were most problematic for shellfish fisheries and marine life in California and southern Oregon. Recurrent *Pseudo-nitzschia* blooms at the northern California HAB "hotspot" continued to impact shellfish fisheries in northern California and southern Oregon. Bloom activity was especially persistent in southern Oregon, resulting in closures of the mussel and razor clam fisheries and contributing to the delayed opening of the 2024-25 commercial Dungeness crab fishery in Oregon by about two weeks. A large marine mammal stranding event related to a *Pseudo-nitzschia* bloom and domoic acid also occurred in Southern California, from July to August with a resurgence in September (Appendix N). This marks the third consecutive year that this region has witnessed such an event.

Pseudo-nitzschia HABs can cost tens of millions of dollars in lost revenue, particularly for the commercial Dungeness crab fishery, and cause a range of sociocultural impacts in fishing communities. A summary of management actions in the commercial Dungeness crab fishery in response to domoic acid and other issues, such as poor body condition and marine life entanglement risk, is shown in Figure 3.16. Since the massive 2015-16 HAB event, domoic acid contamination requiring evisceration or delay of the opening of the season has mostly impacted the fishery in Oregon and Washington. Management actions related to marine life entanglement risk (spatial closures, gear or depth restrictions) or poor crab body condition have occurred in all three states, and have largely overshadowed domoic acid related management actions in California since 2019. Note, however, that exceedances of domoic acid in Dungeness crab did sometimes occur in some regions of California prior to the eventual opening of the season, but the fishery opening was delayed during that time because of management actions regarding marine life entanglement risk and/or meat quality assessments. The toxin cleared from samples, in tandem with the resolution of the non-biotoxin factors, prior to the season opening. As such, this did not result in management action specific to domoic acid.

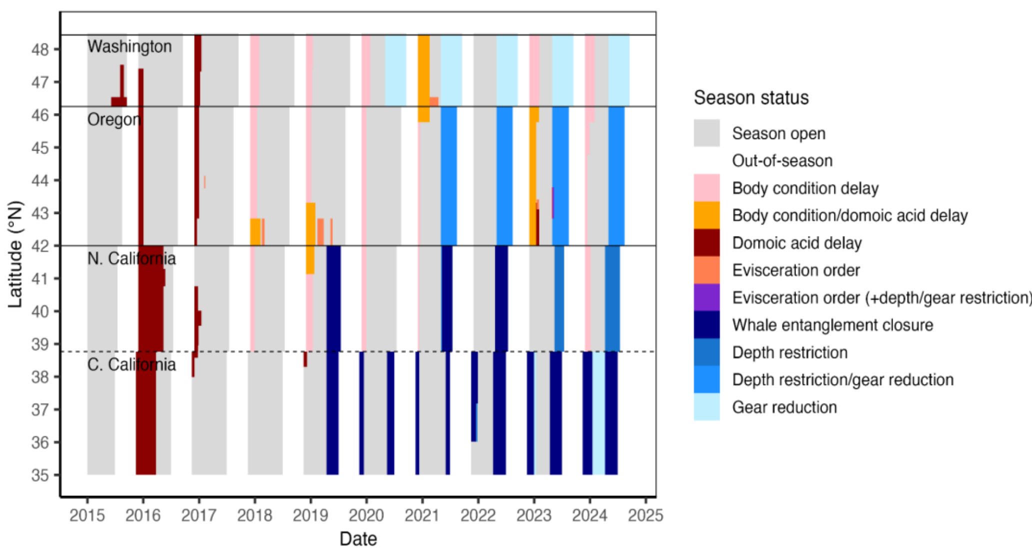

Figure 3.16: The spatial-temporal history of closures and management restrictions in the U.S. West Coast Dungeness crab fishery from 2015 to 2024, both HAB and non-HAB related. Solid black lines indicate state borders and the dashed line indicates the border between the Northern and Central California management zones. Gray shading indicates the commercial Dungeness crab fishing season in each region.

The past year was unusual in that there was a large-scale bloom of the toxic dinoflagellate *Alexandrium catenella* that closed or prompted consumption advisories for bivalve shellfish fisheries in all three coastal states and sickened people in Oregon with paralytic shellfish poisoning. There was also an unusual bloom of the non-toxic dinoflagellate genus *Tripos* in Washington that extended into northern Oregon and raised public concern and impacted commercial oyster markets. Not since 1995 has a *Tripos* bloom of this magnitude occurred in Washington. Warmer temperatures and stratified water column conditions are generally favorable for dinoflagellates. State level details of HAB dynamics and human health and fishery impacts are in Appendix O.

4. HUMAN WELLBEING

Key Message

Washington and Oregon experienced shifts in key commercial fishing communities, generally reflecting reductions in fishing diversity and participation. In contrast, in California human wellbeing metrics remained relatively stable compared to the previous five years. Coastwide there was a decrease in revenue concentration for all management groups combined in 2023, although revenue concentrations increased in the Salmon, Coastal Pelagic and Groundfish fisheries.

4.1 Social Vulnerability

Community vulnerability indices measure generalized socioeconomic vulnerability at the scale of the whole community, and thereby allow for inter-community comparisons. As in prior reports, we monitor the Community Social Vulnerability Index (CSVI), derived from social data (e.g. demographics, personal disruption, poverty, housing characteristics, housing disruption, labor force structure) in communities that depend upon commercial and recreational fishing (Norman et al. 2022, Jepson and Colburn 2013, Lewis-Smith and Norman 2024). We also maintain community-level commercial and recreational fishing *engagement* indices, based on an analysis of variables reflecting commercial fishing (e.g., fishery landings, revenues, permits, and processing), recreational fishing (guide and charter permits, recreational retail shops, and marinas), as well as *per capita engagement*, previously referred to as *reliance.* Data for all of these indices are available through 2022.

In Figure 4.1, communities in the upper right quadrants of plots shown are those with relatively high social vulnerability (vertical axis) and either high commercial fishing per capita engagement (horizontal axis) in the left plot, or high recreational fishing per capita engagement (horizontal axis) in the right plot. The commercial and recreational indices are not directly comparable; a lower score in one does not imply lesser relative importance compared to the other. Communities that measure highly in either commercial or recreational per capita engagement, in addition to exhibiting higher social vulnerability values, may be especially socially vulnerable with downturns in fishing.

In 2022, both Tokeland, WA and Westport, WA had relatively high commercial per capita engagement and high social vulnerability (Fig. 4.1, left). Multiple communities with relatively high recreational engagement also had relatively high social vulnerability, particularly in Washington and Oregon (Fig. 4.1, right). Recreational per capita engagement was generally higher in Oregon and Washington communities compared to those in

California. Several communities coastwide were among the most reliant in their respective regions for both commercial and recreational fishing (Fig. 4.1).

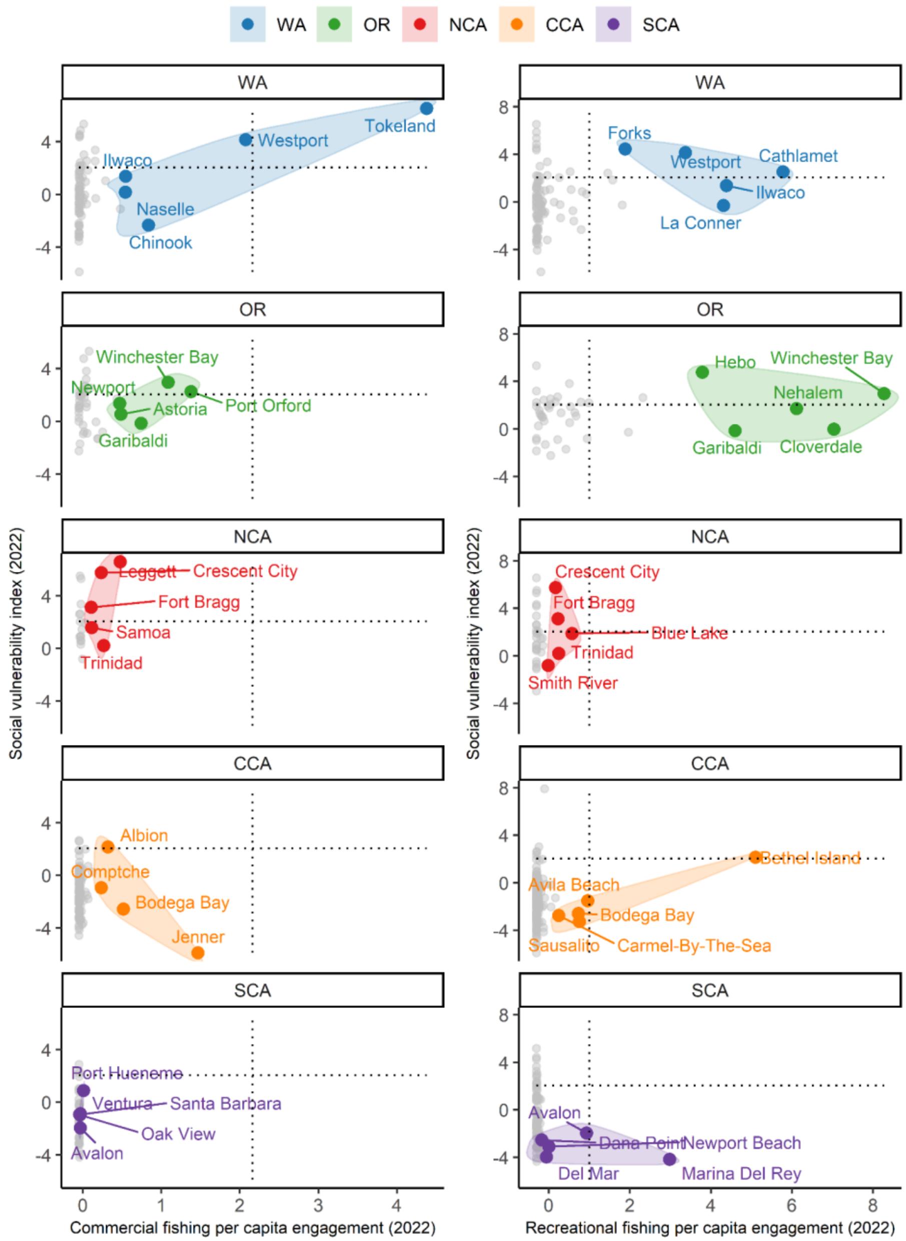

Figure 4.1: Commercial fishing per capita engagement and social vulnerability scores (left) and recreational fishing per capita engagement and social vulnerability scores (right) in 2022 for communities in Washington, Oregon, and northern, central and southern California. The five highest-scoring communities for both forms of per capita engagement are shown for each region. Dotted lines indicate 1 s.d. above the means for all communities.

Colored polygons within the figures group the five community points from each region together to represent cross-regional differences.

Because engagement and social vulnerability indices vary from year to year, we provide similar plots for 2021 in Appendix P, which allow us to identify communities that may have shifted. For example, commercial fishing per capita engagement in Jenner, CA increased in 2022 from 2021 relative to other West Coast communities, moving it into the top five ranking for the Central California region (CCA). The commercial fishing per capita engagement rank for Point Arena, CA declined relative to other communities, removing it from the top five ranking for the CCA (Fig. 4.1, left; Fig. P.1). Communities can move left on the x-axis in years with reduced landings, and therefore may appear to be less dependent on commercial or recreational fishing when in fact they have actually just experienced a difficult year; therefore, these results should be interpreted with care.

Of the highly commercially reliant communities, social vulnerability also increased in Winchester Bay, OR relative to all other top reliant communities in OR in 2022 (Fig. 4.1, left). For communities more reliant on recreational fishing activity, Hebo, OR shifted into the higher end for social vulnerability (Fig. 4.1, right). For additional information, including recreational and commercial fishing total engagement, see Figure P.2 in Appendix P.

4.2 Diversification of Fishery Revenues

Interannual variability in fishing revenue can be reduced by diversifying activities across multiple fisheries or regions, and more diversified fishers also tend to have higher total revenue (Kasperski and Holland 2013). In 2023, revenue diversification, which is measured by how revenue is spread across species groups, declined by 5% from the 2022 level for the current fleet of vessels fishing on the U.S. West Coast and in Alaska, falling to the lowest level observed since 1981 (Figure 4.2a-d). California, Oregon and Washington fleets saw 11%, 15% and 6% decreases in diversification in 2023 relative to 2022. Further information on port-level diversification and temporal diversification can be found in Appendix Q.

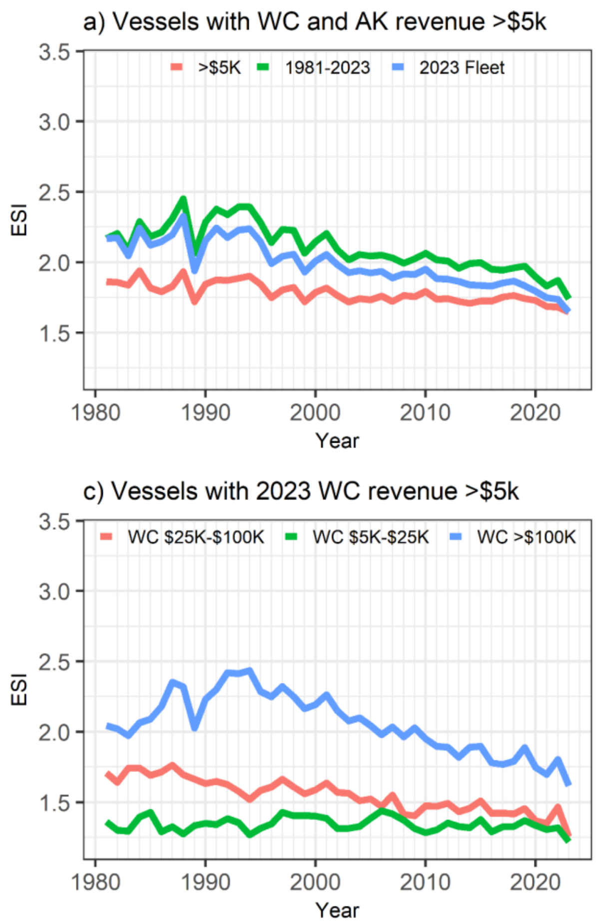

Figure 4.2: Average diversification for West Coast and Alaskan fishing vessels (top left) and for vessels in the 2023 West Coast Fleet, grouped by state (top right), average gross revenue class (bottom left) and vessel length class (bottom right).

The Theil Index is used to assess the geographic concentration of fishing revenues. This Index is calculated annually for all fisheries and specific management groups, at the scale of the 21 port groups previously established for the economic Input-Output model for Pacific Coast fisheries (IO-PAC) (Leonard and Watson 2011). The Theil index measure for the salmon fishery shows a steep increase in 2023, which coincides with a downturn in salmon revenues overall and a concentration of salmon revenues in northern Washington and Oregon ports after salmon fishing closures in 2023 inhibited harvest in California (see Appendix R). CPS and HMS fisheries continue to have the highest Theil Index values, as they have for the last decade, indicating those groups' relatively high concentration of revenue in a smaller number of port groups. See Appendix R for additional information.

4.3 Fisheries Participation Networks

Fisheries participation networks (Fuller et al. 2017, Fisher et al. 2021) provide a visual representation of economically important commercial fisheries for individual communities. Much like species in a food web diagram, in these networks each fishery is depicted as a point known as a node. Pairs of fisheries, like interacting species in a food web, are connected by lines called 'edges.' Edges in a fisheries participation network represent the level of connectivity between two fisheries, and integrate information about vessels participating in both fisheries.

We developed fisheries participation networks representing IO-PAC port groups for the past year (examples in Fig. 4.3; see also Appendix S). Networks for some port groups, like Columbia River, consist only of a single fishery (salmon), while in other port groups (e.g., Santa Barbara) there are almost two dozen connections between fisheries. These snapshots in time depict the portfolios of fisheries that are economically important to individual vessels within a port group, based on a diversity of behaviors and choices at the level of individual vessels over the past year.

It is typical for the number of fisheries on which individual vessels and IO-PAC port groups depend to fluctuate (increase or decrease by one fishery) from year to year. However, in the last five years the number of fisheries in three Oregon port groups (Tillamook, Coos Bay, Brookings) and five California port groups (Eureka, Fort Bragg, San Francisco, Morro Bay, Los Angeles) has declined more substantially (Fig. S5 in Appendix S). For Brookings and San Francisco, this decline in the number of fisheries was accompanied by increasing connectivity (through shared vessel participation in pairs of fisheries), an expected result for networks with fewer nodes (Fig. S6 in Appendix S). However, vessels in Coos Bay, Morro Bay, and Los Angeles not only participated in fewer fisheries but those fisheries were also less well-connected over the last five years (Figs. S5-S6 in Appendix S). Declines in connectivity can in turn reduce resilience to environmental or regulatory shocks (e.g., Fisher et al. 2021).

The Puget Sound, Astoria, Monterey, and San Diego port groups exhibited an increasing trend in the number of fisheries over the last five years, with all but Astoria showing a corresponding and expected decline in connectivity (Figs. S5-S6 in Appendix S). In contrast, in Astoria not only is there a positive trend in the number of fisheries in its network, but those fisheries are increasingly connected. Port groups with high connectivity have a greater ability to move effort between fisheries and thus substitute for lost revenue from a fishery that is closed or has a poor year.

Finally, for the WA Coast port group, the average number of fisheries and the connectivity between them were below long-term averages, though there was not a clear recent trend (Figs. S5-S6 in Appendix S). Future work to evaluate the causes and potential impacts of these patterns of fisheries participation could prove fruitful, especially in the context of historical or potential management actions. See Appendix S for more information.

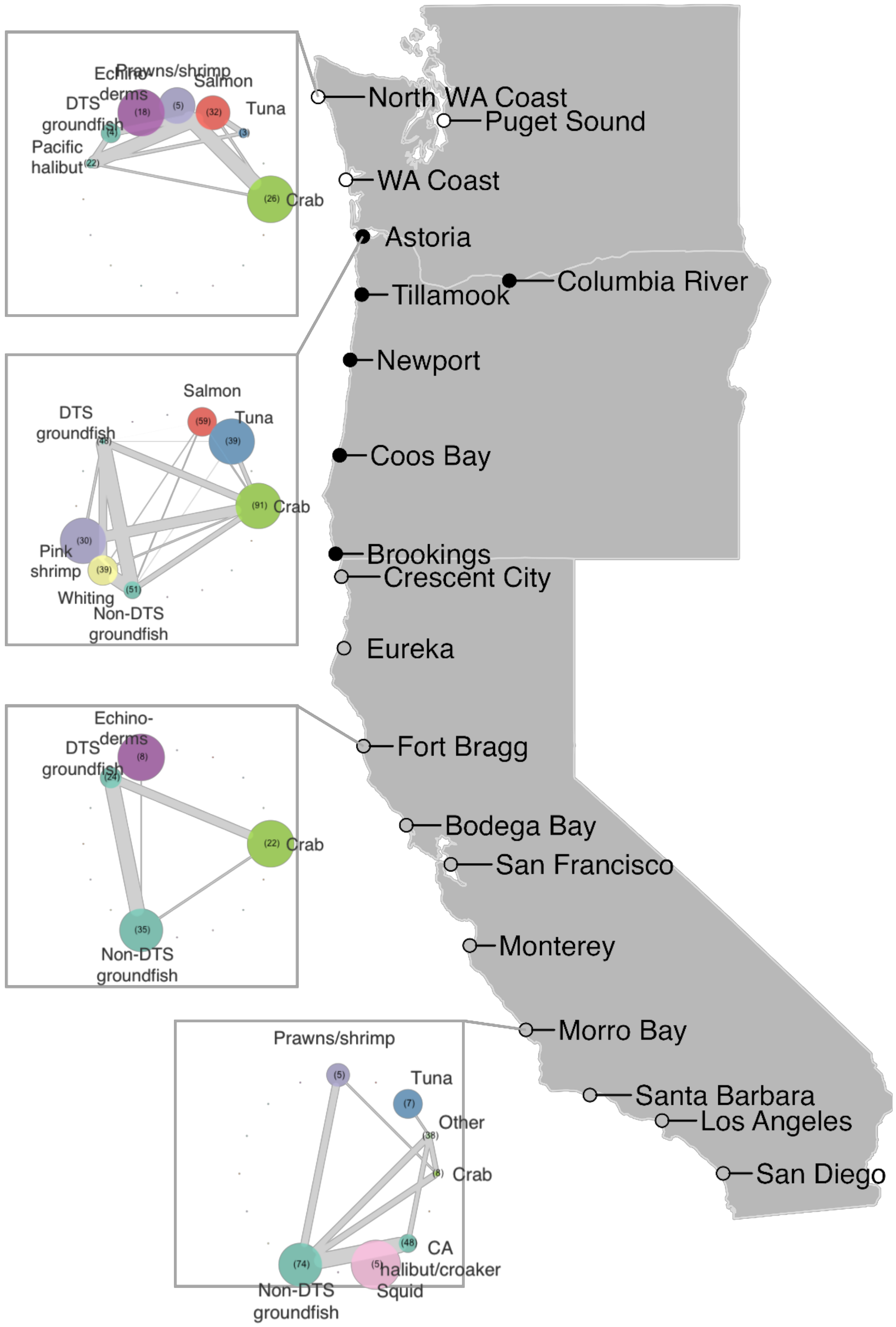

Figure 4.3: Fisheries participation networks for four example IO-PAC port groups (North WA Coast, Astoria, Fort Bragg, Morro Bay), based on November 2023-November 2024 (a Dungeness crab year) landings receipts. Node size is proportional to the median contribution of a given fishery to annual vessel-level revenue; values in parentheses are the number of vessels participating in

the fishery. Thickness of lines ("edges") is proportional to the number of vessels participating in both of the fisheries connected by the lines, and the evenness of revenue generated by each fishery in the pair. All IO-PAC port groups are illustrated in this figure except for Other Coastal WA and Unknown Ports.

5. Fishing and Non-fishing Human Activities

Key Message

In 2024, total coastwide commercial landings declined largely due to a substantial decrease in Pacific whiting landings. However, coastwide landings increased for several commercial fisheries, such as HMS, market squid, and shrimp. Total coastwide revenue also increased, albeit by a small margin. Recreational landings (excluding salmon) were among the lowest of the last 20 years. Recently developed ecosystem indicators for offshore wind energy suitability suggest that the wind energy areas off Humboldt Bay, California may have greater ecosystem productivity tradeoffs than areas to the north and south.

5.1 Coastwide Landings by Major Fisheries

Fishery landings are indicators of ecosystem services provided and also reflect removals from the CCE. In 2024, coastwide total landings were well below the long-term average and decreased 12% from 2023 (Fig. 5.1). This decrease is largely driven by a 31% decrease in Pacific whiting landings from 2023 to 2024, primarily the result of a more southerly distribution of the species and decreased capacity in the mothership sector during the spring of 2024. Landings from 5 of 9 commercial fisheries increased in 2024: market squid (142%), HMS (45%), shrimp (17%), CPS finfish (11%), and salmon (11%). In contrast, landings from Pacific whiting (-31%), crab (-26%), non-whiting groundfish (-11%), and Other species (-5%) fisheries decreased in 2024 from 2023. Over the past five years, no fishery's status was above the long-term average, while salmon, CPS finfish, HMS and Other species landings were below long-term averages. Landings from crab fisheries increased from 2020 to 2024, while landings from Pacific whiting fisheries decreased. There were no commercial landings of salmon in California in 2023 and 2024, as the fishery was closed.

Total revenue in commercial fisheries coastwide increased in 2024 by 3% from 2023, largely driven by an increase in revenue from market squid fisheries in California State-by-state landings and revenue are presented in Appendix T.

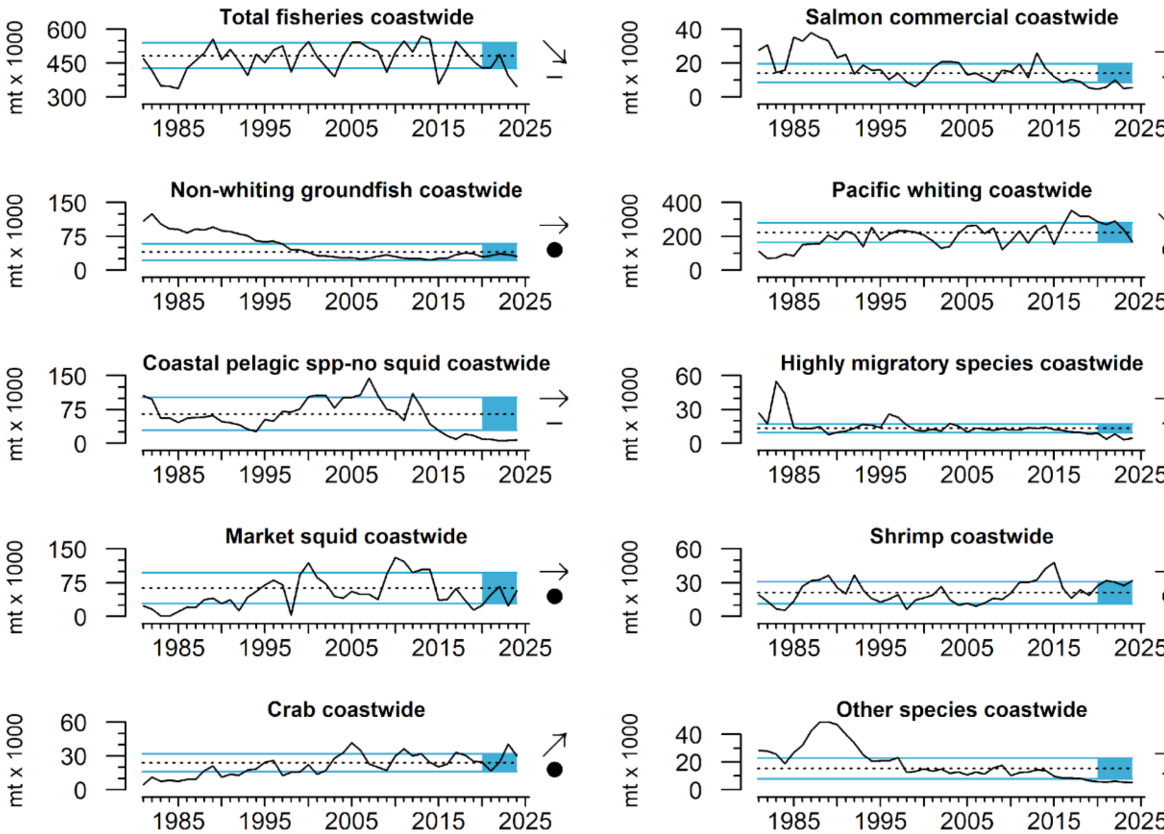

Figure 5.1: Annual landings from West Coast commercial fisheries (data from PacFIN and NORPAC), including total landings across all fisheries, from 1981 - 2024. Data were downloaded from PacFIN and NORPAC on January 10, 2025. Lines, colors, and symbols are as in Fig. 2.1.

Overall, recreational landings have declined from a peak in 2015 and 2024 landings were among the lowest of the available time series (Fig. 5.2). The recent five-year average was nonetheless <1 s.d. below the long-term average. The coastwide time series pattern generally follows landings across the top three targeted species: black rockfish, lingcod and albacore. Recreational salmon landings have varied within ~1 s.d. of long-term averages over the last five years. Notably, the recreational salmon fishery in California was closed in 2023 and 2024, though no recreational salmon landings data from any states in 2024 were available for this report. State-level recreational landings are in Appendix T.

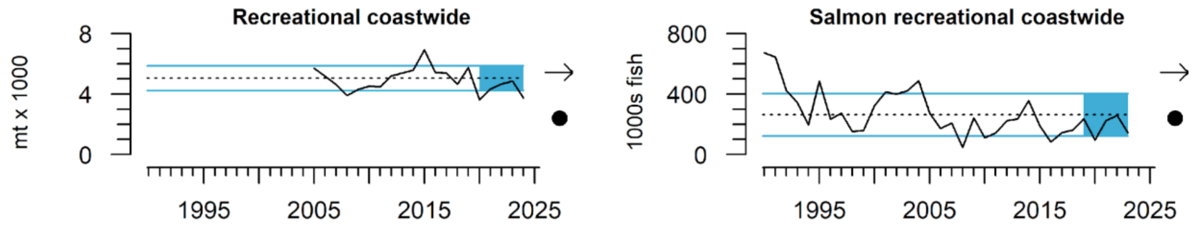

Figure 5.2: Annual landings from most West Coast recreational fisheries from 1981 - 2024 (data from RecFIN) and from recreational salmon fisheries from 1990-2023 (data from PFMC). Data from 2024 are complete through October. Lines, colors, and symbols are as in Fig. 2.1.

5.2 Potential Interactions Between Offshore Wind and Ecosystem Indicators

Federal and state processes to pursue offshore wind energy (OWE) development in CCE have been underway in recent years. Five lease areas for OWE off northern and central California were issued in 2022 and two Wind Energy Areas were designated off Oregon in 2024. A portfolio of indicators is needed that can identify ocean areas important to the overall structure and function of the CCE, and that can track potential ecosystem impacts across all stages of OWE development or for other new ocean-use sectors.

In Appendix U, we present seven broad-scale ecosystem indicators focused on lease areas and other areas under consideration for future OWE development along the northern California coast. The indicators reflect long-term, spatial variation in ecosystem components that help define levels of productivity across the CCE. As such, they are useful for identifying areas that might be more or less suitable for OWE development because of the area's relative importance to the ecosystem. A hotspot of overall ecosystem importance has been identified offshore from Humboldt Bay, CA which may signify this area is less suitable for OWE than areas further to the north or south as a function of the seven ecosystem indicators (Fig. U.1h). Additional indicators of potential interactions with groundfish fisheries are in Figure U.2 in Appendix U. New information on how climate change is projected to affect inferences about the potential for interactions between offshore wind energy development and fisheries can be found in Appendix E.

6. SYNTHESIS

The California Current Ecosystem in 2024 began with a "strong" El Niño, which delayed the normal springtime upwelling signal. However, conditions changed quickly after the delay, to a productive and favorable environment for many species during the summer and fall. As such, the ecological impacts of the El Niño were not as great as similar past events, partially evidenced by the switch back to lipid-rich copepods in the north following spring upwelling, and the average krill abundances off California, which are typically low during El

Niño events. Additionally, forage was observed to be productive and diverse, with high abundances of anchovy and juvenile groundfish. Juvenile salmon in the Northern CCE were also near or above average abundance. This more muted response to the El Niño was likely due to the strong sustained spring and summer upwelling, particularly from central California to southern Oregon - which fueled heightened productivity, and mostly kept marine heatwaves at bay.

While these signs of resilience to the El Niño and marine heatwaves are encouraging, other indicators raise concern. Multiple harmful algal bloom events, including unusual blooms of toxic dinoflagellates, caused an array of impacts, from fishery closures to direct human health impacts. Marine birds were adversely impacted - starvation of pelicans and a significant mortality event for Cassin's auklets likely due to changes in krill availability. Also, habitat compression and high forage levels in nearshore waters were a likely culprit for heightened whale entanglement reports. Social vulnerability increased for most Oregon and Washington commercial and recreational fishing communities in 2022, which may reduce the resilience of coastal communities to the 2024 ecological impacts, including the harmful algal blooms and fishery closures. Further, fisheries participation networks revealed that most IO-PAC port groups saw a reduction in the number of fisheries that vessels participate in and some ports also had less connectivity between fisheries, potentially reducing fisher resilience to environmental and market pressures.

The suite of indicators presented in the ESR support EWG and NOAA Fisheries efforts to develop risk tables for West Coast fisheries. The ocean forecasts (Appendix D) and outlooks for adult salmon returns (Appendix J) highlighted in this year's ESR further enable NOAA scientists and their partners to effectively assess risk associated with ecosystem conditions. Also, the ongoing development of human wellbeing indicators supports Council efforts to better characterize the social and economic conditions of West Coast fishing communities. With impending shifts in fishing communities, including the closure of several Oregon fishing processors in 2024, we expect to see changes in the human wellbeing indicators, including reduced per capita engagement in southern West Coast ports and increased overall engagement in northern West Coast ports.

Looking forward to 2025, we note the system is transitioning back towards La Niña or "neutral" conditions (Appendix D), although current ocean conditions within the CCE do not yet reflect this transition, with massive regions of warmer than normal ocean temperatures as of February 1, 2025 (see NOAA's California Current Marine Heatwave Tracker). Conditions on land show continued drought in the south, and no drought conditions to the north, which is consistent with a La Niña pattern (see the Western Region's Drought Index). Similar to past years, marine heatwaves are forecast to continue in the further offshore regions, with potential incursions into the coastal zone in the summer and fall (Fig. D.2). Even with these challenges, there are positive signs in the outlooks for some Chinook salmon stocks returning to the Columbia Basin and California river basins in 2025 and 2026. With new advances in ocean modeling, we will be able to provide more detailed short-term forecasts (Appendix D), and enhanced understanding of climate variability and change impacts on the CCE and West Coast fisheries and communities (Appendix E).

7. LITERATURE CITED

Abbott JK, Sakai Y, Holland DS (2023) Species, space and time: A quarter century of fishers' diversification strategies on the US West Coast. Fish and Fisheries 24:93–110

Abell R, Thieme ML, Revenga C, et al (2008) Freshwater ecoregions of the world: a new map of biogeographic units for freshwater biodiversity conservation. BioScience 58:403–414

Barth, J. A., S. D. Pierce, B. Carter, A. Y. Erofeev, J. L. Fisher, R. A. Feely, K. C. Jacobson, A. A. Keller, C. A. Morgan, J. E. Pohl, L. K. Rasmuson, and V. Simon, 2024. Widespread and increasing near-bottom hypoxia in the coastal ocean off the United States Pacific Northwest. *Nature Sci. Rep.*, **14**, 3798, https://doi.org/10.1038/s41598-024-54476-0.

Bi R, Maunder MM, Xu H, et al (2024) Stock assessment of skipjack tuna in the eastern Pacific Ocean: 2024 benchmark assessment. https://www.iattc.org/GetAttachment/f57dece1-81ba-4771-8fa8-3362320a368a/SAC-15-04_Skipjack-tuna-benchmark-assessment-2024.pdf

Brodie S, Pozo Buil M, Welch H, Bograd SJ, Hazen EL, et al. (2023) Ecological forecasts for marine resource management during climate extremes. Nature Communications, 14(1):7701.

Burke BJ, Peterson WT, Beckman BR et al (2013) Multivariate models of adult Pacific salmon returns. PLoS One 8:e54134

Busch DS, McElhany P (2016) Estimates of the direct effect of seawater pH on the survival rate of species groups in the California Current Ecosystem. PloS one 11:e0160669

Chan F, Barth J, Lubchenco J, et al (2008) Emergence of anoxia in the California Current Large Marine Ecosystem. Science 319:920–920

Cimino MA, Santora JA, Schroeder I, et al (2020) Essential krill species habitat resolved by seasonal upwelling and ocean circulation models within the large marine ecosystem of the California Current System. Ecography 43:1536–1549

Cluett AA, Bograd SJ, Jacox MG, Pozo Buil M, Hazen E (in review) Pan-basin warming now overshadows robust Pacific Decadal Oscillation.

Demer DA, Zwolinski JP, Byers KA, et al (2012) Prediction and confirmation of seasonal migration of Pacific sardine (*Sardinops sagax*) in the California Current Ecosystem

Dyson K, Huppert DD (2010) Regional economic impacts of razor clam beach closures due to harmful algal blooms (HABs) on the Pacific coast of Washington. Harmful Algae 9:264–271

Food and Drug Administration(2011) Fish And Fishery Products Hazards And Controls Guidance (Fourth Edition). Rockville, MD: US Department of Health and Human Services

Feely RA, Sabine CL, Hernandez-Ayon JM, et al (2008) Evidence for upwelling of corrosive" acidified" water onto the continental shelf. Science 320:1490–1492

Fiechter J, Edwards CA, Moore AM (2018) Wind, circulation, and topographic effects on alongshore phytoplankton variability in the California Current. Geophysical Research Letters 45:3238–3245

Fiechter J, Santora JA, Chavez F, et al (2020) Krill hotspot formation and phenology in the California Current Ecosystem. Geophysical research letters 47:e2020GL088039

Field JC, Miller RR, Santora JA, et al (2021) Spatiotemporal patterns of variability in the abundance and distribution of winter-spawned pelagic juvenile rockfish in the California Current. PloS one 16:e0251638

Fisher JL, Peterson WT, Rykaczewski RR (2015) The impact of El Niño events on the pelagic food chain in the northern California Current. Global Change Biology 21:4401–4414

Fisher MC, Moore SK, Jardine SL, et al (2021) Climate shock effects and mediation in fisheries. Proceedings of the National Academy of Sciences 118:e2014379117

Fuller EC, Samhouri JF, Stoll JS, et al (2017) Characterizing fisheries connectivity in marine social–ecological systems. ICES Journal of Marine Science 74:2087–2096

Gladics AJ, Suryan RM, Parrish JK, et al (2015) Environmental drivers and reproductive consequences of variation in the diet of a marine predator. Journal of Marine Systems 146:72–81

Goldstein T, Zabka TS, DeLong RL, et al (2009) The role of domoic acid in abortion and premature parturition of California sea lions (*Zalophus californianus*) on San Miguel Island, California. Journal of wildlife diseases 45:91–108

Harvey CJ, Garfield NT, Williams GD, Tolimieri N (2021a) Ecosystem Status Report of the California Current for 2020-21: A Summary of Ecosystem Indicators Compiled by the California Current Integrated Ecosystem Assessment Team (CCIEA). NOAA Technical Memorandum NMFS-NWFSC-170. https://doi.org/https://doi.org/10.25923/x4ge-hn11

Harvey CJ, Garfield NT, Williams GD, Tolimieri N (2021b) California Current Integrated Ecosystem Assessment (CCIEA) California Current ecosystem status report, 2021. Report to the Pacific Fishery Management Council. March 2021, Agenda Item I.1.a.

Harvey CJ, Garfield NT, Williams GD, Tolimieri N (2022) California Current Integrated Ecosystem Assessment (CCIEA) California Current ecosystem status report, 2022. Report to the Pacific Fishery Management Council. March 2022, Agenda Item I.1.a.

Harvey CJ, Garfield NT, Williams GD, Tolimieri N (2023) California Current Integrated Ecosystem Assessment (CCIEA) California Current ecosystem status report, 2023. Report to the Pacific Fishery Management Council. March 2023, Agenda Item I.1.a.

Henson, S., Beaulieu, C., Ilyina, T. *et al.* Rapid emergence of climate change in environmental drivers of marine ecosystems. *Nat Commun* 8, 14682 (2017). https://doi.org/10.1038/ncomms14682

Hobday AJ, Alexander LV, Perkins SE, et al (2016) A hierarchical approach to defining marine heatwaves. Progress in Oceanography 141:227–238

Holland DS, Kasperski S, Abbott JK (2025) Contract and Sustain: Evaluating the results of progressive implementation of limited entry and catch shares in West Coast and Alaska fisheries over four decades. Canadian Journal of Fisheries and Aquatic Sciences

Holland DS, Leonard J (2020) Is a delay a disaster? economic impacts of the delay of the California dungeness crab fishery due to a harmful algal bloom. Harmful Algae 98:101904

International Scientific Committee for Tuna and Tuna-like Species in the North Pacific Ocean (2024) Stock assessment of Pacific bluefin tuna in the Pacific Ocean in 2024. https://isc.fra.go.jp/pdf/ISC24/ISC24_ANNEX13-Pacific_Bluefin_Tuna_Stock_Assessment_in_2024-FINAL.pdf

Jacox MG, Edwards CA, Hazen EL, Bograd SJ (2018) Coastal upwelling revisited: Ekman, Bakun, and improved upwelling indices for the US West Coast. Journal of Geophysical Research: Oceans 123:7332–7350

Jacox MG, Bograd SJ, Fiechter J, Pozo Buil M, Alexander M, Amaya D, Cordero Quiros N, Ding H, Rykaczewski RR (2024) Linking upwelling dynamics and subsurface nutrients to projected productivity changes in the California Current System. Geophysical Research Letters, 51(10):e2023GL108096.

Jepson M, Colburn LL (2013) Development of social indicators of fishing community vulnerability and resilience in the US Southeast and Northeast regions

Kasperski S, Holland DS (2013) Income diversification and risk for fishermen. Proceedings of the National Academy of Sciences 110:2076–2081

Keister JE, Di Lorenzo E, Morgan C, et al (2011) Zooplankton species composition is linked to ocean transport in the Northern California Current. Global Change Biology 17:2498–2511

Keller AA, Wallace JR, Methot RD (2017) The northwest fisheries science center's west coast groundfish bottom trawl survey: History design, and description. NOAA Technical Memorandum NMFS-NWFSC-136. http://doi.org/10.7289/V5/TM-NWFSC-136

Keller, A., L. Ciannelli, W. W. Wakefield, V. Simon, J. A. Barth and S. D. Pierce, 2015. Occurrence of demersal fishes in relation to near-bottom oxygen levels within the California current large marine ecosystem. *Fisheries Oceanography,* **24**, 162-176, https://onlinelibrary.wiley.com/doi/10.1111/fog.12100.

Lefebvre KA, Bargu S, Kieckhefer T, Silver MW (2002) From sanddabs to blue whales: the pervasiveness of domoic acid. Toxicon 40:971–977

Leising A, Hunsicker M, Tolimieri N, Williams G, Harley A (2024) 2023–2024 California Current Ecosystem Status Report. NOAA California Current Integrated Ecosystem Assessment Team, https://doi.org/10.25923/vxen-pf76

Leonard JL, Watson PPS (2011) Description of the input-output model for Pacific coast fisheries. U.S. Dept. Commer., NOAA Tech. Memo. NMFS-NWFSC-111, 64 p.

Lewis-Smith C, Norman K (2024) Developing US West Coast recreational fishing community measures: Applying an index approach in the context of COVID-19 and social vulnerability. Ocean & Coastal Management 255:107236

Lindgren F, Rue H (2015) Bayesian spatial modelling with R-INLA. Journal of statistical software 63:1–25

Liu OR, Ward EJ, Anderson SA, Andrews KS et al. (2023) Species redistribution creates unequal outcomes for multispecies fisheries under projected climate change. Sci. Adv.**9**, eadg5468. DOI:10.1126/sciadv.adg5468

Liu OR, Kaplan IC, Hernvann PY, Fulton EA, et al. (2025) Climate Change Influences via Species Distribution Shifts and Century-Scale Warming in an End-To-End California Current Ecosystem Model. Global Change Biology, 31(1):e70021.

Marshall KN, Kaplan IC, Hodgson EE, et al (2017) Risks of ocean acidification in the California Current food web and fisheries: ecosystem model projections. Global Change Biology 23:1525–1539

McCabe RM, Hickey BM, Kudela RM, et al (2016) An unprecedented coastwide toxic algal bloom linked to anomalous ocean conditions. Geophysical Research Letters 43:10–366

McKibben SM, Peterson W, Wood AM, et al (2017) Climatic regulation of the neurotoxin domoic acid. Proceedings of the National Academy of Sciences 114:239–244

Melin SR, Orr AJ, Harris JD, et al (2012) California sea lions: an indicator for integrated ecosystem assessment of the California Current System. California Cooperative Oceanic Fisheries Investigations Reports 53:140–152

Messié M, Sancho-Gallegos DA, Fiechter J, et al (2022) Satellite-based Lagrangian model reveals how upwelling and oceanic circulation shape krill hotspots in the California Current System. Frontiers in Marine Science 9:835813

Moore SK, Cline MR, Blair K, et al (2019) An index of fisheries closures due to harmful algal blooms and a framework for identifying vulnerable fishing communities on the US West Coast. Marine Policy 110:103543

Moore SK, Dreyer SJ, Ekstrom JA, et al (2020) Harmful algal blooms and coastal communities: Socioeconomic impacts and actions taken to cope with the 2015 US West Coast domoic acid event. Harmful Algae 96:101799

Morgan CA, Beckman BR, Weitkamp LA, Fresh KL (2019) Recent ecosystem disturbance in the Northern California current. Fisheries 44:465–474

Neveu E, Moore AM, Edwards CA, et al (2016) An historical analysis of the California Current circulation using ROMS 4D-Var: System configuration and diagnostics. Ocean Modelling 99:133–151

Norman K, Holland D, Abbott J, Phillips A (2022) Community-level fishery measures and individual fishers: Comparing primary and secondary data for the US West Coast. Ocean & coastal management 224:106191

Peterson WT, Fisher JL, Peterson JO, et al (2014) Applied fisheries oceanography: Ecosystem indicators of ocean conditions inform fisheries management in the California Current. Oceanography 27:80–89

Phillips EM, Chu D, Gauthier S, et al (2022) Spatiotemporal variability of euphausiids in the California Current Ecosystem: insights from a recently developed time series. ICES Journal of Marine Science 79:1312–1326

Pozo Buil M, Jacox M, Fiechter J, Alexander M, et al. (2021) A dynamically downscaled ensemble of future projections for the California Current System. Frontiers Marine Sciences, https://doi.org/10.3389/fmars.2021.612874

Quezada FJ, Tommasi D, Frawley TH, Muhling B, Kaplan I, Stohs S (2023) Catch as catch can: Markets, availability, and fishery closures drive distinct responses among the US West Coast Coastal Pelagic Species fleet segments. Canadian Journal of Fisheries and Aquatic Sciences.

Raghukumar K, Nelson T, Jacox M, et al (2023) Projected cross-shore changes in upwelling induced by offshore wind farm development along the California coast. Communications Earth & Environment 4:116

Riley KL, Wickliffe LC, Jossart JA, MacKay JK, et al (2021) An aquaculture opportunity area atlas for the US Gulf of Mexico. NOAA technical memorandum NOS NCCOS 299. 545 p. DOI:10.25923/8cb3-3r66

Ritzman J, Brodbeck A, Brostrom S, et al (2018) Economic and sociocultural impacts of fisheries closures in two fishing-dependent communities following the massive 2015 US West Coast harmful algal bloom. Harmful Algae 80:35–45

Robertson RR, Bjorkstedt EP (2020) Climate-driven variability in *Euphausia pacifica* size distributions off northern California. Progress in Oceanography 188:102412

Rust L, Gulland F, Frame E, Lefebvre K (2014) Domoic acid in milk of free living California marine mammals indicates lactational exposure occurs. Marine Mammal Science 30:1272–1278

Samhouri JF, Feist BE, Jacox M, Liu OR et al (2024) Stay or go? Geographic variation in risks due to climate change for fishing fleets that adapt in-place or adapt on-the-move. PLOS Climate. DOI: 10.1371/journal.pclm.0000285

Santora JA, Mantua NJ, Schroeder ID, et al (2020) Habitat compression and ecosystem shifts as potential links between marine heatwave and record whale entanglements. Nature communications 11:1–12

Santora JA, Rogers TL, Cimino MA, et al (2021) Diverse integrated ecosystem approach overcomes pandemic-related fisheries monitoring challenges. Nature communications 12:1–10

Selden, Rebecca L., et al. (2020) Coupled changes in biomass and distribution drive trends in availability of fish stocks to US West Coast ports. ICES Journal of Marine Science 77.1: 188-199.

Smith JA, Pozo Buil M, Muhling B, Tommasi D, et al. (2023) Projecting climate change impacts from physics to fisheries: A view from three California Current fisheries. Progress in Oceanography, 211:102973.

Stierhoff KL, Renfree JS, Rojas-González RI, Vallarta-Zárate JP J. R. F.and Zwolinski (2023a) Distribution, biomass, and demography of coastal pelagic fishes in the California Current Ecosystem during summer 2021 based on acoustic-trawl sampling. U.S. Dep. Commer., NOAA Tech. Memo., NOAA-TM-NMFS-SWFSC-676: 85.

Stierhoff KL, Zwolinski JP, Demer DA (2020)Distribution, biomass, and demography of coastal pelagic fishes off Central and Southern California during spring 2021 based on acoustic-trawl sampling. NOAA Tech. Memo. NMFS-SWFSC-xxxx

Stierhoff KL, Zwolinski JP, Refree JS, Demer DA (2023b) Distribution, biomass, and demography of coastal pelagic fishes in the California Current Ecosystem during summer 2022 based on acoustic-trawl sampling. U.S. Dep. Commer., NOAA Tech. Memo., NOAA-TM-NMFS-SWFSC-683:84.

Szoboszlai AI, Thayer JA, Wood SA, et al (2015) Forage species in predator diets: synthesis of data from the California Current. Ecological Informatics 29:45–56

Theil H (1967) Economics and Information Theory (Chicago and Amsterdam). Rand McNally andCo.; North-Holland Publishing Company

Thompson AR, Harvey CJ, Sydeman WJ, et al (2019) Indicators of pelagic forage community shifts in the California Current large marine ecosystem, 1998–2016. Ecological Indicators 105:215–228

Tolimieri N, Wallace J, Haltuch M (2020) Spatio-temporal patterns in juvenile habitat for 13 groundfishes in the California Current Ecosystem. PloS one 15:e0237996

Tommasi D, Stock CA, Hobday AJ, et al (2017) Managing living marine resources in a dynamic environment: the role of seasonal to decadal climate forecasts. Progress in Oceanography 152:15–49

Trainer VL, Moore SK, Hallegraeff G, et al (2020) Pelagic harmful algal blooms and climate change: Lessons from nature's experiments with extremes. Harmful algae 91:101591

Warlick AJ, Liu OR, Layton J, Harvey CJ, Samhouri JF, Hazen EL, Andrews KS (in revision) A framework to evaluate dynamic social and ecological interactions between offshore wind energy development and commercial fisheries: a US West Coast perspective. PLOS Climate.

Welch H, Hazen EL, Briscoe DK, Bograd SJ, Jacox MG, et al. (2019) Environmental indicators to reduce loggerhead turtle bycatch offshore of Southern California. Ecological Indicators, 98:657-64.

Wildermuth RP, Tommasi D, Kuriyama P, Smith J, Kaplan I (2023) Evaluating robustness of harvest control rules to climate-driven variability in Pacific sardine recruitment. Canadian Journal of Fisheries and Aquatic Sciences, 81(8):1029-1051.

Xu H, Maunder MM, Xu H, et al Stock assessment of bigeye tuna in the eastern Pacific Ocean: 2024 benchmark assessment. https://www.iattc.org/GetAttachment/23cfd40e-2865-451a-b63a-b22132a760ab/SAC-15-02_Bigeye-tuna-benchmark-assessment-2024.pdf

Zwolinski JP, Demer DA (2024) An updated model of potential habitat for northern stock Pacific Sardine (*Sardinops sagax*) and its use for attributing survey observations and fishery landings. Fisheries Oceanography 33:e12664

Zwolinski JP, Demer DA, Cutter Jr GR, et al (2014) Building on fisheries acoustics for marine ecosystem surveys. Oceanography 27:68–79

Appendix A — CONTRIBUTORS TO THIS REPORT

NWFSC, NOAA Fisheries Mr. Kelly Andrews, Dr. Brian Burke, Mr. Jeff Cowen, Mr. Christopher Dailey (co-editor), Dr. Blake Feist, Ms. Jennifer Fisher, Dr. Correigh Greene, Dr. Thomas Good, Dr. Daniel Holland, Dr. Mary Hunsicker (co-editor), Dr. Kym Jacobson, Dr. Isaac Kaplan, Ms. Su Kim, Mr. Connor Lewis-Smith, Dr. Owen Liu, Dr. Stephanie Moore, Dr. Stuart Munsch, Dr. Karma Norman, Ms. Amanda Phillips (co-editor), Dr. Jameal Samhouri, Dr. Kayleigh Somers, Dr. Nick Tolimieri (co-editor), Dr. John Wallace, Dr. Amanda Warlick, Mr. Curt Whitmire, Dr. Jen Zamon

AFSC, NOAA Fisheries Dr. Stephen Kasperski, Dr. Sharon Melin

SWFSC, NOAA Fisheries Dr. Eric Bjorkstedt, Dr. Steven Bograd, Ms. Lynn deWitt (co-editor), Dr. John Field, Dr. Elliott Hazen, Dr. Michael Jacox, Dr. Andrew Leising (co-editor), Dr. Nate Mantua, Dr. Barbara Muhling, Mr. Josiah Renfree, Dr. Tanya Rogers, Mr. Keith Sakuma, Dr. Jarrod Santora, Dr. Kevin Stierhoff, Dr. Andrew Thompson, Dr. Brian Wells,

California State Polytechnic University, Humboldt Ms. Roxanne Robertson

Oregon State University Dr. Jack Barth, Ms. Anna Bolm, Ms. Elizabeth Daly, Mr. William Kennerley, Ms. Cheryl Morgan, Dr. Rachael Orben, Dr. Stephen Pierce, Ms. Samantha Zeman

NOAA Fisheries West Coast Region Ms. Jennifer (Lilah) Ise, Mr. Dan Lawson, Ms. Lauren Saez

Pacific States Marine Fishery Commission Mr. Toby Auth, Mr. Gregory Williams (co-editor)

University of California-San Diego Dr. Dan Rudnick

University of California-Santa Barbara Dr. Chris Free

University of California-Santa Cruz Dr. Megan Cimino, Dr. Jerome Fiechter, Ms. Rebecca Miller, Dr. Antonella Preti, Dr. Travis Richards, Dr. Isaac Schroeder, Dr. Juan Zwolinski

California Department of Public Health Ms. Christina Grant, Ms. Ali Hossain, Mr. Duy Truong, Ms. Vanessa Zubkousky-White

California Department of Fish and Wildlife Ms. Christy Juhasz

CA Office of Environmental Health Hazard Assessment Dr. Shannon Murphy, Dr. Beckye Stanton

Oregon Department of Fish and Wildlife Ms. Kelly Corbett, Mr. Matthew Hunter

Washington Department of Fish and Wildlife Mr. Zachary Forster, Dr. Matt George, Dr. Scott Pearson

Washington Department of Health Ms. Tracie Barry, Mr. Jerry Borchert

Beach Watch (Greater Farallones Association and Greater Farallones & Cordell Bank National Marine Sanctuaries) Ms. Kirsten Lindquist, Ms. Jan Roletto

BeachCOMBERS Ms. Kirby Bartlett

Coastal Observation and Seabird Survey Team Ms. Jackie Lyndsay, Dr. Julia Parrish

Monterey Bay Aquarium Research Institute Dr. Monique Messie

Farallon Institute Dr. William Sydeman, Ms. Sarah Ann Thompson

Point Blue Conservation Science Ms. Meredith Elliott, Dr. Jaime Jahncke, Dr. Mike Johns, Mr. Peter Warzybok

Appendix B — SUMMARY INFOGRAPHICS for 2024-25

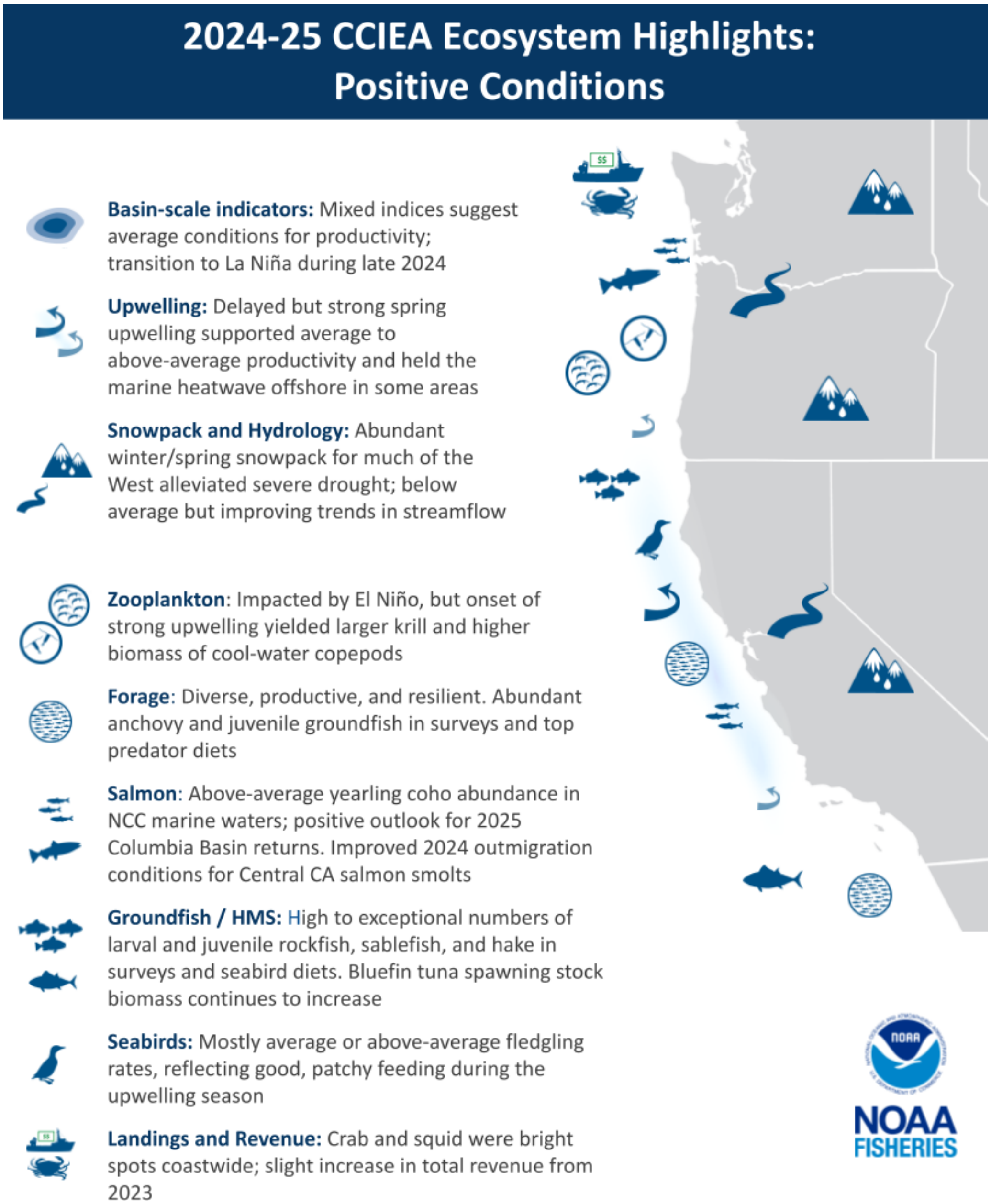

2024-25 CCIEA Ecosystem Highlights: Unfavorable / Risk Factors

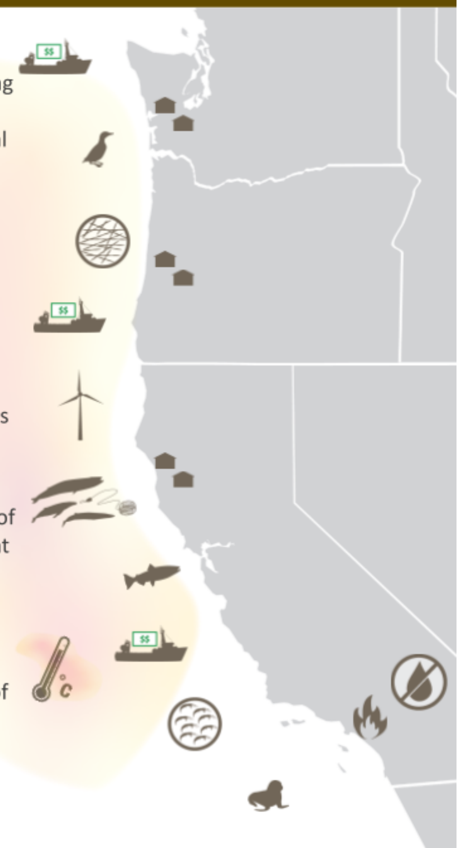

Ocean Temperatures & Marine Heatwave: Strong El Niño conditions in winter/spring 2024 and overall ocean warming in the NE Pacific. Seasonal repeat of MHW conditions post-Blob

Terrestrial Disturbances: Emerging drought conditions in southwest during late 2024; Santa Ana winds fan devastating coastal fires

Zooplankton: Below average northern copepod biomass during El Niño; winter ichthyoplankton index lowest of 27-y time series

Chinook Salmon: Less favorable ocean conditions for NCC juvenile salmon. Thiamine deficiency impacts in CA natural-area fish

Seabirds & Sea lions: : Unusually high mortality of Cassin's auklets and brown pelicans; lowest count of sea lion pup births since Blob

Whale Entanglement: Increasing trend for humpbacks

HABs: HAB activity continued through summer of 2024, leading to fisheries closures & impacts to marine life and human health

Mixed Ocean Uses: Impacts of wind lease area locations continue to come into focus with new ecosystem indicator portfolios

Fishery Landings & Revenue: Closure of CA ocean salmon fishery; Declining catches for most sectors, most notably Pacific whiting

Coastal Communities: Shifting human wellbeing metrics for fishing-reliant communities of OR & WA; Revenue diversification fell to lowest level since 1981

NOAA FISHERIES

Appendix C — LIST OF FIGURES AND DATA SOURCES

Figure 1.1: Map of the California Current Ecosystem (CCE) and U.S. West Coast Exclusive Economic Zone (EEZ) created by B. Feist, NMFS/NWFSC. GIS layers of freshwater ecoregions derived from TNC & WWF (2008), based on Abell et al. (2008).

Figure 2.1: Oceanic Niño Index data are from the NOAA Climate Prediction Center (https://origin.cpc.ncep.noaa.gov/products/analysis_monitoring/ensostuff/ONI_v5.php). PDO data are from N. Mantua, NMFS/SWFSC, and are served on the CCIEA ERDDAP server (https://oceanview.pfeg.noaa.gov/erddap/tabledap/cciea_OC_PDO.html). North Pacific Gyre Oscillation data are from E. Di Lorenzo, Georgia Institute of Technology (http://www.o3d.org/npgo/).

Figure 2.2: Standardized sea surface temperature anomaly plots were created by A. Leising, NMFS/SWFSC, using SST data from NOAA's optimum interpolation sea surface temperature analysis (OISST; https://www.ncei.noaa.gov/products/optimum-interpolation-sst); SST anomaly calculated using climatology from NOAA's AVHRR-only OISST dataset. MHW conditions are delineated by values of the normalized SST + 1.29 SD from normal. Methods for tracking and classifying heatwaves are described in Thompson et al. 2019b and at the CCIEA blocktracker website project page.

Figure 2.3: Newport Hydrographic (NH) line temperature data from J. Fisher, NMFS/NWFSC. Glider data along CalCOFI lines are from D. Rudnick and obtained from https://spraydata.ucsd.edu/projects/CUGN/.

Figure 2.4: Daily 2024 values of BEUTI and CUTI are provided by M. Jacox, NMFS/SWFSC; detailed information about these indices can be found at https://go.usa.gov/xG6Jp.

Figure 2.5: Habitat compression index estimates developed and provided by J. Santora, NMFS/SWFSC, and I. Schroeder, NMFS/SWFSC, UCSC.

Figure 2.6: Dissolved oxygen data from bottom mooring CE07 (https://oceanobservatories.org/site/ce07shsm/) obtained from NSF Ocean Observatories Initiative (2024). Newport Hydrographic (NH) line dissolved oxygen data are from J. Fisher, NMFS/NWFSC.

Figure 2.7: Newport Hydrographic (NH) line aragonite saturation state data provided by J. Fisher, NMFS/NWFSC.

Figure 2.8: Snow-water equivalent data were derived from the California Department of Water Resources snow survey (http://cdec.water.ca.gov/) and the Natural Resources Conservation Service's SNOTEL sites in WA, OR, CA and ID (http://www.wcc.nrcs.usda.gov/snow/). Data compilation and summary calculations by S. Munsch, NMFS/NWFSC, Ocean Associates, Inc.

Figure 2.9: Minimum and maximum streamflow data were provided by the US Geological Survey (http://waterdata.usgs.gov/nwis/sw). Data compilation and summary calculations by S. Munsch, NMFS/NWFSC, Ocean Associates, Inc.

Figure 3.1: Copepod biomass anomaly data were provided by J. Fisher, NMFS/NWFSC.

Figure 3.2. Krill data were provided by E. Bjorkstedt, NMFS/SWFSC SWFSC, Cal Poly, Humboldt and R. Robertson, Cooperative Institute for Marine Ecosystems and Climate (CIMEC) at Cal Poly, Humboldt.

Figure 3.3: Cumulative estimated CPS biomass data from the 2024 summer CPS survey. Surveys typically span the area between Cape Flattery and San Diego, but in some years also include Vancouver Island, Canada (2015-2019) and portions of Baja CA (2021-2022). Data and figure provided by K. Stierhoff, NMFS/SWFSC and J. Zwolinski, UCSC and NMFS/SWFSC.

Figure 3.4: Pelagic forage data from the Northern CCE from B. Burke, NMFS/NWFSC and C. Morgan, OSU/CIMRS. Data are derived from surface trawls taken during the NWFSC Juvenile Salmon & Ocean Ecosystem Survey (JSOES; https://www.fisheries.noaa.gov/west-coast/science-data/ocean-ecosystem-indicators-pacific-salmon-marine-survival-northern). Similarity analysis and cluster plot by A. Thompson, NMFS/SWFSC.

Figure 3.5: Pelagic forage data from the Central CCE were provided by J. Field, T. Rogers, K. Sakuma, and J. Santora, NMFS/SWFSC, from the SWFSC Rockfish Recruitment and Ecosystem Assessment Survey (https://go.usa.gov/xGMfR). Similarity analysis and cluster plot by A. Thompson, NMFS/SWFSC.

Figure 3.6: Pelagic forage larvae data from the Southern CCE were provided by A. Thompson, NMFS/SWFSC, from spring CalCOFI surveys (https://calcofi.org/); data were not collected in 2020 due to survey cancellations associated with the COVID pandemic. Similarity analysis and cluster plot by A. Thompson, NMFS/SWFSC.

Figure 3.7: Data for at sea juvenile salmon provided by B. Burke, NMFS/NWFSC and C. Morgan, OSU/CIMRS, from surface trawls taken during the NWFSC Juvenile Salmon and Ocean Ecosystem Survey (JSOES).

Figure 3.8: Stoplight table of indicators related to salmon in the northern CCE courtesy of B. Burke, J. Fisher, and K. Jacobson, NMFS/NWFSC, and C. Morgan, and S. Zeman, OSU/CIMRS (https://www.fisheries.noaa.gov/west-coast/science-data/ocean-ecosystem-indicators-pacific-salmon-marine-survival-northern#stoplight-table).

Figure 3.9: Stoplight table of indicators and qualitative outlook for 2025/2026 Sacramento River Fall, Central Valley Spring, and Klamath River Fall Chinook salmon returns courtesy of C. Greene and S. Munsch, NMFS/NWFSC.

Figure 3.10: Estimates of juvenile abundance for West Coast groundfish were provided by N. Tolimieri, NMFS/NWFSC, based on data from the NOAA West Coast bottom trawl survey (https://www.fisheries.noaa.gov/west-coast/science-data/us-west-coast-groundfishbottom-trawl-survey).

Figure 3.11: Annual distribution maps of West Coast juvenile sablefish were provided by N. Tolimieri, NMFS/NWFSC, based on data from the NOAA West Coast bottom trawl survey. Data available via API download from: https://www.webapps.nwfsc.noaa.gov/data/map

Figure 3.12: Albacore, swordfish, and bluefish tuna diet data provided by A. Preti and T. Richards, UCSC.

Figure 3.13: Seabird fledgling production data at nesting colonies at Yaquina Head, OR provided by R. Orben and W. Kennerley, OSU.

Figure 3.14: California sea lion data provided by S. Melin, NMFS/AFSC.

Figure 3.15: Whale entanglement data provided by D. Lawson and L. Saez, NMFS/WCR.

Figure 3.16: Figure adapted from Free et al. (2022) using news releases from the California, Oregon, and Washington Departments of Fish and Wildlife.

Figure 4.1: Community social vulnerability index (CSVI), commercial fishery reliance, and recreational fishing reliance data provided by C. Weng (NEFSC), L. Colburn (NMFS/OST), K. Norman, NMFS/NWFSC, and C. Lewis-Smith, NMFS/NWFSC, PSMFC, based on data derived from the US Census Bureau's American Community Survey (ACS; https://www.census.gov/programs-surveys/acs/), PacFIN (http://pacfin.psmfc.org), ESRI business analyst, and guide and charter license data from Oregon and Washington state.

Figure 4.2: Fishery revenue diversification estimates were provided by D. Holland, NMFS/NWFSC, and S. Kasperski, NMFS/AFSC, utilizing data provided by PacFIN (http://pacfin.psmfc.org) and AKFIN (https://akfin.psmfc.org).

Figure 4.3: Fishery Participation Network data and analyses provided by J. Samhouri, NMFS/NWFSC, with data derived from PacFIN (http://pacfin.psmfc.org).

Figure 5.1: Data for commercial landings are from PacFIN (http://pacfin.psmfc.org) and NORPAC (North Pacific Groundfish Observer Program). Data acquired and plotted by K. Andrews, NMFS/NWFSC.

Figure 5.2: Data for recreational landings are from RecFIN (http://www.recfin.org/) and the CDFW Pelagic Fisheries and Ecosystem Data Sharing index). Data acquired and plotted by K. Andrews, NMFS/NWFSC.

Appendix D — CLIMATE AND ECOSYSTEM FORECASTS

Based on feedback from the PFMC and its associated subcommittees (Agenda Item H.1.b Supplemental EAS Report, March 2023; Agenda Item H.1.b Supplemental EWG Report 1 , March 2024), we now present short-term ecosystem predictions in this standalone appendix. Expanded ocean forecasting capabilities in active development under NOAA's Climate, Ecosystems, and Fisheries Initiative (CEFI) will enable additional and improved ecosystem forecasts in coming years, building from regional modeling efforts such as JISAO Seasonal Coastal Ocean Prediction of the Ecosystem (J-SCOPE).

A separate appendix is provided for long-term climate and ecosystem projections (Appendix E). Outlooks for adult Chinook salmon returns to the Columbia basin and California river basins are presented in the salmon appendix (Appendix J).

Forecasts for 2025

ENSO

The El Niño - Southern Oscillation (ENSO) is the best source of predictability for marine ecosystem conditions in the CCE. El Niño events tend to produce warm ocean conditions and lower productivity, while La Niña tends to produce the opposite. Thus, in considering how conditions are likely to evolve in 2025, we start with forecasts of ENSO.

There are currently weak La Niña conditions in the equatorial Pacific, which are expected to persist through early spring. Around April, ENSO is expected to shift to a neutral state, which is favored to persist through fall 2025 (Fig. D.1). Given the current and predicted ENSO conditions, we do not expect strong ENSO impacts on the CCE through fall 2025.

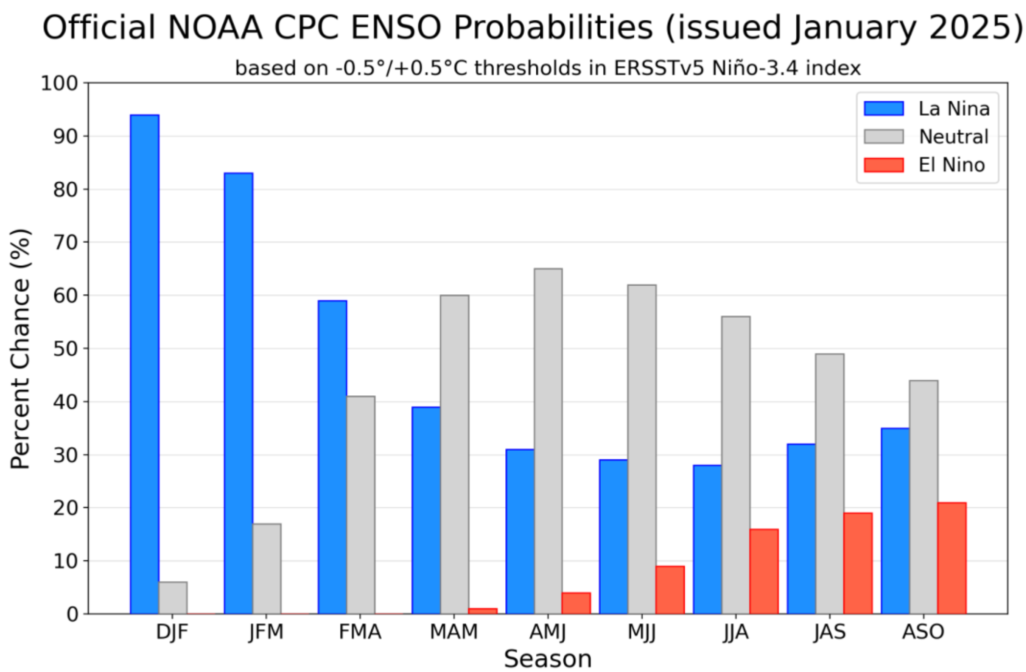

Figure D.1: CPC ENSO forecast, indicating the chances of El Niño, La Niña, or ENSO-neutral conditions for 3-month periods based on an ensemble of climate model forecasts. Accessed Jan. 21, 2025 at https://iri.columbia.edu/our-expertise/climate/forecasts/enso/current/.

Marine Heatwaves

Since 2022, NOAA has provided marine heatwave (MHW) forecasts, updated monthly. The latest forecasts for the Northeast Pacific indicate low probabilities of MHWs in the US EEZ through spring of 2025, associated with SST anomalies near zero (Fig. D.2). From summer into fall, MHW likelihoods increase considerably, particularly north of Cape Mendocino, with forecast probabilities exceeding 50%. This increase in MHW probabilities nearshore is in contrast to the 2024 pattern of decreasing MHW likelihoods during the year. Farther offshore, elevated chances of MHWs are present and increasing throughout 2025, continuing a pattern in recent years of persistent warm waters and MHWs offshore.

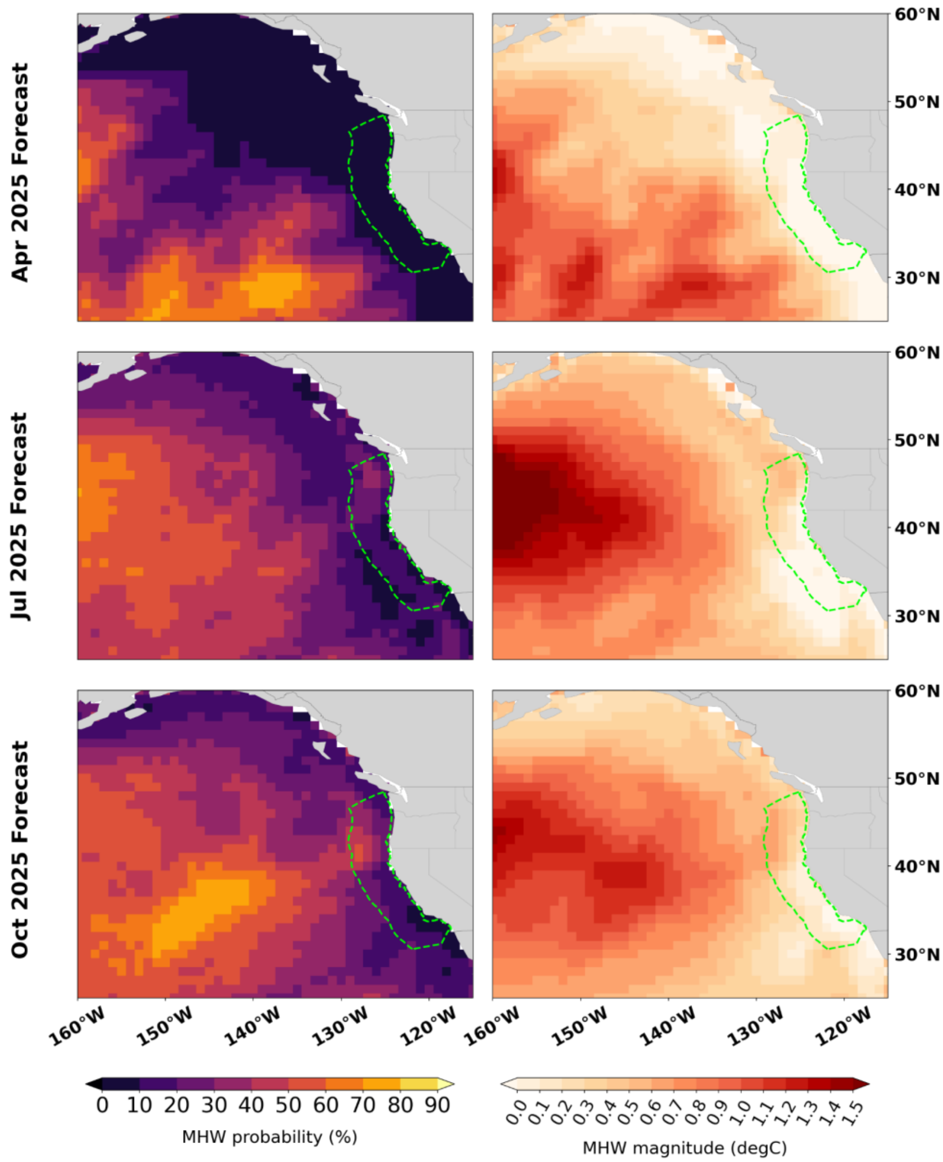

Figure D.2: Forecast likelihood of marine heatwaves in the Northeast Pacific Ocean through summer/fall 2025. (Left) Forecast MHW probability and (right) forecast SST anomaly for three months (top-bottom; April, July, October). The U.S. EEZ is outlined in green. Forecasts are updated each month and are available from psl.noaa.gov/marine-heatwaves.

Temperature Observations To Avoid Loggerheads (TOTAL)

As an example of how we could expand model-based forecasts in years to come, we present an experimental forecast of the Temperature Observations To Avoid Loggerheads (TOTAL) tool. The TOTAL tool tracks anomalies of SST in the Southern California Bight with an alert indicating that 6-month average SST anomalies have exceeded a threshold of ~0.8°C and there is an increased likelihood of Loggerhead turtle presence (and potential interaction risk) in the area based on historical data (Welch et al. 2019). A retrospective analysis found that using climate model forecasts, TOTAL could be predicted months in advance, potentially providing advance warning of risks (Brodie et al. 2023).

The latest experimental TOTAL forecast (as of writing in January 2025) shows low risk of a TOTAL alert throughout 2025 (Fig. D.3). Since spring of 2024, the TOTAL index has steadily declined to its current state, near zero. Neutral to slightly cool values in the SCB are expected to continue through spring, with TOTAL alert likelihoods under 5%. Thereafter, warming is predicted, though the forecast chance of an alert remains under 10% through August.

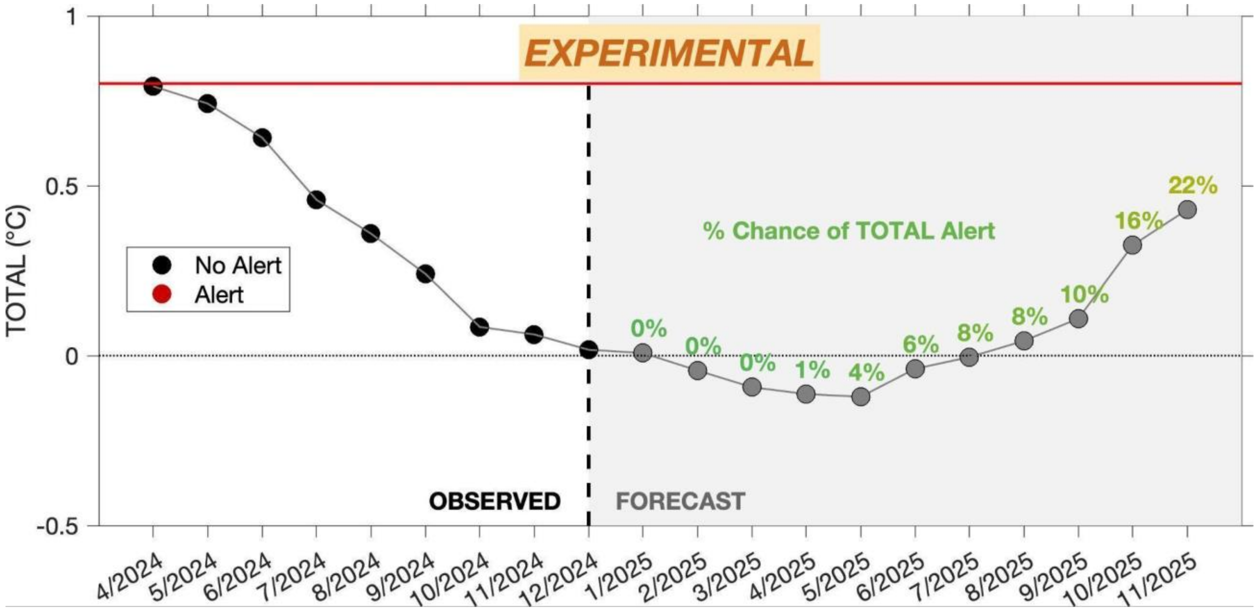

Figure D.3: Forecast likelihood of a Temperature Observations To Avoid Loggerheads (TOTAL) alert in 2025. TOTAL was designed to indicate increased risk of Loggerhead turtle interactions; an alert occurs when the 6-month average sea surface temperature anomaly in the Southern California Bight exceeds ~0.8°C. Predicted TOTAL values are indicated on the y-axis for recent observations (black dots) and forecasts (gray dots). Numbers above forecast dots indicate the predicted chance of a TOTAL alert occurring each month.

Broader Ecosystem Impacts

The strong El Niño event of winter 2023-2024 provided the basis for a range of ecosystem predictions related to expected environmental conditions (see Table D.1 and related discussion below). This year as of January 2025, ENSO conditions are weakly La Niña, heading quickly toward neutral. In the absence of a moderate-to-strong ENSO event, predictive skill for the CCE is reduced, and a good null hypothesis is "damped persistence". Damped persistence means that existing anomalies will persist, but will trend toward a normal state. The rate at which existing anomalies decay depends on the variable in question – anomalies in physical conditions (e.g., SST) or primary productivity can fade quite quickly, while other anomalous states (e.g., in species responses) may persist much longer.

Uncertainty in climate and ecosystem predictions

To contextualize the use of forecast information in decision making, we offer a brief discussion of forecast uncertainty. In this context, one must recognize that decisions made based on forecasts will not be perfect, but should be better than what is possible with no forecasts. As an analogy, if someone could win 60% of blackjack hands, they would become rich over time, despite losses along the way.

For ecosystem forecasts, there are three key sources of uncertainty: (1) uncertainty in how the climate itself will evolve, (2) noise in environmental and ecological relationships, and (3) changes over time in environmental and ecological relationships (also known as "nonstationarity"). We briefly describe each source of uncertainty and how it can be accounted for in physical and biological models. For more detailed discussion, please see the 2023-2024 Climate Change Appendix.

1. When predicting what will happen in coming weeks and months, the greatest source of uncertainty is internal variability – unpredictable change that occurs due to the naturally chaotic nature of the climate (the "butterfly effect"). In order to account for this uncertainty, climate forecasts (like weather forecasts) are actually made up of many forecasts from which one can obtain the likelihood of an outcome given uncertainty.
2. Often, our understanding of responses between environmental variables, or between species and their environments, are based on empirical correlations. These relationships are imperfect. For example, El Niño increases the likelihood of a warm CCE, but cold CCE conditions are still possible during El Niño. Thus, individual years may deviate from the "expected" outcome, but the relationship still provides useful information, enabling predictions that are better than if climate were ignored altogether.
3. Non-stationarity refers to when a relationship between variables has changed such that past correlations no longer apply. Concerns of nonstationarity can be mitigated by (1) relying on environmental-biological relationships that are more mechanistic (e.g., modeling species responses to spatially proximate ocean conditions rather than large-scale climate indices), and (2) using ensembles of ecological models with different formulations to capture uncertainty and identify robust responses.

Revisiting forecasts from 2024

In last year's ESR (Table E1 in Appendix E: Developing indicators of climate variability and change) we presented a list of predictions for 2024. Here, we briefly evaluate those predictions, and their influence on our assessment of the ecosystem, as a means to weigh the merits of similar predictions in the future.

The major prediction from last year, issued by NOAA's Climate Prediction Center, was for a moderate-to-strong El Niño during the winter of 2023-24. That forecast was correct and by the time of last year's ESR, observations were already confirming the onset of the event.

Given the developing El Niño, the CCIEA team compiled a suite of likely impacts in 2024, which are presented here along with what ultimately was observed (Table D.1).

Table D.1. Predicted and observed environmental and biological conditions in the CCE impacts during 2024. Potential impacts (predictions) were assembled by the CCIEA team for last year's report. Observed impacts were compiled for this year's report based on available data. Color indicates match of potential to observed impact, green = good match, yellow = partial or unclear, red = did not match.

Species/ index	Potential Impact	Observed Impacts
Snow water equivalent	More initial snowpack, then warmer weather transitions to rain instead of snow	As predicted
Habitat compression	Habitat compression through spring	As predicted
Marine heatwaves	Decreasing likelihood nearshore, increasing likelihood offshore	As predicted
Copepods	Increase in southern (lipid poor) species and increase in species richness	As predicted, then quick rebound after El Niño
Krill	Lowered abundance, lower adult sizes	As predicted, then quick rebound after El Niño
Anchovy	Continued relatively high numbers but likely lower than past few years	As predicted
Market squid	Lower abundance and northward shift	Lower abundance in all surveys, northward shift not clear. Fisheries catch increased from previous year
Rockfish	Dominated by larvae due to poor survival of later (pelagic juvenile) stages	High larval and YOY abundances
Sablefish	Larger and closer to shore	Unclear from assessment
Salmon	Poorer conditions for all stages	Some conditions were poorer, but not all. Effects were spatially, temporally, and species dependent
Sea lions	Reduced pup weights/productivity	Pup counts lower, weights not yet measured for 2024 cohort
Harmful algal blooms	Increased HAB activity and subsequent closures	As predicted, though less HAB activity in north

We included two types of predictions last year: (1) physical forecasts that rely on climate models (El Niño, snow water equivalent, marine heatwaves) and (2) qualitative predictions of species responses, based on expert opinion drawn from past observations and scientific studies. In both cases, our outlooks were generally correct, in large part because outcomes aligned with our expectations for the impacts of El Niño based on past events. However, there were some details which our forecasts were unable to represent. First, despite the confident forecasts of an El Niño event, predictions of its strength and duration were less certain. The 2023-24 El Niño transitioned quite abruptly in late April to favorable strong upwelling conditions. In turn, some parts of the system recovered quickly, as evidenced by a rapid change in the plankton community to a more favorable state (i.e. a return to more lipid rich copepod species in the north, and larger krill sizes in the south). Second, we did not make detailed predictions for different salmon species, times, and locations, rather providing a more generalized forecast. While our forecast for salmon was therefore correct for some locations/times/species, it did not generalize well to the entire range of conditions salmon experienced; future forecasts of this nature may be more useful if made more specific to better address the complexity and diversity of different salmon stocks. Last, for market squid, we were unable to clearly identify if there was a true range shift or just a change in abundance overall; additional further analysis in this case might be able to make this determination.

In 2024, we were relatively confident in our forecasts, owing to the strong El Niño event. These predictions were largely accurate, though unsurprisingly some details were missed. In future years, our confidence in predictions will vary. Reduced confidence may occur, for example, in years of ENSO neutral conditions or when expected environmental-biological relationships are observed to be failing. When uncertainty is very large, due to the climate state or to insufficient observations/knowledge to draw upon, making a forecast may be inappropriate or may be accompanied by significant caveats. Nonetheless, there is clearly a growing foundation from which to make physical and ecosystem forecasts, recognizing the importance of including estimating confidence in those forecasts.

Appendix E — DEVELOPING INDICATORS OF CLIMATE VARIABILITY AND CHANGE

Setting the Context

Climate change is upon us. The North Pacific Ocean has warmed to the point that long-term warming trends are overshadowing natural variability and confounding past relationships between the CCE and basin-scale Pacific variability. For example, while positive phases of the PDO are generally associated with warm conditions in the CCE, and negative PDO with a cold CCE, this paradigm has been upset by long-term warming. In recent years (2021-2024), the CCE has been anomalously warm despite a negative PDO favoring cooler conditions (Cluett et al., in review).

Climate shapes risk to meeting fisheries management objectives by affecting the distribution, seasonal timing, productivity, abundance, and physiology of marine species, as well as influencing fishing practices. For instance, changes in productivity can influence projections of rebuilding timelines and estimated reference points used in harvest setting processes. Shifts in distribution can affect the regional availability of target species or the risk of bycatch of non-target species. These and other connections between climate change, ecology, socioeconomic dynamics, and management procedures provide essential context for navigating ecosystem change.

There is a continually growing body of research on future climate change and its impacts in the California Current. As such, here we summarize past research – including information from recent reports – with a focus on groundfish and CPS. We then highlight several insights that are new for this year.

Current state of knowledge

Ocean and biogeochemical change

Under future climate change scenarios, robust projections in the California Current System include ocean warming (both surface and subsurface), increased stratification, reduced mixed layer depth, deoxygenation, and acidification (Pozo Buil et al. 2021). While the magnitude of these changes varies among models and scenarios, the sign of change is consistent. Under a high-emissions scenario (RCP8.5), climate change trends in many physical and chemical trends emerge (exceed natural variability) by mid-century; mitigation scenarios delay that time of emergence (Henson et al. 2017). Lower emissions scenarios are expected to produce qualitatively similar but less pronounced effects. Changes in primary production are less certain – most but not all models suggest decreased productivity under future climate change (Jacox et al. 2024).

Distribution and abundance of groundfish and CPS

Focusing on the DTS complex of groundfish (dover sole, shortspine thornyhead, longspine thornyhead, and sablefish), Liu et al. (2023) projected that the oceanographic changes summarized above would lead to declining coastwide abundance of sablefish and shortspine thornyhead, which would also shift offshore into deeper waters. Projected changes in the distributions of Dover sole and longspine thornyhead were smaller, with abundance remaining near constant or increasing.

A suite of different ecosystem models all projected a northward shift in the northern subpopulation of Pacific sardine, though there was no consensus on whether coastwide biomass would increase or decrease (Smith et al. 2023). Distribution changes for anchovy are projected to be much smaller, though an increased likelihood of "bust" periods is projected for the coastwide anchovy population (Leising et al. 2024). Wildermuth et al. (2023) found that the current sardine assessment process can effectively track changes in population status under a changing climate, and that effective management will likely depend on frequent/responsive monitoring and assessment, as well as better understanding of climate-driven recruitment changes.

Vulnerability and risk for groundfish and CPS fleets

Climate-driven risks to groundfish fleets are expected to be greater to the north (off Washington/Oregon) than farther south (Samhouri et al. 2023). The increased risk is because (1) current fishing grounds in the northern CCS are projected to experience higher exposure to climate change (more warming, greater shifts required to keep pace with bottom temperatures) and (2) communities in the northern CCS have greater economic dependence on these fisheries. When comparing two approaches for adapting to climate change, Samhouri et al. (2023) found that moving to follow shifting fish stocks is likely to be more effective than diversifying portfolios while remaining in place (Samhouri et al. 2023).

The projected northward distribution shift for the northern subpopulation of Pacific sardine is expected to increase landings in the Pacific Northwest while decreasing landings in California (Smith et al. 2023), though the potential effects of shifts in the southern subpopulation have not yet been modeled. Quezada et al. (2023) identified multiple segments of west coast CPS fisheries (small scale vs industrial, local vs wide-ranging, specialist vs generalist), and identified mobility and the ability to switch between target species as two qualities that will confer future adaptation potential.

New for 2025

Ecosystem perspective on CPS and groundfish change

Above, we summarized previously published findings on projected impacts of climate change on Pacific sardine, northern anchovy, and four species of groundfish (the DTS complex). The underlying analyses considered each species individually, without taking into account the potential for species interactions (predation, competition, etc.) and fishing dynamics to modify climate impacts. They also did not consider the metabolic effects of ocean warming explicitly.

A recently published study using the Atlantis ecosystem model (Liu et al. 2025) addressed these shortcomings and expanded the focus from 6 species to 38 interacting functional groups (including 24 groundfish, 2 HMS, 6 CPS, along with 6 other groups of marine mammals and sharks). The study projected changes in biomass (Fig. E.1), abundance, and weight at age due to the combined effects of warming and species distribution shifts over the 21st century. Overall, effects of spatial shifts had larger impacts on species than did the effects of warming alone (Fig. E.1). At a coastwide scale, projected changes in biomass from 2013 until 2100 are relatively greater for CPS (approximately ± 25%) than for the DTS complex of groundfish or for Pacific hake (± 5%). The direction of change in biomass is species-dependent, and results from changes in spatial distribution (which affects overlap between predators and prey and fisheries harvest) that can be enhanced or counteracted by the effects of ocean warming on growth and fecundity.

Projected species responses are influenced by three-dimensional physical and biogeochemical variability in the California Current ecosystem (Pozo Buil et al. 2021), and assumed constraints on the ability of pelagic versus bottom-dwelling species to obtain climate refugia by moving horizontally (usually northward) or vertically (usually deeper). Projected changes are not expected to be spatially uniform throughout the CCE – for example, the northern subpopulation of Pacific sardine will decline in the southern CCE but increase in the northern CCE, while DTS species are expected to experience more pronounced offshore shifts in the northern CCE than in the southern CCE.

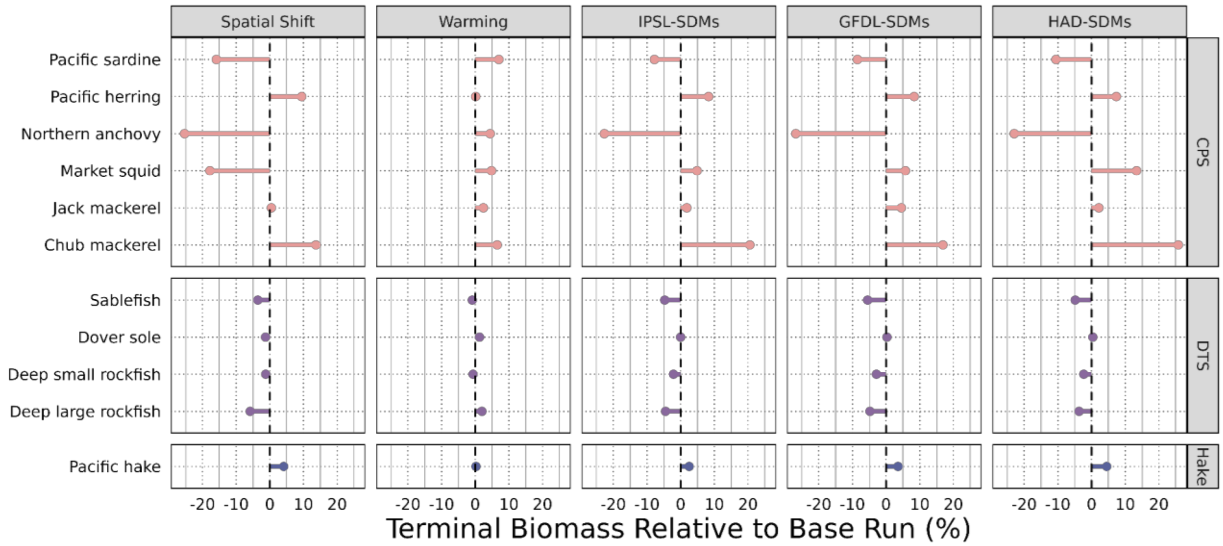

Figure E.1. Projected biomass change from 2013-2100 for each functional group (rows) in each Atlantis scenario (columns) relative to a Base scenario. The dashed line indicates no change between a given scenario and the Base scenario, which has no species distribution shifts or ocean warming. The five scenarios shown here include a Spatial Shift scenario with species distribution models (SDMs) integrated into the Atlantis ecosystem model, a Warming scenario affecting metabolic processes that favor higher growth for consumers, and one scenario for each of three Earth System Models (ESMs) combining the effects of Spatial Shifts and Warming. The three ESMs are from the NOAA Geophysical Fluid Dynamics Laboratory (GFDL-ESM2M), Institut Pierre-Simon Laplace (IPSL-CM5A-MR) and the Met Office Hadley Centre (HadGEM2-ES). Reproduced from Liu et al. (2025).

Climate change alters potential overlap of fisheries and offshore wind

One of the implications of climate change-driven shifts in the distribution of fishery species comes from the potential disparity between overlapping ocean uses today versus in the future. In a forthcoming paper, Warlick et al. (in revision) considered the change in biomass of three groups of groundfish species within historical fishing grounds that intersect with areas designated for the development of offshore wind. The groups included species caught as part of the DTS groundfish bottom trawl, non-DTS groundfish bottom trawl, and midwater rockfish trawl fisheries. The variability in response among the three target species groups includes the offshore shift in DTS species in relation to fishing grounds near Eureka, CA, the shift to the shelf-break of non-DTS species associated with fishing grounds near Coos Bay, OR, and the overall 10-fold projected decline in midwater species biomass adjacent to fishing grounds in Brookings, OR. Furthermore, Warlick et al. (in revision) projected that portions of areas designated for offshore wind development will witness increased biomass of DTS and non-DTS bottom trawl species in the future (Fig. E.2ab, red shading within black polygons). Overall, compared to using only historical information on species distributions, these findings suggest that consideration of climate change fundamentally affects inferences about the potential for interactions between offshore wind energy development and fisheries.

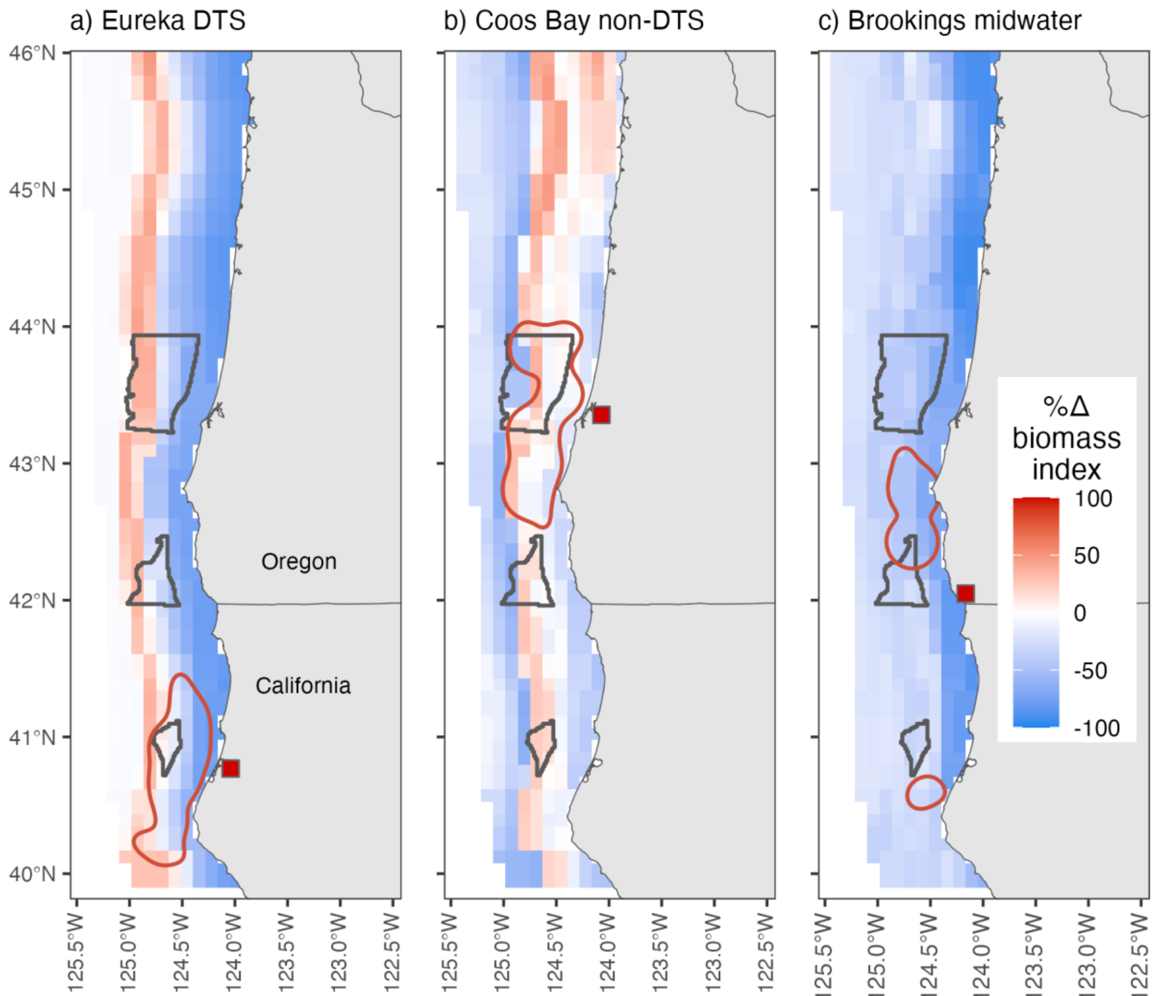

Figure E.2. Proposed offshore wind energy Call Areas in Oregon and Wind Energy Areas in California (black outlines), historical fishing footprints from commercial landings from 1994 to 2020 (red outlines), and the average percent change in projected biomass index of targeted species (gridded heatmap) for three example fishing fleets. The % Delta biomass index shows the change from the present (2020) to the end of the century (2050-2100), based on results from Liu et al. (2023). Reproduced from Warlick et al. in revision.

Appendix F — CLIMATE AND OCEAN INDICATORS

Link to main section: Climate and Ocean Drivers

F.1 Basin-scale Climate/Ocean Indicators at Seasonal Time Scales

These plots show seasonal averages and trends of the three basin-scale climate forcing indicators shown in the main report in Figure F.1.

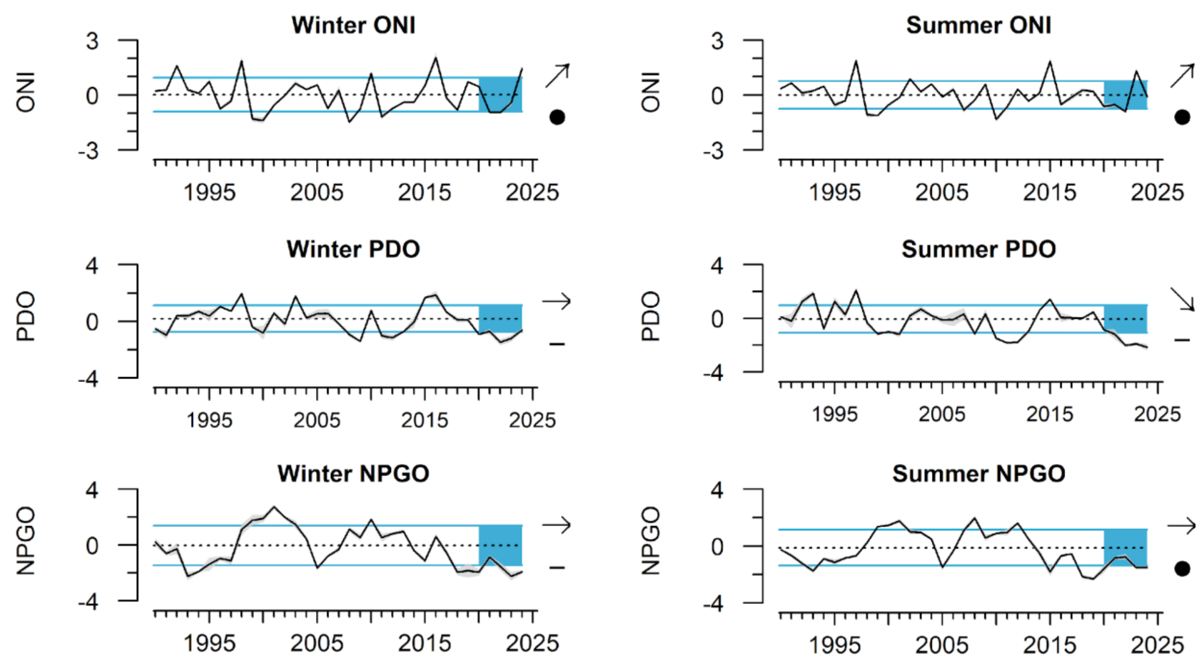

Figure F.1: Winter (Jan-Mar) and Summer (July-Sep) values for the basin-scale climate indicators: Ocean Niño Index (ONI), Pacific Decadal Oscillation (PDO), and North Pacific Gyre Oscillation (NPGO) through 2024. Mean and s.d. for 1991-2020. Lines, colors, and symbols are as in Fig. 2.1.

Satellite data, which has been collected in a similar fashion since 1982, allows for a basin-scale view of sea surface temperature (SST) at up to daily and sub-degree (spatial) resolution. Here we show seasonal averages of SST anomalies (the difference from climatology) across the NE Pacific (Fig. F.2). Winter saw anomalously high SST along the west coast, which was an expression of the El Niño (Fig. F.2. Left). Spring and summer 2024 saw a return to anomalously warm waters offshore, which continues the trend during the past several years, and is primarily the result of continued offshore marine heatwaves. Nearshore waters, however, showed cooler than average conditions during the summer and fall, due to average to strong upwelling in these regions during those seasons. Fall 2024 saw a shift in anomalously warm temperatures to offshore and to the south of the region.

Over the past five years, NE Pacific SSTs generally have been warmer than average (Fig. F.2, middle). Recent trends are diverging, with some areas experiencing cooling (Fig. F.2 right, blue regions) and others experiencing warming (e.g., coastal waters during winters; Fig. F.2 right).

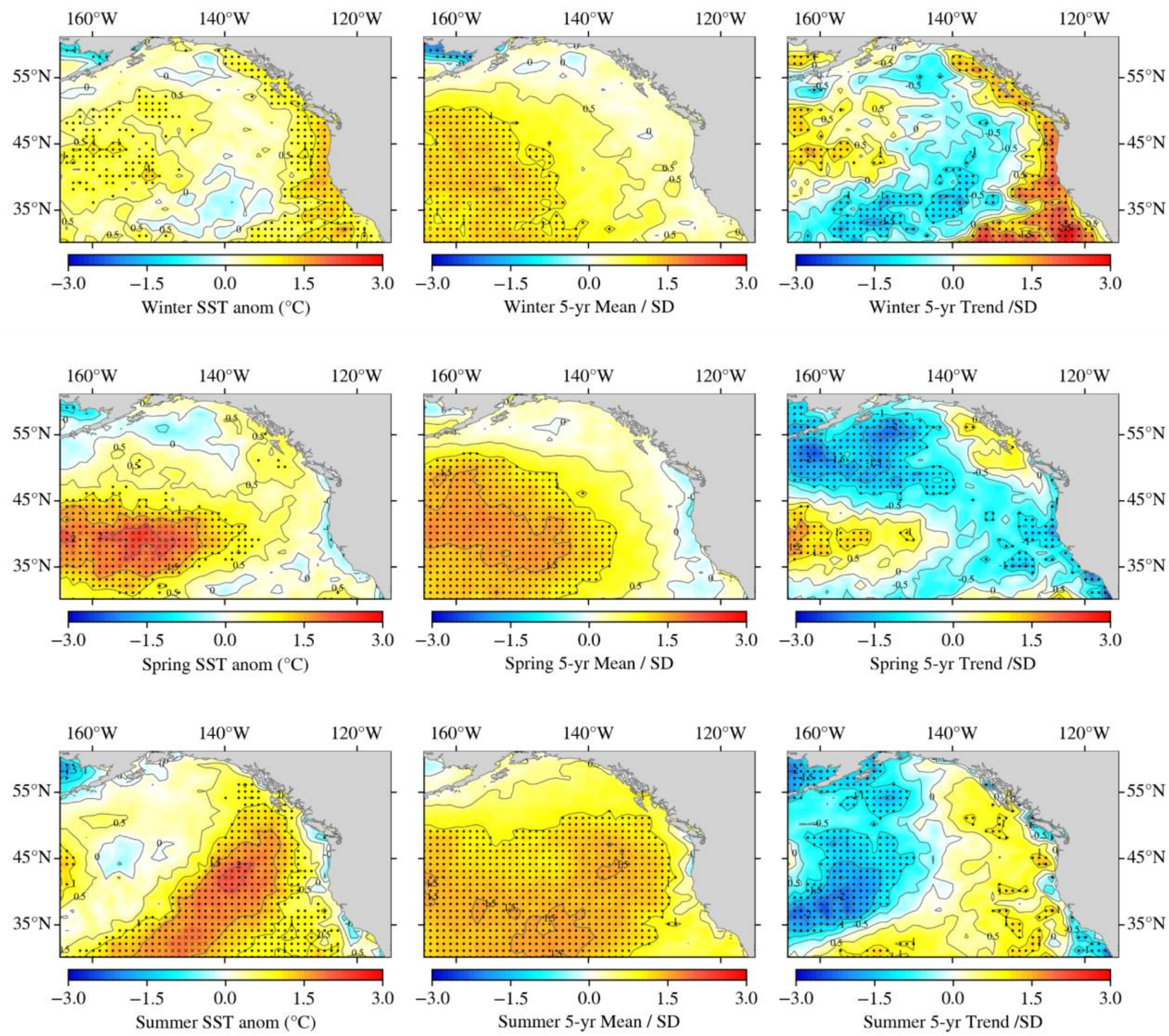

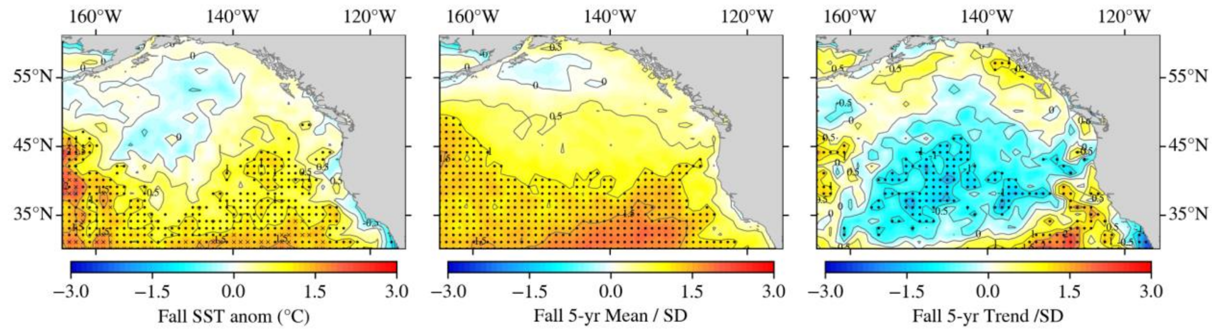

Figure F.2: Left: Sea surface temperature (SST) anomalies in 2024, based on 1982-present satellite time series in winter (Jan-Mar) spring (Apr-Jun) summer (July-Sept), and fall (Oct-Dec). Center: Mean SST anomalies for 2020-2024. Right: trends in SST anomalies from 2020-2024. Black dots mark cells where the anomaly was >1 s.d. above the long-term mean (left, middle) or where the trend was significant (right). Black x's mark cells where the anomaly was the highest in the time series.

Glider data has become an increasingly useful tool for analyzing trends in subsurface water temperatures over time. The following series of plots represents data from subsurface gliders, which generally sample in onshore-offshore transects on a weekly to monthly basis, and have been in service long enough for the development of climatologies, which are then used to compute temperature anomalies. Examination of these subsurface anomalies over time suggests that during 2024 subsurface temperatures off OR were generally cooler than previous years, except for the beginning of the year during the El Niño period (Fig. F.3). Off Northern CA, subsurface temperatures were also generally cool, although during the summer, the intrusion of the marine heatwave can be seen in the upper 50m for several periods Fig. F.4. Off Monterey Bay, 2024 saw warmer than normal surface and subsurface temperatures Fig. F.5. From Pt. Conception south (Fig. F.5), there has been an increase in stratification, due to a return of deeper waters (>50m) to a more "normal" temperature (e.g. anomalies close to zero), while surface waters remained anomalously warm, as in previous years.

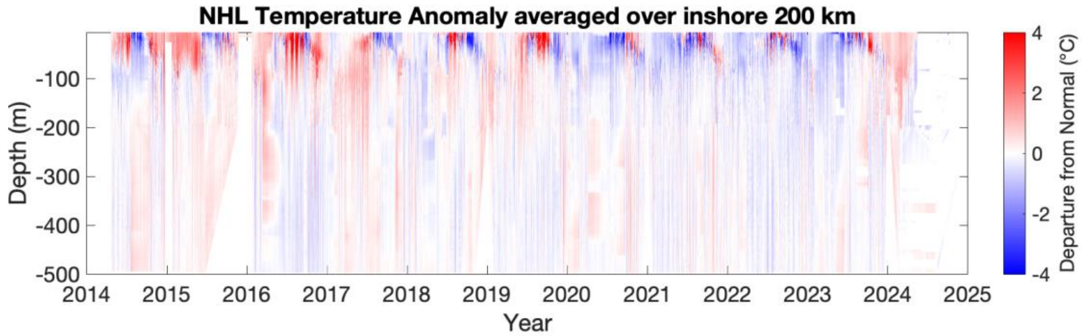

Figure F.3: Time-depth plot of average subsurface temperature anomalies from the shore to 200 km offshore along the Newport Hydrographic Line, based on OSU-OOI coastal endurance array gliders (https://ceoas.oregonstate.edu/ocean-observatories-initiative-ooi). Climatology based on monthly averages created over 2014-2022

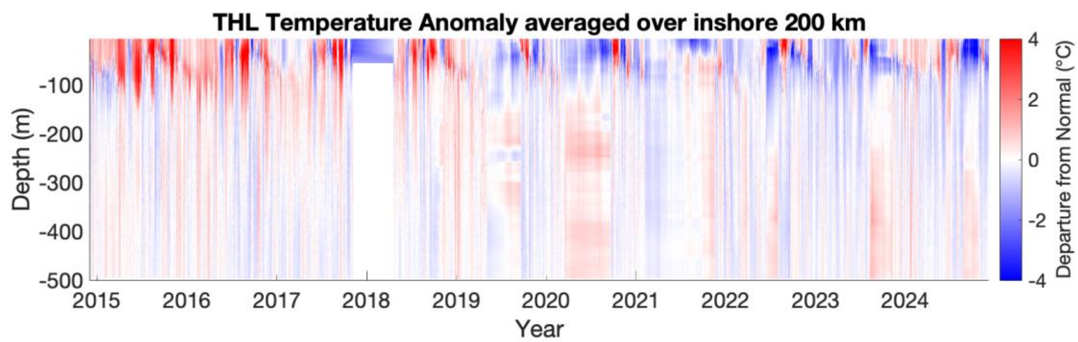

Figure F.4: Time-depth plot of average subsurface temperature anomalies from the shore to 200 km offshore along the Trinidad Head Line. Data courtesy of CeNCOOS and NANOOS.

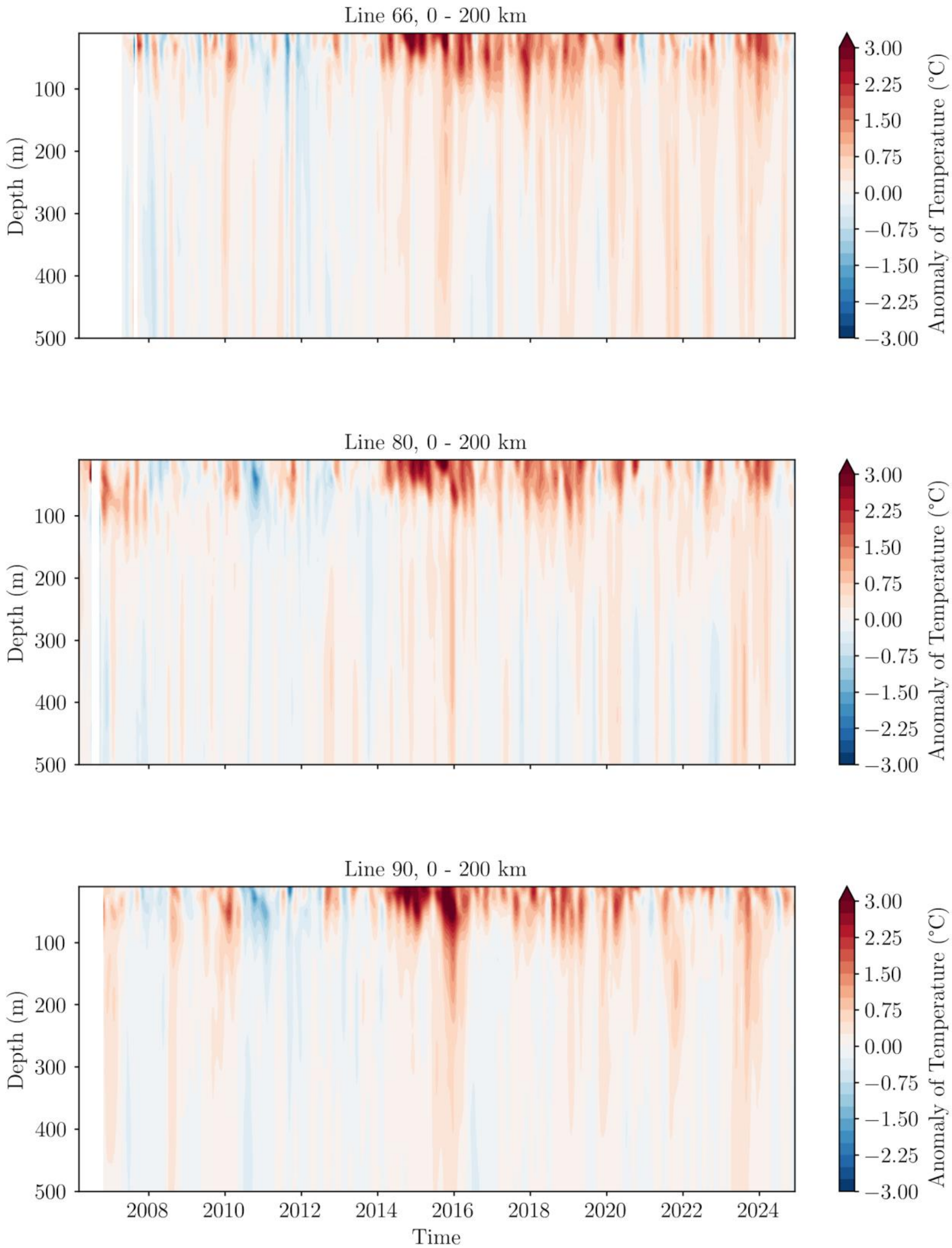
Line 66, 0 - 200 km
Line 80, 0 - 200 km
Line 90, 0 - 200 km
Depth (m)
100
200
300
400
500
2008
2010
2012
2014
2016
2018
2020
2022
2024
Time
3.00
2.25
1.50
0.75
0.00
−0.75
−1.50
−2.25
−3.00
Anomaly of Temperature (°C)

Figure F.5: Time-depth plot of average subsurface temperature anomalies from the shore to 200 km offshore along CalCOFI lines 66, 80, and 90 based on Spray gilder data and climatology. Data from the California Underwater Glider Network are provided by Dr. Dan Rudnick, Scripps Institution of Oceanography Instrument Development Group (doi: 10.21238/S8SPRAY1618).

The CCE is an upwelling dominated system, with the interaction between upwelling, stratification, and source water properties controlling much of coastal temperatures, nutrient input, and overall productivity. Time series of upwelling indices (CUTI and BUTI, Fig. 2.4) provide information on upwelling strength and nutrient content at sub-seasonal frequency and upwelling phenology, and allow interannual comparisons of seasonal upwelling timing and frequency. Additionally, the calculation of cumulative upwelling allows for a comparison of the total amount of upwelling a region receives during the entire course of the year (Fig. F.6). Cumulative upwelling is calculated as the daily summation of upwelling values (additive for positive upwelling, and subtractive for negative upwelling - aka downwelling) starting on January 1 and ending on December 31. These plots demonstrate that cumulative upwelling in 2024 (black lines) was below the climatological average (dashed lines) for most of the year for the northern latitudes, and for the winter and spring, followed by an increase to above average levels for mid latitudes, and the most southern location, reflecting the depression and delay of upwelling due to El Niño, followed by the rapid spring transition to strong upwelling, particularly in the mid latitudes.

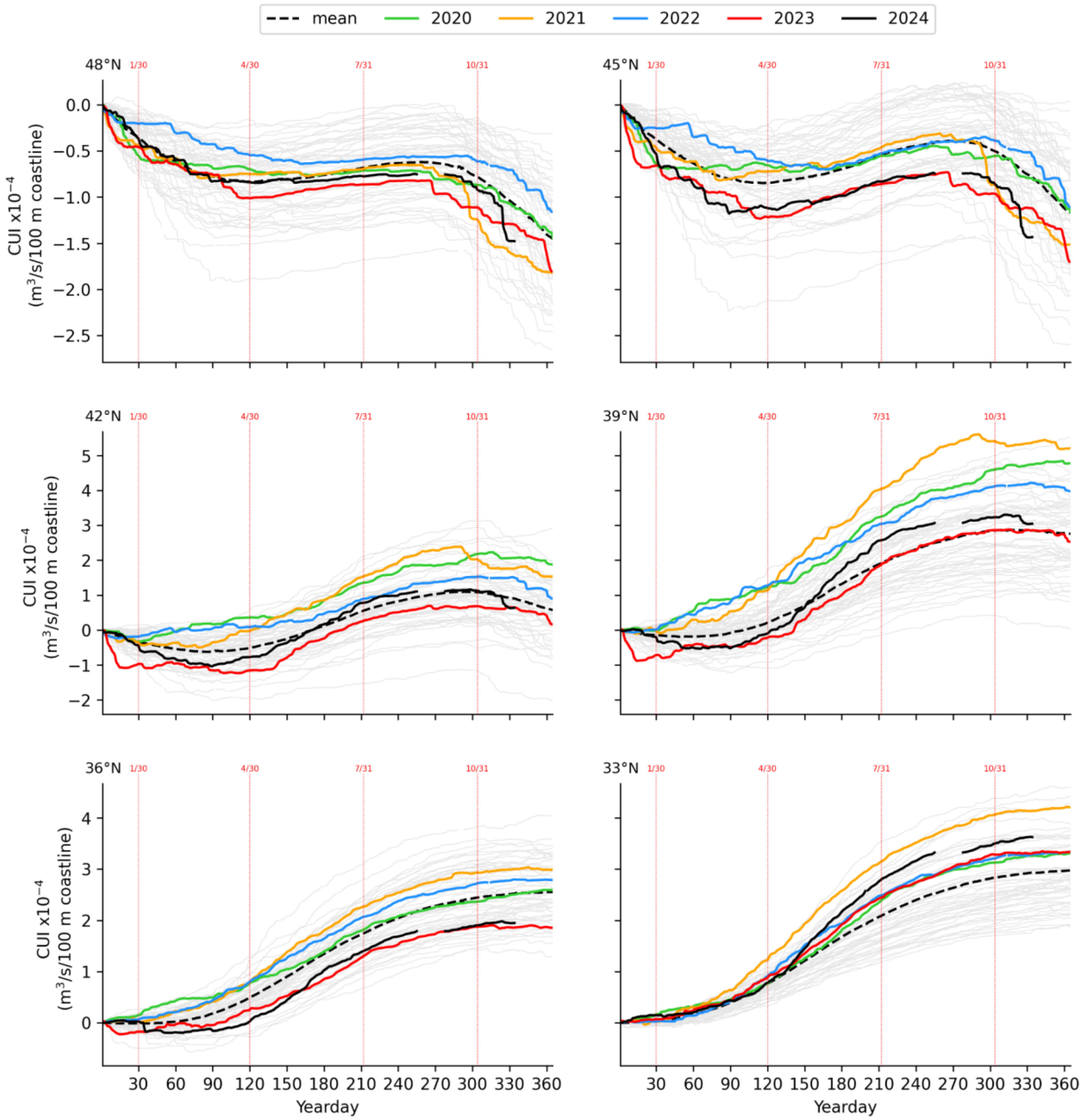

Figure F.6: Cumulative upwelling index (CUI) calculated for respective locations throughout the CCE for 2024 and the prior four years for comparison. CUI based on the Bakun upwelling index. Mean based on 1967-2024.

F.2 Assessing Marine Heatwaves in 2024

There is growing recognition that marine heatwaves can have strongly disruptive impacts on the CCE (e.g., Morgan et al. 2019). Based on an analysis of sea surface temperature anomalies (SSTa) obtained from satellite measurements (https://www.ncei.noaa.gov/products/optimum-interpolation-sst), we define marine heatwaves as 1) times when normalized SSTa >1.29 s.d. (90th percentile) of the long-term SSTa time series at a location, and 2) lasting for >5 days; these are analogous to the thresholds suggested in Hobday et al. 2016. Here, we further report on statistics concerning large heatwaves (LHW) which were tracked through space and time, with LHW defined as those heatwaves with an area > 400,000 km^2 (these denote the top 20% of all heatwaves by area as measured since 1982 when satellite data became available for tracking). 2024 saw extensive coverage of the US West Coast EEZ by El Niño (which is essentially another kind of marine heatwave) during January to mid March, and then again in late August into early September, and then a third period in late October (See red and yellow regions in Fig. F.7). The coverage during the summer and fall was not due to El Niño, which subsided in April, but rather a repeat of the now typical offshore marine heatwaves that tend to develop offshore during late spring, expand during the spring and summer, and develop within coastal waters of the EEZ during summer and fall. Strong upwelling in much of the late spring and summer helped lessen intrusion of the heatwave into the EEZ. This 2024 event was the 6th largest by area, and 5th longest marine heatwave recorded since monitoring began in 1982 (Fig. F.8). *Note: the underlying climatology used for SST anomaly analysis has changed from 1982-2010, to now encompass 1982-2020; hence small changes in the retrospective analysis of tracked heatwaves reported in Fig. F.6 as compared to previous years' reports (fewer total tracked heatwaves N, and a downgrading of maximum area for the 2022 event).

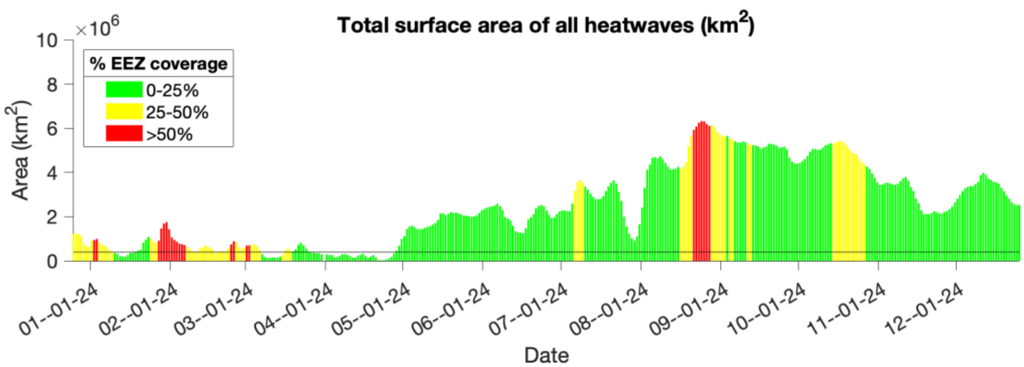

Figure F.7: Areas of North Pacific marine heatwaves during 2024. The horizontal line represents 400,000 km^2, the area threshold that we use for tracking individual events over time (top 15% of heatwaves by area). Color indicates the percentage of the US West Coast EEZ that was in heatwave state.

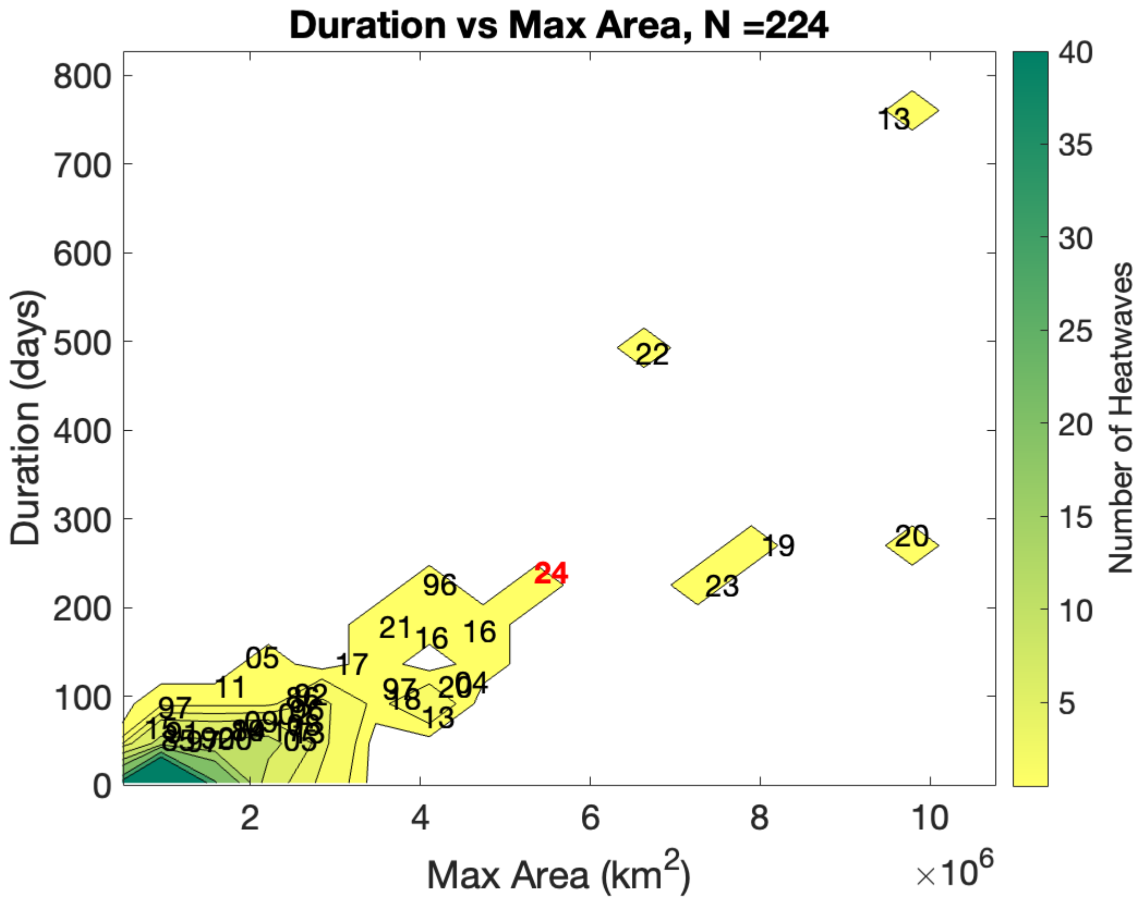

Figure F.8: Duration and maximum areas of NE Pacific large marine heatwaves, 1982-2024. Shading indicates the number of heatwaves (out of 236). Outliers are marked with numbers indicating the year the heatwave formed, with 2024 marked in red.

F.3 Habitat Compression Index

Spatial variability in patterns of upwelling, including the distribution of upwelled water and associated development of hydrographic fronts, is important for ecosystem monitoring and assessment of marine heatwaves and ecosystem shifts that can impact coastal fishing communities. Coastal upwelling creates a band of relatively cool coastal water, which is suitable habitat for a diverse and productive portion of the CCE food web. Monitoring the area and variability of upwelling habitat provides regional measures of habitat compression—an indicator to monitor the incursion of offshore warming (e.g., from heatwaves or reduced upwelling conditions) over shelf waters, which relates to shifts in the pelagic forage species community in space and time. Santora et al. (2020) applied principles of ecosystem oceanography and integration of fisheries surveys to develop the Habitat Compression Index (HCI) to quantify how offshore warming during the 2013–2016 marine heatwave and previous warming events restricted the cool upwelling habitat to a narrower-than-normal band along the coast. This compression of habitat consequently altered prey community composition and distribution, spatial aggregation patterns of top predators, and contributed to increased rates of whale entanglements in fixed fishing gear originating from California.

HCI is derived from the CCE configuration of the Regional Ocean Modeling System (ROMS) model with data assimilation (Neveu et al. 2016), and is estimated in four biogeographic provinces within the CCE: 30°-35.5°N, 35.5°-40°N, 40°-43.5°N, and 43.5°-48°N. HCI is defined as the area of monthly averaged ROMS model temperatures at a depth of 2 m that fall below a temperature threshold. Each region/month has a unique temperature threshold, based on its distinct historic climatology. Winter and spring means for central California are shown in the main body of the report (Fig. 2.5). Winter and spring means for all four regions are shown here, in Figure F.9, and demonstrate the strong, coastwide compression effect of the El Niño event in early 2024 (HCI values closer to zero).

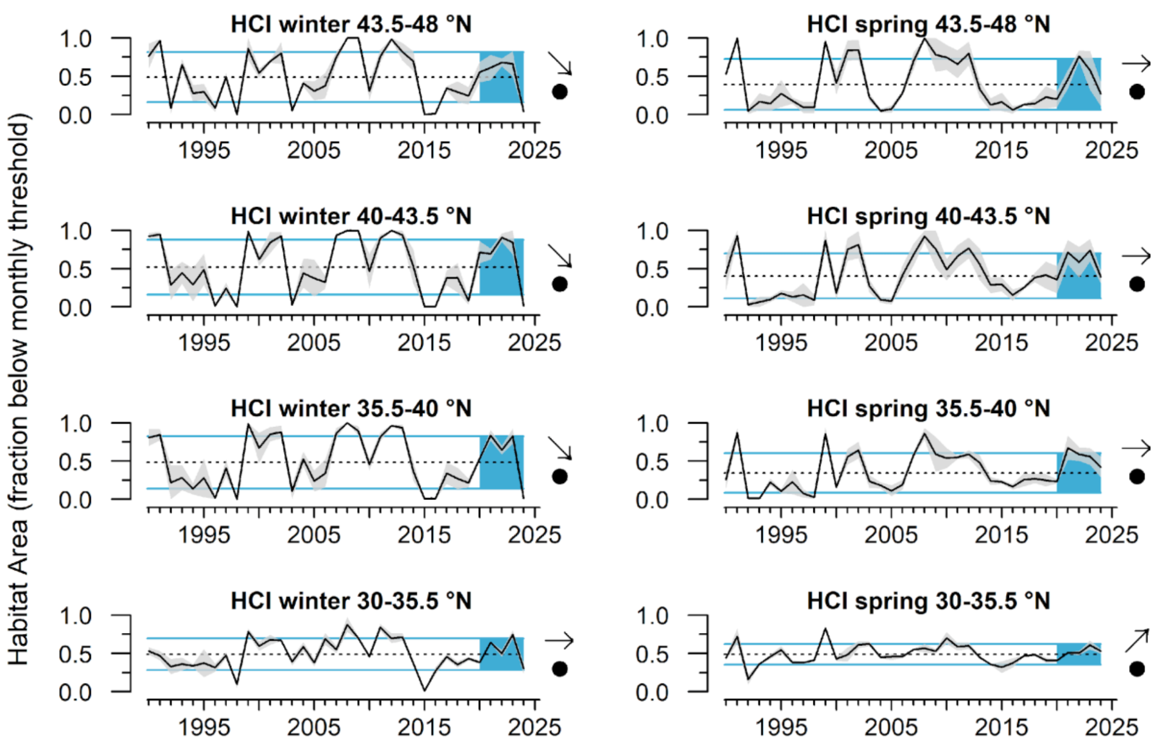

Figure F.9: Mean winter (January - March) and spring (April - June) habitat compression index by region, 1990 - 2024. Values near 1 indicate greater coverage of cool surface waters, while values near 0 indicate greater compression of cool habitat by warmer water. Gray envelope indicates ±1 s.e. Data provided by J. Santora, NMFS/SWFSC, and I. Schroeder, NMFS/SWFSC, UCSC. Lines, colors, and symbols are as in Fig. 2.1.

F.4 Seasonal Dissolved Oxygen and Ocean Acidification Indicators

Nearshore dissolved oxygen (DO) depends on many processes, including currents, upwelling, air–sea exchange, and community-level production and respiration in the water column and benthos. DO is required for organismal respiration; low DO can compress habitat and cause stress or die-offs for sensitive species. Waters with DO levels <1.4 mL/L (~2 mg/L, note unit change) are considered to be hypoxic; such conditions may occur on the shelf following the onset of spring upwelling, and continue into the summer and early fall months until the fall transition vertically mixes shelf waters. Upwelling-driven hypoxia occurs because upwelled water from deeper ocean sources tends to be low in DO, and microbial decomposition of organic matter in the summer and fall increases overall system respiration and oxygen consumption, particularly closer to the seafloor (Chan et al. 2008).

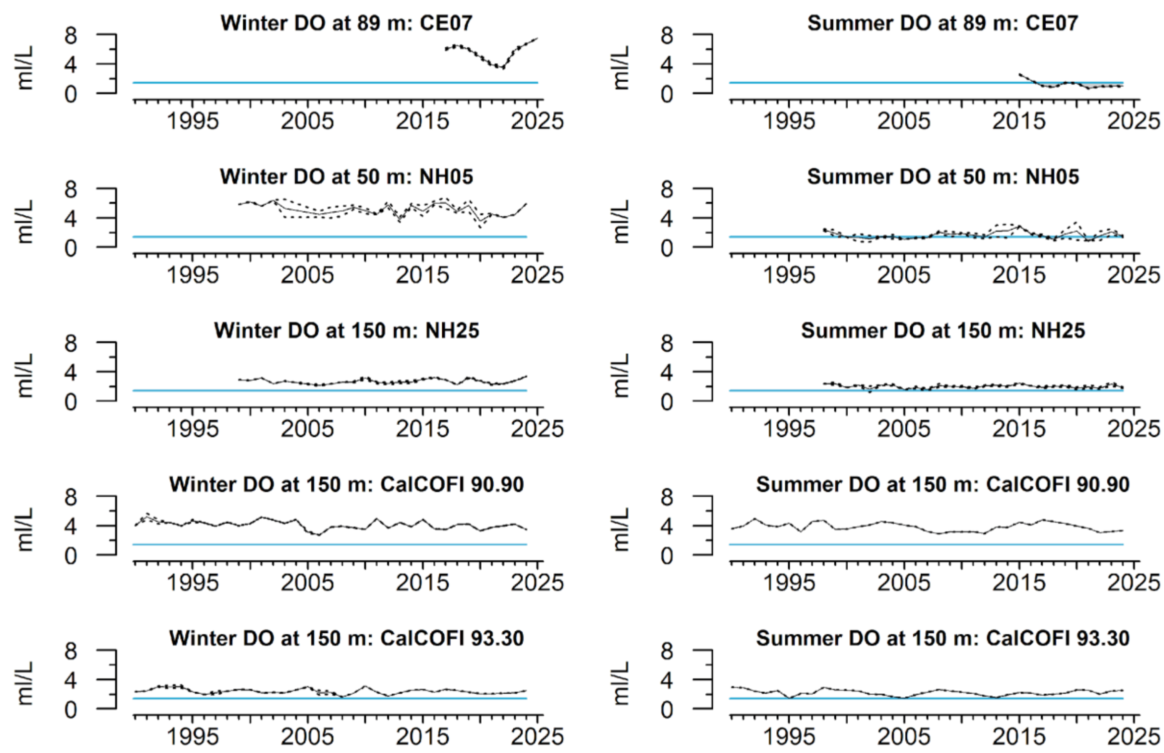

Figure F.10: Dissolved oxygen in winter (January - March) and summer (July-December) off of Washington (CE07), Oregon (NH), and southern California (CalCOFI) for 1990 - 2024. Gray envelope indicates ±1 s.e.

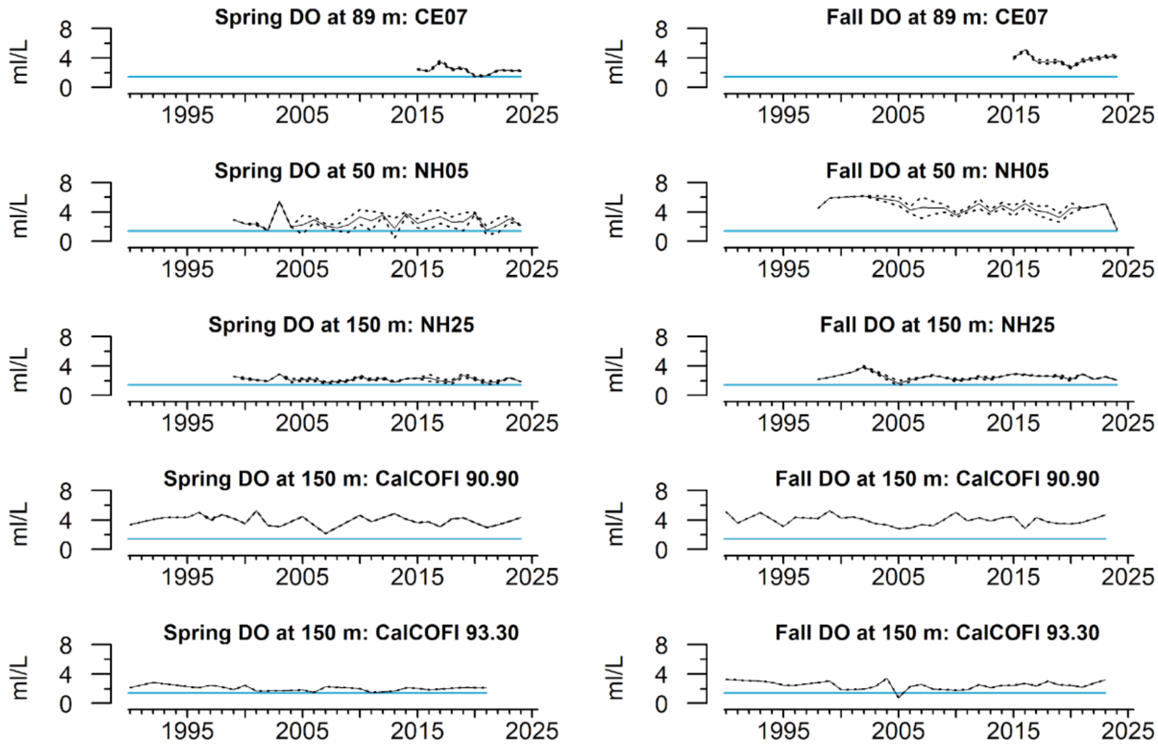

Figure F.11: Dissolved oxygen in spring (April-June) and fall (October-December) off of Washington (CE07), Oregon (NH), and southern California (CalCOFI) for 1990 - 2024. Gray envelope indicates ±1 s.e.

Annually, on the JSOES surveys conducted mid-summer, CTD casts are taken which include measurements of oxygen levels (Fig. F.10, F.11). Figure F.12 shows the June map of oxygen compiled from this survey. This year's oxygen distribution in June supports the higher frequency measurements reported above; most waters off Washington remained above hypoxic levels during the summer, with regions off Oregon being very near the threshold of hypoxia.

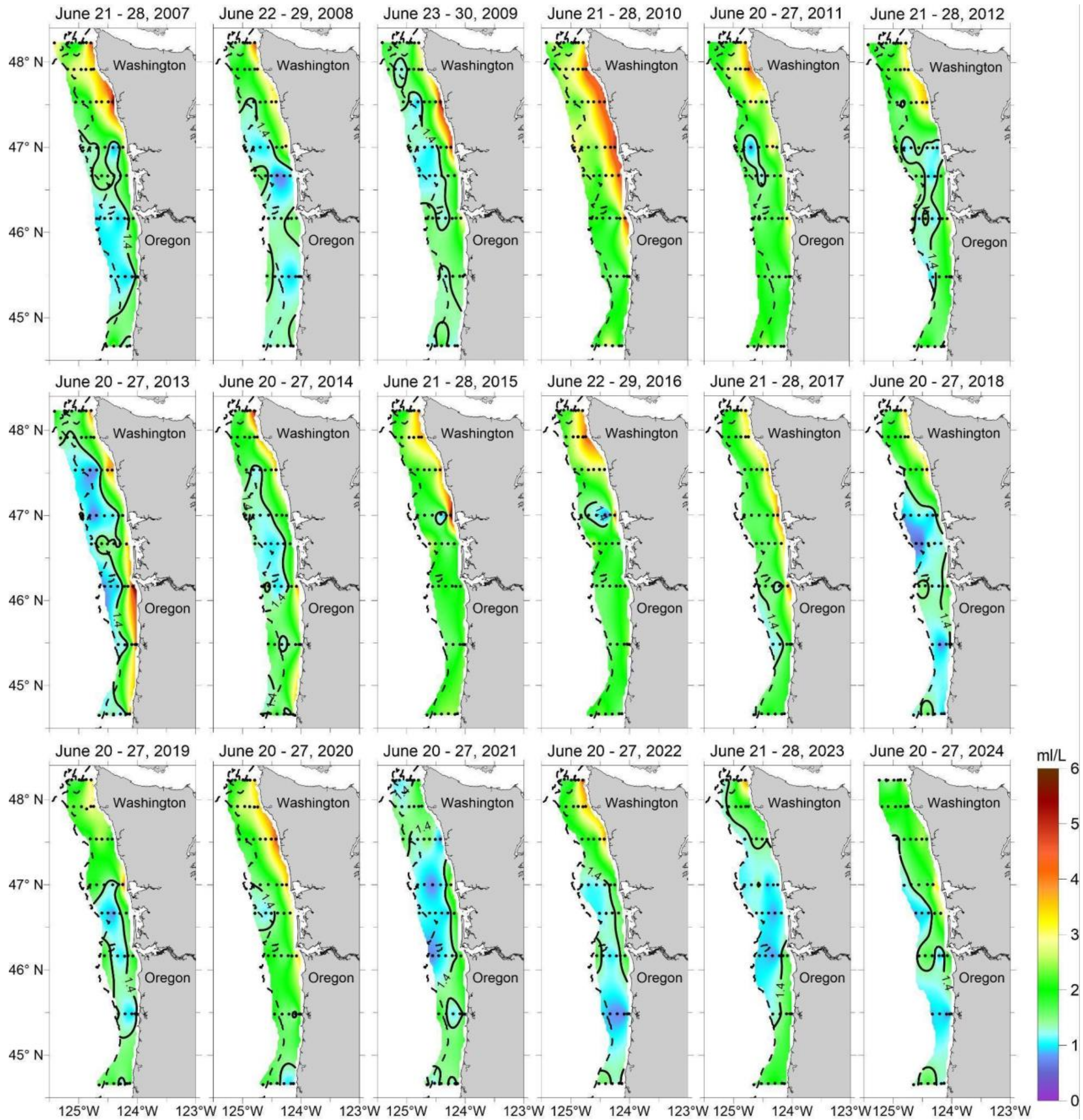

Figure F.12: Near-bottom dissolved oxygen levels (ml/L) collected from CTD casts during the June JSOES survey, 2007-2024. Solid contour represents the 1.4 mL/L hypoxia threshold; dashed contour is the 200 m isobath (shelf break); dots represent data collection locations (stations). Data provided by C. Morgan, OSU/CIMRS

Examining oxygen levels over the wider region, additional near-bottom environmental data were collected on groundfish trawls from May 19 to October 15, 2024, as part of NOAA's annual groundfish survey (Fig. F13). Areas of near-bottom hypoxia (DO < 61 µmol/kg) were found inshore of the continental shelf break (200-m isobath) north of Coos Bay, OR, and between Cape Mendocino and Point Reyes, CA. Areas of relatively high near-bottom dissolved oxygen were found elsewhere on the shelf off the US west coast. These patterns are generally consistent with previous results, but the near-bottom DO over Pacific Northwest waters were quite low similar to the 2021 upwelling season (Keller et al., 2015; Barth et al., 2024).

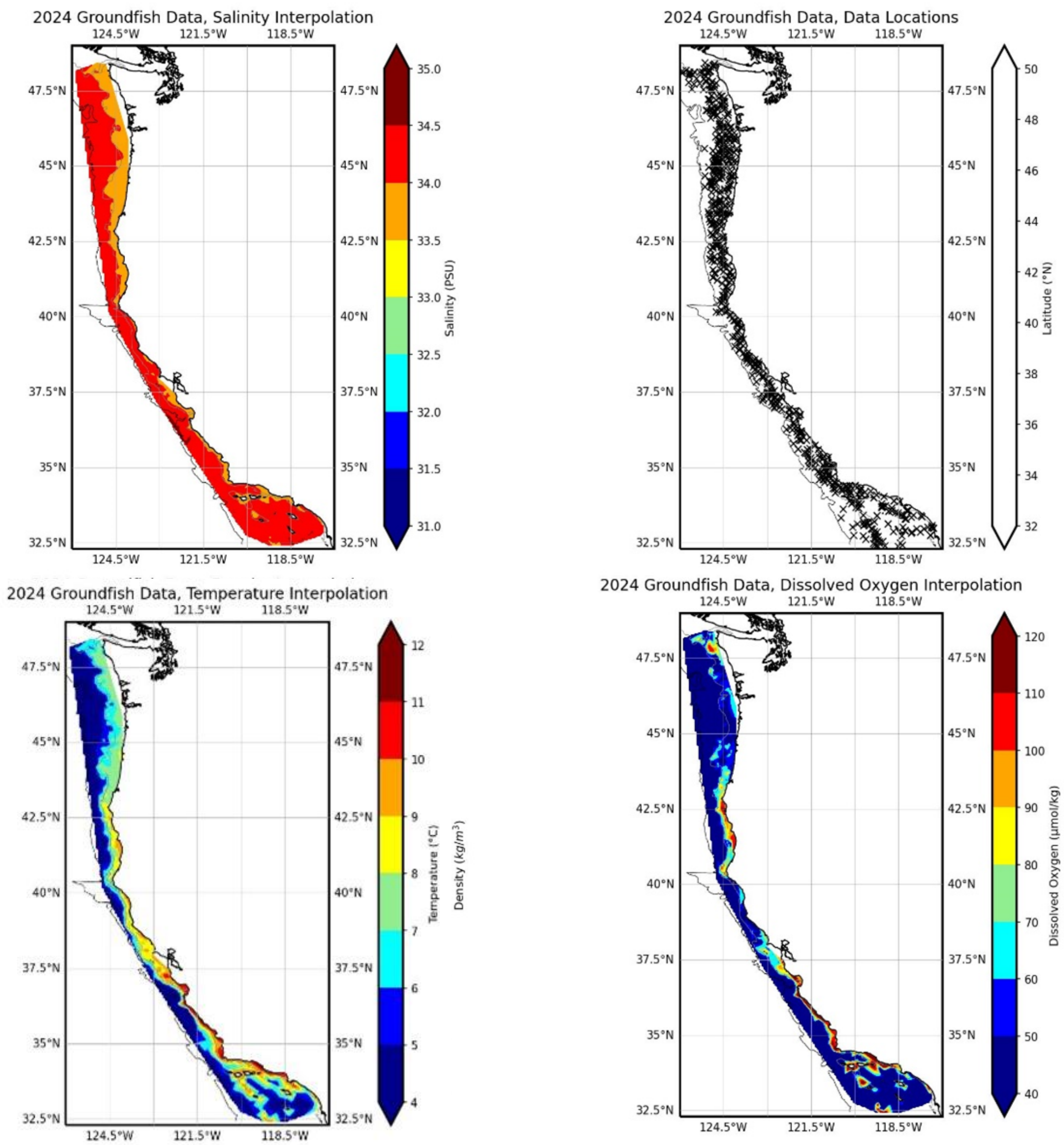

Figure F.13: Distributions of near-bottom salinity (upper left), temperature (lower left), data locations (upper right), and dissolved oxygen (lower right) from the 2024 NOAA Groundfish trawl survey conducted from May 19 to October 15. These whole-coast plots can be compared with those from previous years as in Keller et al. (2015). Station locations in upper right; isobaths are 200 and 2000 m. Figures courtesy of Jack Barth and Sean Coleman, Oregon State University. Data collected and provided by the Fisheries Resource

Analysis and Monitoring Division, Northwest Fisheries Science Center, NOAA Fisheries (Aimee Keller, Victor Simon, Peter Frey, James Fellows).

Ocean acidification (OA) occurs when atmospheric CO_2 dissolves into seawater, reduces seawater pH and carbonate ion levels. Upwelling transports low oxygen, acidified waters from deeper offshore onto the continental shelf, where increased community-level metabolic activity can further exacerbate OA (Feely et al. 2008). A key measure of OA is aragonite saturation state, which is related to availability of aragonite (a form of the mineral calcium carbonate) to form or dissolve. Aragonite saturation <1.0 indicates relatively acidified, corrosive conditions that are stressful for many CCE species, particularly shell-forming invertebrates. OA impacts on these species can propagate through marine food webs and potentially affect fisheries (Marshall et al. 2017). Aragonite saturation states tend to be lowest during spring and summer upwelling, and highest in winter.

Figure F.14 shows time series of winter and summer aragonite saturation from near bottom at stations NH05 and NH25.

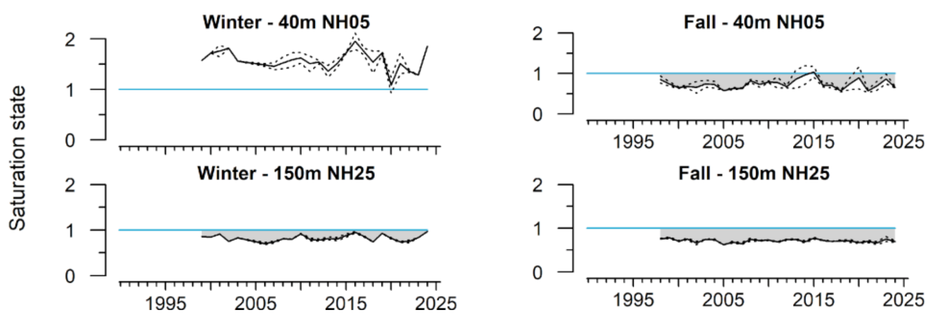

Figure F.14: Winter (Jan-Mar) and summer (Jul-Sep) mean aragonite saturation states at stations NH05 and NH25 off Newport, OR, 1998 - 2024. The blue line indicates aragonite saturation state = 1.0, below which are corrosive conditions for many shell-forming species. Dotted lines indicate ± 1.0 s.e. Data provided by J. Fisher, NMFS/NWFSC, OSU.

The corrosive water on the shelf at NH05 is largely driven by seasonal upwelling, where upwards of 80% of the water column falls below the aragonite saturation threshold each summer (Fig. F.15).

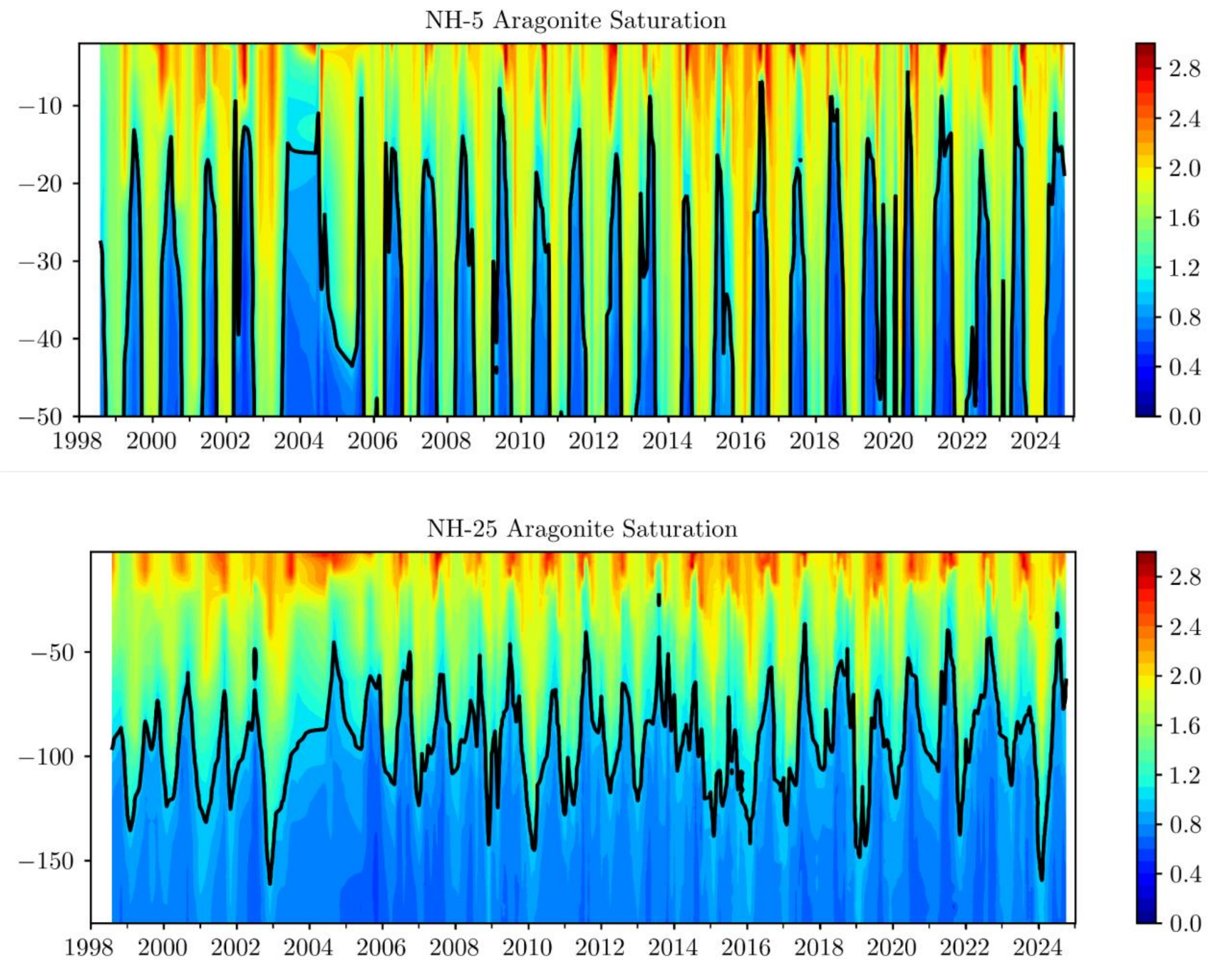

Figure F.15: Aragonite saturation state profiles for stations NH05 and NH25 off Newport, OR. Depths (y-axis) are in m. Black line indicates the depth at which aragonite saturation state = 1.0. Data provided by J. Fisher, NMFS/NWFSC, OSU.

Appendix G — SNOWPACK, STREAMFLOW, AND STREAM TEMPERATURE

Link to main section: Snowpack and Hydrology

Freshwater habitat indicators are reported based on a hierarchical spatial framework. The framework facilitates comparisons of data at the right spatial scale for particular users, whether this be the entire California Current, ecoregions within the CCE, or smaller spatial units. The framework we use divides the region encompassed by the CCE into ecoregions (Fig. 1.1), and ecoregions into smaller physiographic units. Freshwater ecoregions are based on the biogeographic delineations in Abell et al. (2008), see also www.feow.org, who define six ecoregions for watersheds entering the California Current, three of which comprise the two largest watersheds directly entering the California Current (the Columbia and the Sacramento-San Joaquin Rivers). Within ecoregions, we summarized data at scales of evolutionary significant units (ESUs) and 8-field hydrologic unit classifications (HUC-8). Status and trends for all freshwater indicators are estimated using space-time models that account for spatial and temporal autocorrelation (Lindgren and Rue (2015))

Snow-water equivalent. Snow-water equivalent (SWE) is measured using data from the California Department of Water Resources snow survey program (California Data Exchange Center, cdec.water.ca.gov) and The Natural Resources Conservation Service's SNOTEL sites across Washington, Oregon, California and Idaho. Snow data are converted into SWEs based on the weight of samples collected at regular intervals using a standardized protocol. Measurements on April 1 are considered the best indicator of maximum extent of SWE; thereafter snow tends to melt rather than accumulate.

Anomalies of SWE in 2024 were typical of El Niños across the Pacific's mountain ranges, with northerly ecoregions receiving average or lower snowpack, and with most Oregon Cascades and Sierra Nevada areas at higher levels (Fig. G.1). This situation helped Oregon and California recover from drought conditions, but also resulted in extensive flooding in California.

The outlook for snowpack in 2025 is limited to cumulative snowpack through February 2, an imperfect predictor of SWE in April. Thus far, SWE in the Mountain West has been well above median levels in much of Northern California, Oregon, and parts of Washington (Fig. G.1), near median in Idaho, and below median in northern Washington and the Southern Sierra Nevada. It remains too soon to say whether patterns will change by the end of this winter, although atmospheric conditions suggest a continuing pattern over the next few months.

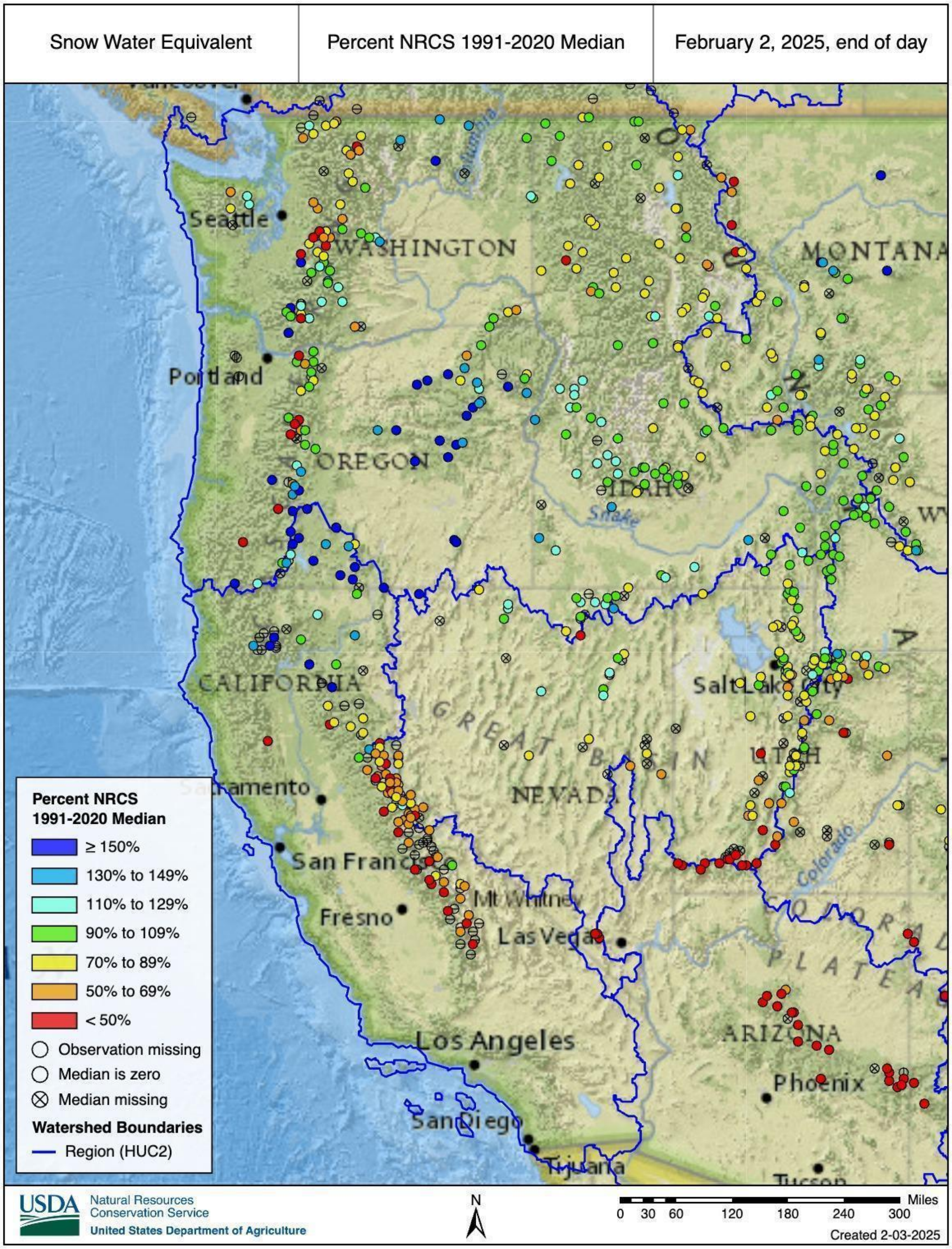
Snow Water Equivalent
Percent NRCS 1991-2020 Median
February 2, 2025, end of day
Seattle
WASHINGTON
MONTANA
Portland
OREGON
IDAHO
Snake
CALIFORNIA
GREAT BASIN
NEVADA
Salt Lake City
UTAH
Colorado
COLORADO PLATEAU
Sacramento
San Francisco
Fresno
Mt Whitney
Las Vegas
Los Angeles
San Diego
Tijuana
ARIZONA
Phoenix
Tucson
Percent NRCS 1991-2020 Median
≥ 150%
130% to 149%
110% to 129%
90% to 109%
70% to 89%
50% to 69%
< 50%
Observation missing
Median is zero
Median missing
Watershed Boundaries
Region (HUC2)
USDA Natural Resources Conservation Service
United States Department of Agriculture
N
0 30 60 120 180 240 300 Miles
Created 2-03-2025

Figure G.1: Snow water equivalent (left panel) and total precipitation (right panel) as of February 2, 2025, relative to the 1991-2020 median. Data are from the California Data Exchange Center and the Natural Resource Conservation Service SNOTEL database. Open circles indicate stations that either lack current data or long-term median data.

Stream temperature. Mean maximum stream temperatures in August were determined from 446 USGS streamgages with temperature monitoring capability. While these gages did not necessarily operate simultaneously throughout the period of record, at least two gages provided data each year in all ecoregions. Stream temperature records are limited in California, so two ecoregions (Sacramento/San Joaquin and Southern California Bight-Baja) were combined. Maximum temperatures exhibit strong ecoregional differences in absolute temperature (for example, Salish Sea and Washington Coast streams are much cooler on average than California streams).

The most recent 5 years have been marked by stream temperatures that have been above average across nearly all ecoregions (Fig. G.2). Trends show evidence of a latitudinal cline, rising in the northern ecoregions (Salish Sea and Washington Coast, Columbia Glaciated), and declining or steady in Columbia Unglaciated, Oregon, and California ecoregions. Despite recent patterns, 2024 water stream temperatures were close to long-term averages in all ecoregions.

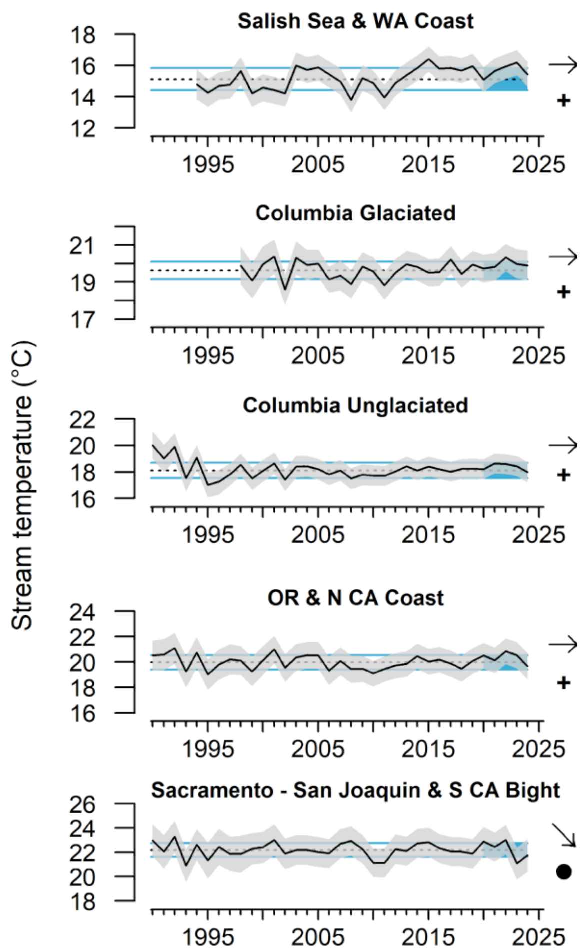

Figure G.2: Mean maximum stream temperatures in August measured at 466 USGS gages from 1990 - 2024. Gages include both regulated (subject to hydropower operations) and unregulated systems, although trends are similar when these systems are examined separately. Error envelopes represent 95% credible intervals (CI). Lines, colors and symbols are as in Fig. 2.1.

Minimum and maximum streamflow. Flow is derived from active USGS gages with records that are of at least 30 years' duration (waterdata.usgs.gov/nwis/sw). Daily means from 213 gauges were used to calculate annual 1-day maximum and 7-day minimum flows (Fig. G.3, Fig. G.4). These indicators correspond to flow parameters to which salmon populations are most sensitive. We use standardized anomalies of streamflow time series from individual gages.

Ecoregional patterns in snowpack (Fig. G.1) translated to similar patterns in stream flow. Maximum stream flows were below average in all ecoregions, and 2024 was the third lowest year of the time series for the Columbia Glaciated ecoregion. Minimum stream flows (Fig. G.3) continued a downward trend in low flows for the three northern ecoregions, and

2024 was the sixth lowest year of the time series for the Columbia Glaciated ecoregion. However, the three southern ecoregions witnessed higher than average August low flows in 2024, and low flows in the Southern California Bight were their highest in the 1981-2024 record.

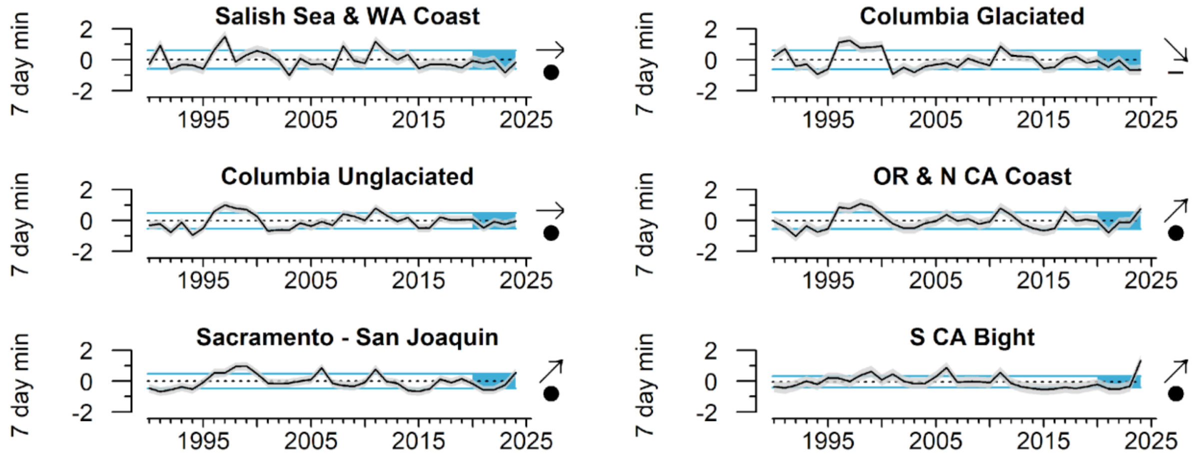

Figure G.3: Anomalies of 7-day minimum streamflow measured at 213 gages in six ecoregions from 1990 - 2024. Gages include regulated (subject to hydropower operations) and unregulated systems, though trends are similar when these systems are examined separately. Gray envelopes represent 95% credible intervals. Lines, colors and symbols are as in Fig. 2.1.

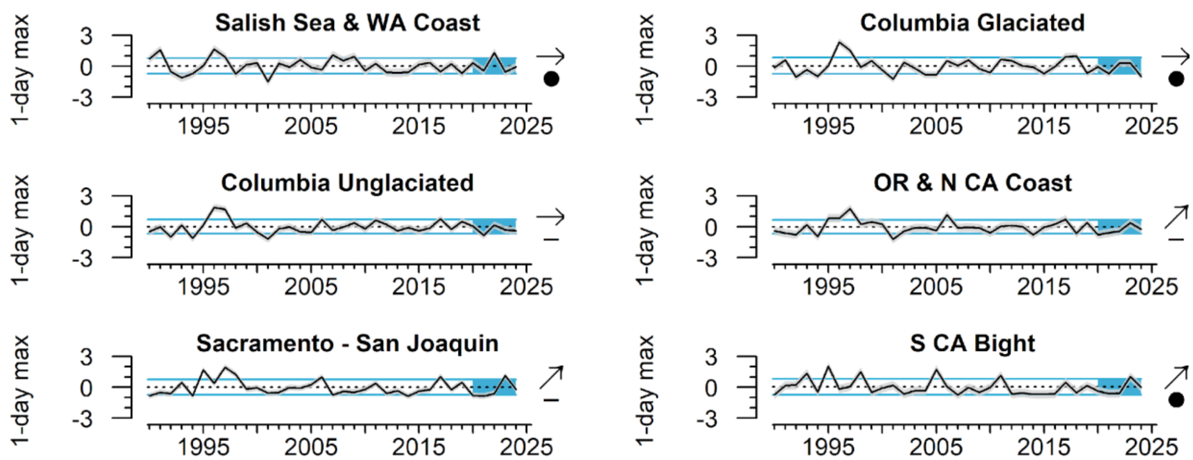

Figure G.4: Anomalies of 1-day maximum streamflow measured at 213 gages in six ecoregions from 1990 - 2024. Gauges include both regulated (subject to hydropower operations) and unregulated systems, although trends are similar when these systems are examined separately. Gray envelopes represent 95% credible intervals. Lines, colors and symbols are as in Fig. 2.1.

Appendix H — COASTAL PELAGIC SPECIES

Link to main section: Coastal pelagic species

Acoustic-trawl method (ATM) surveys have been used by the NOAA Southwest Fisheries Science Center in most years since 2006 to map the distributions and estimate the abundances of coastal pelagic fish species (CPS) in the coastal region from Cape Flattery to San Diego, California (e.g., Demer et al. 2012; Zwolinski et al. 2014; Stierhoff et al. 2020). In some years, the surveys were expanded to include portions of Vancouver Island, Canada and Baja California, Mexico (Stierhoff et al. 2023a, b). The surveys cover waters to at least the 1,000-fathom (1829 m) isobath, or 65 km from shore. The five most abundant CPS in this domain are northern anchovy, Pacific herring, Pacific sardine, jack mackerel, and Pacific mackerel. The ATM combines data from echosounders, which record CPS echoes, and trawls, which produce information about the species composition, sizes, and ages of the fishes.

The 2024 summer survey was conducted aboard NOAA Ship *Reuben Lasker* with sampling in the core area from Punta Eugenia, Baja California to Cape Scott, British Columbia between 26 June and 30 September (Stierhoff et al., In prep., Fig. H.1). Additionally, two charter fishing vessels, *Lisa Marie* and *Long Beach Carnage,* sampled nearshore (within 5 NM from shore) between San Diego, California and to Cape Flattery, Washington, including around the northern Channel Islands (Fig. H.2).

Acoustic backscatter from CPS was mapped throughout the core and nearshore survey areas. In the core region, trawl samples were mostly northern anchovy south of San Francisco, jack mackerel between San Francisco and Newport, Oregon, and Pacific Herring off northern Oregon, Washington, and Vancouver Island (Fig. H.1).

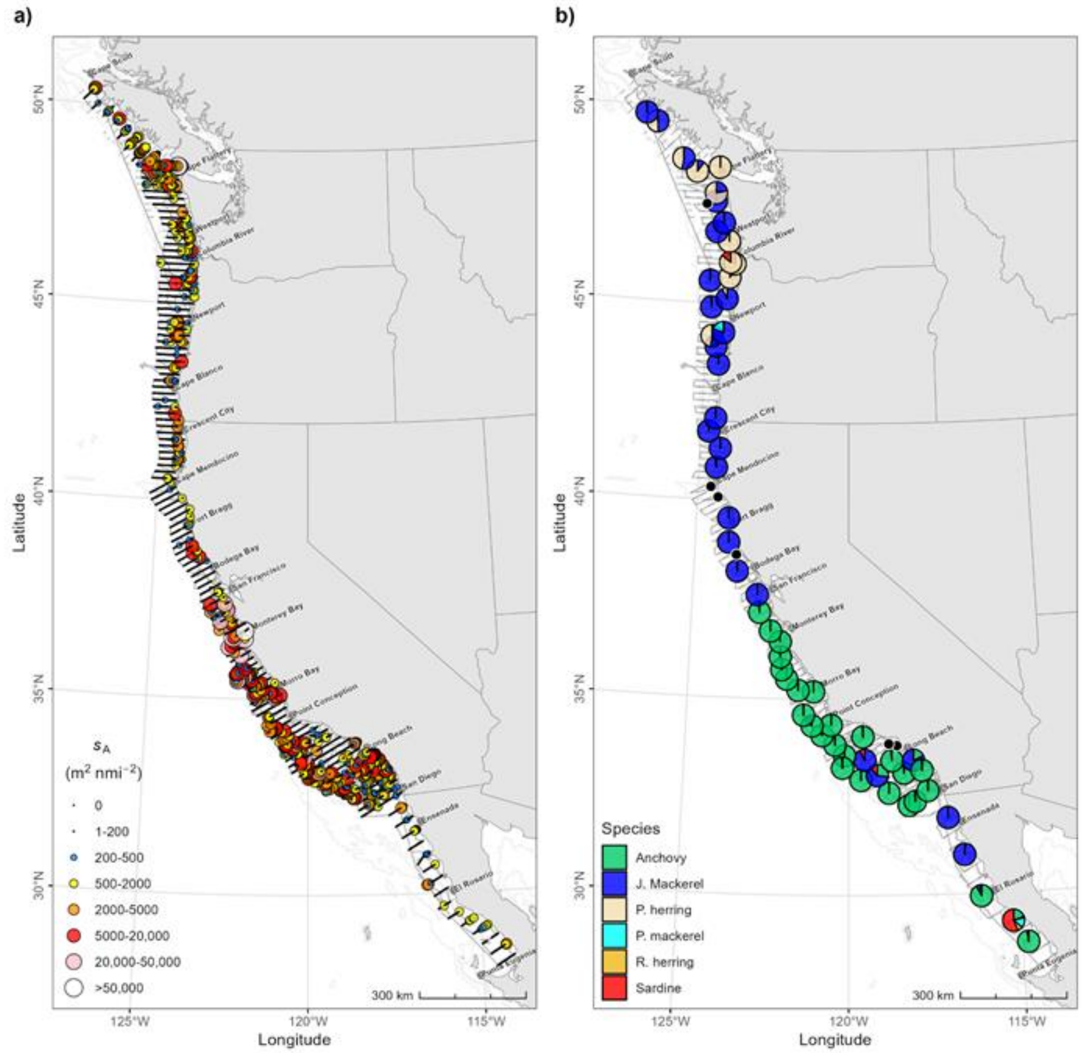

Figure H.1: Data from the 2024 summer CPS survey in the core survey area as sampled by FSV Lasker, including: a) integrated 38-kHz volume backscatter coefficients attributed to CPS, and b) the proportion of CPS backscatter based on the nearest nighttime trawl catch.

In the nearshore region, purse seine samples contained mostly Pacific sardine, northern anchovy, and Pacific mackerel south of San Francisco, and jack mackerel and Pacific herring north of San Francisco. Pacific sardine were caught primarily in the nearshore area, with those from the northern stock caught off Monterey Bay and San Francisco, and those from the southern stock caught south of Point Conception. (Fig. H.2).

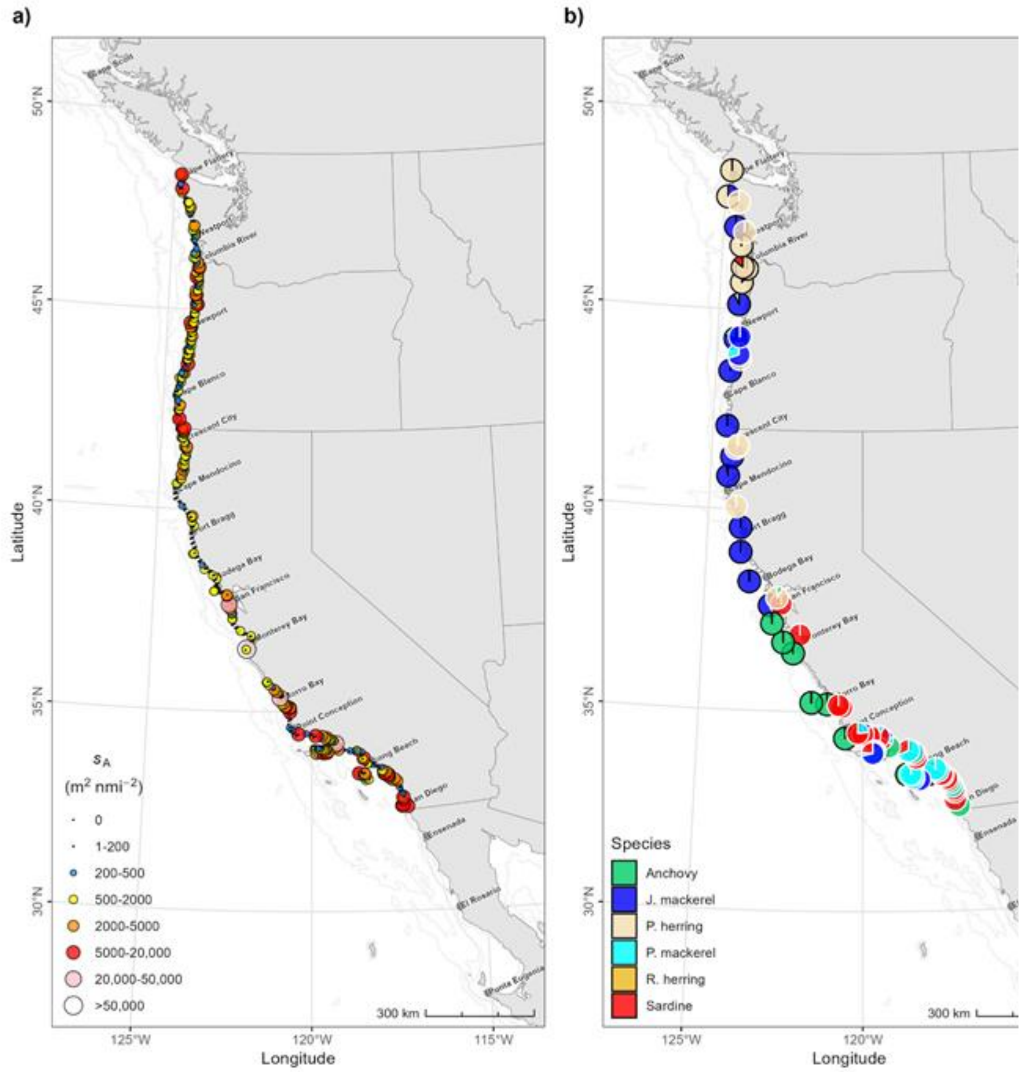

Figure H.2: Data from the 2024 summer CPS survey in the nearshore survey area as sampled by two fishing vessels, including: a) integrated 38-kHz volume backscatter coefficients attributed to CPS, and b) the proportion of CPS backscatter based on the nearest purse seine catch.

The survey-estimated summer CPS biomasses were dominated by northern stock Pacific sardine from 2008 until 2013, jack mackerel in 2014 and 2015, and then the central stock of northern anchovy since 2015, when it began to resurge (see Fig. 3.4 in Leising et al. 2024). Based on observations from the 2024 survey, the CPS assemblage continues to be dominated by the central stock of northern anchovy and jack mackerel, with the biomass of Pacific sardine, Pacific herring, round herring, and Pacific mackerel remaining low (Data not shown, Stierhoff et al., in prep.)

Appendix I — REGIONAL FORAGE AVAILABILITY

Link to main section: Regional Forage Availability

I.1 Northern California Current Forage

The Northern CCE survey (known as the Juvenile Salmon Ocean Ecology Survey, JSOES) occurs in June and targets juvenile salmon in surface waters off Oregon and Washington (Fig. 1.1). It also collects adult and juvenile (age 1+) pelagic forage fishes, market squid, and gelatinous zooplankton with regularity. A Nordic 264 rope trawl is towed at the surface (upper 20 m) for 15 - 30 min at approximately 6.5 km/hr. The gear is fished during daylight hours in near-surface waters, which is appropriate for targeting juvenile salmon.

In 2024, catches of juvenile chum salmon were over 1 s.d. above the long-term survey mean, while juvenile sockeye catches were just above the long-term mean; with a significantly increasing 5 year trend for chum, and no trend for sockeye (Fig. I.1, top).

Among non-salmonids, catches of many species have been dynamic since the values associated with the 2013-2016 marine heatwave (Fig. I.1). Catches of age-0 sablefish were close to average again in 2024, and well below the sharp peak in 2020. Pacific pompano (butterfish), a warmer-water fish whose catches peaked in 2016, were close to the time series average in 2024. Catches of market squid in 2024 decreased slightly compared to 2023 and were near the time series average. While this survey is not designed to accurately estimate biomass of YOY rockfishes, the prevalence of YOY rockfishes in the survey (i.e., the proportion of stations at which YOY rockfishes were caught) was noted as being high in 2024 (Data not shown, Morgan et al., in prep).

Among the gelatinous zooplankton off Washington and Oregon, beginning in 2015 community composition transitioned from dominance of the large, cool-water sea nettle jellyfish (*Chrysaora fuscescens*) to the more offshore-oriented water jellyfish (*Aequorea* spp.). By 2019, both had returned to roughly average densities. In 2024, catches of sea nettles, water jellies, egg yolk jellies and moon jellies all increased (Fig. I.1), with catches of water jellies being more than 1 s.d. above the mean for the past two years. Egg yolk and moon jellies are species that tend to be associated with warmer or offshore water masses, and thus may be reflecting the El Niño and/or marine heatwave presence this past year.

The JSOES program also samples off Oregon and southern Washington in May. During this survey a fine-mesh liner is added to the Nordic trawl to directly sample prey of juvenile salmon such as juvenile forage fishes and groundfish, krill, and crab megalopae. Juvenile Pacific sardine have been present in the fine-mesh liner catches in all years from 2016 - 2024 (no survey in 2020). The 2024 catches had the highest prevalence of juvenile sardine, i.e. present at all sampling locations, and higher than average biomass (Data not shown, Morgan et al., in prep). Also, since 2015, newly hatched larval Pacific sardine have been caught in bongo samples from nearshore waters on the Newport Hydrographic Line off Oregon.

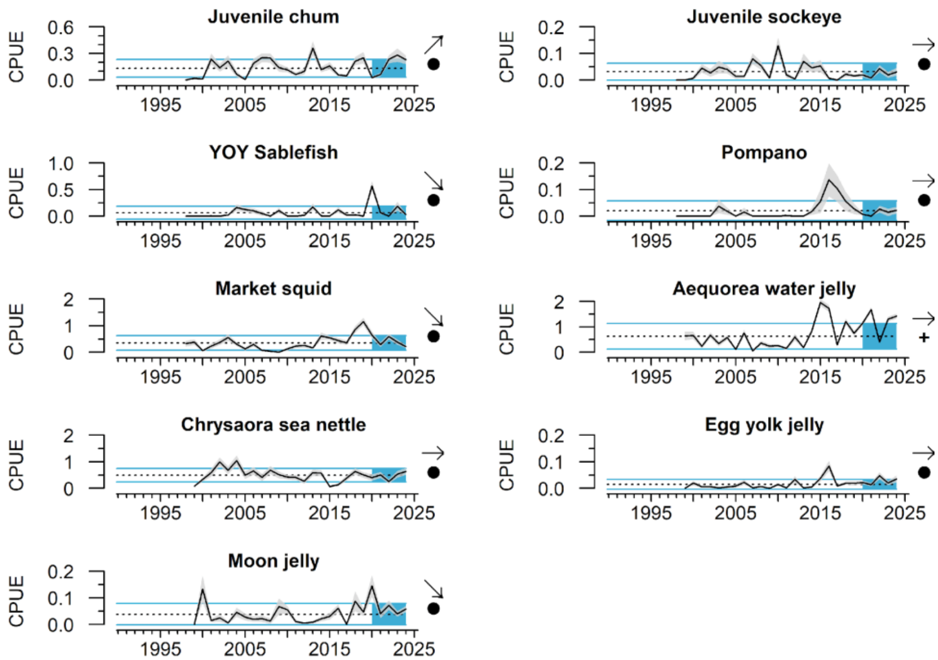

Figure I.1: CPUE (log_{10}(number/km+1)) for pelagic species in the Northern CCE, 1998 - 2024. Lines, colors, and symbols are as in Fig. 2.1.

Preliminary results from a parallel survey, which samples waters north of Cape Mendocino using the same methodology as the survey for the Central CCE (see Appendix I.2), suggest a high diversity of forage in this region in 2024 (e.g. squid, krill, jellies, smelts, juvenile fishes), but low to moderate overall biomass. One exception was YOY rockfish, which were highly abundant. These results generally align with observations reported by some commercial and recreational fishermen during a Fishermen and Scientists roundtable in Newport, Oregon in November 2024.

I.2 Central California Current Forage

The Central CCE forage survey (known as the Rockfish Recruitment and Ecosystem Assessment Survey, RREAS) samples much of the West Coast each May to mid-June, using midwater trawls sampling between 30 and 45 m depths during nighttime hours. The survey targets young-of-the-year (YOY) rockfish species and a variety of other YOY and adult forage species, market squid, adult krill, and gelatinous zooplankton. Juvenile rockfish, anchovy, krill, and market squid are among the most important prey for CCE predators (Szoboszlai et al. 2015). Time series presented here are from the "Core Area" of that survey, centered off Monterey Bay (Fig. 1.1). Catch data were standardized by using a delta-GLM to estimate year effects while accounting for spatial and temporal covariates to yield relative abundance indices, shown with their approximate 95% confidence limits

(Santora et al. 2021). The 2024 survey effort in the "Core Area" was comparable to previous years apart from 2020.

Standardized anomalies of log-transformed catch indices of key forage taxa in 2024 suggest continued high abundance of adult northern anchovies, with a marked increase in YOY anchovy to more than 1 s.d. above the mean (Fig. I.2). Catches of Pacific sardine showed a marked decrease compared to 2023, to near 1 s.d. below the mean. The anchovy and sardine results in this region are consistent with findings from a coastwide acoustic-trawl CPS survey in 2024 (see Appendix H).

The survey observed high abundances of YOY rockfish and YOY Pacific hake again in 2024 (Fig. I.2). YOY rockfish catches were at the highest level since the 2015-16 marine heatwave. Krill abundance increased compared to 2023; coastwide RREAS data indicate that krill abundance has been generally higher in northern areas relative to southern areas in recent years. Myctophids (lanternfishes) also increased to near 1 s.d. above the long-term average levels observed in recent years. Catches of market squid were slightly less abundant in 2024, while octopus abundance slightly increased to near-average levels. The cumulative results of these trends indicate a fairly productive ecosystem, with anchovy continuing to dominate the forage community but with a greater abundance of alternative forage, and with only market squid showing a declining trend.

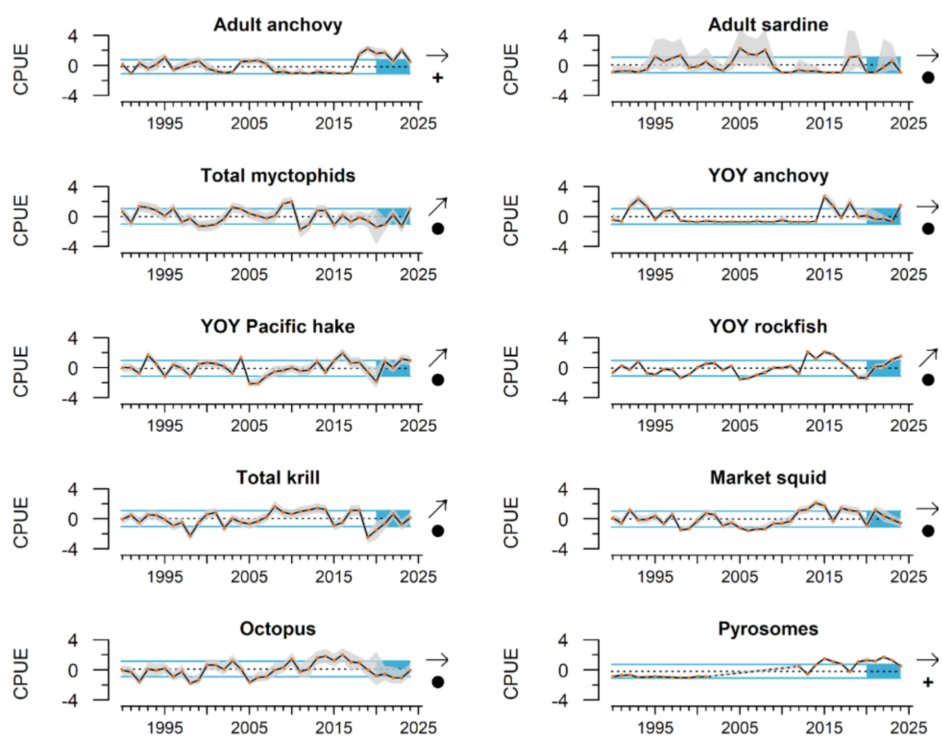

Figure I.2: CPUE (delta-GLM index and 95% CL) anomalies of a subset of key forage groups in the Core Area of the Central CCE, 1990 - 2024. Lines, colors, and symbols are as in Fig. 2.1.

I.3 Southern California Current Forage

Abundance indicators for forage in the Southern CCE come from fish and squid larvae collected in the spring (May-June) across all core stations of the CalCOFI survey (Fig. 1.1). Larval data are indicators of the relative regional abundances of adult forage fish, such as sardines and anchovy, and other species, including certain groundfish, market squid, and mesopelagic fishes. The survey samples a variety of fish and invertebrate larvae (<5 d old) from several taxonomic and functional groups, collected via oblique vertical tows of fine mesh Bongo nets to 212 m depth. In 2020, the spring larval survey was cancelled due to COVID-19, and thus no data are available for that year, but survey operations resumed in 2021.

Catches of larval anchovy in spring 2024 were slightly down from 2023 but still at a historically high level. (Fig. I.4). Larval California smoothtongue (a mesopelagic species) , although at lower abundance this year, has also continued to remain relatively high since 2019. Market squid paralarvae, which were absent from 2013-2017, increased steadily and significantly since 2017, had the second highest abundance of the time series in 2022, but were absent in 2023 and 2024, reflecting lowered abundances of this group throughout the CCE during 2024. Catches of larval sardines have been low since 2012 and remained low in 2024. Southern mesopelagic species increased dramatically in 2015 and remained relatively abundant in 2024. Both hake and rockfish had high larval abundances in 2024, greater than 1 s.d. above the long term mean. Moreover, larval hake abundance in 2024 was the highest in the time series. Recent trends for most species or species groups were non-significant.

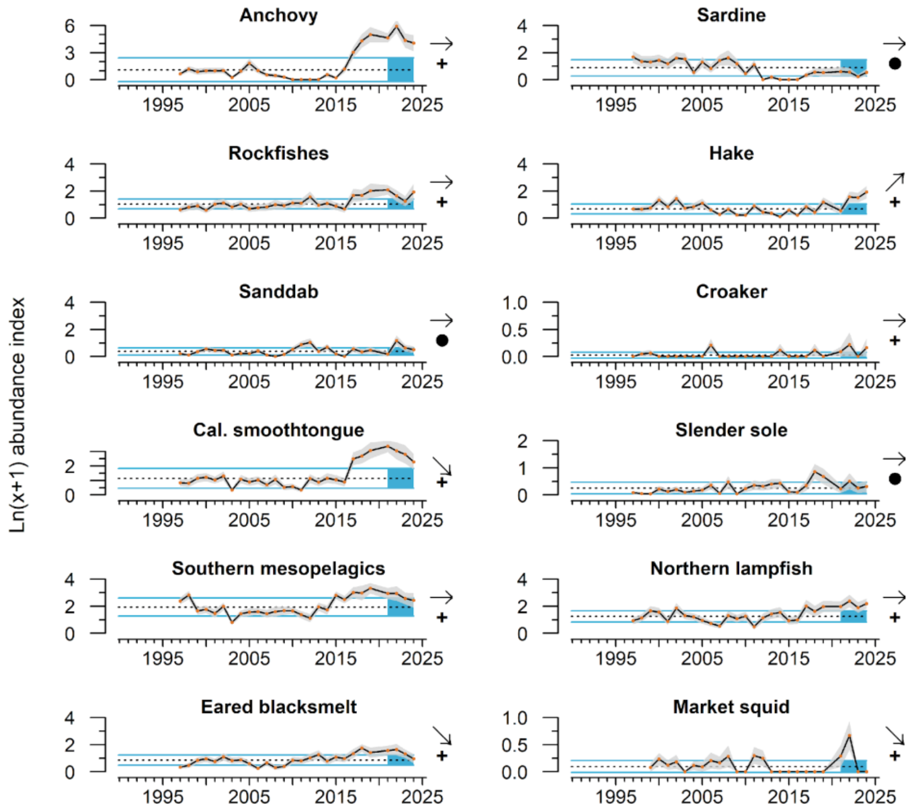

Figure I.4: Mean abundance (ln(x+1)) index of the larvae of key forage species in the Southern CCE, from spring CalCOFI surveys during 1997 - 2024 (no data from 2020). Lines, colors, and symbols are as in Fig. 2.1.

I.4 Pyrosomes and Salps

Catches of pyrosomes (warm-water pelagic tunicates) in research surveys in the "core area" off central California (Fig. 1.1) remained high and declined slightly from last year (Fig. I.3). Salps were moderately abundant in the central CCE. Pyrosome catches and salps were considered low in the northern CCE (data not shown; B. Wells, NMFS/SWFSC).

Appendix J — SALMON

Link to main section: Salmon indicators

J.1 Salmon Stoplight Table Format

For the stoplight tables presented in Figure 3.8 and below in Section J.3, we use color to represent anomalous years. The statistically based format used to develop these tables produces five bins that are determined relative to a fixed baseline reference period (see Harvey et al. 2023). In this format, we assumed a normal distribution for each of the indicators, estimating a mean and standard deviation for the base period. For each cell within a given indicator, we determined how many standard deviations the values were from their respective base period mean and used a five-color set to indicate whether a value was >2 s.d. below the mean, within 1 and 2 s.d. below the mean, within 1 s.d. of the mean in either direction, 1 to 2 s.d. above the mean, or >2 s.d. above the mean.

J.2 Ecosystem Indicator-based Outlooks for Chinook Salmon Escapement in the Columbia River Basin

The main body of the report features a stoplight table (Fig. 3.8) that provides a qualitative, ecosystem-based outlook of returns of adult Columbia Basin Chinook salmon in 2025 and 2026, based on indicators of conditions affecting marine growth and survival of smolts that outmigrated in 2023 and 2024. Two related quantitative analyses, which are still being refined in response to feedback from the SSC-ES and other partners, use a summary metric of the stoplight table, a new stock-specific metric (B. Burke, unpublished), and counts of adult salmon returns to Bonneville Dam.

In these analyses, models are fit to past adult return data and use the most recent ecosystem indicator data to predict what returns will be for cohorts that have gone to sea but not yet returned. Both models are founded on linear regressions of single ecosystem indicators versus counts of adult fish at Bonneville Dam (Fig. J.1, black points), though this approach can easily be applied to measures of salmon survival rather than adult counts. The first model uses a Dynamic Linear Model with the first principal component (PC1) from a Principal Component Analysis of the stoplight table as a covariate. The data used in this "Stoplight PC1 model" is therefore limited to years included in the stoplight table (1998-2024). The second model is a simple linear regression using a Covariance Map Index of Sea Surface Temperature (CMISST; B. Burke, unpublished), which is a metric derived by calculating the similarity of SST spatial patterns in the North Pacific Ocean to a stock-specific nominal pattern. Because SST data are available for a longer period, this "CMISST" model uses data starting in 1980 and continuing through 2024.

For smolts that went to sea in 2023 (which should dominate adult returns in 2025), the count estimates are mostly above the averages for the past ten years (Table J.1). For adults that will return in 2026, the models consistently suggested lower adult returns in 2025 than for those that went to sea in 2023 (Table J.1). This is not too surprising as the mean rank of indicators in the Columbia stoplight table was 11.7 for smolts that went to sea in 2023 and 15.4 for smolts in 2024 (Fig. 3.8); higher rank suggests poorer ocean survival).

Return estimates from the Stoplight and CMISST models were similar, though the CMISST model consistently suggested higher adult returns than the Stoplight PC1 model (Table J.1). Uncertainty in the estimates (95% prediction intervals, colored vertical ribbons in (Fig. J.1) is relatively high, particularly for fall Chinook salmon.

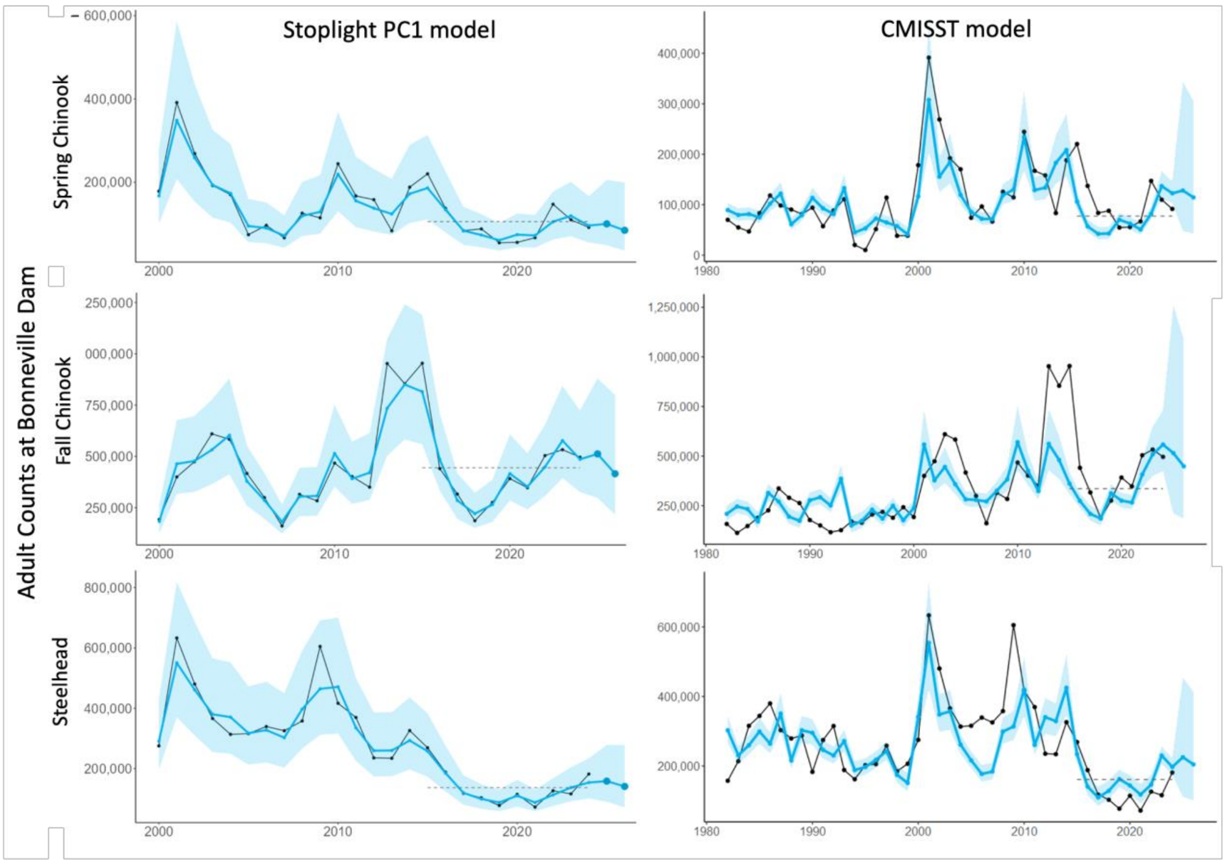

Figure J.1: Observed (black lines) and modeled (blue lines) adult salmon counts at Bonneville Dam for spring Chinook salmon (top row), fall Chinook salmon (middle row), and steelhead (bottom row). Left panels are forecasts with the "Stoplight PC1" model, and right panels are forecasts with the "CMISST" model. Years on the x-axes are adult return years (covariate data were lagged by 2 years before running models). Shaded areas are 95% confidence intervals (or prediction intervals for 2025 and 2026). Gray dashed lines are the recent 10-year average.

Although Figure 3.8 represents a general description of ocean conditions related to multiple populations, we acknowledge that the importance of any particular indicator will vary among salmon species and runs. These analyses represent progress toward greater distinction among different Salmon Evolutionary Significant Units (ESUs) than some results shared in previous ecosystem status reports. NOAA scientists and partners continue to refine stock-specific salmon outlooks such as the CMISST approach by using both correlative and mechanistic methods that can identify and optimally weight the indicators for each response variable in which we are interested. We will continue to work with the Council and advisory bodies to identify data sets for Council-relevant stocks for which analyses like these could be possible.

Table J.1: Counts of adult salmonids (in thousands) at Bonneville Dam, including the most recent 10-year mean (2015-2024) and estimates from the Stoplight and CMISST models.

	10-year mean	Stoplight 2025	Stoplight 2026	CMISST 2025	CMISST 2026
Spring Chinook	77	100	84	128	114
Fall Chinook	336	512	416	514	448
Steelhead	161	158	141	225	205

J.3 Ecosystem Conditions for Chinook Salmon in California

Rebuilding plans in 2019 for Sacramento River (SRFC) and Klamath River fall Chinook salmon runs (KRFC) prompted annual updates of habitat indicators for these two stocks (see Harvey et al. 2021b), which have been expanded to include Central Valley Spring-run Chinook salmon (CVSC) to inform risk assessment for this otherwise unassessed stock. These putative indicators ranged across the salmon life cycle and include factors relevant to adult spawning, incubation and emergence, freshwater/delta residence, and early marine residence phases, as well as hatchery influences (see Leising et al. (2024)).

Since last year's ESR, the authors have begun to distill 46 indicators detailed in previous ESRs into a shorter list of key indicators to concisely highlight ecosystem states that best predict salmon recruitment (Table J.2).

Table J.2: Definitions of habitat and recruitment indicators, and data sources, for three salmon stocks: Sacramento River Fall Chinook (SRFC), Central Valley Spring-run Chinook (CVSC), and Klamath River Fall Chinook (KRFC).

Life-stage	Abbreviation	Time period	Expected effect	Reference	Stock
Adult spawners					
Spawner counts	Spawners		+	Friedman et al. 2019	KF, SF, CS
Fall closures of Delta Cross Channel	CChannel.F	Se-Oc	+	Rebuilding plan	SF
Low flows during upstream migration	Flows.U	Se-Oc*	+	Strange et al. 2012	KF, SF, CS
Temperatures during upstream mainstem	Temp.U	Se-Oc*	-	Fitzgerald et al. 2020	KF, SF
Holding period flows in Butte Creek	Flows.H	Jn-Se	+	USFWS, 1995	CS

Holding temperature in Butte Creek	Temp.H	Jn-Se	-	USFWS, 1995	CS
Prespawn mortality rate	PrespawnM		-	USFWS, 1995	CS
Incubation and emergence					
Fall-winter low flows in tributaries (7Q10)	Flows.I	Oc-De*	+	Jager et al. 1997	KF, SF, CS
Egg-fry temperatures (avg of max daily)	Temp.I	Oc-De*	-	Friedman et al. 2019	KF, SF, CS
Egg-fry productivity	FW.surv		+	Hall et al. 2018	KF, SF, CS
Freshwater/delta residence					
Winter-spring tributary flows	Flows.T	Fe-My	+		CS
Winter-spring mainstem outmigration flows	Flows.O	De-My	+	Friedman et al. 2019	KF, SF, CS
Delta outflow index	Delta	Ap-Jl	+	Reis et al. 2019	SF, CS
7-day flow variation (SD)	SDFlow.O	De-My	-	Munsch et al. 2020	KF, SF, CS
Maximum flushing flows	Max.flow	No-Mr	+	Jordan et al. 2012	KF
Total annual precipitation	Precip	Annual	+	Munsch et al. 2019	KF, SF, CS
Spring outmigration temperatures	Temp.O	My-Jn	-	Munsch et al. 2019	KF, SF, CS
Spring closures of Delta Cross Channel	CChannel.S	Fe-Jl	+	Perry et al. 2013	SF, CS
Days floodplain bypasses were accessible	Floodpln	Annual	+	Limm and Marchetti 2009	SF, CS
Marine residence					
Coastal sea surface temperature	CSTarc	Mr-My	-	Wells et al. 2008	KF, SF, CS
North Pacific Index	NPI	Mr-My	+	Wells et al. 2008	KF, SF, CS
North Pacific Gyre Oscillation	NPGO	Mr-My	+	Wells et al. 2008	KF, SF, CS
Marine predation index	Predation		-	Friedman et al. 2019	SF, CS
Krill length**	Prey	Mr-Se	+	Robertson & Bjorkstedt 2020,	
Robertson et al. in prep.	KF				
Hatchery releases					
Release number	Releases		+	Sturrock et al. 2019	KF, SF, CS
Prop net pen releases	Net.pen		+	Sturrock et al. 2019	SF, CS
Release timing relative to spring transition	FW.Timing	Ja-Au	+	Satterthwaite et al. 2014	KF, SF, CS
Release timing relative to peak spring flow	M.Timing	Ja-Au	+	Sykes et al. 2009	KF, SF, CS

Since the mid-1980s, key indicator states have generally worsened over time, with some variation among years (see Fig. 3.8). Much of this pattern was driven by a rise in incubation, outmigration, and sea surface temperatures as well as recent droughts and a long-term decline in Sacramento River natural area spawners. Indeed, physical habitat conditions were especially poor for year classes that outmigrated in 2015 and 2016 (and returned predominantly in 2017 and 2018), and below average states have generally become more frequent thereafter. Different from other indicator patterns, the marine predation index during the early marine phase was especially severe for SRFC juveniles that outmigrated in 2005-2007 (and returned predominantly in 2007-2009), but has been relatively stable across other periods; this index is linked to common murre diets on SE Farallon Island. Notably, some indicators for year classes that migrated to sea in the past two years and are mostly yet to return or be harvested have approached more average or better levels. Improving indicators include SRFC incubation temperature, SRFC & CVSC outmigration flows, sea surface temperature, and North Pacific Index.

Outlooks for 2024-2026 return years

Because habitat metrics are leading indicators, linear statistical models that describe recruitment as a function of indicators in stoplight charts can be used to make predictions of future recruitment (harvest and spawners). As shown in Figure J.3, indicator-based models provide outlooks two years in advance of adult returns. For example, because most commercially harvested Chinook salmon in California are three-year olds, returns in 2026 will primarily reflect spawning and incubation conditions in 2023 and outmigration conditions in 2024. Below we summarize projected returns for 2025-2026 return years (2022-2023 brood years). For methodology see the Technical Documentation (Appendix V).

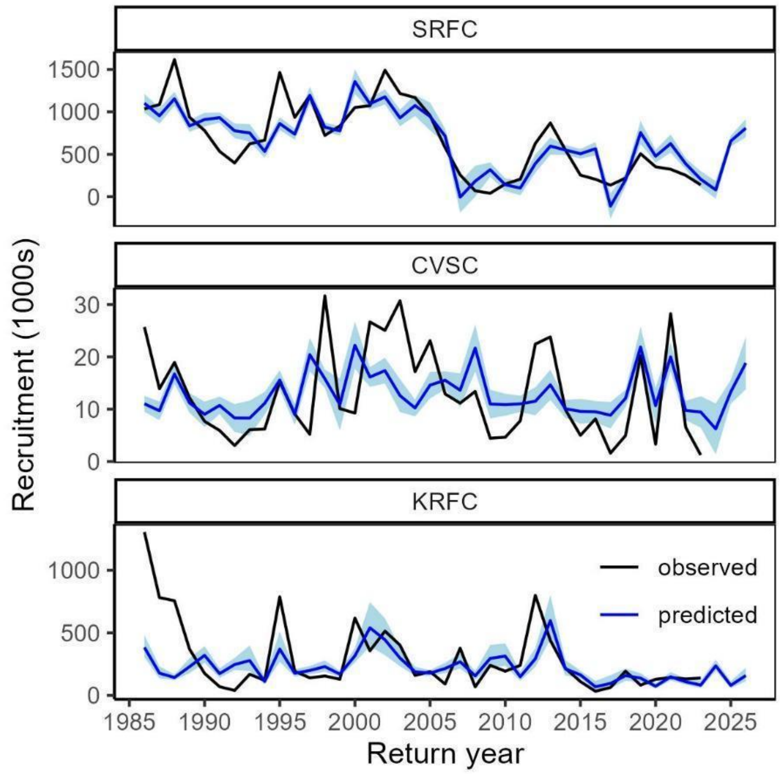

Fig. J.3 Observed recruitment and model-predicted recruitment. Stock-specific models were informed by stock-specific indicators in stoplight charts. Ribbons show one standard error above and below predictions.

Sacramento River Fall Chinook salmon: With a couple of exceptions, habitat indicators for SRFC in brood years 2022 and 2023 improved compared to previous (poor) years (Fig. 3.9). For example, incubation temperatures declined by up to two degrees and outmigration flows more than tripled. Consequently, indicator-based outlooks for Sacramento Fall Chinook recruitment (i.e., the Sacramento Index) in 2025 and 2026 are projected to improve from the 5th percentile (time domain for all California stock outlooks: 1986-2026) in 2024 to the 45th and 63rd percentiles in 2025 and 2026, respectively (Fig. J.3). One note of caution is that thiamine levels in eggs from the 2022 and 2023 broods indicate high levels of deficiency that could cause upward of 25% egg-fry mortality in natural spawners.

Central Valley Spring-run Chinook salmon: Like SRFC, CVSC runs experienced improving conditions recently, and so are projected to rebound from a time-series worst projected return in 2024. These projected increases are driven by improvements to outmigration flows in 2023 and 2024 outmigration years and smolts per spawner measured at traps in Butte Creek in 2024 (Fig. 3.9). The indicator-based outlooks are in the 63rd and 88th percentile for adults returning to hatcheries and natural areas in 2025 and 2026, respectively (Fig. J.3). These projections are also tempered by observations of high rates of thiamine deficiency; this may be a particular concern in a stock that largely depends on natural-origin spawning populations that did not benefit from thiamine supplementation in hatcheries.

Klamath River Fall Run Chinook salmon: For brood year 2022, habitat indicators improved slightly from the previous year but were still mixed (Fig. 3.9). In particular, near-average spawners, incubation and sea surface temperatures, and above average North Pacific Index did not fully offset higher outmigration temperatures, resulting in an outlook of ocean age-3 recruitment in the 5th percentile for 2025. Improvements in outmigration temperatures the following year, combined with above average North Pacific Index, results in an improved 33rd percentile outlook for the 2026 return that is nevertheless just above observed recruitment in 2023 (Fig. J.3). KRFC are less likely to be affected by thiamine deficiency, as anchovies are not a key prey item. As noted in the main body of this report, removal of the lowest four dams on the Klamath River in 2024 also adds uncertainty for adult return outlooks, which primarily will start affecting the 2027 adult return year.

As suggested by the SSC-ES in September 2022 (see H.1.a SSC-ES Report 1 March 2023), the CCIEA team is working with the STT and other advisory bodies to clarify how the indicator-based outlooks described above are interpreted and used. A primary purpose of developing quantitative indicator-based outlook models is to validate stoplight indicators. For example, these models can help assess the relative importance of individual indicators and identify non-stationary relationships among indicators and salmon metrics. The models are not necessarily intended for forecasting abundances in the coming years but can support the development of risk tables. For example, for one-year-out predictions, these indicator-based outlooks are intended to complement existing forecasts (sibling regressions for KRFC, jack-based regressions for SRFC, none for CVSC) by considering a wider range of factors that may capture effects on biological processes not well represented by sibling counts alone (e.g., changes in maturation rates or natural mortality after the first year in the ocean), or in the case of CVSC, that are available in time to potentially inform management. Considering these additional factors may inform the degree of precaution (or lack thereof) managers may want to apply when considering the forecasts arising from formally approved methods.

Appendix K — GROUNDFISH

Link to main section: Groundfish

K.1 Juvenile groundfish abundance

Strong year classes can determine age structure and set stock size for marine fishes, and may also indicate favorable environmental conditions, increased future catches, and impending potential bycatch issues. Here, we provide estimates of juvenile abundance for 13 species of West Coast groundfishes including four from the DTS assemblage (Dover sole, shortpine and longspine thornyheads, and sablefish). This assemblage is a valuable West Coast groundfish fishery, and bycatch of some species, like small sablefish and shortspine thornyheads, can impact other fisheries such as the at-sea hake fishery.

Relative abundance (scaled to 0-1) of the juveniles of 13 groundfish species is shown in Figure K.1. The data represent juvenile abundance but not recruitment because it was necessary to combine multiple age classes for most species, with some exceptions. Data are from the NOAA Fisheries West Coast Groundfish Bottom Trawl Survey (WCGBTS). Juvenile sablefish abundance was high in 2024 (Fig. K.1) but comparable to the last 3-4 years. Longspine thornyhead showed a large increase in 2022 and 2023 but slightly lower abundance in 2024 (Fig. K.1). The abundance of arrowtooth flounder juveniles has declined over the last three years, while multiple species showed longer-term decreases in juvenile abundance, but less recent variability.

Note, in previous reports, a single distribution model was used for all species. For 2024, models were tailored to individual species by evaluating multiple error distributions and different forms of depth (linear, smoothed, quadratic), so there are some minor changes in the time series, most notably the extremely high sablefish abundance in 2022 is more muted in the updated analysis. See the online Technical Documentation and/or Appendix V for details.

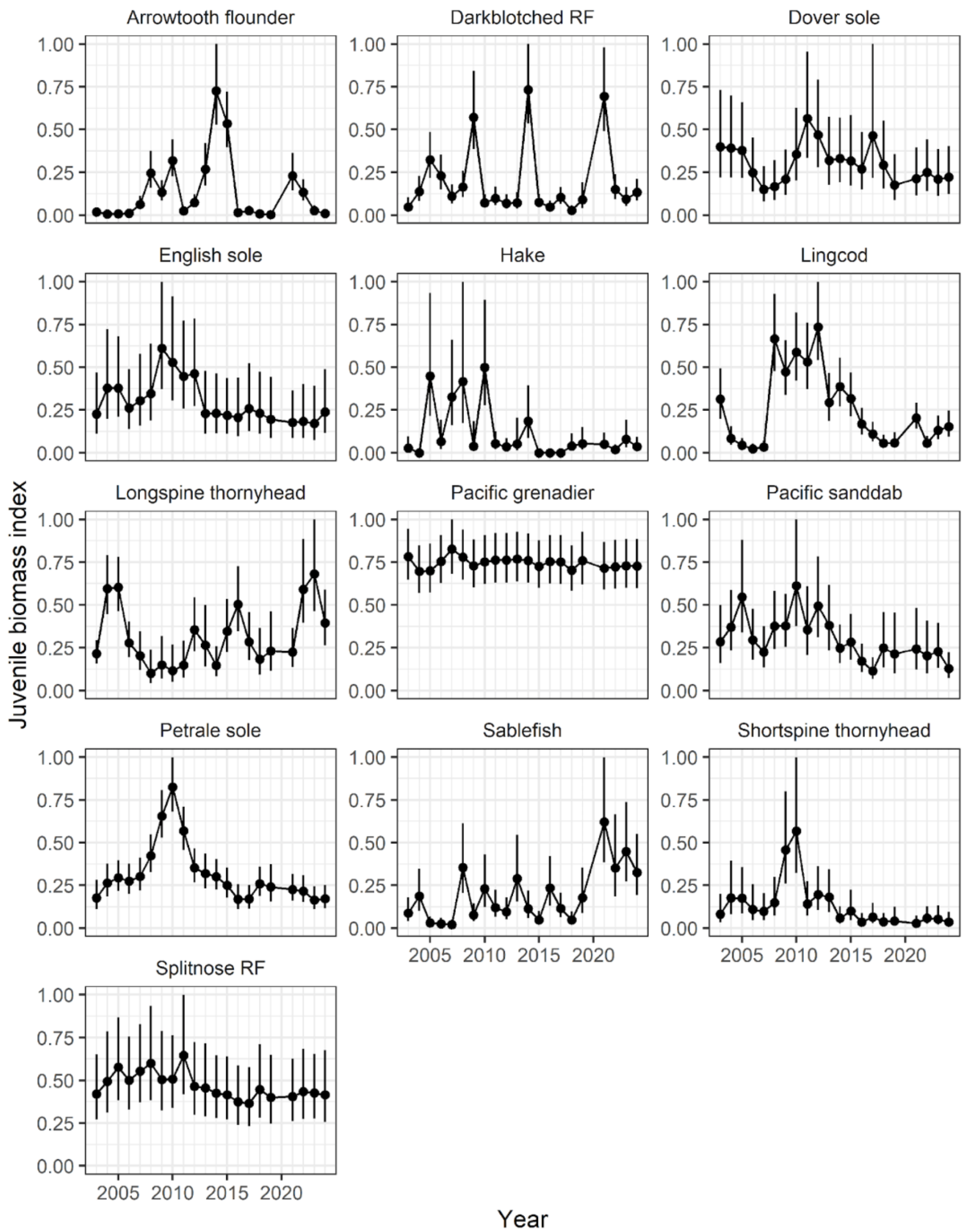

Figure K.1: Abundance indexes of 13 juvenile groundfishes from the WCGBTS for 2002-2024. No data are available from 2020 due to COVID restrictions. Error bars represent 95% CL. Total biomass was scaled to 0-1 by dividing by the maximum CL for that species.

The size structure of sablefish in 2024 compared to other years (Fig. K.2) suggests a combination of good recruitment and abundant, relatively small age-1 individuals from 2023, perhaps due to density dependence impacting growth of the strong 2023 cohort. Fish less than 29 cm are typically age-0 fishes (Tolimieri et al. 2020), and in many years there is a mode of smaller fish around 25 cm (Fig. K.2). However, in 2022 and 2024 there are many fish in the 27-30 cm range, suggesting relatively slow growth of the previous year's cohort, which may have been the result of density-dependent growth following high abundances in 2021 and 2023.

For sablefish, recent increases in juvenile abundance coincide with probability of occurrence and abundance in the northern portion of the west coast from 2014 onwards, including strong coast-wide recruitment in recent years (Fig. 3.11). When longspine thornyhead juveniles were abundant, they tended to occur in the northern and southern portions of the coast (Fig. K.3).

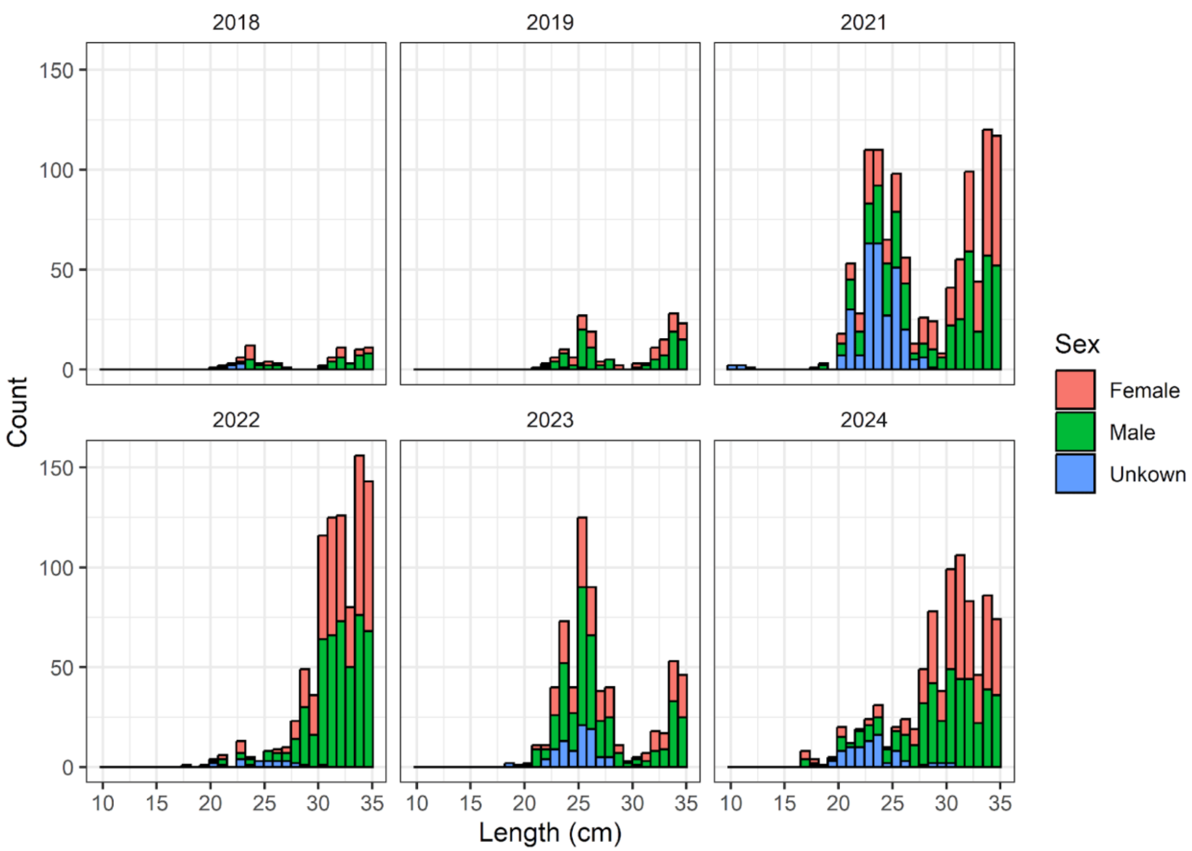

Figure K.2: Size distributions of sablefish less than or equal to 35 cm for recent years.

We examined variability in the distribution of sablefish (Fig. 3.11) and longspine thornyhead (Fig. K.3) because juvenile abundance of both species was high over the last 3-4 years. The following results are from species distribution models using delta-lognormal error distributions, which combine a presence/absence model and abundance-when-present model to estimate biomass. Probability of occurrence was calculated from the presence/absence model, while abundance is the estimate from the full species distribution model.

Occurrence of sablefish (Fig. 3.11a) shifted north after about 2014, although high juvenile abundance was still associated with coastwide recruitment (Fig. 3.11b). See also Section 3.4

Juvenile longspine thornyheads were both more frequent (Fig. K.3a) and more abundant (Fig. K.3b) at depth than in shallower regions. Probability of occurrence tended to be higher at the northern and southern ends of the West Coast.

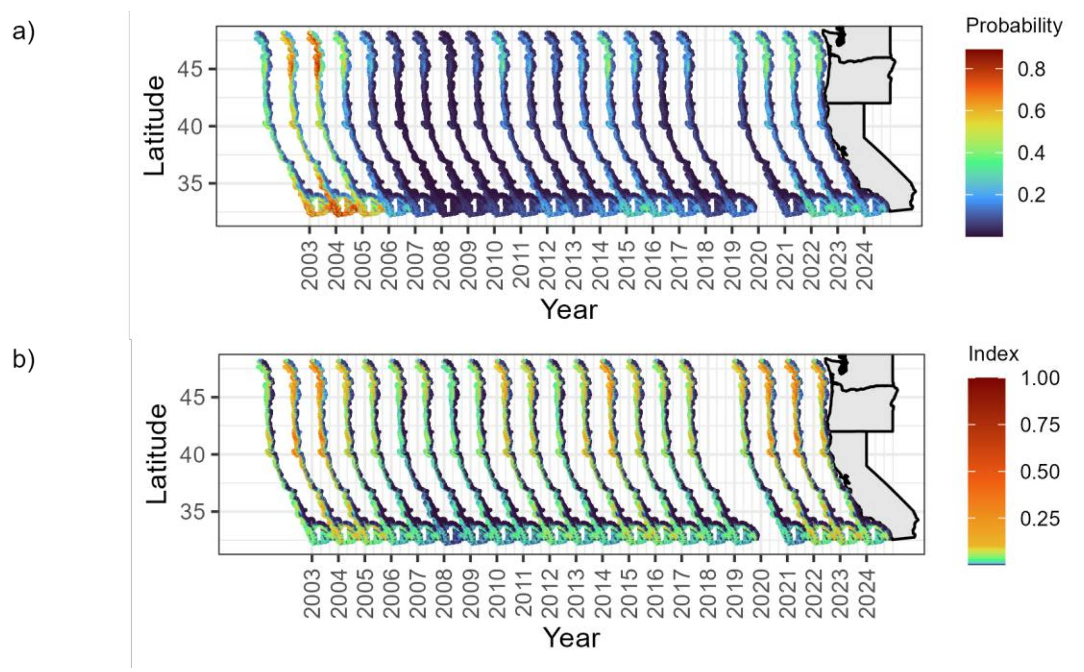

Figure K.3: Distribution of juvenile longspine thornyheads along the west coast from the species distribution model. a) probability of occurrence, and b) index of abundance (scaled to 0-1).

K.2 Juvenile sablefish: Availability to hake and salmon ports

Bycatch of juvenile sablefish can impact other fisheries, especially the hake (Pacific whiting) and salmon fisheries. The relative availability of juvenile sablefish (≤ 29 cm) was calculated for selected ports along the West Coast that have high hake or salmon catches.

Biomass from the analysis of juvenile abundance (Section K.1) was summed within 232 km of a port for hake ports and within 65 km of a port for salmon ports.

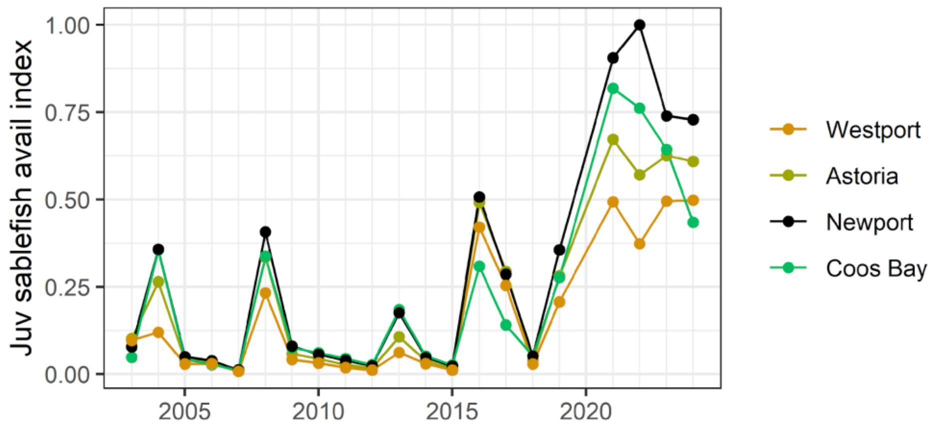

Figure K.4: Index of availability of juvenile sablefish (≤ 29 cm) to selected ports along the West Coast that fish heavily for Pacific hake. Availability was calculated within a 232 km radius. Annual values were scaled to 0-1 by dividing by the maximum observed biomass.

In 2024, the availability of juvenile sablefish to most hake ports was similar to 2023 (Fig. K.4), with the exception of Coos Bay where availability has declined consistently since 2021. Newport and Astoria had the highest relative abundance of juvenile sablefish within the 232 km fishing radius.

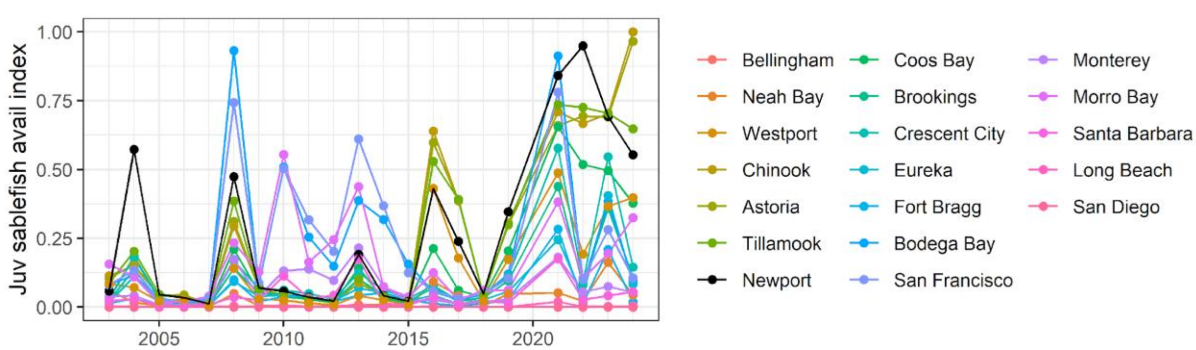

Figure K.5: Index of availability of juvenile sablefish (<30 cm) to selected ports along the West Coast that fish for salmon. Availability was calculated within a 65 km radius. Annual values were scaled to 0-1 by dividing by the maximum observed biomass.

For salmon ports, the availability of juvenile sablefish within a 65 km radius from the port was medium to high in 2023 but declined in 2024, with a few exceptions (Fig. K.5). Availability increased for Astoria, Chinook, Westport, and Morro Bay.

K.3 Center of gravity for groundfishes

Shifts in groundfish spatial distributions can impact the availability of target species to fisheries as well as bycatch rates. We used species distribution models to evaluate potential shifts in groundfish distributions over time (following Selden et al. 2020, but with models run in the sdmTMB package). We tracked changes in the center of gravity (CoG) of groundfish stock biomass distributions using the WCGBTS data (Keller et al. 2017). We applied these analyses to 12 species that compose a large component of groundfish landings, or that have broader management interest. For this report model structures were updated to include a delta-lognormal model structure with depth included as a smoothed variable. This change resulted in better residuals and muted some of the previous high values, but produced otherwise quantitatively and qualitatively similar results. See Technical Details for more information. Note, these analyses are for total biomass for each species, not juvenile biomass as in the previous section.

The CoG of lingcod, longnose skate, petrale sole, and sablefish has shifted to the north over time (Fig. K.6). For sablefish, the northern shift over the past 10 years returned the CoG to approximately 41.5 °N, about a degree farther north than in 2003. This shift may be due to recent strong recruitment along the northern West Coast (Fig. 3.11). For petrale sole the pattern was similar, although the CoG shift was only about 0.5 °N to 42.5 °N. Some species like shortbelly rockfish and shortpine thornyhead shifted north over the last 20 or so years, but their distribution over the last ~10 years has been variable but the changes not directional.

The CoG of Dover sole and several other groundfish species varied over time with no clear latitudinal trend (Fig. K.6).

Estimates of the relative availability of groundfish biomass to fishing ports over the same period are in the next section and long-term projections of groundfish species distributions under climate change are included in Appendix E.

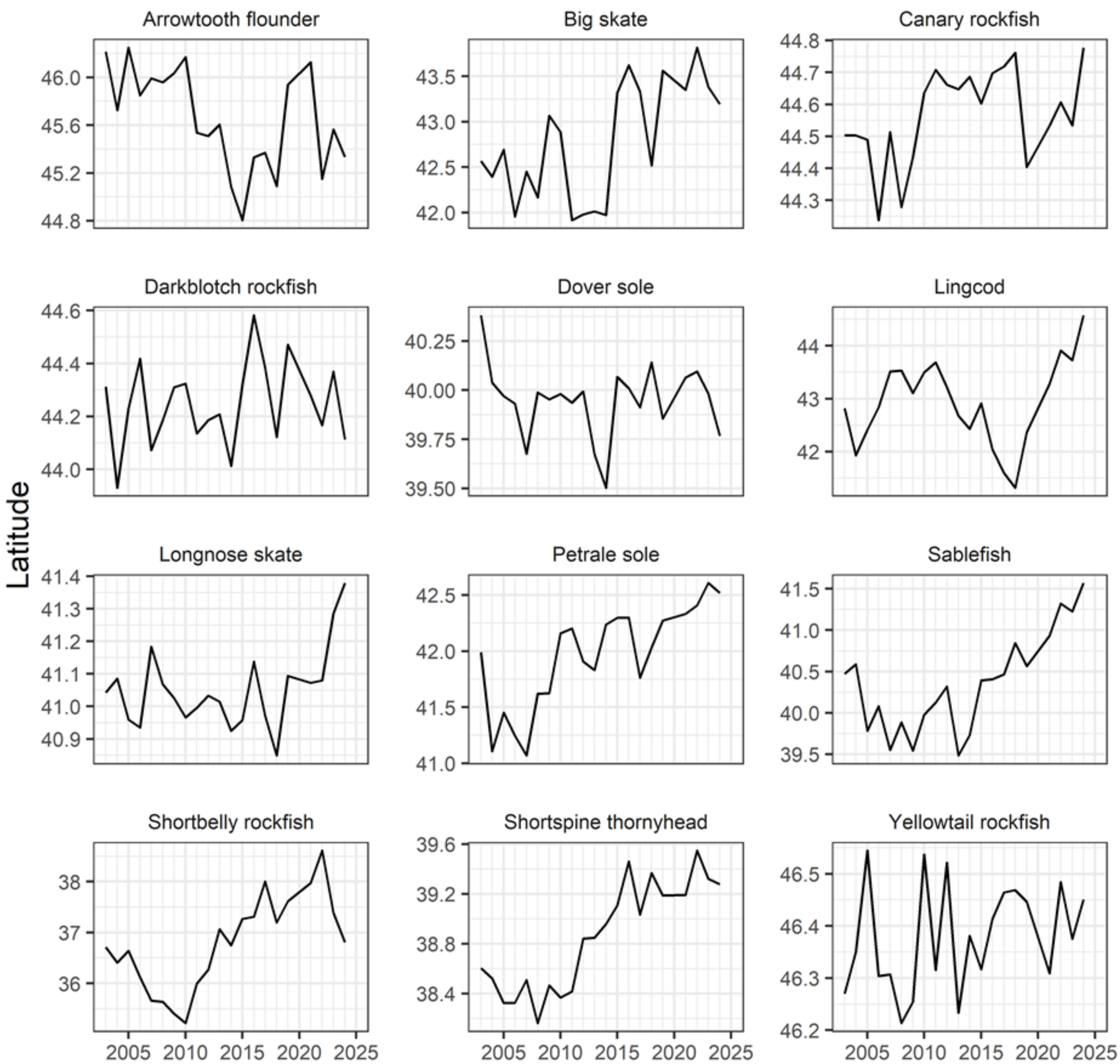

Figure K.6: Center of gravity of biomass of 12 groundfish species along the West Coast.

K.4 Availability of groundfishes to ports

The spatial distribution of a species' biomass impacts its availability to individual ports and represents a difference in fishing opportunity to fleets. We used the results of the spatial distribution models in Appendix K.3 to calculate availability of groundfish to ports. Biomass available to a port was determined for each port by summing the biomass within a radius from that port based on the 75th quantile of the distance traveled from port to harvest of species of interest, weighted by catch (Fig. K.7), as measured by trawl logbooks. See Selden et al. (2020) and the Technical Documentation for more details.

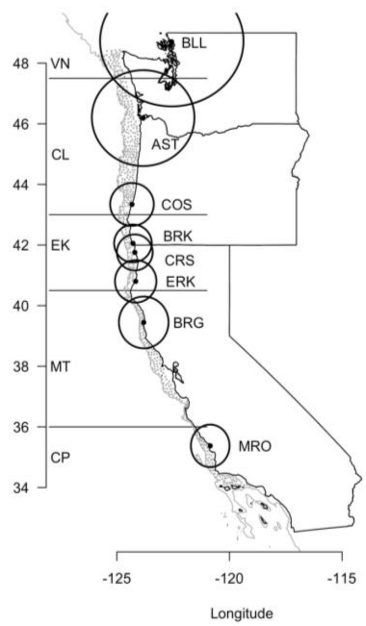

Figure K.7: Location of ports used in the Availability Analysis. The radii of the black circles centered on each port represent the areas within which groundfish availability is estimated (see text). Ports are Bellingham Bay (BLL), Astoria (AST), Charleston (Coos Bay, COS), Brookings (BRK), Crescent City (CRS), Eureka (ERK), Fort Bragg (BRG) and Morro Bay (MRO). Gray line is the 1200-m contour.

Fishers delivering to the northern ports of Astoria and Bellingham typically had access to more fish than other ports, with the exception of shortbelly rockfish (Fig. K.8). Shortbelly were more available to central/southern ports including Brookings, OR and Morro Bay, CA. While there has been interannual variability, the overall relationships among ports has remained fairly stable over the past decade. However, sablefish have become much more available to fishers from Astoria over the last five years.

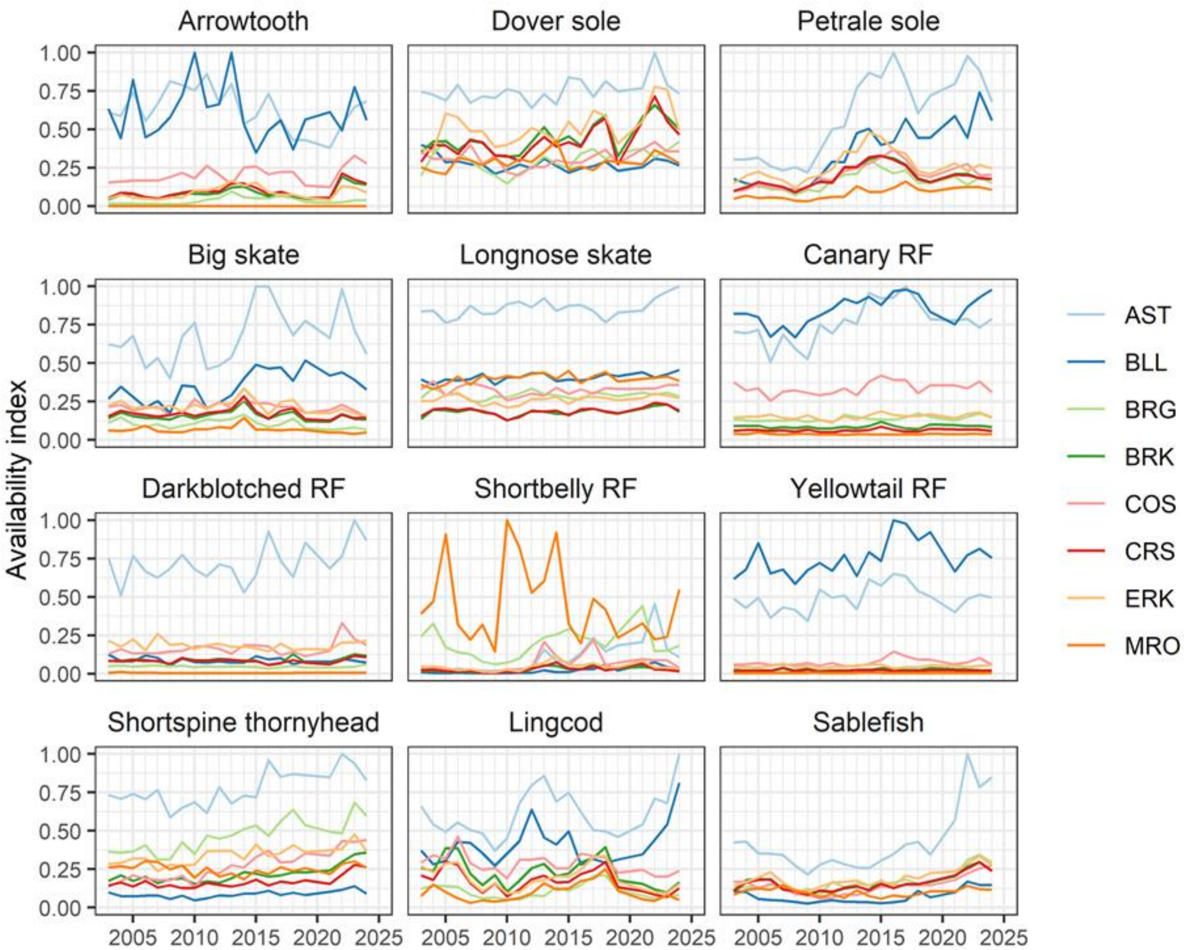

Figure K.8: Indices of availability of biomass of twelve (12) groundfish species to selected ports along the West Coast. Ports are Bellingham Bay (BLL), Astoria (AST), Charleston (Coos Bay, COS), Brookings (BRK), Crescent City (CRS), Eureka (ERK), Fort Bragg (BRG) and Morro Bay (MRO). Total biomass was scaled to 0-1 by dividing each estimate by the maximum observed yearly biomass for that species.

Appendix L — HIGHLY MIGRATORY SPECIES (HMS)

Link to main section: Highly Migratory Species

L.1 HMS Stock Assessment Information

Biomass and recruitment estimates for many HMS stocks that occupy the California Current are available from stock assessments conducted by collaborators under the International Scientific Committee for Tuna and Tuna-like Species in the North Pacific Ocean (ISC) or the Inter-American Tropical Tuna Commission (IATTC). The only assessment updates since last year's ecosystem status report are for Pacific bluefin tuna, skipjack tuna, and bigeye tuna.

The 2024 bigeye tuna assessment underwent several changes since the last benchmark assessment (Xu et al. 2024) The assessment uses a risk analysis approach, encompassing three levels of hypotheses structured hierarchically to address the main uncertainties in the assessment. The time-series shown here are multi-model estimates. The 2024 skipjack tuna assessment is a significant improvement over the 2022 interim assessment (Bi et al. 2024). It reflects major advancements in the assessment methodologies and incorporates new data sets, including tagging data. The Pacific bluefin tuna assessment also included some improvements to the model used in the last (2022) benchmark assessment (ISC 2024). One of the major changes made was to shorten the assessment time period to start in 1983 instead of 1952. This adjustment was implemented because more reliable data were available after 1983. For all species, we emphasize that the status and trends symbols shown in Figure L.1 and Figure L.2 reflect short-term patterns relative to time series averages (with a period of reference of 1991-2020), and do not necessarily reflect reference points based on, e.g., unfished stock biomass.

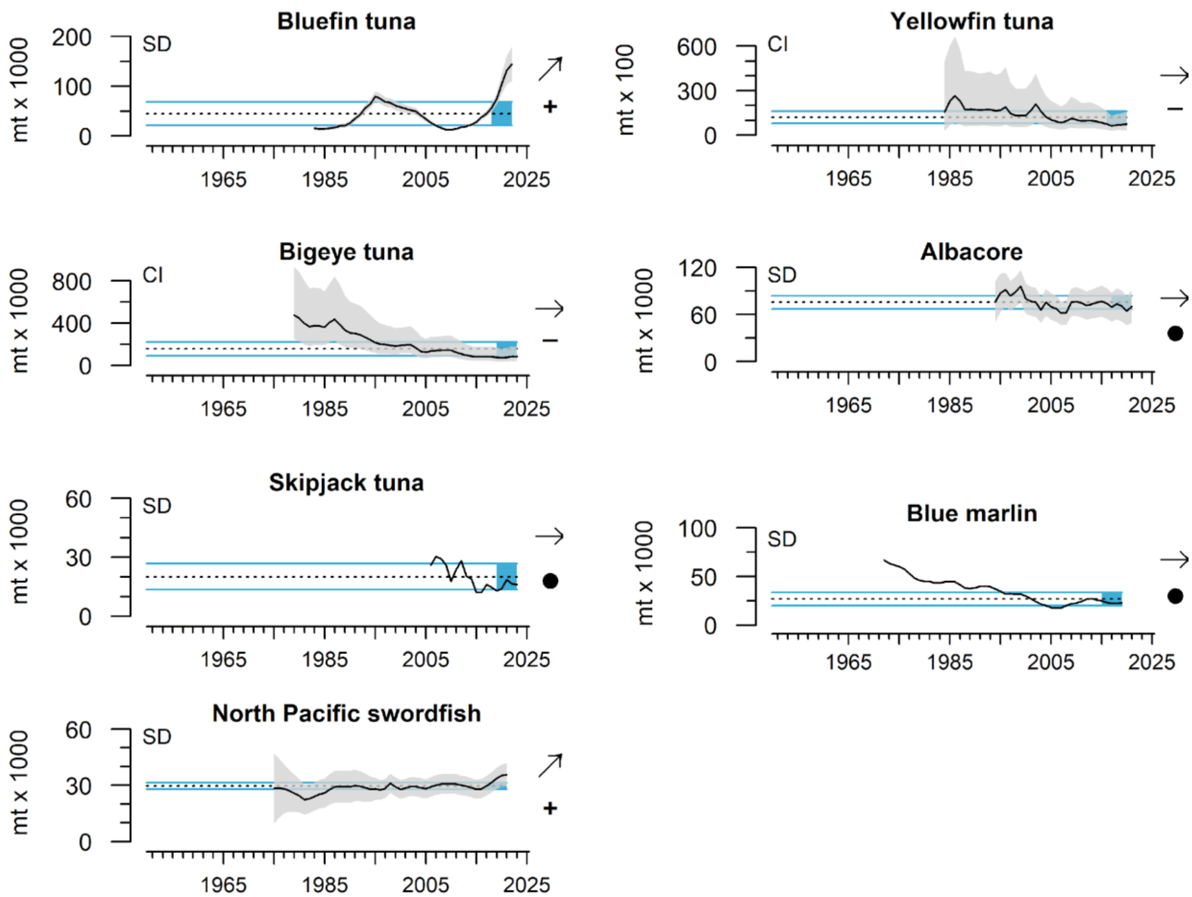

Figure L.1: Spawning biomass for highly migratory species in the north Pacific. The type of error envelope is indicated in the upper left of each panel: SD = ±1 s.d.; SE = ±1 s.e.; CL = ±95% C.L. Assessment dates were: Albacore (2023), Bigeye tuna (2024), Blue marlin (2021), Bluefin tuna (2024), Eastern Pacific swordfish (2012), Skipjack tuna (2024), North Pacific swordfish (2023), and Yellowfin tuna (2020). Lines, colors, and symbols are as in Fig. 2.1.

The most recent spawning stock biomass estimates range from >1 s.d. above the assessment time series average (bluefin tuna, swordfish) to ~1 s.d. below average (yellowfin tuna, bigeye tuna), with generally wide error estimates (Fig. L.1). Estimated SSBs of bluefin tuna and swordfish have positive five-year trends. HMS recruitment trends from the most recent assessments are generally trending either neutrally (bluefin tuna, skipjack tuna, swordfish) or positively (bigeye tuna, yellowfin tuna, blue marlin) typically with high uncertainty (Fig. L.2). One exception is albacore tuna, which has a negative five-year recruitment trend, albeit with high uncertainty.

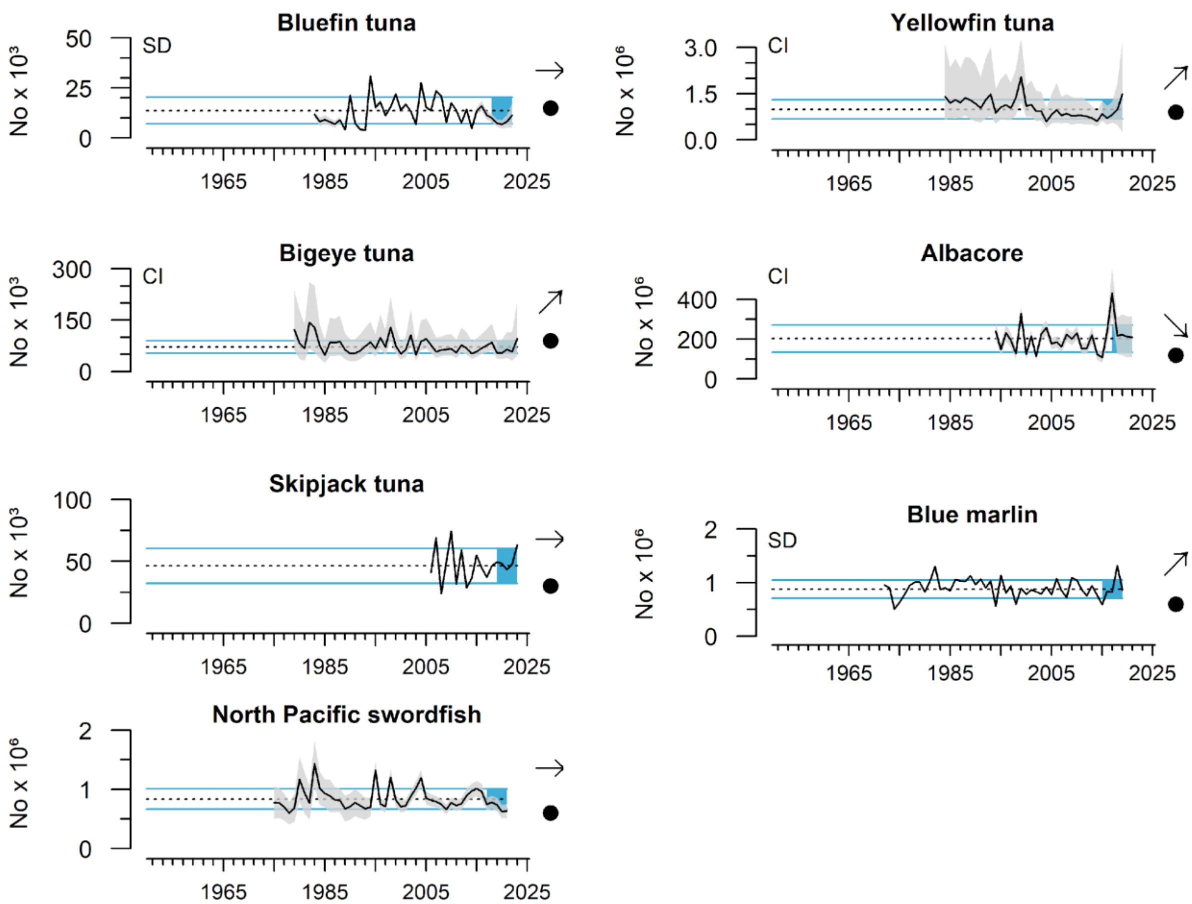

Figure L.2: Recruitment for highly migratory species in the North Pacific. The type of error envelope is indicated in the upper left of each panel: SD = ±1 s.d.; SE = ±1 s.e.; CL = ±95% C.L. Assessment dates were: Albacore (2023), Bigeye tuna (2024), Blue marlin (2021), Bluefin tuna (2024), Eastern Pacific swordfish (2012), Skipjack tuna (2024), North Pacific swordfish (2023), and Yellowfin tuna (2020). Lines, colors, and symbols are as in Fig. 2.1.

L.2 HMS Diet Information

Highly mobile predators are capable of responding rapidly to spatial shifts in oceanographic conditions and prey fields. Quantifying the diets of highly migratory fishes in the CCE can complement existing trawl-based assessments of the available forage, provide insight into how forage varies over time and space, as well as provide a direct metric of forage utilization. Albacore Tuna, Bluefin Tuna, and Broadbill Swordfish are opportunistic predators that consume a wide variety of prey taxa across a range of depths and habitats.

Albacore, Bluefin, and Swordfish stomachs were provided by commercial and recreational fishers, and prey were identified from whole or hard part remains and are reported as a mean proportional abundance. Diet data for four key prey groups are summarized in Figure 3.12 in the main section, and a broader subset of prey species are presented here focusing on prey that are either themselves under a management plan, or considered ecosystem component species, to highlight their links to highly migratory species. Juvenile Albacore Tuna were collected off Northern California, Oregon, and Washington during the summer and fall fishing season. Bluefin Tuna were collected by recreational fishers in the Southern California Bight from spring until early fall. Swordfish were collected off Southern and Central California during the commercial drift gillnet season (August 15th through January 31st). Swordfish stomachs are classified by the year the fishing season began (stomachs from January are assigned to the previous year's fishing season). Data are available through 2023 for all three highly migratory species (see Figs. L3, L4 and L5).

During a Fishermen and Scientist roundtable in November 2024, Oregon fishermen noted a 'market basket' feed pattern for Albacore Tuna, coho salmon and other fish predators, which suggests that a wide variety of prey were available to these predators in summer and early fall in the northern CCE.

Figure L.3: The proportion of prey items in Bluefin tuna diets, 2008-2023. Lines, colors, and symbols are as in Fig. 2.1.

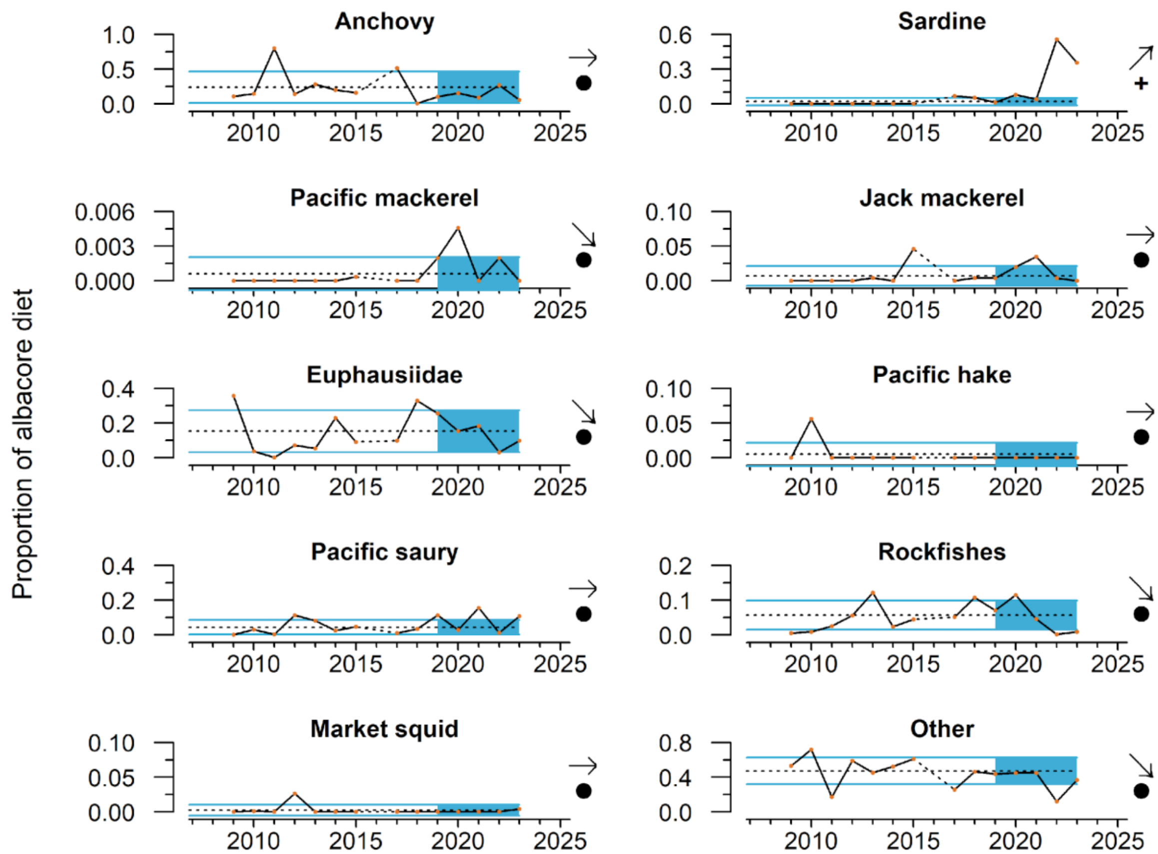

Figure L.4: The proportion of prey items in Albacore diets, 2009-2023. Lines, colors, and symbols are as in Fig. 2.1.

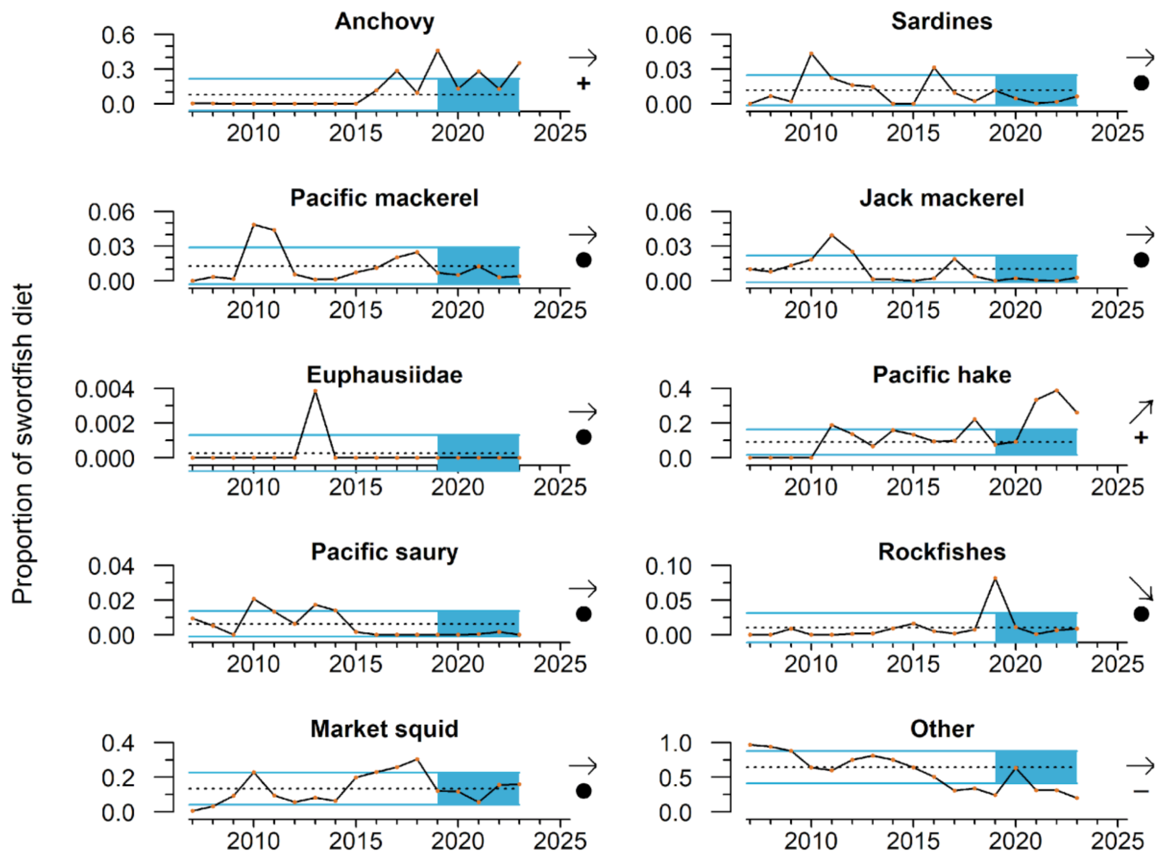

Figure L.5: The proportion of prey items in Swordfish diets, 2007-2023. Lines, colors, and symbols are as in Fig. 2.1.

Appendix M — SEABIRD PRODUCTIVITY, DIET, AT-SEA DENSITY, AND MORTALITY

Link to main section: Seabirds

M.1 Seabird Productivity

Seabird population productivity, as measured through indicators of reproductive success, tracks marine environmental conditions and often reflects forage production near breeding colonies. We monitor and report on standardized anomalies of fledgling production per pair of breeding adults for one species at Destruction Island, Washington and three species at Yaquina Head, Oregon in the Northern CCE and five species on Southeast Farallon Island in the Central CCE. Collectively, these focal species span a range of feeding habits and ways of provisioning their chicks, and thus provide a broad picture of the status of foraging conditions.

- **Brandt's cormorants** forage primarily on pelagic and benthic fishes in waters over the shelf, generally within 20 km of breeding colonies; they return to the colony during the day to deliver regurgitated fish to their chicks.
- **Cassin's auklets** forage primarily on zooplankton near or on the shelf break, generally within 30 km of colonies; they forage by day and night and return to the colony at night to feed chicks.
- **Common murres** forage primarily on pelagic fishes in waters over the shelf and near the shelf break, generally within 80 km of colonies; they return to the colony during daylight hours to deliver single whole fish to their chicks.
- **Pelagic cormorants** forage primarily on pelagic and benthic fishes in waters over the shelf, generally within 20 km of breeding colonies; they return to the colony during the day to deliver regurgitated fish to their chicks.
- **Pigeon guillemots** forage primarily on small benthic and pelagic fishes over the shelf in the nearshore environment, generally within 10 km of colonies; they return to the colony during the day to deliver single fish to chicks.
- **Rhinoceros auklets** forage primarily on pelagic fishes over the continental shelf, generally within 50 km of colonies; they return to the colony after dusk to deliver multiple whole fish to their chicks.

Northern CCE

In the Northern CCE, productivity of rhinoceros auklets is monitored on Destruction Island, located 6 km off the outer coast of Washington. In 2024, rhinoceros auklet chick productivity was just below the long-term average. Fledgling production has shown an increasing trend since 2021, when it reached its lowest level since 2008 (Fig. M.1).

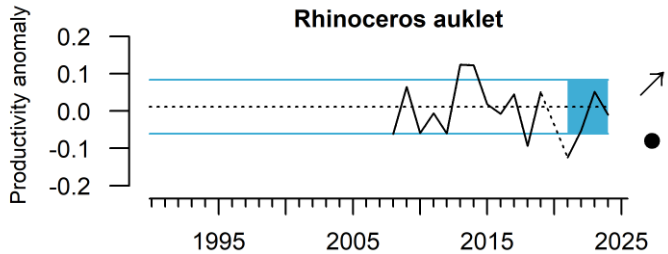

Figure M.1: Standardized productivity anomalies for rhinoceros auklet breeding at Destruction Island, WA through 2024. Data courtesy of S. Pearson, WDFW. Lines, colors, and symbols are as in Fig. 2.1.

The productivity of common murres and Brandt's and pelagic cormorants is monitored at Yaquina Head on the central Oregon coast. Fledgling production in 2024 varied among these three monitored seabird species (Fig. 3.13). Brandt's cormorant fledgling production was above average in 2024 and has been significantly greater than the long-term average over the past five years. Common murres experienced near breeding failure again in 2024, a drop from the average chick production in 2023; chick productivity has also oscillated between average and very low for the past five years. Bald eagle disturbance at this location again contributed to near breeding failure at this site, although high success of common murres breeding at a neighboring colony suggests Yaquina Head murres were more limited by predation than bottom-up factors (Kennerley and Orben, unpubl. data). Pelagic cormorants nested later than usual at Yaquina Head in 2024, fledging far fewer chicks per nest than in 2023; chick productivity has also been quite variable over the past five years.

Central CCE

On the central California coast, productivity of several seabird species is monitored on Southeast Farallon Island, located 48 km west of San Francisco Bay. In 2024, productivity was good for most of the monitored species (Fig. M.2). Pigeon guillemots, Cassin's auklets, rhinoceros auklets, and common murres fledgling production was near average and showed continuing recovery from production that was well below average in 2019. In contrast, the productivity of Brandt's cormorants declined to well below average in 2024, a deviation from positive productivity anomalies observed over the last ten years. The cause is not known with certainty but appears to be part of normal variability. Poor local conditions during winter and early spring associated with the El Niño likely limited prey resources and led to poor adult condition when initiating breeding. Pairs that bred in May and June abandoned those attempts, while those that bred later enjoyed improved ocean conditions and prey abundance. Clutch sizes were small in 2024 (~2 eggs/nest instead of 4-5), and hatching success was low (<20%), leading to fledging success for those that hatched of approximately 50%. All these factors suggest birds that were energetically stressed earlier in the breeding season and not able to support successful breeding attempts.

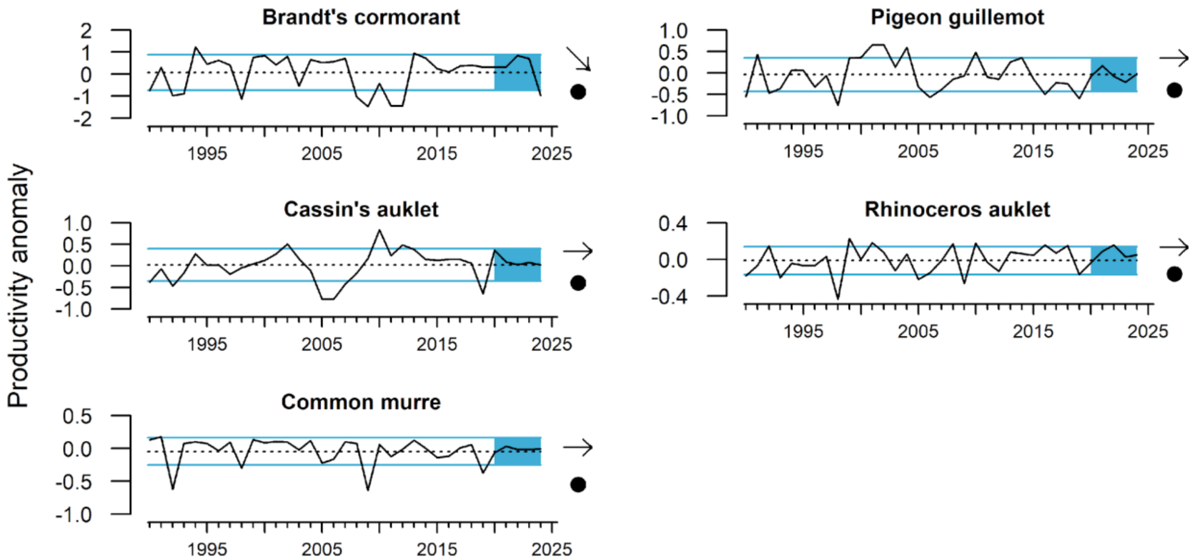

Figure M.2: Standardized productivity anomalies for five seabird species breeding at Southeast Farallon Island, CA through 2024. Data courtesy of Jaime Jahncke, Point Blue Conservation Science. Lines, colors, and symbols are as in Fig. 2.1.

M.2 Seabird Diets

Seabird diet composition during the breeding season often tracks marine environmental conditions and reflects production and availability of forage within regions of the CCE. Here, we present seabird diet data from the northern and central regions to help shed light on foraging conditions in 2024.

Northern CCE

Rhinoceros auklet chick diet data have been collected at Destruction Island, WA since 2008 (Fig. M.3). In 2024, northern anchovy jumped to 17% of the diet, after being nearly absent from diet samples since 2018. The RREAS and CPS surveys indicate that anchovy were abundant in the Central and Southern CCE, however catches of anchovy in the northern region were low and Pacific herring were more prevalent (Sections 3.2.1 & 3.2.2, and Appendices I & H). The proportion of Pacific herring in the diet was just above the long-term mean, around which it has hovered since a peak in 2018. The proportion of Pacific sand lance in the diet in 2024 was above average, as it was in 2023. The peak value for sand lance in 2021 (62%) results in the recent short-term mean being significantly above the long-term mean, even while the short-term trend is negative over that same time. Smelts comprised just under half of the observed chick diet in 2024; resulting in a recent short-term mean significantly greater than the long-term mean and an increasing short-term trend. This is consistent with the high number of smelt collected by the May NCC ecosystem survey off the Oregon and Washington coasts (Appendix I). Rockfish juveniles formed a relatively small (4%) proportion of the observed rhinoceros auklet chick diet in 2024, close to the long-term mean.

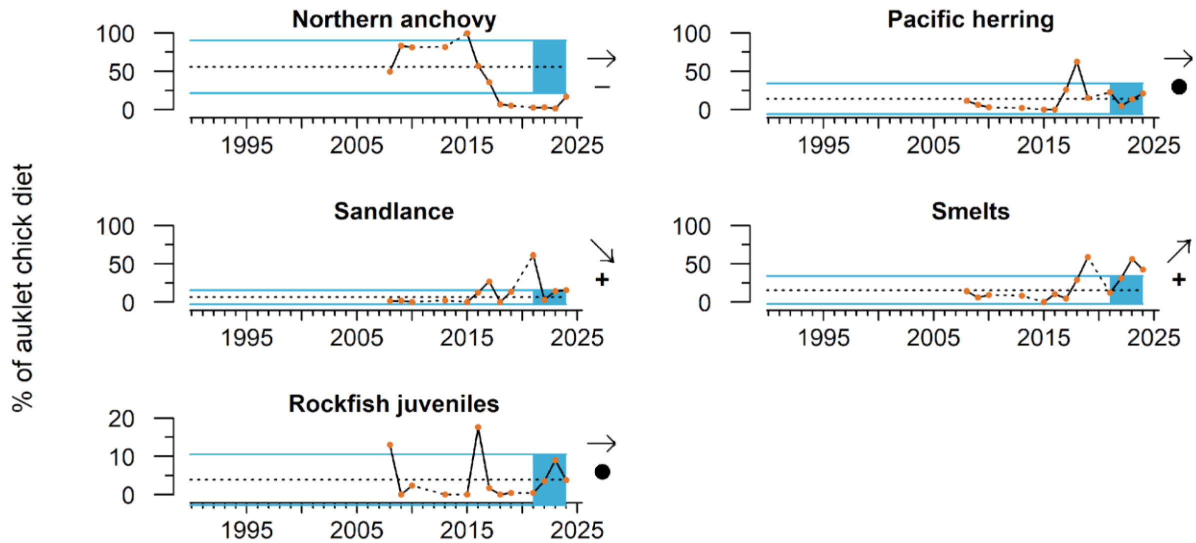

Figure M.3: Percentages of key prey items delivered to rhinoceros auklet chicks at Destruction Island, WA through 2024. Data courtesy of S. Pearson, WDFW. Lines, colors, and symbols are as in Fig. 2.1.

Common murre chick diet data have been collected at Yaquina Head, OR since 1998 (Fig. M.4). Smelts have dominated the diet of common murres at Yaquina Head since 2010, and in 2024, the proportion of smelts in diets was well above average, resulting in an increasing short-term trend. The proportion of Pacific sand lance was below average, resulting in a short-term decline. The proportion of herring and sardines in the chick diet was below average in 2024. Flatfishes comprised a very small proportion of the chick diet in 2024, as they have since peaking at 33% in 2018. The proportion of rockfish juveniles in the chick diet in 2024 was above average as it was in 2023 and showed an increasing trend over the last five years. High numbers of young-of-year rockfish have been caught in this region by the NCC ecosystem survey over the past few years as well (Appendix I). Pacific salmon juveniles were not documented in the chick diet in 2024; the peak of salmon in chick diets in 2021 (16%) results in a short-term mean significantly greater than the long-term mean even while its short-term trend is declining over the same period. Notably, Pacific salmon comprised 10% of over 200 common murre bill loads in 2024 at a colony further north at Haystack Rock in Cannon Beach, OR (Kennerley and Orben, unpubl. data).

The prevalence of these fishes in Yaquina Head murre diet has been associated with high murre reproductive success (Gladics et al. 2015), and common murre productivity was high at a nearby murre colony in Depoe Bay, OR (Kennerley and Orben, unpubl. data). Thus, nearby ocean conditions were likely favorable for common murre reproduction but negated by eagle disturbance.

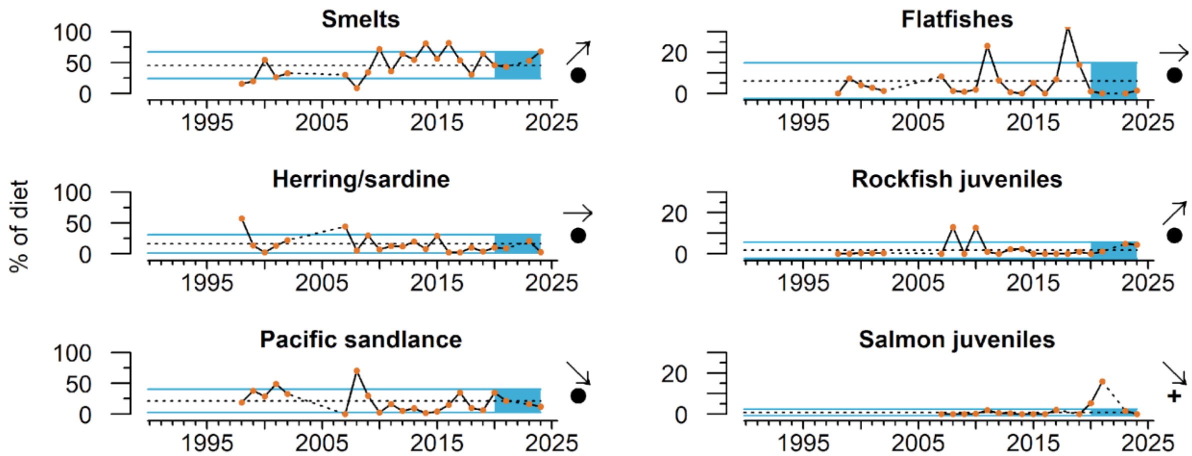

Figure M.4: Percentages of key prey items delivered to common murre chick diets at Yaquina Head, OR through 2024. Data courtesy of R. Orben, Oregon State University. Lines, colors, and symbols are as in Fig. 2.1.

Central CCE

Diet data have been collected for seabirds at breeding colonies on Southeast Farallon Island for more than 30 years. These colonies are close to the most intense upwelling region in the California Current and are thus a valuable source of information about system productivity and prey availability to higher trophic levels. In 2024, most piscivorous birds at this colony relied less on northern anchovy and more on juvenile rockfish for the first time in several years (Fig. M.5). The proportion of rockfish juveniles in the diet of Brandt's cormorants in 2024 was one of the highest observed and showed an increasing trend over the last five years. By contrast, the proportion of northern anchovy in the diet was well below average and the lowest observed since 2015, resulting in a declining short-term trend. The diet in 2024 showed reduced numbers of fish in samples; reduced reliance on northern anchovy was also observed, which has been associated with poor productivity. Similar trends were observed in the time series of rockfish and anchovy in the diets of rhinoceros auklets and common murres. These patterns reflect the increasing trend of juvenile rockfish in the Central CCE in recent years, however adult and juvenile anchovy were abundant in this region in 2024 as well (Fig. I.3).

While low relative to other prey, the proportion of Pacific salmon in the diet of common murres in 2024 was near the long-term mean and showed an increasing short-term trend, driven by results from 2023 and 2024. For planktivorous Cassin's auklets, the proportion of cold-water taxa such as krill (primarily *Euphausia pacifica* and *Thysanoessa spinifera*) was above average in 2024 (Fig. M.5) and has oscillated around the long-term mean since 2019. This general pattern is consistent with trends in krill abundance off central California over the same time period (Figure I.3). Mysids, which are warm-water taxa, dropped out of the diet in 2024.

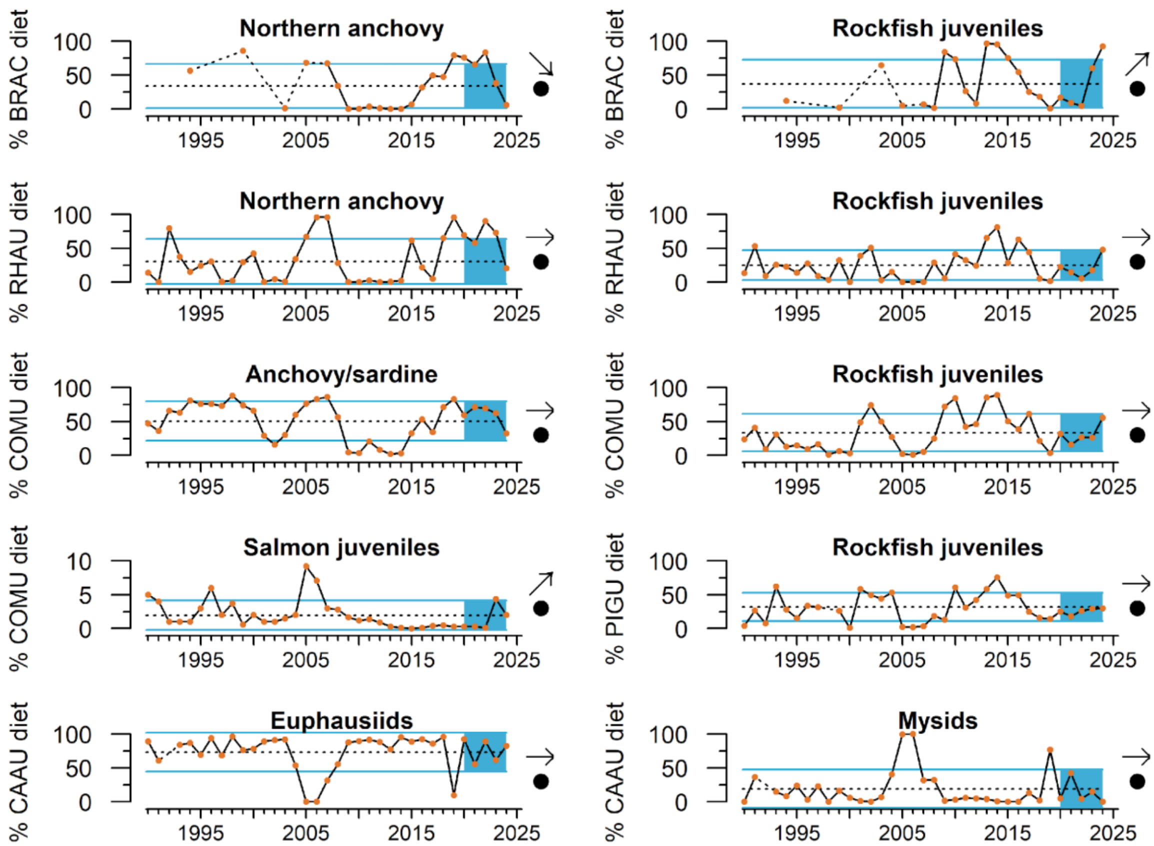

Figure M.5: Percentages of key prey items delivered to seabird chicks at Southeast Farallon Island, CA through 2024. BRAC = Brandt's cormorant; RHAU = rhinoceros auklet; COMU = common murre; PIGU = pigeon guillemot; CAAU = Cassin's auklet. Data provided by J Jahncke, Point Blue Conservation Science. Lines, colors, and symbols are as in Fig. 2.1.

M.3 Seabird At-Sea Density

Seabird densities on the water during the breeding season can track marine environmental conditions and may reflect regional production and availability of forage. Data from this indicator type can establish habitat use and may be used to detect and track seabird population movements or increases/declines as they relate to ecosystem change. We monitor and report on at-sea densities of three focal seabird species in the Northern, Central, and Southern CCE.

- **Sooty shearwaters** migrate to the CCE from the southern hemisphere in spring and summer to forage near the shelf break on a variety of schooling pelagic fish, squid and krill.

- **Common murres** and **Cassin's auklets** are resident species that feed primarily over the continental shelf; Cassin's auklets prey mainly on zooplankton and small fish, while common murres target a variety of pelagic fish.

Northern CCE

At-sea density patterns varied among focal species and among CCE regions in 2024. In the Northern CCE, sooty shearwater and common murre densities were below average (Fig. M.6, top row), while the Cassin's auklet densities were slightly above average. The sooty shearwater density anomaly in 2024 was considerably higher than in the previous two years; this resulted in a positive short-term trend even though the short-term mean was below the long-term mean. The Cassin's auklet density anomaly in 2024 has been above average for the last three years, resulting in a short-term mean greater than the long-term mean. The common murre density anomaly has been below average in recent years and this trend continued in 2024. Recent means and trends should be interpreted with care, as no data were collected in 2020 or 2021 due to COVID-19 restrictions.

Central CCE

In 2024, observations of common murre densities in May/June surveys were well above average, while sooty shearwater and Cassin's auklet densities were near average and well below average, respectively. Common murre and sooty shearwater density anomalies show short-term means greater than the long-term mean, while the Cassin's auklet density anomaly has been below average since 2014 (Fig. M.6, middle row).

Southern CCE

Sooty shearwater and Cassin's auklet densities were below average in late March/April 2024, and common murre at-sea densities were above average (Fig. M.6, bottom row). No data were collected in 2020 or 2021 due to COVID-19 restrictions, thus recent means and trends should be interpreted with care.

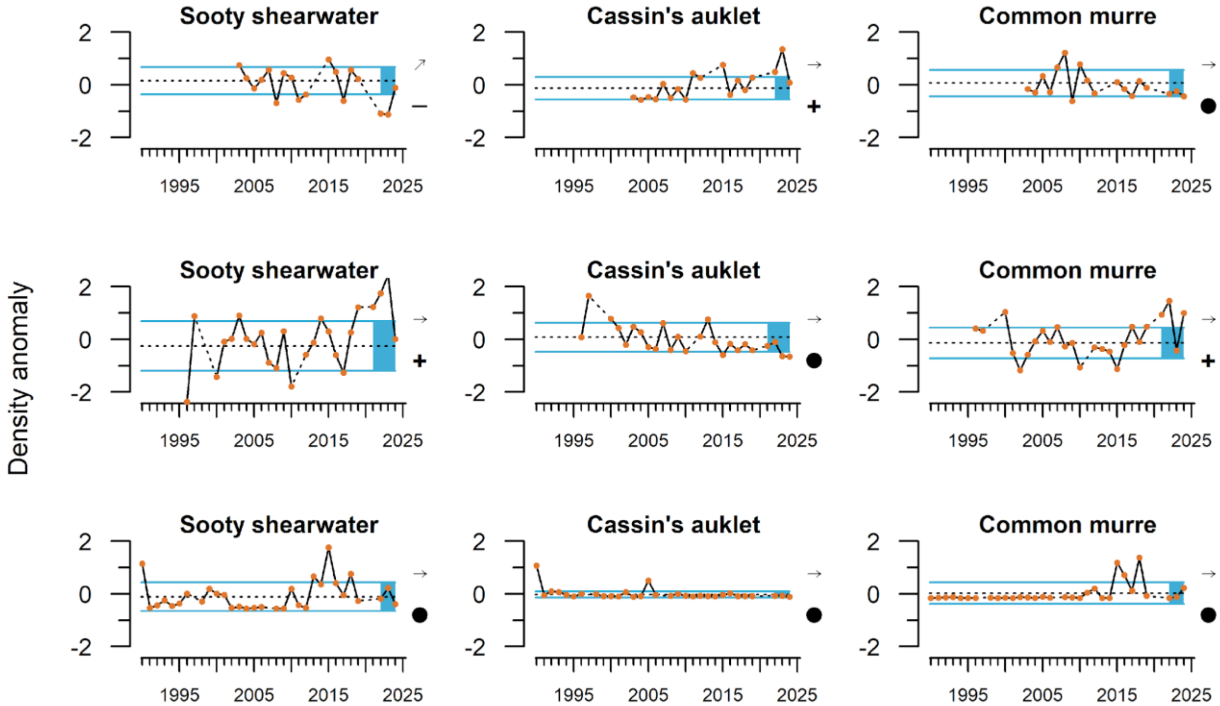

Figure M.6: Anomalies in spring/summer at-sea densities of sooty shearwaters, Cassin's auklets and common murres in the Northern (top), Central (middle), and Southern (bottom) CCE. Data are shipboard counts, transformed as ln(bird density/km^2 +1) and expressed as an anomaly relative to the long-term mean. Seabird density data from the Northern CCE were collected and provided by Dr. Jeannette Zamon (NOAA). Seabird density data from the Central and Southern CCE are collected on SWFSC RREAS and CalCOFI surveys, respectively, and are provided by Dr. William Sydeman. Lines, colors, and symbols are as in Fig. 2.1.

At-sea surveys in the Southern CCE conducted in late July/August 2024 documented a number of warm-water seabird species, including a record number of boobies (family Sulidae). These subtropical/tropical seabirds are becoming more common off the California coast, and the nine observed in 2024 consisted of four different species, including red-footed, masked, Nazca, and Cocos/brown boobies. Other notable warm-water species included black-vented shearwaters, Cook's petrel , and record numbers of elegant terns; for the terns, this is consistent with the continuing pattern of their northward range expansion from Mexico into California (W. Sydeman, unpubl. data).

M.4 Seabird Mortality

Monitoring of dead beached birds provides information on the health of seabird populations, ecosystem health, and unusual mortality events, such as those observed during the anomalously warm and unproductive years of 2014-2016. In January 2024, an unusual level of Cassin's auklet mortality was reported on monitored beaches in the Northern and Central regions of the CCE. There was also a die-off and strandings of brown pelicans on beaches of central and southern California in the spring of 2024. The birds were emaciated, though there was no evidence of avian influenza or domoic acid poisoning. Their regional food supply seemed adequate, as anchovy were abundant in those regions (Appendix I). However, local prey availability may have been the issue. Prolonged periods of unusually strong winds in California in April and May may have interfered with the pelicans' ability to forage, or intraspecific competition for food resources in nearshore areas may have been intensified from increasing pelican populations over the last several years.

Northern CCE

Encounter rates for beachcast Cassin's auklet were well above average in 2024, as documented by the University of Washington-led Coastal Observation And Seabird Survey Team (COASST). In early January, Cassin's Auklets began washing ashore in Oregon, Washington, and Northern California in unexpected numbers, with encounter rates on some beaches rivaling levels seen during the unusual mortality event in January 2015. Encounter rates reported for common murre, northern fulmar, and sooty shearwater below average in 2024 (Fig. M.7).

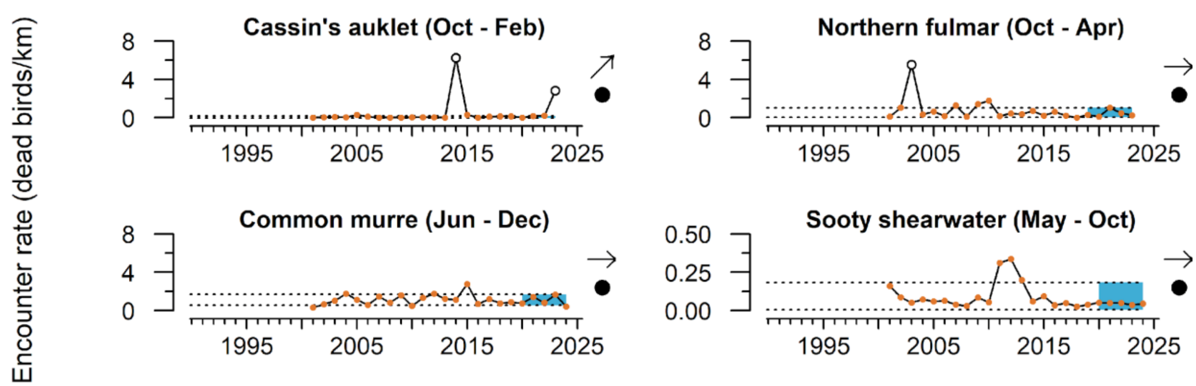

Figure M.7: Encounter rates of dead beachcast birds in Washington, Oregon and northern California. The mean and trend of the last five years (blue shaded area) are evaluated relative to the mean and s.d. of the full time series with the outliers (open circles) removed. Dotted lines indicate ±1 s.d. of the full time series with outliers removed. Data provided by the Coastal Observation and Seabird Survey Team. Symbols at right are as in Fig. 2.1.

Central CCE

The Beach Watch program monitors beaches in northern and central California. Encounter rates of beachcast Cassin's auklet were well above average on beaches from Point Arena to Point Año Nuevo in 2023/2024 and showed a significant positive trend as well as an elevated short-team mean. Above average encounter rates were reported for Brandt's cormorant and sooty shearwater; however these values were lower than the peak value reported for both species in 2020, which resulted in significant negative trend for both species over the last five years. For common murre and northern fulmar, encounter rates in 2023/2024 were below average (Fig. M.8).

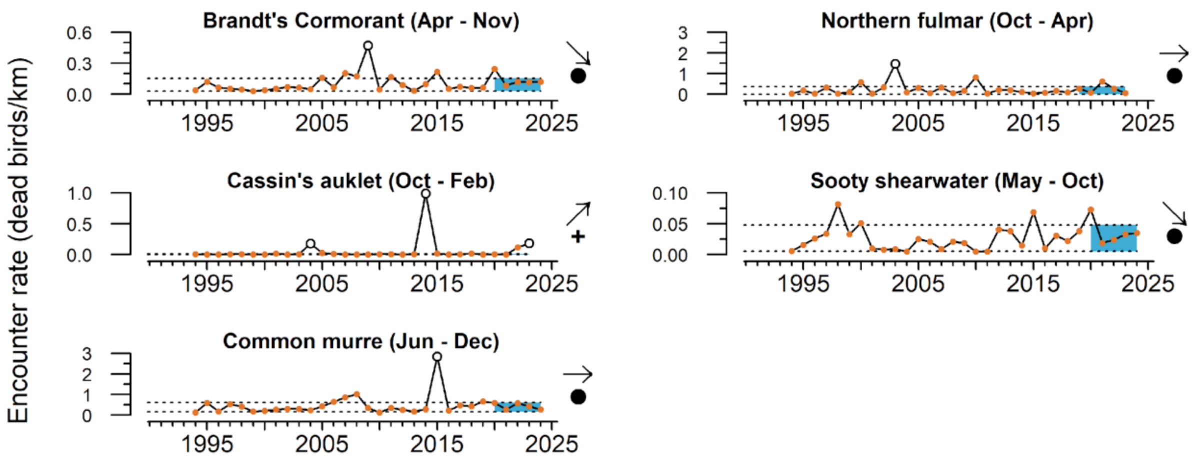

Figure M.8: Encounter rate of dead beachcast birds in north-central California through 2024. The mean and trend of the last five years (blue shaded area) are evaluated relative to the mean and s.d. of the full time series with the outliers (open circles) removed. Dotted lines indicate ±1 s.d. of the full time series with outliers removed. Data provided by Beach Watch. Symbols at right are as in Fig. 2.1.

The Beach Combers program also documented above average encounter rates of beachcast Cassin's auklet on North Coast (Point Año Nuevo to Point Sur, California) and Central Coast (Point Sur to Point Conception, California) beaches in 2023/2024, with a significant positive trend for beaches in Northern California in recent years. Brandt's cormorant encounter rates were above average on the North Coast but below average on Central Coast beaches. For sooty shearwater and common murres, encounter rates were below average on the North Coast and above average on the Central Coast. Below average encounter rates were reported for northern fulmar on beaches in both regions, resulting in significant negative trends over the last five years (Fig. M.9).

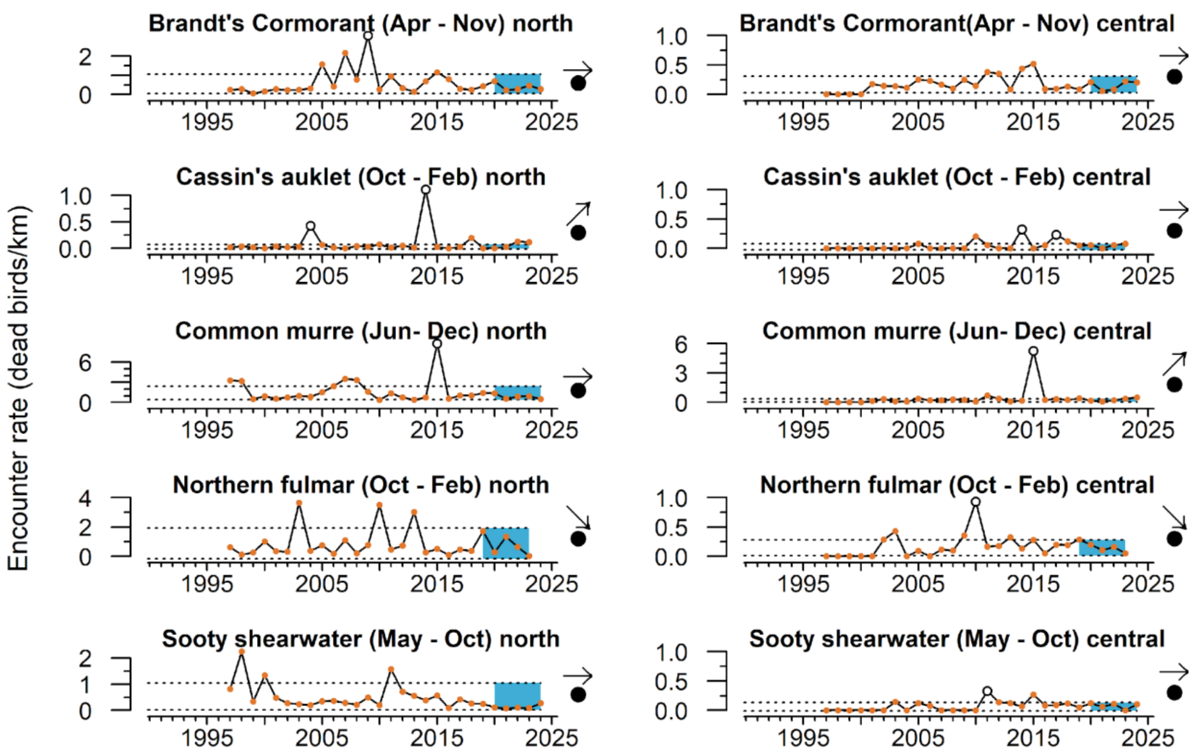

Figure M.9: Encounter rate of dead beachcast birds in central California through 2024. The mean and trend of the last five years (blue shaded area) are evaluated relative to the mean and s.d. of the full time series with the outliers (open circles) removed. Dotted lines indicate ±1 s.d. of the full time series with outliers removed. Data provided by BeachCombers. Symbols at right are as in Fig. 2.1.

Appendix N — MARINE MAMMALS

Link to main section: Marine Mammals

N.1 California Sea Lion Pup Indicators

California sea lions are sensitive indicators of prey availability and composition in the central and southern CCE. Sea lion pup counts at the San Miguel Island colony relate to prey availability and nutritional status for gestating females from October to June, while pup growth from birth to age 7 months is related to prey availability to lactating females from June to March. These metrics have been shown to be good indicators of forage quality and abundance even when the sea lion population is at or near carrying capacity (Melin et al. 2012). Pup counts have been updated for the 2024 cohort and can be found in Figure 3.14 in Section 3.7. Two pup condition indices, weight and growth, were updated through the 2023 cohort at the time of writing this report. These indices are presented below.

In March 2024, NOAA scientists weighed pups from the 2023 sea lion pup cohort born the previous summer. The average weight of female pups was 4% below the time series average and 14.7% below the 2022 cohort (Fig. N.1). The growth rate was 11% below the time series average (Fig. N.1) indicating that pups experienced slow growth during the winter of 2023-2024. Data for the current 2024-25 winter were not yet available at the time of this writing.

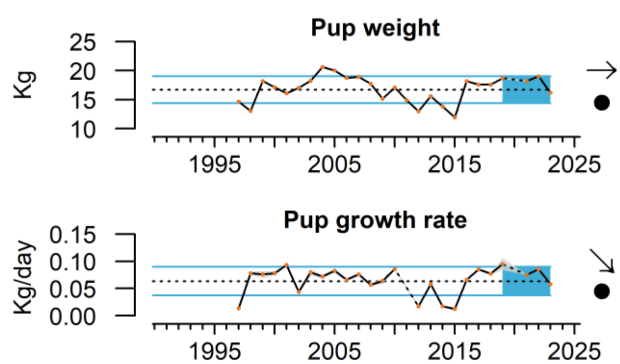

Figure N.1: California sea lion pup weight and growth on San Miguel Island for the 1997 - 2023 cohorts. Lines, colors, and symbols are as in Fig. 2.1; dashed lines indicate years of missing data.

The average weight and growth rate were within the range of values observed during previous mild to moderate El Niño events, and the timing of El Niño conditions between October 2023 to March 2024 overlapped with the period of pup dependency and early pregnancy for adult sea lions. There is no prey information for this period, but El Niño conditions typically lead to reduced prey availability for nursing females making it more difficult for them to support lactation for their pups, and resulting in poor condition of pups and lower pup growth rates, like those observed for the 2023 cohort.

By April 2024, in time for weaning, high abundance of anchovy, and average abundance of other primary prey, such as hake, rockfish, and jack mackerel were recorded in the foraging areas of nursing females and weaned pups. The availability of these prey in the spring and summer typically would lead to successful weaning, births and pup survival. However, the lower live pup count for the 2024 cohort indicates that additional factors negatively offset the improved foraging conditions (see Fig. 3.14 in Section 3.7).

For instance, two harmful algae blooms (April-June 2024 and August-September 2024) resulted in high levels of domoic acid, a neurotoxin, in California sea lion haulouts and rookeries, including Año Nuevo Island and the Farallon Islands. The blooms extended throughout the foraging range of pregnant and lactating California sea lions and persisted throughout the most vulnerable period of pup rearing during the summer and early fall, when pups are solely dependent on their mother's milk for nutrition. Domoic acid toxicity can result in abortions by transplacental transmission (Goldstein et al. 2009) and pup mortality from lactation transmission (Rust et al. 2014) or starvation due to death of the mother. Stranding centers and researchers in the field observed higher than average premature pupping and strandings along the Central California coast. Stranding centers reported 100s of California sea lions presenting with domoic acid toxicity symptoms throughout summer 2024 (see NOAA Fisheries, The New Lede, SCCOOS sites).

Fearing that premature pupping could be due to H5N1 avian influenza that caused significant mortality in South American sea lions (*Otaria flavescens*) and fur seals (*Arctocephalus australis*) (Szteren et al. 2024), dead California sea lion pups were sampled and no positive infections were found. Other factors such as population demographics may also have contributed to the drop-off in the 2024 pup count.

N.2 Whale Entanglements

Total confirmed entanglements have remained fairly consistent for the last five years after declining from a high in 2015-2016 (Fig. N.2). The trend in total entanglements is driven largely by incidents with humpback whales, which are the most frequently entangled species confirmed in absolute numbers. Confirmed entanglements of killer whales increased after 2020 and have fluctuated between 0-2 whales per year.

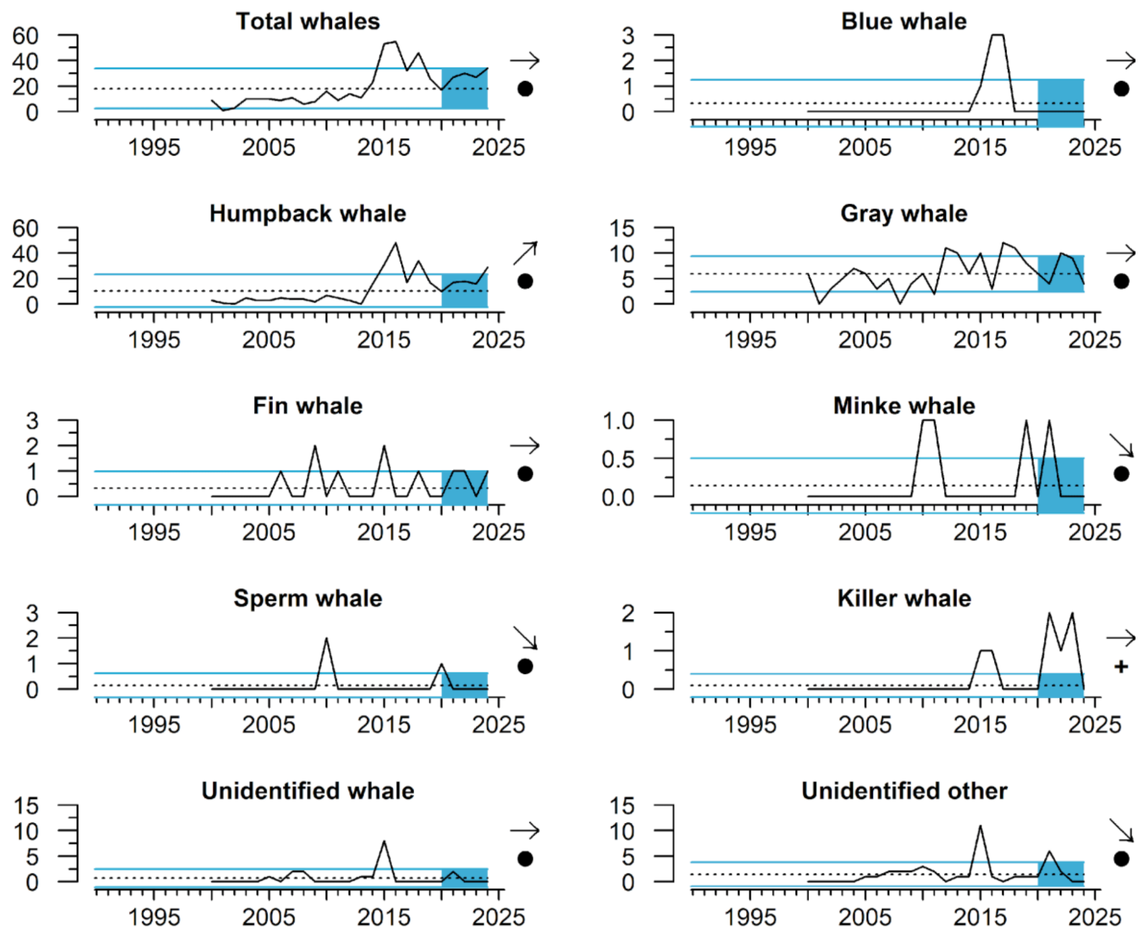

Figure N.2: Numbers of whales (both alive and dead) reported as entangled in fishing gear along the West Coast from 2000 - 2024. Data from 2024 are preliminary.

Appendix O — HARMFUL ALGAL BLOOMS

Link to main section: HABs

Harmful algal blooms (HABs) of diatoms in the genus *Pseudo-nitzschia* have been a recurring concern along the West Coast. Certain species of *Pseudo-nitzschia* can produce the toxin domoic acid, which can accumulate in filter feeders and extend through food webs to cause harmful or lethal effects on people, marine mammals, and seabirds (Lefebvre et al. 2002; McCabe et al. 2016). Because domoic acid can cause amnesic shellfish poisoning in humans, fisheries are delayed, closed, or operate under special orders or health advisories when domoic acid concentrations exceed regulatory thresholds for human consumption. Shellfish fisheries such as razor clam, Dungeness crab, rock crab, and spiny lobster are especially impacted by management actions related to domoic acid, such as fishery closures or delays of openings that can cost tens of millions of dollars in lost revenue, and a range of sociocultural impacts in fishing communities (Dyson and Huppert 2010; Ritzman et al. 2018; Holland and Leonard 2020; Moore et al. 2020), including a "spillover" of fishing effort into other fisheries.

Ocean conditions associated with marine heatwaves, El Niño events or positive PDO regimes may further exacerbate domoic acid toxicity and fishery impacts, and domoic acid toxicity tracks anomalies of southern copepod biomass (Figure 3.1) (McCabe et al. 2016; McKibben et al. 2017). The largest and most toxic HAB of Pseudo-nitzschia on the West Coast occurred in 2015, coincident with the 2013-2016 marine heatwave, and caused the longest-lasting and most widespread HAB-related fisheries closures on record (McCabe et al. 2016; Moore et al. 2019; Trainer et al. 2020). Closures and delays in the opening of West Coast crab fisheries resulted in the appropriation of >$25M in federal disaster relief funds (McCabe et al. 2016).

According to thresholds set by the U.S. Food and Drug Administration, domoic acid levels ≥20 parts per million (ppm) trigger actions for all seafood and tissues except Dungeness crab viscera, for which the level is >30 ppm (California applies this to rock crab viscera as well) (FDA 2011). Under evisceration orders, Dungeness crab can be landed when the viscera exceeds the threshold but the leg meat does not, provided that the crabs are eviscerated by a licensed processor. Oregon was the first West Coast state to pass legislation allowing evisceration, in November 2017, followed by California in October 2021. Washington adopted an emergency evisceration rule in February 2021, and is considering legislation to grant long-term authority for issuing evisceration orders.

A summary of management actions in the Dungeness crab fishery in response to domoic acid and other issues, such as poor body condition and marine life entanglement risk, is shown in Figure 3.16. Since the massive 2015-16 domoic acid event, the majority of management actions impacting the commercial fishery in California were related to marine life entanglement risk; in contrast, domoic acid contamination requiring evisceration or delay of the opening of the season as well as poor body condition has mostly impacted the fishery in Oregon and Washington. Note, however, that exceedances of domoic acid in Dungeness crab did sometimes occur in some regions of California prior to the eventual opening of the season, but the fishery opening was delayed during that time because of management actions regarding marine life entanglement risk and/or meat quality assessments. The toxin cleared from samples, in tandem with the resolution of the non-biotoxin factors, prior to the season opening. As such, this did not result in management action specific to domoic acid. To date, evisceration orders have primarily been used in Oregon and usually mid-season. In general, there has been a preference to delay the season opener rather than open under an evisceration order when domoic acid levels have been high at the start of the season (although the fishery did open under an emergency evisceration order in southern Washington in 2021).

Conditions in 2024 seemed to be more favorable for blooms of dinoflagellates, including toxic and nuisance species, compared to previous years. A coastwide bloom of *Alexandrium catenella* rapidly developed in May and sickened 44 people in Oregon with paralytic shellfish poisoning (PSP) before shellfish fisheries were closed. In Washington, there was also an unusual bloom of the dinoflagellate genus *Tripos* developed in October and colored shellfish tissues orange. While not toxic, the discoloration raised public concern and impacted commercial markets for oysters. This was the first time that a *Tripos* bloom of this magnitude has occurred in Washington since 1995. It is not yet clear what caused this shift in species abundance to favor dinoflagellates, but this functional group generally prefers warmer temperatures and stratified water column conditions.

O.1 Domoic Acid and Paralytic Shellfish Toxin in Washington

Low levels of domoic acid were still detectable in Washington razor clams at the start of 2024 following a particularly toxic bloom of *Pseudo-nitzschia* that occurred in the fall of 2023 (Fig. O.2). These low levels persisted through the spring, but did not exceed regulatory limits for human consumption or interfere with shellfish fisheries. In 2024, blooms of *Pseudo-nitzschia* occurred in early May and again in August, but despite the high cell abundances, particularly in August, they did not result in any significant accumulation of domoic acid in shellfish tissues. Levels of domoic acid in Washington Dungeness crab viscera collected in November and December 2024 ranged from below the detection threshold to < 3 ppm, but the commercial fishery was delayed until at least January 15, 2025 due to meat quality.

While diatoms generally remained dominant, dinoflagellates (both harmful and non-harmful) comprised a larger portion of the phytoplankton species assemblage in 2024 compared to previous years. In late May, a widespread and rapidly evolving toxic bloom of *Alexandrium* was observed along the outer coast and shortly after in Willapa Bay and Grays Harbor. The bloom caused widespread closures of commercial and recreational harvest of bivalve shellfish, including razor clams, manila clams, and oysters, due to unsafe levels of paralytic shellfish toxins (PSTs). While shellfish closures impacted state run bivalve fisheries along Washington's southern coast, the razor clam fishery within the Quinault Indian Nation's (QIN) usual and accustomed fishing areas continued to test below the PSP action level and remained open. Favorable conditions for dinoflagellates persisted through the summer and into the fall, and an unusual bloom of *Tripos spp*. developed in October.

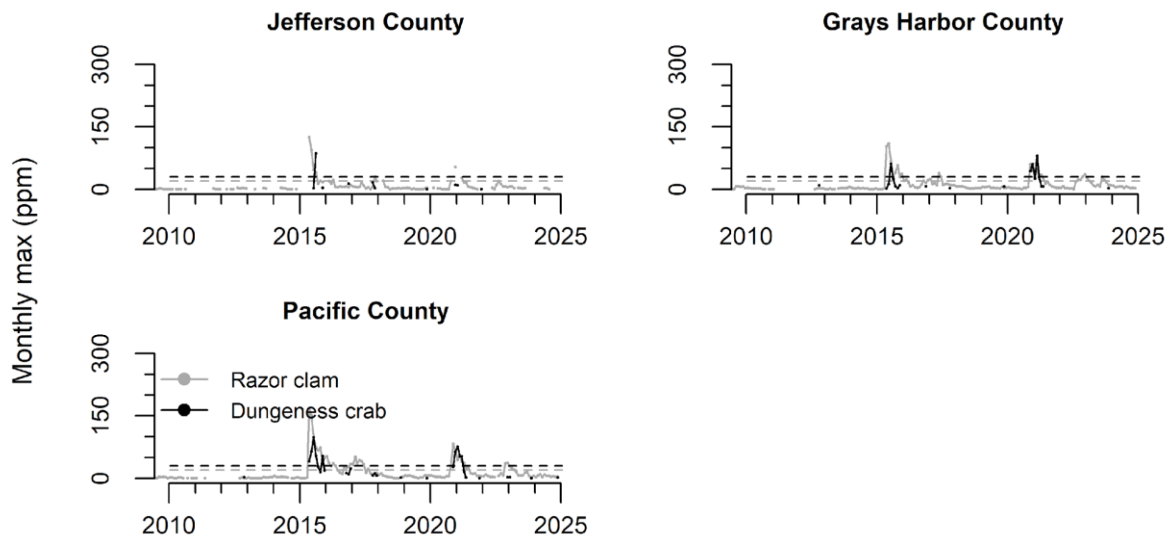

Figure O.2: Monthly maximum domoic acid concentration in razor clams and Dungeness crab viscera from 2010 - 2024 by coastal counties in Washington (north to south). Horizontal dashed lines are the management thresholds of 20 ppm (clams, gray) and 30 ppm (crab viscera, black). Data compiled by the Washington Department of Health, from samples collected and analyzed by a variety of local, tribal, and state partners.

O.2 Domoic Acid and Paralytic Shellfish Toxin in Oregon

Domoic acid exceedances resulted in multiple closures of Oregon shellfish fisheries in 2024. At the beginning of 2024, domoic acid levels were still elevated in bivalve shellfish along the southern Oregon coast in response to a particularly toxic bloom of *Pseudo-nitzschia* in the fall of 2023 (Fig. O.3). *Pseudo-nitzschia* blooms persisted throughout much of the summer and fall of 2024 in southern Oregon and northern California. This region is associated with a northern California "hot spot" that emerged in 2015 (Trainer et al. 2020). This persistent bloom activity eventually culminated in closures in mussel harvest (August 9, 2024 to October 11, 2024) from Cape Blanco to the OR/CA border. Razor clam harvest was also closed (July 26, 2024 to October 25, 2024) from Cape Blanco to the OR/CA border and the closure was extended northward to Cascade Head on October 25, 2024. Thus, the razor clam fishery was closed on over half of the Oregon coast through December 2024.

Levels of domoic acid in Oregon Dungeness crab viscera remained below the regulatory threshold throughout 2024 until November when exceedances occurred on the southern Oregon coast. The opening of the 2024-25 commercial crab season was delayed coastwide to December 16, 2024 due to a combination of low meat recovery in four harvest areas and elevated domoic acid detected in crab viscera in harvest areas K and L (Cape Blanco to the OR/CA border). The commercial and recreational bay crab fisheries from Cape Blanco to the OR/CA border were closed from November 14 through December 4, 2024. The opening of the ocean recreational crab fishery in this area was delayed by three days to December 4, 2024.

In late May of 2024, biotoxin levels of Paralytic Shellfish Toxin (PST) rapidly increased in mussels in the north-central coast of Oregon. This rapid increase resulted in 44 individuals having Paralytic Shellfish Poisoning symptoms, with 7 being hospitalized. PST levels were at or above record levels in all commercial and recreational bivalves including; mussels, razor clams, oysters, and all bay clams. This disrupted both commercial and recreational harvest during optimal harvest time frames through much of June, with nearly the entire coast closed to all bivalve harvest. By the middle of July, PST levels had depurated to below the FDA closure threshold which allowed harvest to occur.

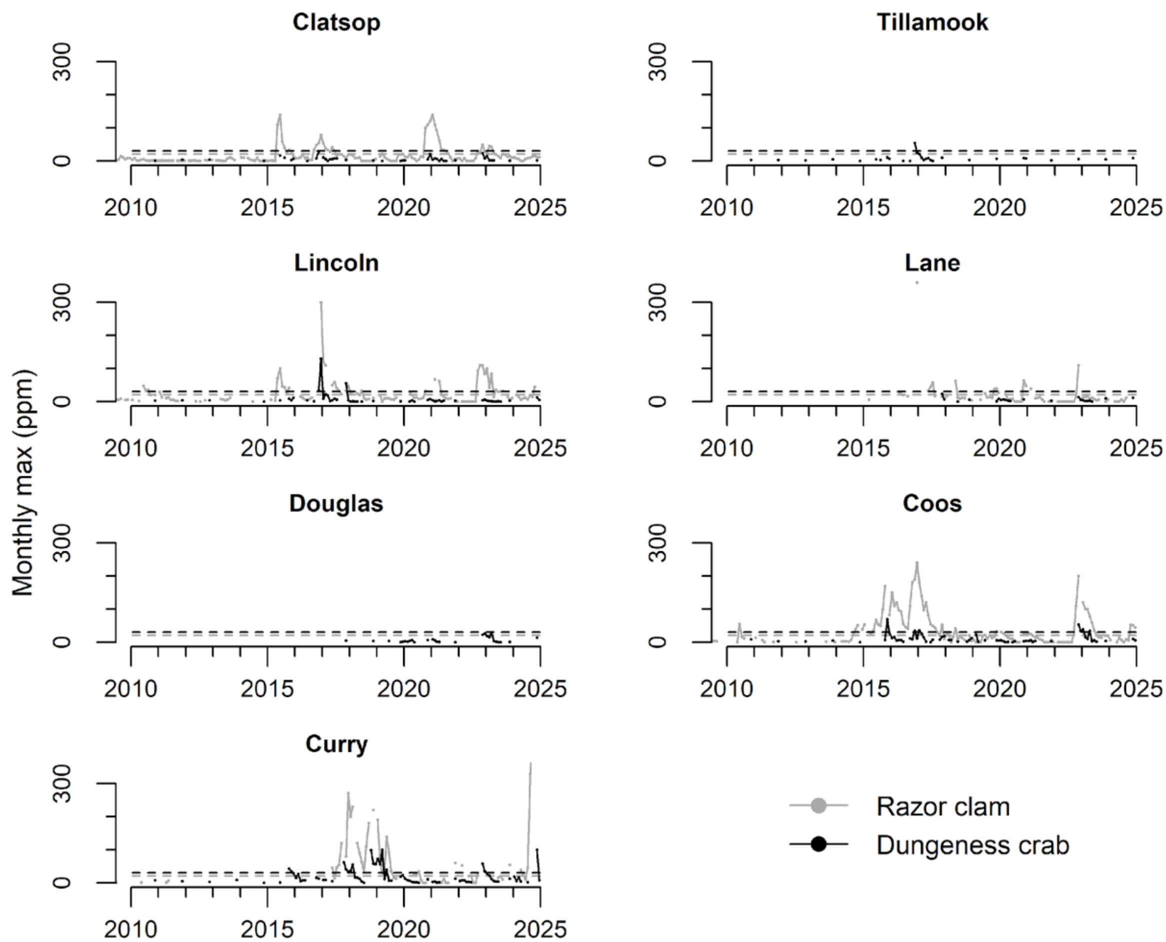

Figure 0.3: Monthly maximum domoic acid concentration in razor clams and Dungeness crab viscera from 2010 - 2024 by coastal counties in Oregon (north to south). Horizontal dashed lines are the management thresholds of 20 ppm (clams, gray) and 30 ppm (crab viscera, black). Razor clam tissue sampling is

conducted twice monthly from multiple sites across the Oregon coast. Data compiled and reported by Oregon Department of Fish and Wildlife from analyses conducted by the Oregon Department of Agriculture.

O.3 Domoic Acid and Paralytic Shellfish Toxin in California

Domoic acid closures persisted in 2024 for the recreational razor clam fishery in northern California. The razor clam fishery closure in Del Norte County was issued on November 9, 2023 and did not open once in 2024 (Fig. O.4). The razor clam fishery in Humboldt County closed on May 2, 2024 and remained closed through the end of the year.

A major domoic acid event in central and southern California developed in July 2024 and lasted more than 3 months. The *Pseudo-nitzschia* bloom resulted in the strandings of hundreds of marine mammals, almost exclusively adult female California sea lions with a few adult Northern fur seals and long- and short-beaked common dolphins. The marine animal rescue centers are also documenting animals exhibiting chronic domoic acid effects with neurological and cardiac damage evident with necropsy. A domoic acid-related health advisory warning against the consumption of sport-harvested bivalve shellfish from Santa Barbara County was instituted on August 8 to September 3, and again for September 26 through October 23, 2024. The commercial shellfish harvester located in the Santa Barbara Channel was closed due to domoic acid from August 7 to August 21 and October 2 to October 16, 2024.

The northern rock crab fishery remained closed in two areas due to domoic acid concerns (see https://wildlife.ca.gov/fishing/ocean/health-advisories); these areas have not been open since November 2015. During the fall of 2024, there were several sites that tested above domoic acid alert levels in the viscera and meat of Dungeness crab. Domoic acid exceedances in the viscera (> 30 ppm) were detected at Russian River in Sonoma County, Eel River in Humboldt County, and Klamath River and George Reef in Del Norte County. The recreational Dungeness crab fishery was delayed in northern California from the CA/OR border (42° 0.00' N latitude) to the southern boundary of the Reading Rock State Marine Reserve, Humboldt County, based on a meat sample testing above the alert level (≥ 20 ppm). The area opened on December 9, 2024 about one month after the recreational season start date of November 2, 2024. The commercial Dungeness crab fishery was delayed due to meat quality testing and the inability to complete a quality test due to domoic acid concerns in northern California, and also in central California due to the presence of high numbers of whales, particularly humpbacks. This is the sixth consecutive year that the commercial Dungeness crab fishery has been delayed in California because of insufficient meat quality and/or marine mammal entanglement risk concerns.

In 2024, Paralytic Shellfish Toxins (PST) were detected in bivalve shellfish in the majority of coastal counties in California (except for Santa Barbara and Ventura) from May through December; however, the amount and level of PSTs detected were not out of the ordinary for the California coast. Levels of PSTs in bivalve shellfish exceeded the regulatory limit for human consumption in July in multiple counties along the coast: Del Norte, Humboldt, Sonoma, Marin, Santa Cruz, and Monterey. PST exceedances also occurred in August in Santa Cruz County and in September in Monterey County. The highest level detected was 840 ug/100 g PSTs in mussels in Del Norte County collected July 9, 2024. Recreational bivalve shellfish advisories were issued for the affected counties. There were no commercial shellfish closures due to PSTs in 2024.

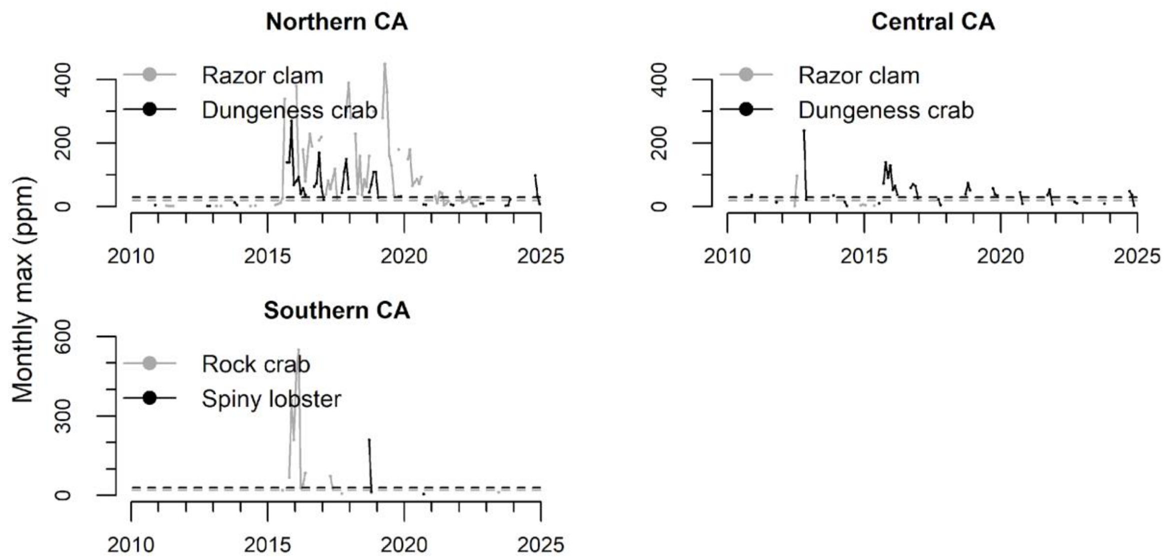

Figure O.4: Monthly maximum domoic acid concentration in razor clams, Dungeness crab, rock crab, and spiny lobster from 2010 - 2024 in California (Northern CA: Del Norte to Mendocino counties; Central CA: Sonoma to San Luis Obispo counties; Southern CA: Santa Barbara to San Diego counties). Note that there were no rock crab or spiny lobster samples for 2024. Horizontal dashed lines are the management thresholds of 20 ppm (clams and lobsters, gray) and 30 ppm (crab viscera, black). Data compiled by the California Department of Public Health from samples collected by a variety of local, tribal, and state partners.

Appendix P: SOCIAL VULNERABILITY OF COMMERCIAL and RECREATIONAL FISHING-DEPENDENT COMMUNITIES

Link to main section: Social Vulnerability

Communities adjacent to the California Current engage with marine ecosystems for their economic, social, and cultural well-being. This appendix features indicators and analyses of human wellbeing, relating to the risk profiles and adaptive capacities of coastal communities in the face of environmental and socio-economic pressures, to help track progress toward meeting National Standard 8 (NS-8) of the Magnuson-Stevens Act, as well as monitoring these communities with an interest in fisheries management. NS-8 states that fisheries management measures should “provide for the sustained participation of [fishing] communities” and “minimize adverse economic impacts on such communities.”

Community Social Vulnerability Index (CSVI) as an indicator of social vulnerability in coastal communities that depend upon commercial fishing was presented in Section Section 4.1 of the main report. To gain further insight into community vulnerability in relation to commercial fishing, fishing dependence, which can be expressed in terms of engagement, reliance, or by a composite of both, can be considered in relation to CSVI. Engagement refers to the total extent of fishing activity in a community; it can be expressed in terms of commercial activity (e.g., landings, revenues, permits, processing, etc). Reliance, or per capita engagement, measures the engagement relative to the population size of a community; thus, in two communities with equal engagement, the community with the smaller population would have a higher reliance on its fisheries activities.

We have developed index measures for community-level recreational fishing engagement and reliance, and related them to CSVI. As with the commercial fishing index construction, following the method proposed by Jepson and Colburn (2013), data directly linking place-based communities to the economic aspects of recreational fishing, which could be attributed to specific calendar years, were compiled from six distinct sources as inputs for the measures. Charter and guide permit data collected by state managers were obtained and linked to Census-Designated Place (CDP) based communities. Additionally, historic fishing tackle business location data was compiled from Data Axel, the provider of business location data to Environmental Systems Research Institute’s (ESRI) business analyst application. Marina business location data was also obtained from ESRI and ESRI’s provider. These data enable interannual comparisons and allow for future replicate iterations.

In the main body of the report, Figure 4.1 plots CSVI against commercial and recreational *reliance* (per capita engagement) for the five most reliant communities respectively for 2022 from each of the five regions of the CCE. Similar plots are presented here for 2021 for comparison (Fig. P.1). Since the commercial and recreational indices are measured separately, their scores are not directly comparable; a lower score in one does not imply lesser relative importance compared to the other. Fishing reliance can be volatile: communities can move left on the x-axis in years with reduced landings, and may thus appear to be less dependent on commercial fishing when in fact they have actually just experienced a difficult year; therefore, these results should be interpreted with care. These same qualifications apply to recreational fishing reliance measures. These data are difficult to ground truth and interpreting trends requires further study.

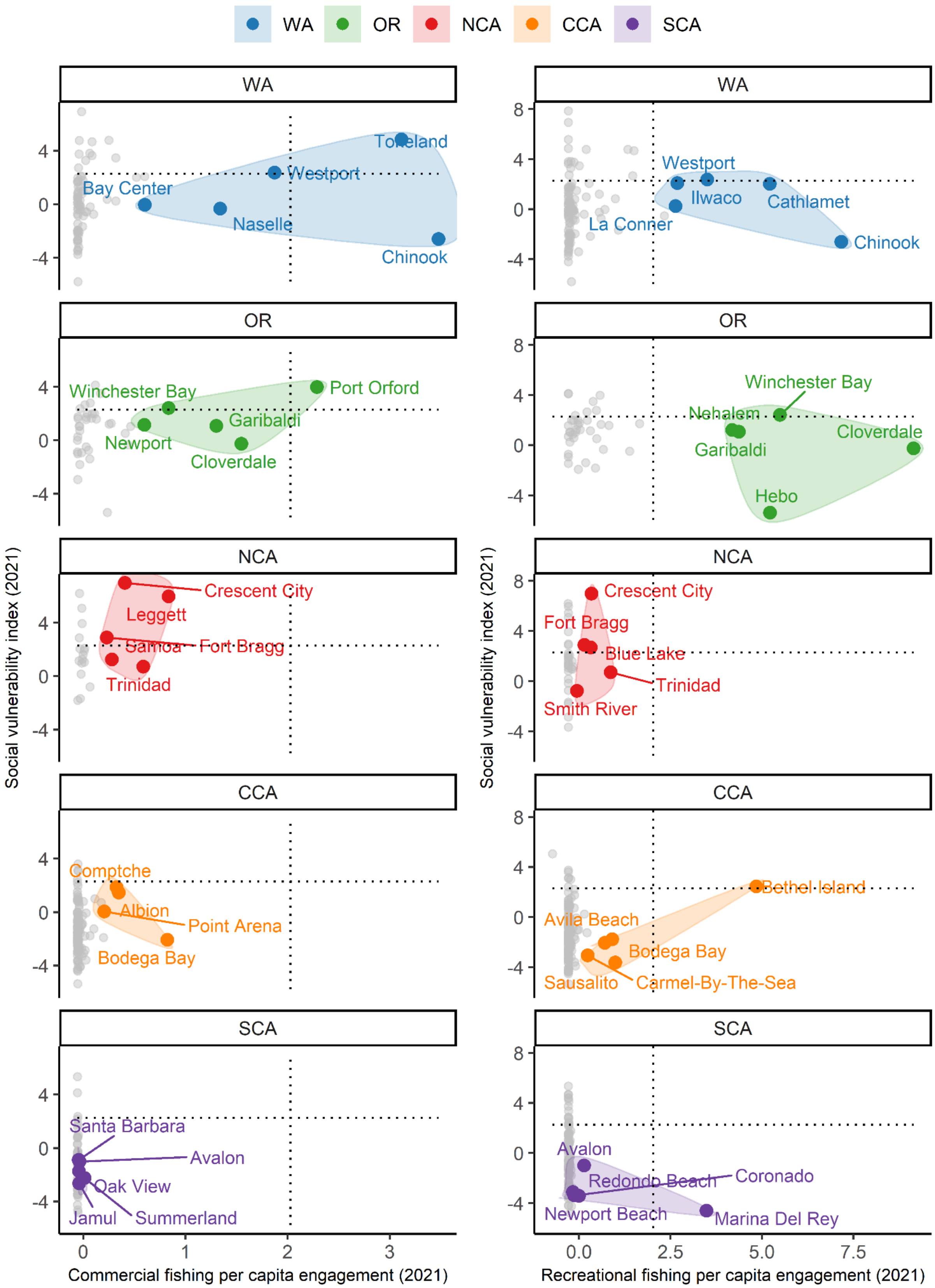

WA
OR
NCA
CCA
SCA
Social vulnerability index (2021)
Commercial fishing per capita engagement (2021)
Recreational fishing per capita engagement (2021)
Tokeland
Westport
Bay Center
Naselle
Chinook
Ilwaco
Cathlamet
La Conner
Winchester Bay
Port Orford
Garibaldi
Newport
Cloverdale
Nehalem
Hebo
Crescent City
Leggett
Samoa
Fort Bragg
Trinidad
Blue Lake
Smith River
Comptche
Albion
Point Arena
Bodega Bay
Bethel Island
Avila Beach
Sausalito
Carmel-By-The-Sea
Santa Barbara
Avalon
Oak View
Jamul
Summerland
Redondo Beach
Coronado
Newport Beach
Marina Del Rey

Figure P.1: Commercial fishing per capita engagement and social vulnerability scores (left) and recreational fishing per capita engagement and social vulnerability scores (right) in 2021 for communities in Washington, Oregon, and northern, central and southern California. The five highest-scoring communities for both forms of fishing per capita engagement are shown for each region. Dotted lines indicate 1 s.d. above the means for all communities. Colored polygons within the figures group the five community points from each region together to represent cross-regional differences.

Similar to the above plot, Figure P.2 shows highly engaged West Coast commercial and recreational fishing communities and their corresponding social vulnerabilities in 2022. Of note are the groupings of communities above and to the right of the dashed lines, which mark at least 1 s.d. above the mean of both indices as averaged across all communities. Several communities were not in that quadrant in the per capita engagement plot (Fig. 4.1) do fall into that quadrant for the total engagement plot. For commercial engagement, this includes Westport, WA; Port Orford, OR; and Crescent City, Fort Bragg, and Los Angeles, CA (Fig. P.2). For total recreational engagement, Los Angeles was the only relatively highly vulnerable community that was not also highly vulnerable in the per capita recreational engagement plot (Fig. 4.1).

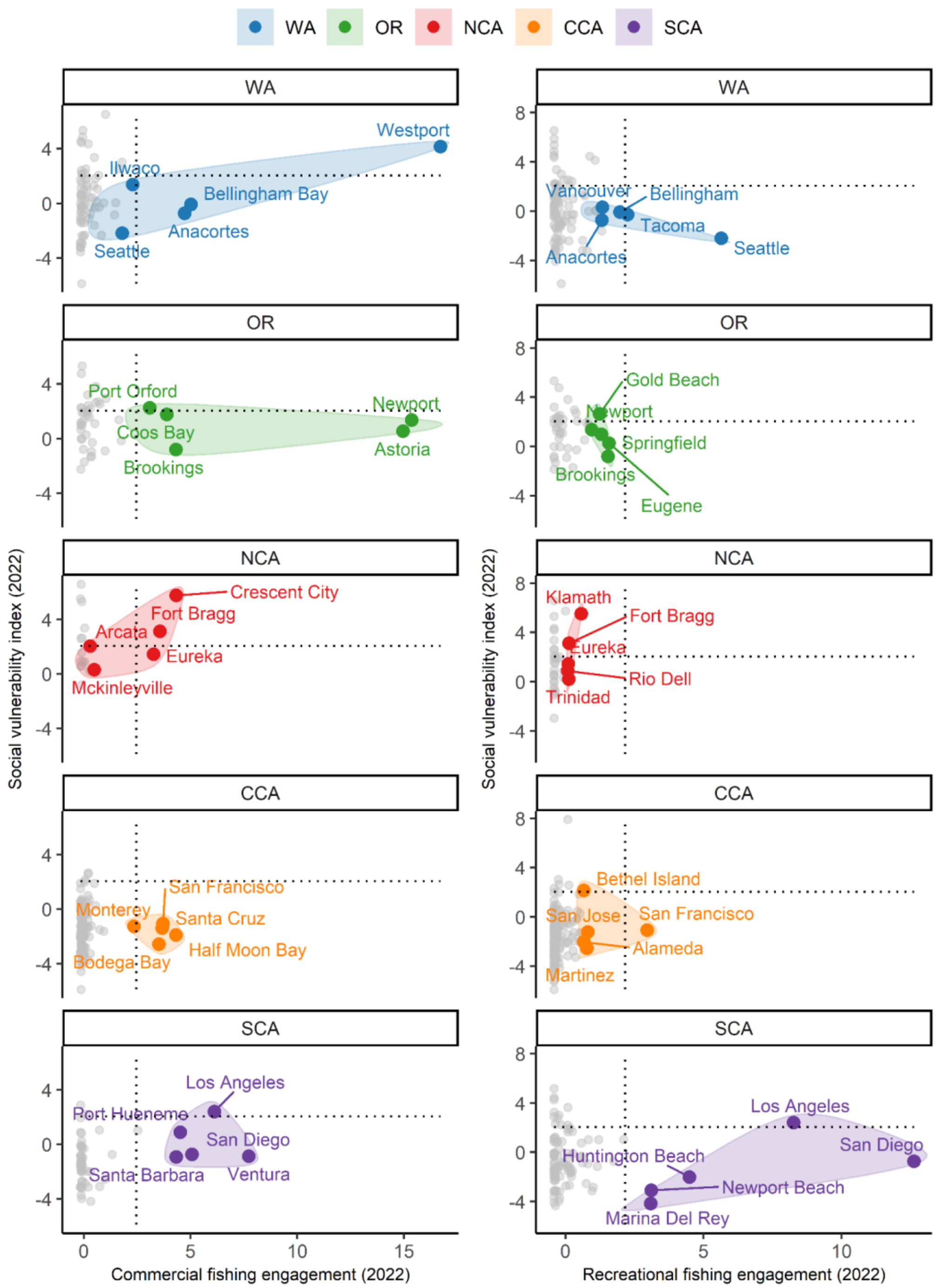

Figure P.2: Commercial (left) and recreational (right) fishing engagement with social vulnerability scores in 2022 for communities in Washington, Oregon, and northern, central and southern California. The five highest-scoring communities for fishing engagement are shown for each region. Dotted lines indicate 1 s.d. above the means for all communities.

To provide further insight into longer-term changes in the social vulnerability of both top commercial and recreational engaged and reliant coastal communities, Figure P.3 displays the CSVI categorically with annual scores provided as categorical rankings. Dark red reflects a relatively high vulnerability, representing scores at or above 1 standard deviation greater than the mean, light red is medium high (between 0.5 and 0.99 standard deviation above the mean), light blue is medium (0 to 0.49 standard deviation above the mean) and dark blue is low (negative standard deviation).

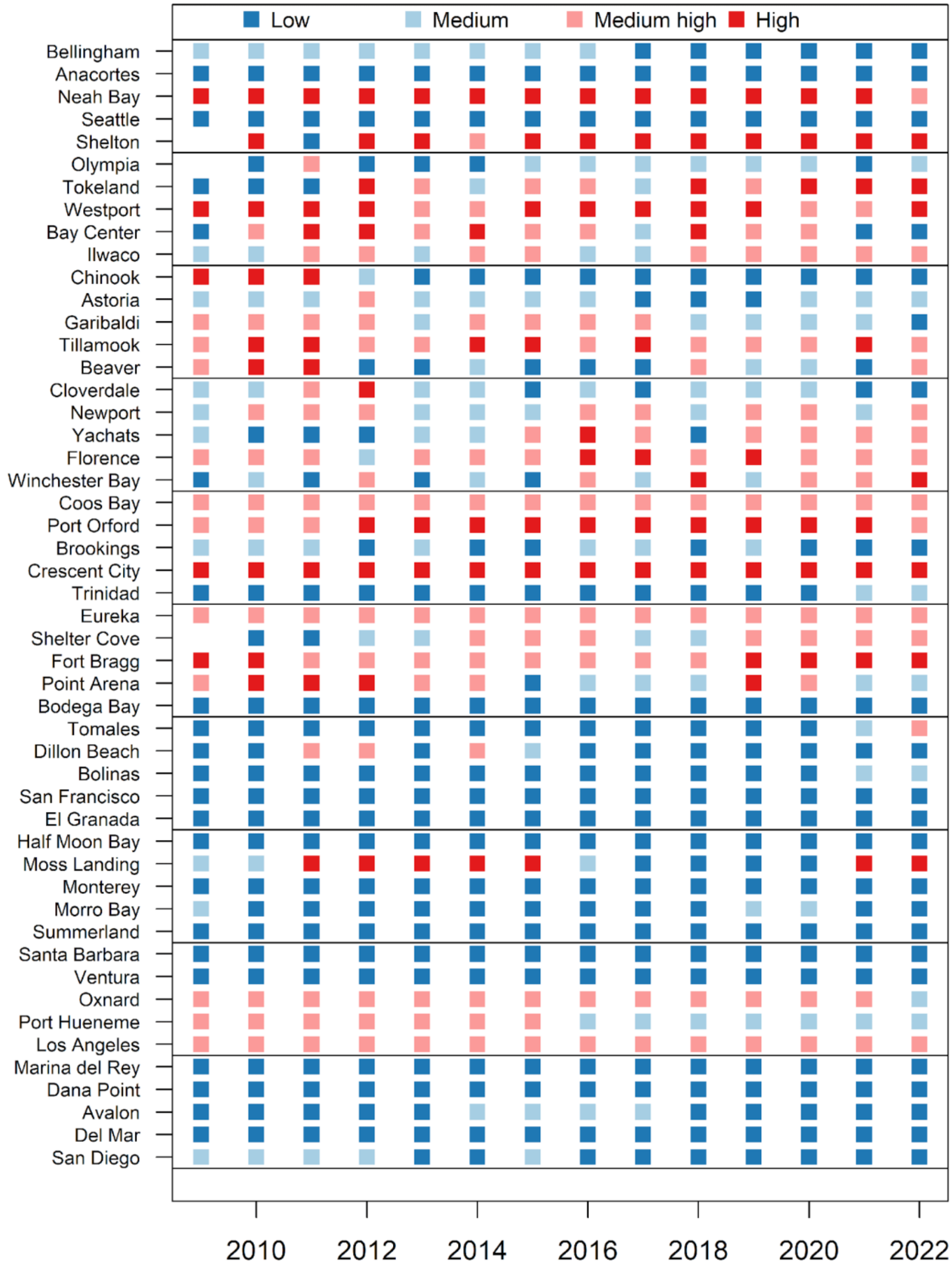

Figure P.3: Categorical social vulnerability scores for fishing communities with high-ranking commercial and recreational concerning engagement and *reliance scores from 2009 to 2022. Communities are arranged approximately from north to south.*

Appendix Q — FLEET DIVERSIFICATION INDICATORS FOR MAJOR WEST COAST PORTS

Link to main section: Diversification of Fisheries Revenue

Catch and price from many fisheries exhibit high interannual variability, leading to high variability in fisher's revenue, but variability can be reduced by diversifying activities across multiple fisheries or regions (Kasperski and Holland 2013). Individuals may have good reasons to specialize, including reduced costs or greater efficiency; thus while diversification may reduce income variation, it does not necessarily promote higher average profitability.

We use the Effective Shannon Index (ESI) to examine diversification of fishing revenue for more than 28,000 vessels fishing off the West Coast and Alaska over the last 40 years. In the main body of the report (Fig. 4.2), ESI increases as revenues are spread across more fisheries, and more evenly across fisheries; ESI = 1 when a vessel's revenues are from a single species group and region; ESI = 2 if revenues are spread evenly across 2 fisheries; ESI = 3 if revenues are spread evenly across 3 fisheries; and so on. If revenue is not evenly distributed across fisheries, then the ESI value is lower than the number of fisheries a vessel enters.

There has been a moderate decline in average fishery diversification since the mid-1990s or earlier for most vessel classifications (see main report, Fig. 4.2). Changes in diversification are due both to entry and exit of vessels and changes on an individual vessel level. Although vessels remaining in the fishery have become less diverse on average over time, less diversified vessels have been more likely to exit and newer entrants have generally been more diversified than those who left (Abbott et al. 2023). Within the average trend there are wide ranges of diversification levels and strategies, and some vessels remain highly diversified.

As is true with individual vessels, the variability of landed value at the port level is reduced with greater diversification of landings. Revenue diversification scores are highly variable year-to-year for some ports, making it difficult to discern trends. Some major ports have seen long-term declines in fishery diversification. Almost all major West Coast ports in Washington, Oregon and Northern California saw a decline in fishery diversification in 2023 relative to 2022 with the exceptions of Bellingham, WA and Ventura, CA where species diversification increased (Fig. Q.1).

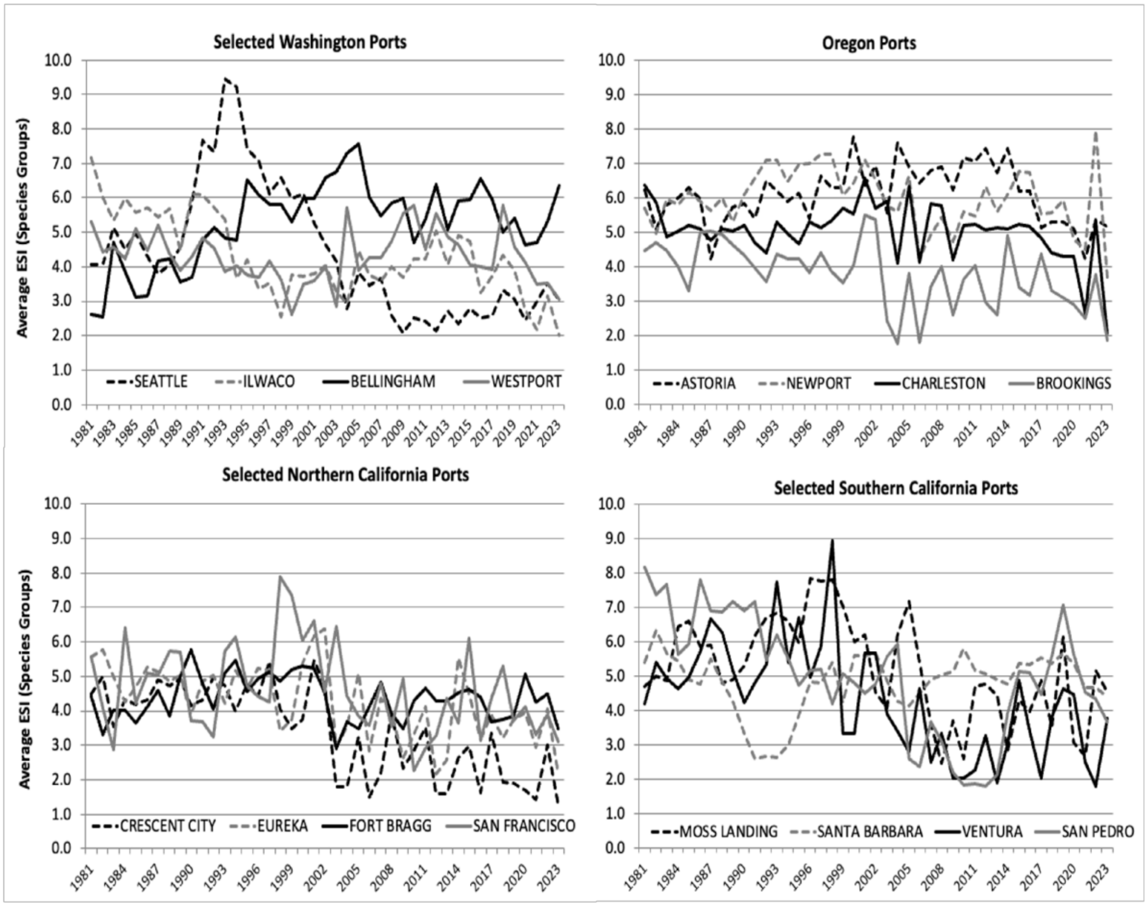

Figure Q.1: Trends in fishery revenue diversification in major U.S. West Coast ports, grouped by state. Data from D. Holland (NMFS/NWFSC) and S. Kasperski (NMFS/AFSC).

Diversification can take other forms. Spreading effort and catch over the year, or simply fishing more weeks of the year, can both increase revenue and decrease interannual variation of revenue just as species diversification does. In fact, Abbott et al. (2023) showed that reductions in revenue variation associated with species diversification can be explained mainly by increased temporal diversification, which can be achieved by fishing in multiple fisheries but also by fishing for more weeks of the year in a single fishery.

Below, Figure Q.2 shows temporal diversification for the same vessel groups and classes shown in the main body (Fig. 4.2). Here we use an Effective Shannon Index that reflects how widely and evenly vessel revenues are spread across weeks of the year as an indicator of temporal diversification. Like the species diversification metric, this index increases the more weeks of the year a vessel has revenue and the more evenly that revenue is distributed across weeks. A vessel fishing 15 weeks of the year with the same revenue each of those weeks would have a temporal ESI of 15, and that number would decline as revenue is spread less evenly over the 15 weeks.

Unlike species diversification, which has been trending down since the early 1990s for most vessel groups, temporal diversification generally trended up though the early 2000's and oscillated without a clear trend through 2014. However, since 2014, temporal diversification has declined for most vessel groups other than West Coast vessels with average revenue under $25K (Fig. Q.2 and see Holland et al. 2025 for further analysis) and that trend continued in 2023. There was a small increase in 2022 for some vessel groups, but the average remains well below the 2014 high.

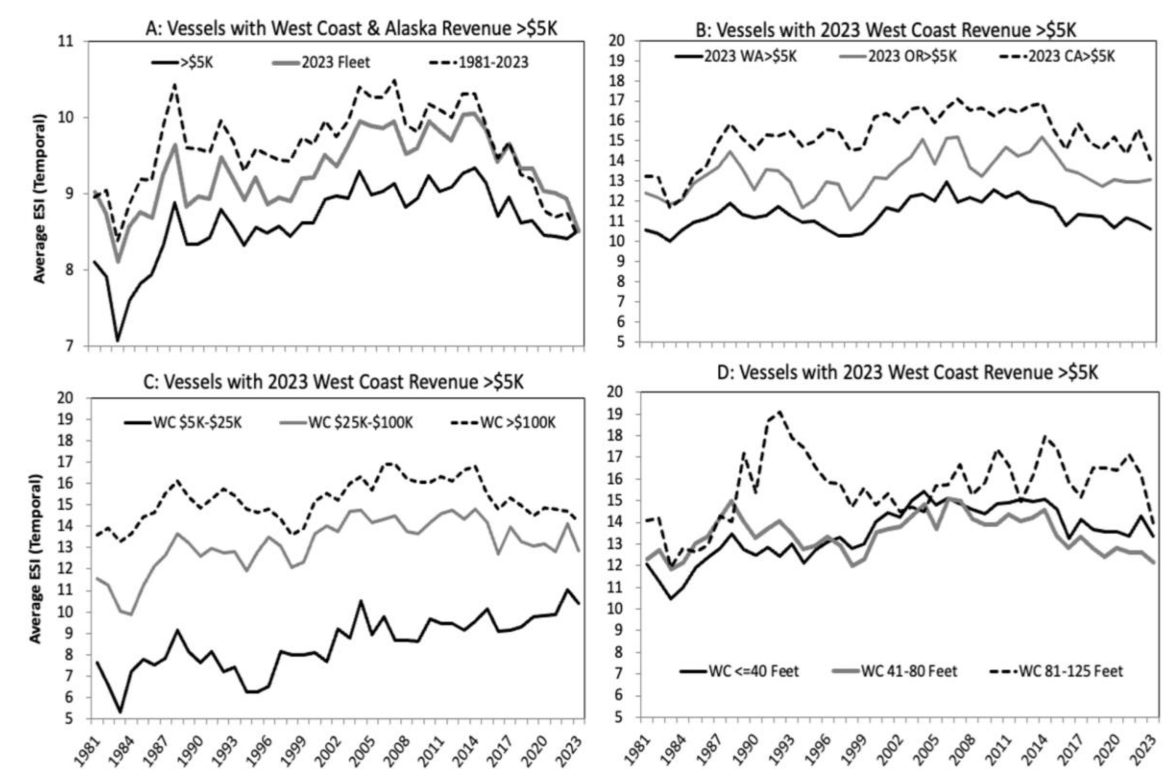

Figure Q.2: Trends in average temporal diversification for U.S. West Coast and Alaskan fishing vessels with over $5K in average revenues (top left) and for vessels in the 2023 West Coast Fleet with revenues over $5K, grouped by state (top right), by average gross revenue class (bottom left) and by vessel length class (bottom right). Data from D. Holland (NMFS/NWFSC).

Appendix R — PORT-LEVEL REVENUE CONCENTRATION

R.1 The Theil Index

Over the past four reports, we have worked with the SSC-ES to develop an index of the concentration or consolidation of ex-vessel fishery revenue in ports on the West Coast. The Theil index is an annual measure of geographic concentration of fishery revenue (Theil 1967). It is one approach to assessing if fishery access to opportunities is changing within and across ports and/or FMPs. The Theil index estimates the difference between observed revenue concentration and theoretical revenue concentration with equal distribution across ports; higher values indicate greater concentration in a subset of ports.

Annually, we calculate the Theil index for all fisheries and for specific fishery management groups, at the scale of the 21 port groups previously established for the economic Input-Output model for Pacific Coast fisheries (IO-PAC) (Leonard and Watson 2011).

The annual Theil index values for total commercial fishing revenue and six management groups are presented in Figure R.1. The total revenue trend is relatively flat with low values in each year for the over 40-year time period, suggesting total fishery revenue has not experienced dramatic changes in geographic concentration. Between 2022 and 2023 (the most recent year of data analyzed), there was a decrease in the overall Theil index value for all fisheries. When considering individual management groups, there are distinctions in the overall degree of geographic concentration. CPS and HMS fisheries continue to have the highest Theil index values, as they have for the last decade, indicating those groups' relatively high concentration of revenue in a smaller number of port groups.

The salmon fishery shows relatively high short-term variability, though a steep increase in the 2023 Theil index measure for salmon coincides with a downturn in salmon revenues overall, a concentration of salmon revenues in northern Washington and Oregon ports for 2023, and salmon fishing closures in 2023 which inhibited harvest in Northern California (see below). This index may provide the Council with relevant information on particular fisheries and port groups where revenue concentrations are changing, as a basis for evaluating trade-offs related to NS-8 considerations under the Magnuson–Stevens Act, in which fisheries management measures should "provide for the sustained participation of [fishing] communities" and "minimize adverse economic impacts on such communities."

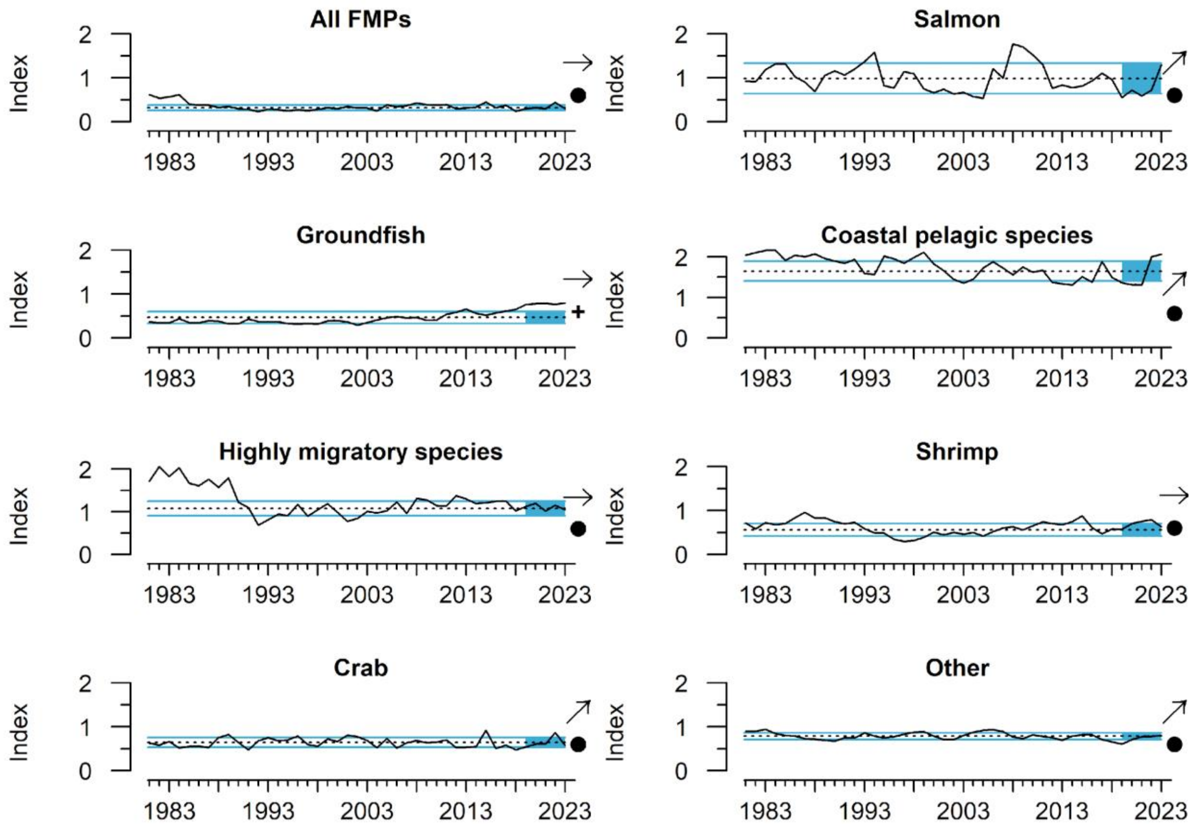

Figure R.1: Theil index estimation of commercial fishery revenue concentration in West Coast IO-PAC port groups, 1981 - 2023. Increasing values indicate greater concentration of revenue in a smaller number of port groups.

Theil index values for CPS revenues on the West Coast have been decreasing in geographic concentration over the last 40 years but increased in 2022 and 2023. Prior to the removal of Humboldt squid, Pacific bonito, Pacific herring and round herring from the CPS FMP as requested by the CPSMT in mid 2022, the Theil index for CPS appeared constant across the last 40 years. This was primarily due to the northern ports CPS revenue consisting of Pacific herring in addition to the southern port concentration of market squid (data not shown). Without the influence of Pacific herring on revenue, market squid has become less consolidated in southern ports, shifting north, and has driven the CPS Theil index value lower over the last 40 years. However, the recent increase in the Theil index reflects an increase in CPS revenue in Santa Barbara with less CPS revenue in other Port groups (Fig. R.2).

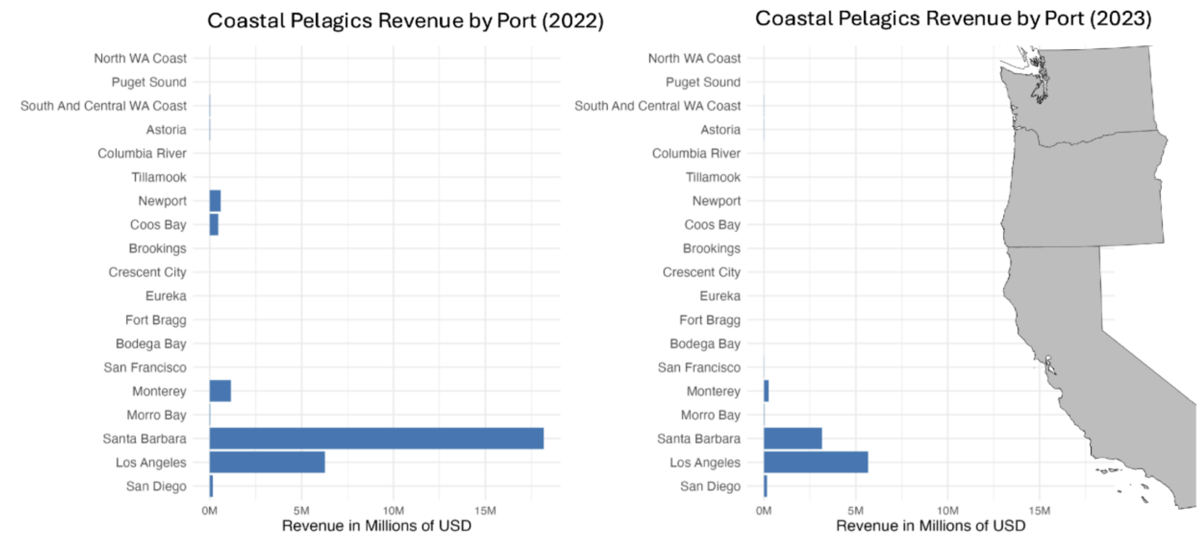

FigureR.2: Coastal Pelagic FMP revenue for 2022 (left) and 2023 (right) across IO-PAC port groups.

Salmon revenues are lower overall, and limited to northern ports, with the implementation of salmon fishing closures in California (Fig. R.3). Accordingly, the Theil index measures for salmon show a steep increase from 2022 to 2023 (Fig. R.1). The Theil index results generally suggest that the commercial salmon fishery has seen its diminished revenues more geographically concentrated, and an examination of revenue changes between 2022 and 2023 indicate that this increasing concentration is limited to ports in Washington and Oregon (Fig. R.3).

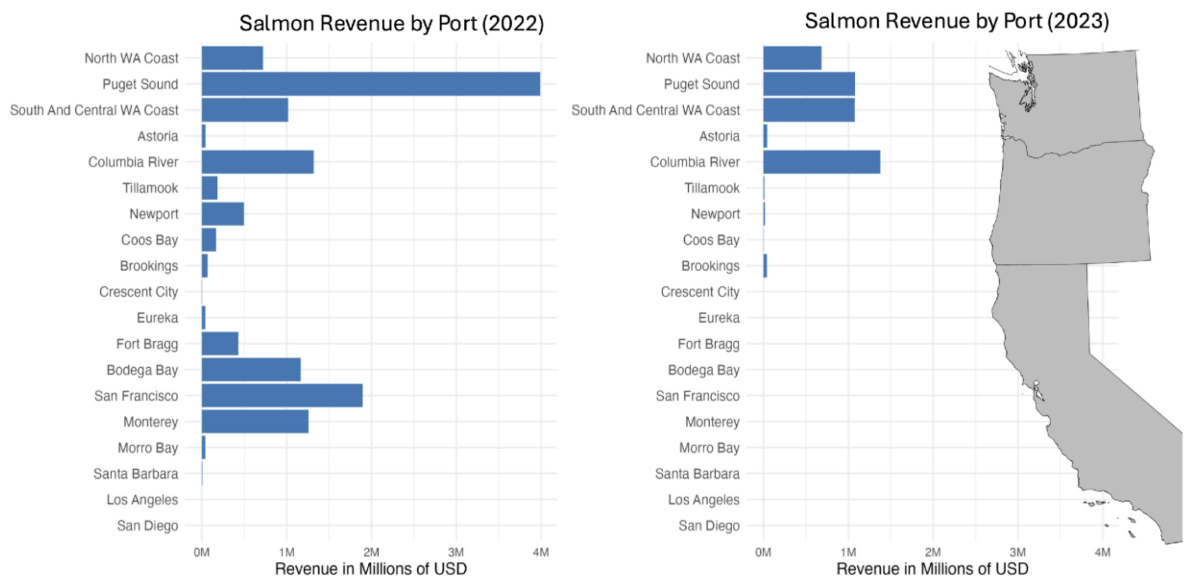

Figure R.3: Salmon FMP revenue for 2022 (left) and 2023 (right) across IO-PAC port groups.

Appendix S — FISHERIES PARTICIPATION NETWORKS

Fisheries participation networks may add levels of social and economic detail or context to other analyses in this report, such as those related to the community vulnerability, fishery diversification, and port-level revenue concentration. As such, fisheries participation networks offer one way to respond to requests from the EAS and EWG for deeper characterization of social and economic conditions in West Coast fishing communities, information relevant to meeting NS-8 under the Magnuson–Stevens Act, and may be informative for PFMC IRA Project 2.

We developed vessel-level fisheries participation networks, which provide a visual representation of the portfolio of fisheries that are economically-important to individual vessels within a port group (Fuller et al. 2017; Fisher et al. 2021). The networks are derived from landings receipts and summarized annually from week 46 in one year through week 45 in the following year (e.g., November 2020 to November 2021) to capture the beginning of the Dungeness crab fishing season. Fisheries landings data were retrieved from the Pacific Fisheries Information Network (PacFIN; http://pacfin.psmfc.org) database. We note that in Washington, fish tickets include a port assigned based on the actual port of landing or derived from the license database; prior to 2018, most port data were derived (see Table S1).

To focus the analysis on vessels that derive a substantial amount of income from commercial fishing, we include only vessels that generate at least $5,000 annually in total fisheries revenue. In addition, vessels must generate at least $500 of revenue from a given fishery (node) to be included as participants in that fishery. We assume that economically-important fisheries are those that contribute to at least a median of 10% of the annual revenue of associated vessels. Vessels are represented in all port groups for which their landings meet these conditions. To maintain confidentiality, we include only fisheries with at least three vessels participating in a port group.

In network graphs, node size represents the median proportional contribution of a fishery to annual vessel-level revenue; it is scaled relative to the fishery with the maximum median proportional contribution to annual vessel-level revenue in each network, summarized by port group. Therefore, node sizes are not comparable across port groups, only within them. The edges connecting pairs of nodes indicate that vessels participate in both fisheries, and the widths of these edges scale with the number of vessels exhibiting this behavior, as well as the total amount and evenness of revenue generation from each pair of fisheries. As with node sizes, edge widths are not comparable across port groups, only within them.

Fisheries participation networks representing IO-PAC port groups in the past year (November 2023 to November 2024) consisted of one to nine fisheries nodes, with 0–21 links between the fisheries within each network (Figs. 4.3, S.1 - S.4); all IO-PAC port groups are illustrated in these figures except for Other Coastal WA and Unknown Ports.

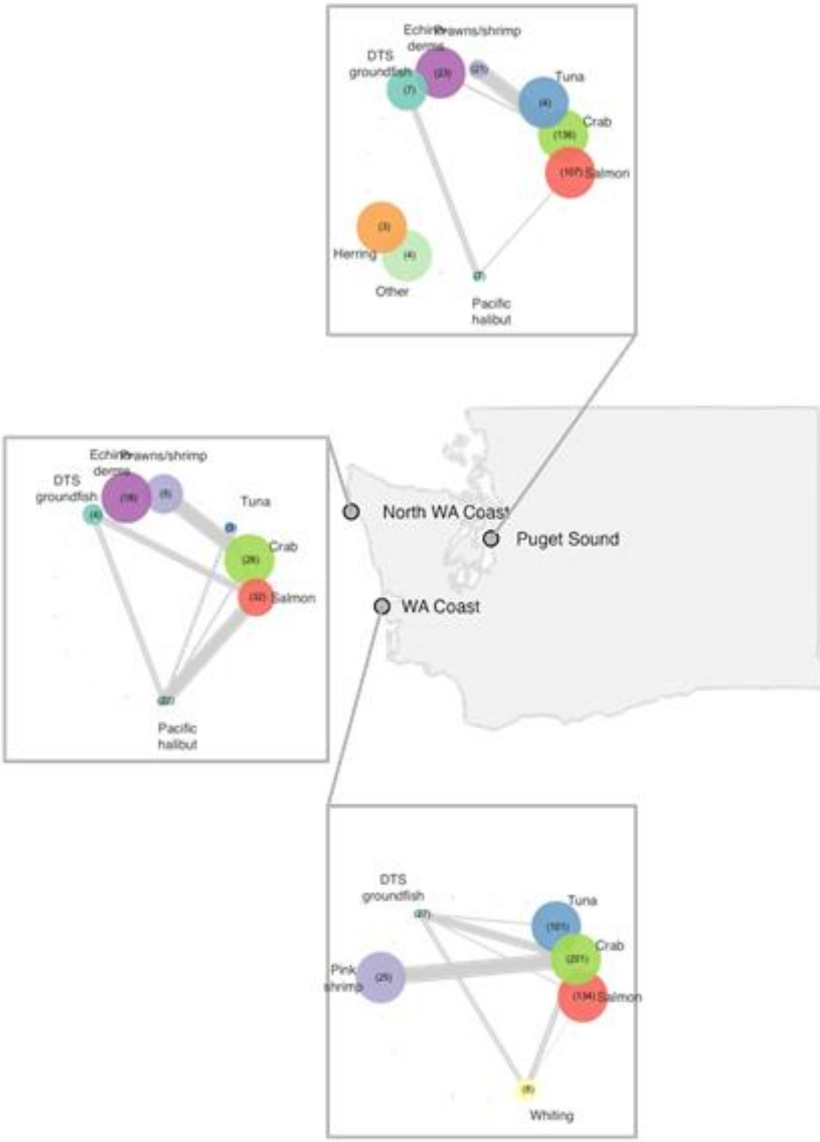

Figure S.1: Fisheries participation networks for IO-PAC port groups in Washington, based on November 2023-November 2024 (a Dungeness crab year) landings receipts. Node size is proportional to the median contribution of a given fishery to annual vessel-level revenue; values in parentheses are the number of vessels participating in the fishery. Thickness of lines ("edges") is proportional to the number of vessels participating in both of the fisheries connected by the lines, and the evenness of revenue generated by each fishery in the pair. Data and analyses provided by J. Samhouri (NMFS/NWFSC), with data derived from PacFIN (http://pacfin.psmfc.org).

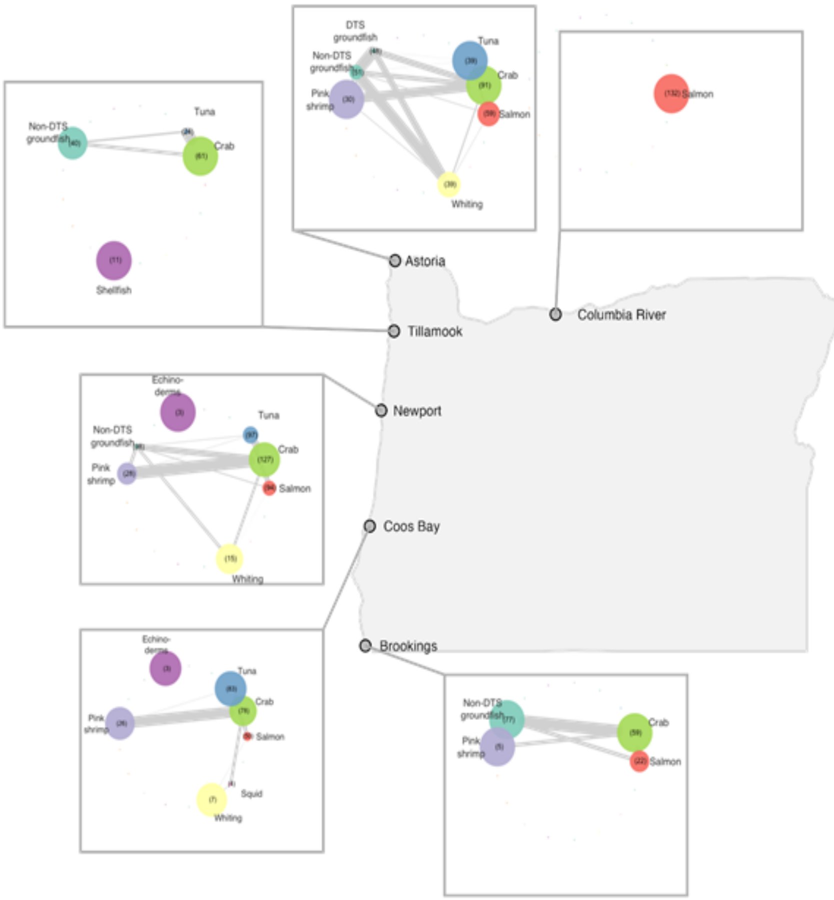

Figure S.2: Fisheries participation networks for IO-PAC port groups in Oregon, based on November 2023-November 2024 (a Dungeness crab year) landings receipts. Node size is proportional to the median contribution of a given fishery to annual vessel-level revenue; values in parentheses are the number of vessels participating in the fishery. Thickness of lines ("edges") is proportional to the number of vessels participating in both of the fisheries connected by the lines, and the evenness of revenue generated by each fishery in the pair. Data and analyses provided by J. Samhouri (NMFS/NWFSC), with data derived from PacFIN (http://pacfin.psmfc.org).

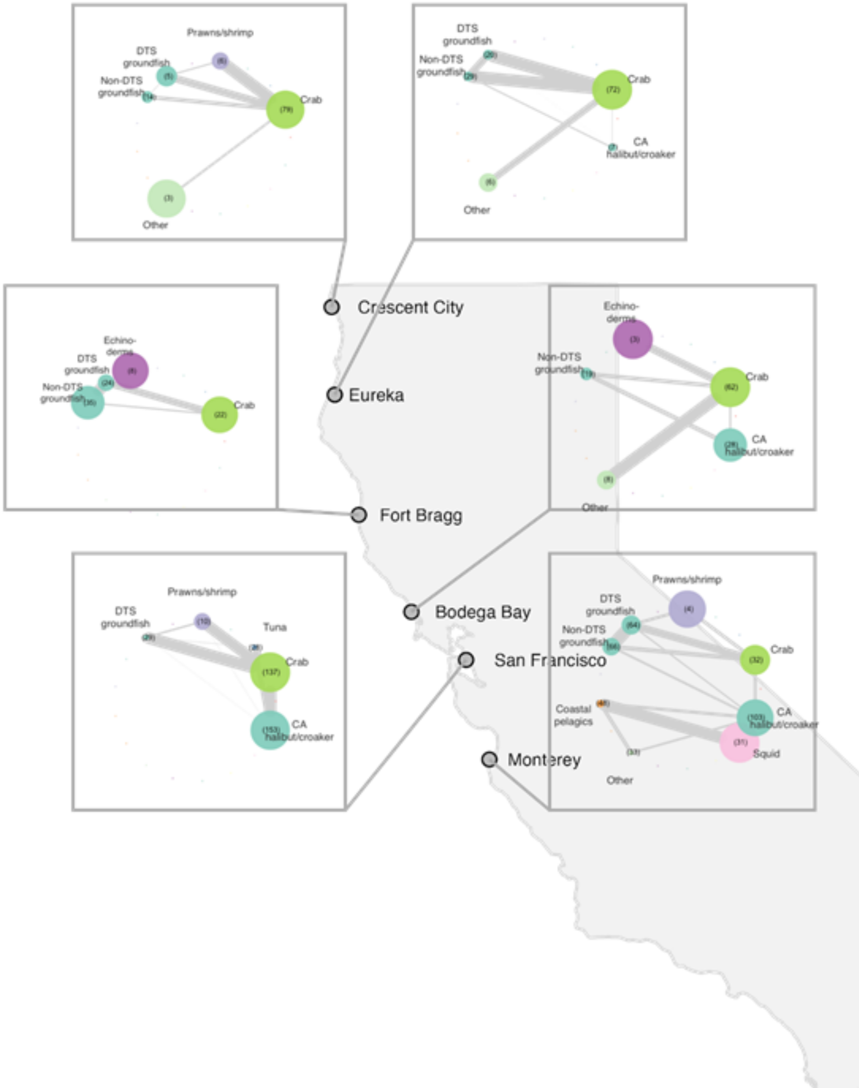

Figure S.3: Fisheries participation networks for IO-PAC port groups in Northern California, based on November 2023-November 2024 (a Dungeness crab year) landings receipts. Node size is proportional to the median contribution of a given fishery to annual vessel-level revenue; values in parentheses are the number of vessels participating in the fishery. Thickness of lines ("edges") is proportional to the number of vessels participating in both of the fisheries connected by the lines, and the evenness of revenue generated by each fishery in the pair. Data and analyses provided by J. Samhouri (NMFS/NWFSC), with data derived from PacFIN (http://pacfin.psmfc.org)

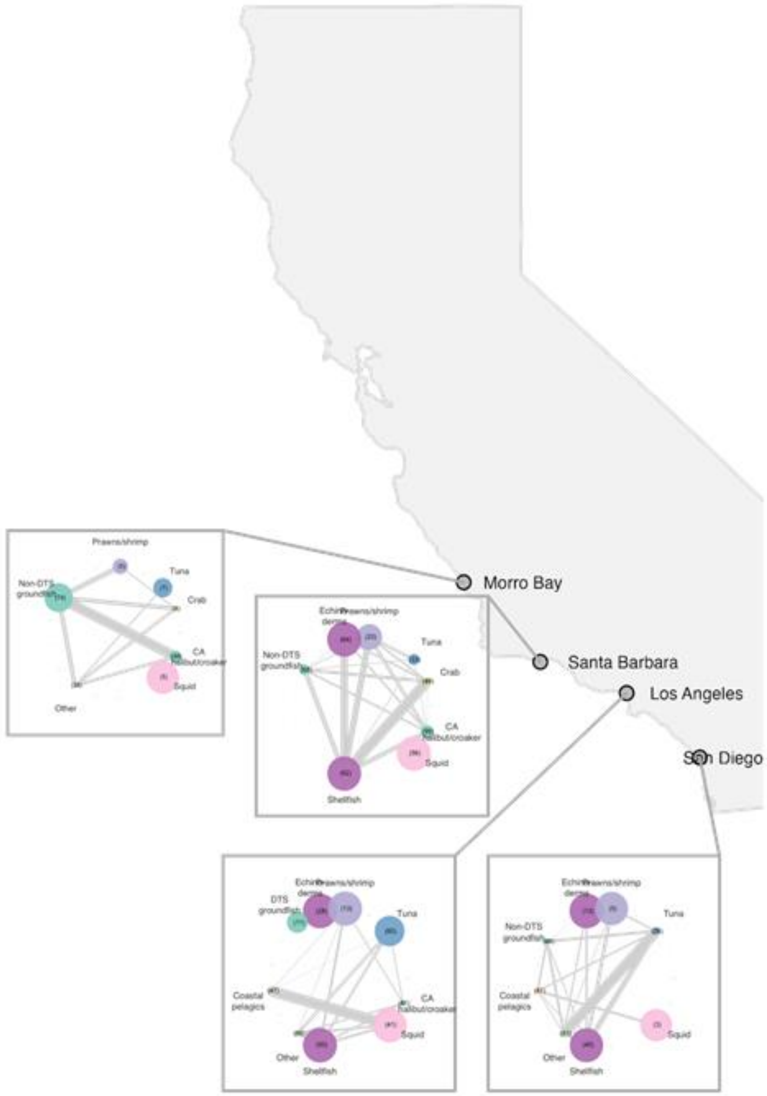

Figure S.4: Fisheries participation networks for IO-PAC port groups in Southern California, based on November 2023-November 2024 (a Dungeness crab year) landings receipts. Node size is proportional to the median contribution of a given fishery to annual vessel-level revenue; values in parentheses are the number of vessels participating in the fishery. Thickness of lines ("edges") is proportional to the number of vessels participating in both of the fisheries connected by the lines, and the evenness of revenue generated by each fishery in the pair. Data and analyses provided by J. Samhouri (NMFS/NWFSC), with data derived from PacFIN (http://pacfin.psmfc.org).

Tracking changes in networks over time may support Council activities by providing insight into how fishing communities are changing and potentially adapting to external forces such as changing stock availability, climate, regulations (such as rebuilding plans), and economic and social systems. To that end, we present time series for each port group of the number of fisheries (Fig S.5) and of a network metric called Edge Density within the participation networks from 2004-2024 (Fig S.6). The number of fisheries indicates how varied the types of economically-important, commercial fishing opportunities are within a port group (the nodes in the networks in Figs. S.1 - S.4). Edge Density, which we refer to below as connectivity, represents the extent to which nodes within a network are connected (the lines in the networks in Figs. S.1 - S.4) by vessels that participate in multiple fisheries. Declines in Edge Density imply less well-connected fisheries and a simplification of network structure, which can in turn reduce resilience to environmental or regulatory shocks (e.g., Fisher et al. 2021). In contrast, networks with high edge density suggest that fishers have greater ability to move effort between fisheries and thus substitute for lost revenue from a fishery that is closed or has a poor year.

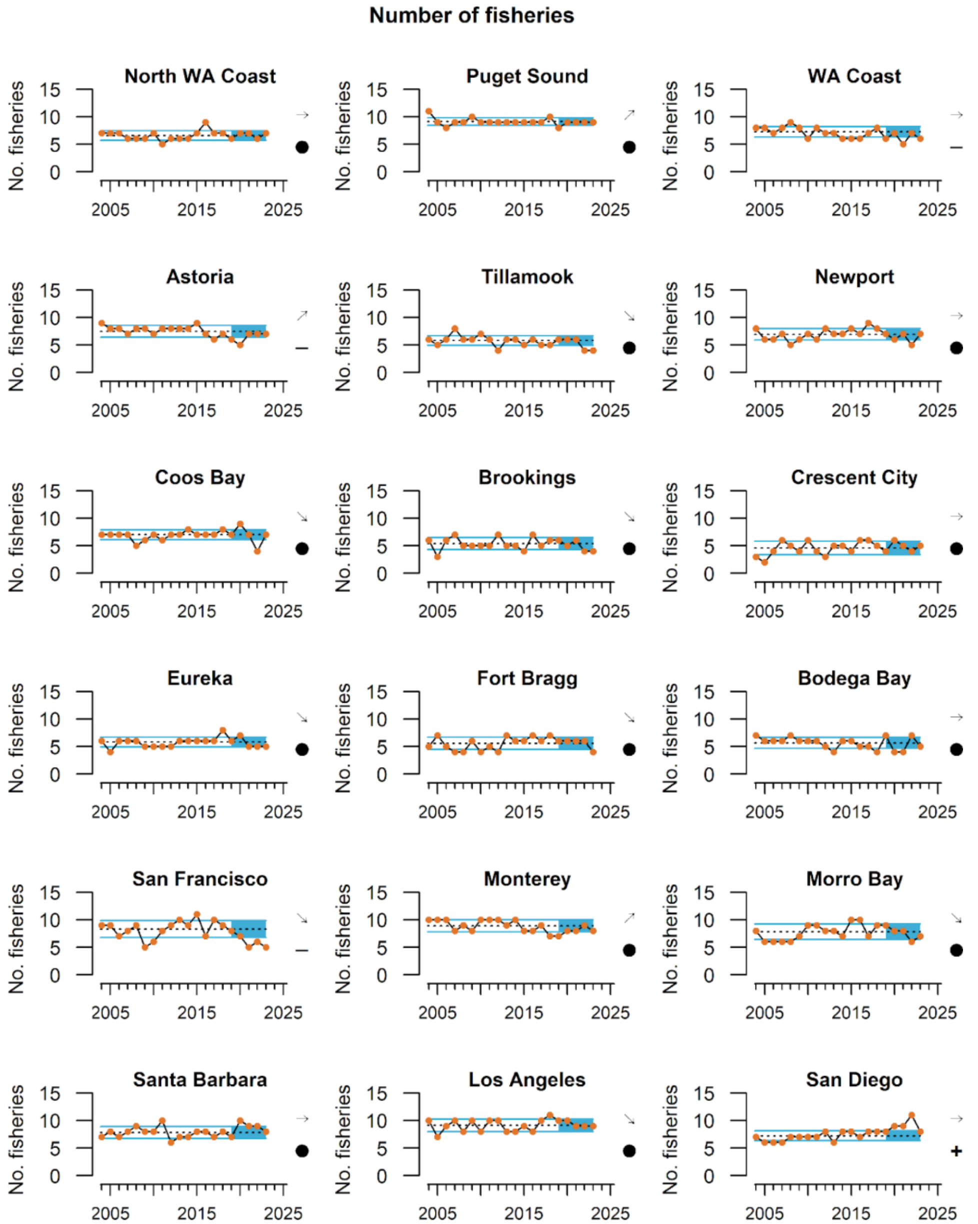

Figure S.5: Number of fisheries (nodes) represented in fisheries participation networks for IO-PAC port groups from Nov 2004 - Nov 2024. More fisheries indicate greater variation in the types of commercial fishing opportunities within a port group. Each year represents landings from Nov of the previous year through Nov of the labeled year. Port groups not shown: Other Coastal Washington, Columbia River, and Unknown Ports. Data and analyses provided by J. Samhouri (NMFS/NWFSC), with data derived from PacFIN (http://pacfin.psmfc.org).

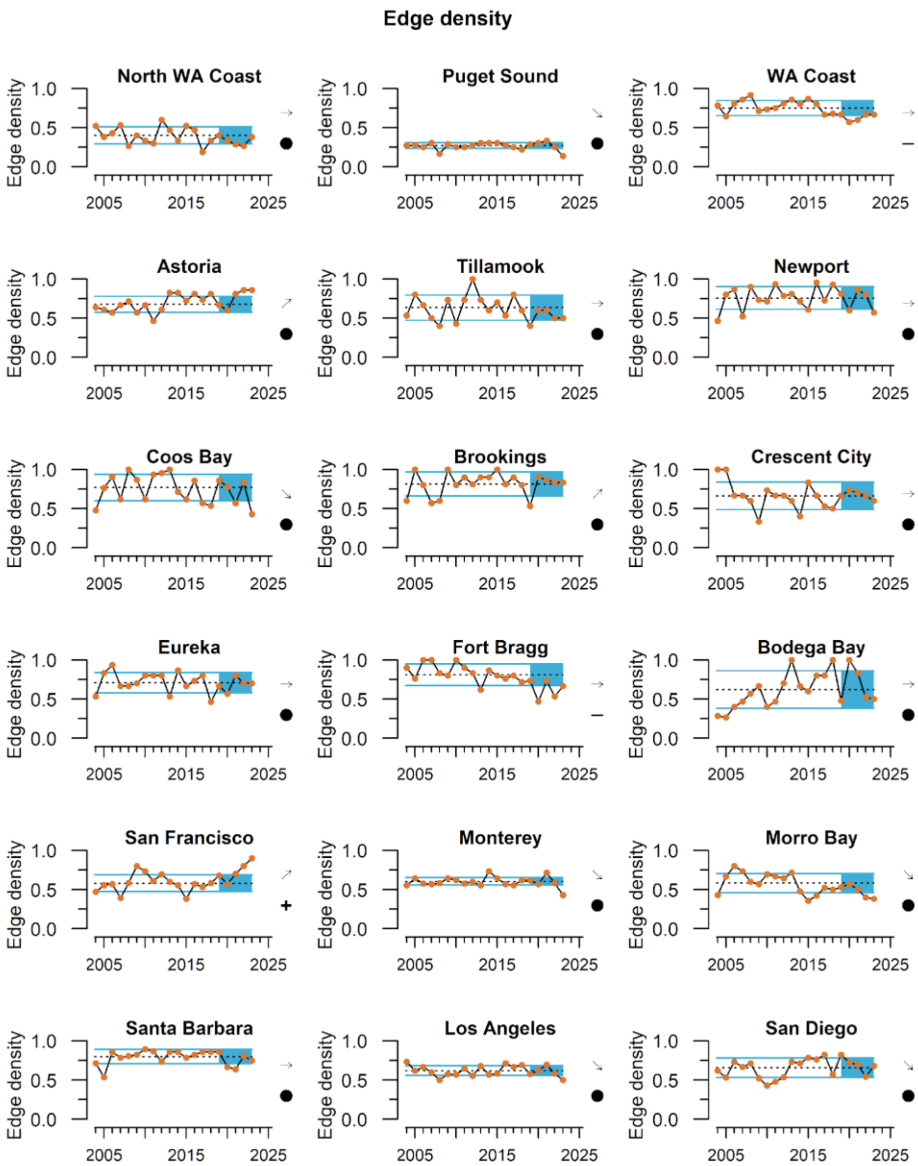

Figure S.6: Edge Density in fisheries participation networks for IO-PAC port groups from Nov 2004 - Nov 2024. Higher edge densities correspond to greater connectivity in fishery participation among all vessels represented in the network. Note that edge density scales with network size (it is easier to achieve a high density in a low complexity network), so comparisons across networks of different sizes should be interpreted carefully. All other figure specifications are identical to Figure S.5.

Table S1. Summary of WDFW landings receipts (fish tickets), indicating the percentage of receipts, landings, and revenue that included port information that was not derived from the WDFW license database, was derived, or the port derivation is unknown. Years refer to crab years, as in the Fisheries Participation Networks (e.g., 2023 reflects November 2023 (week 46) - November 2024 (week 45)).

	Port Not Derived			Port Derived			Unknown if Port Derived		
Year	% of Tickets	% of Landings	% of Revenue	% of Tickets	% of Landings	% of Revenue	% of Tickets	% of Landings	% of Revenue
2003	0.0%	0.0%	0.0%	98.3%	91.5%	71.5%	1.7%	8.5%	28.5%
2004	0.0%	0.0%	0.0%	98.1%	89.9%	69.0%	1.9%	10.1%	31.0%
2005	0.0%	0.0%	0.0%	98.2%	90.6%	67.0%	1.8%	9.4%	33.0%
2006	0.0%	0.0%	0.0%	98.1%	88.7%	65.7%	1.9%	11.3%	34.3%
2007	0.0%	0.0%	0.0%	98.1%	87.7%	68.8%	1.9%	12.3%	31.2%
2008	0.0%	0.0%	0.0%	98.2%	88.2%	66.8%	1.8%	11.8%	33.2%
2009	0.0%	0.0%	0.0%	98.4%	89.1%	71.2%	1.6%	10.9%	28.8%
2010	0.0%	0.2%	0.0%	98.6%	90.0%	74.7%	1.3%	9.9%	25.3%
2011	0.2%	0.4%	0.0%	98.4%	89.8%	73.8%	1.4%	9.8%	26.1%
2012	0.0%	0.0%	0.0%	98.4%	91.5%	72.0%	1.6%	8.5%	28.0%
2013	0.0%	0.0%	0.0%	98.5%	88.5%	72.7%	1.5%	11.5%	27.3%
2014	0.1%	0.0%	0.1%	98.1%	86.0%	71.6%	1.9%	13.9%	28.3%
2015	0.7%	3.9%	0.3%	96.6%	83.3%	71.0%	2.7%	12.8%	28.7%
2016	17.9%	50.6%	4.3%	74.5%	38.7%	66.2%	7.6%	10.8%	29.4%
2017	19.1%	50.3%	4.3%	45.9%	25.5%	35.3%	35.1%	24.2%	60.3%
2018	25.5%	63.0%	0.0%	38.2%	13.2%	0.0%	36.3%	23.8%	0.0%
2019	23.5%	72.8%	0.0%	33.1%	6.2%	0.0%	43.5%	21.0%	0.0%
2020	25.2%	71.6%	0.0%	32.9%	10.0%	0.0%	41.8%	18.4%	0.0%
2021	20.1%	66.5%	0.0%	37.1%	10.0%	0.0%	42.7%	23.5%	0.0%
2022	24.6%	72.3%	0.0%	34.1%	7.7%	0.0%	41.3%	20.0%	0.0%
2023	28.9%	74.5%	0.0%	29.0%	7.3%	0.0%	42.1%	18.2%	0.0%

Appendix T — STATE-BY-STATE FISHERY LANDINGS AND REVENUES

Link to main section: Coastwide Landings by Major Fisheries

The Council and EWG have requested information on state-by-state fisheries landings and revenues; these values are presented here. Commercial landings and revenue data are best summarized by the Pacific Fisheries Information Network (PacFIN; pacfin.psmfc.org), and recreational landings are best summarized by the Recreational Fisheries Information Network (RecFIN; www.recfin.org). Data from 1981 to 2024 were downloaded from PacFIN and RecFIN on January 10, 2025. Landings provide the best long-term indicator of fisheries removals. Revenues are calculated based on consumer price indices in 2024 dollars. Status and trends are estimated relative to a frame of reference of 1991-2020.

T.1 State-by-State Landings

Total fisheries landings in Washington were >1 s.d. below the long-term average and decreased from 2020 to 2024, with the lowest total landings in the time series observed in 2024 (Fig. T.1). These patterns were driven primarily by a decrease in Pacific whiting landings over the last five years, including a 28% decrease in 2024 from 2023. Commercial crab was the only fishery in Washington with a significantly increasing 5-year trend. Commercial shrimp landings were >1 s.d. above the long-term average, while salmon, Pacific whiting, and HMS landings were >1 s.d. below the long-term average. All other major commercial fisheries showed no trends and were within 1 s.d. of the long-term average from 2020 to 2024.

Total recreational catch data (excluding salmon and halibut) in Washington were complete through October 2024 and varied within 1 s.d. of the long-term average from 2020 to 2024 (Fig. T.1). Recreational landings of Chinook and coho salmon were within 1 s.d. of the long-term average from 2019 to 2023 (2024 data were not available at time of this report).

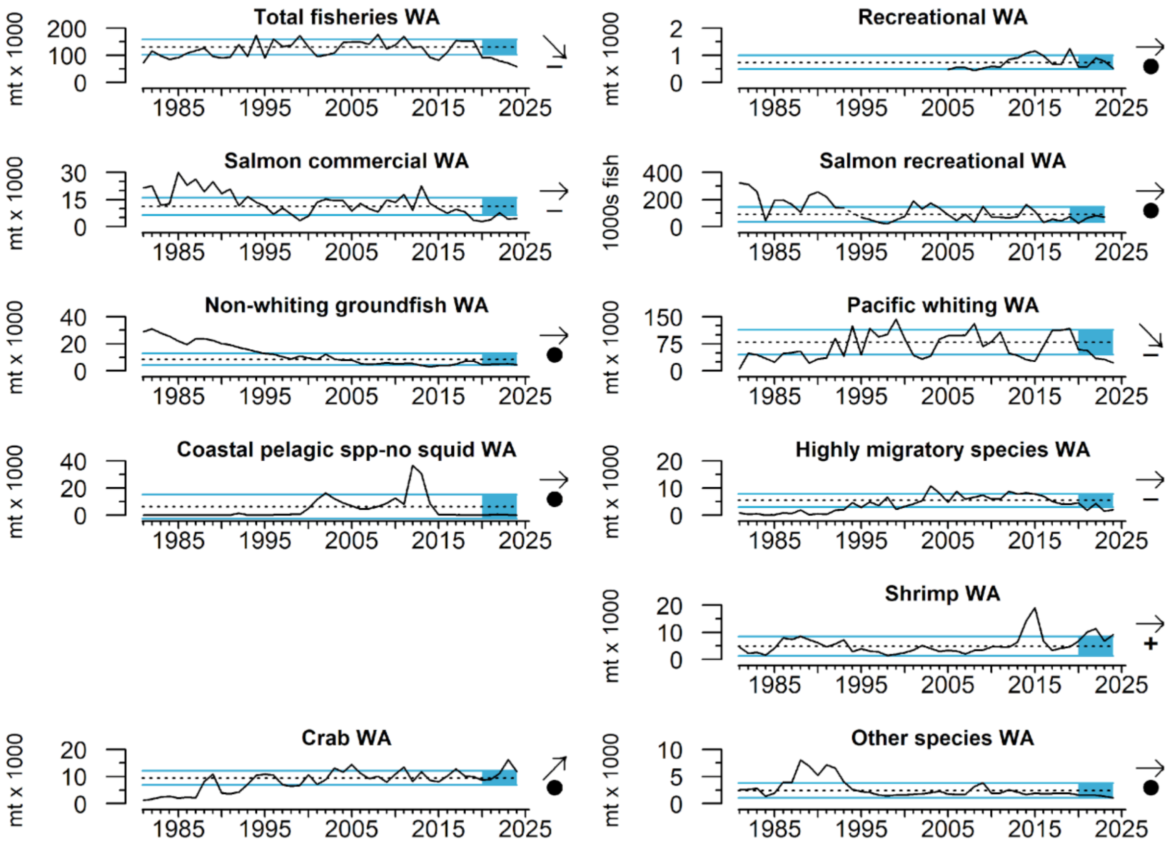

Figure T.1: Annual Washington landings from West Coast commercial (data from PacFIN) and recreational (data from RecFin) fisheries, including total landings across all fisheries from 1981 - 2024. Lines, colors, and symbols are as in Fig. 2.1.

Total fisheries landings in Oregon decreased 24% in 2024 from 2023, and decreased by >1 s.d. of the long-term average, but the five-year mean from 2020 to 2024 was still >1 s.d. above the long-term average (Fig. T.2). Similar to Washington, these patterns were driven primarily by landings of Pacific whiting, which decreased and were >1 s.d. above the long-term average for the most recent five years. Commercial landings of crab increased by >1 s.d. of the long-term average from 2020 to 2024. Landings of shrimp and Pacific whiting were >1 s.d. above the long-term average, while landings of HMS were >1 s.d. below the long-term average over the last five years. Landings of market squid in Oregon ports have dropped to near 0 levels in 2023 and 2024. Commercial landings of all other commercial fisheries showed no significant recent trends and had short-term averages within 1 s.d. of long-term averages.

Recreational fisheries landings data (excluding salmon and Pacific halibut) in Oregon were complete through October 2024 and have increased by >1 s.d. of the long-term average from 2020 to 2024 primarily due to an increasing trend in landings of albacore (Fig. T.2). Recreational landings of Chinook and coho salmon showed no significant recent trend, and have been within 1 s.d. of the long-term average since 2019 (2024 data were not available at time of report).

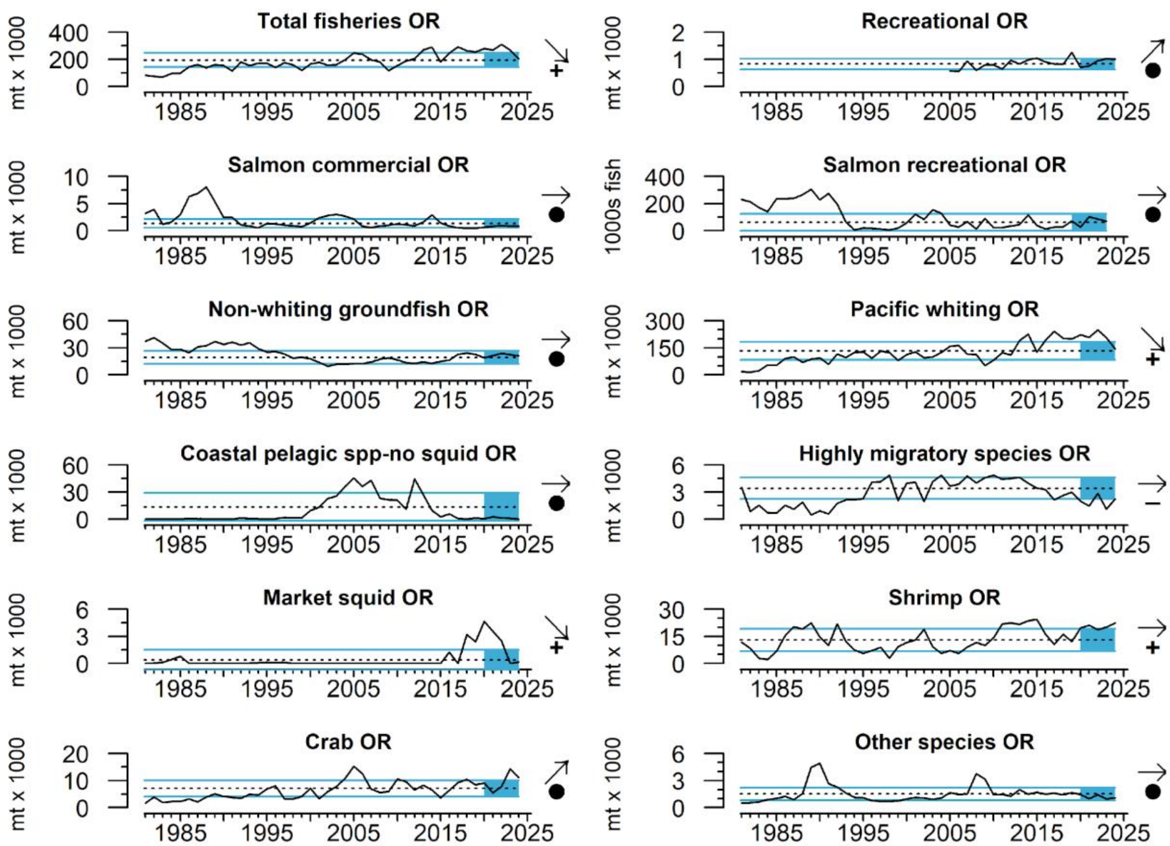

Figure T.2: Annual Oregon landings from West Coast commercial (data from PacFIN) and recreational (data from RecFin) fisheries, including total landings across all fisheries from 1981 - 2024. Lines, colors, and symbols are as in Fig. 2.1.

Total fisheries landings in California increased 48% in 2024 from 2023, but were >1 s.d. below the long-term average from 2020 to 2024 (Fig. T.3). Landings for CPS finfish, shrimp and Other species were >1 s.d below the long-term average over the last five years. Commercial salmon landings decreased by >1 s.d. of the long-term average because the fishery was closed in 2023 and 2024. All other major fisheries showed no significant trends and were within 1 s.d. of long-term averages over the last five years.

Recreational landings data (excluding salmon, Pacific halibut and HMS) in California were complete through October 2024. Recreational landings were >1 s.d. below the long-term average over the past five years (Fig. T.3). The low status level was largely due to relatively low levels of landings for lingcod and vermilion rockfish over the last five years. Similar to commercial fisheries, the recreational salmon fishery in California was closed in 2023 and again in 2024.

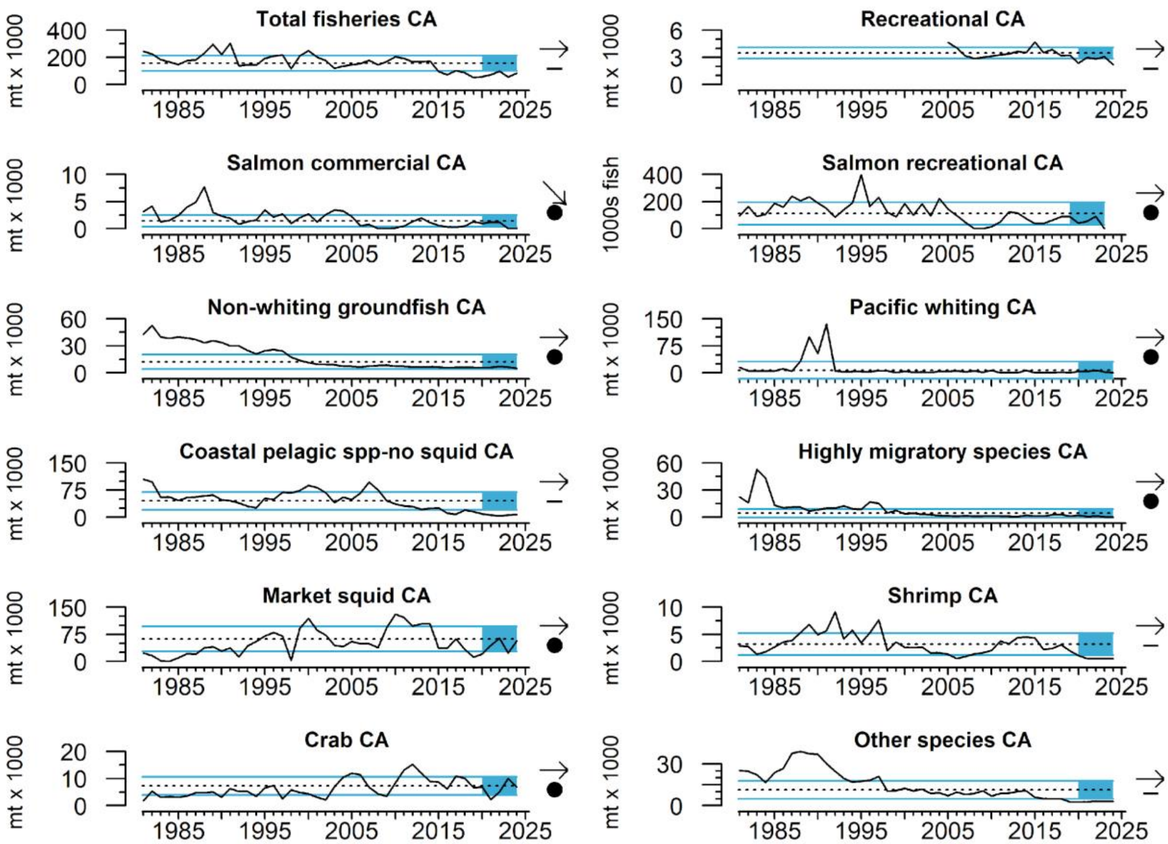

Figure T.3: Annual California landings from West Coast commercial (data from PacFIN) and recreational (data from RecFin) fisheries, including total landings across all fisheries from 1981 - 2024. Lines, colors, and symbols are as in Fig. 2.1.

T.2 Commercial Fisheries Revenue

Total revenue across U.S. West Coast commercial fisheries in 2024 increased by 3% from 2023, based on data currently available (Fig. T.4). Over the most recent five years, total revenue was highly variable, but remained within 1 s.d. of the long-term average. Recent revenue patterns have been driven by large variation in market squid revenues over the last five years and smaller one- or two-year increases in crab, Pacific whiting and HMS revenues since 2020. Revenue for 5 of 9 commercial fisheries increased from 2023 to 2024: market squid (137%), HMS (52%), shrimp (25%), salmon (10%), and CPS finfish (2%). In contrast, Pacific whiting (-19%), non-whiting groundfish (-15%), Other species (-8%) and crab (-4%) fisheries generated less revenue in 2024 than in 2023. Commercial revenue for salmon and HMS fisheries decreased by >1 s.d. of their long-term average from 2020 to 2024. Revenue from salmon, non-whiting groundfish, CPS finfish and HMS was >1 s.d. below long-term averages over the last five years. All other fisheries' revenues showed no trends and were within 1 s.d. of long-term averages.

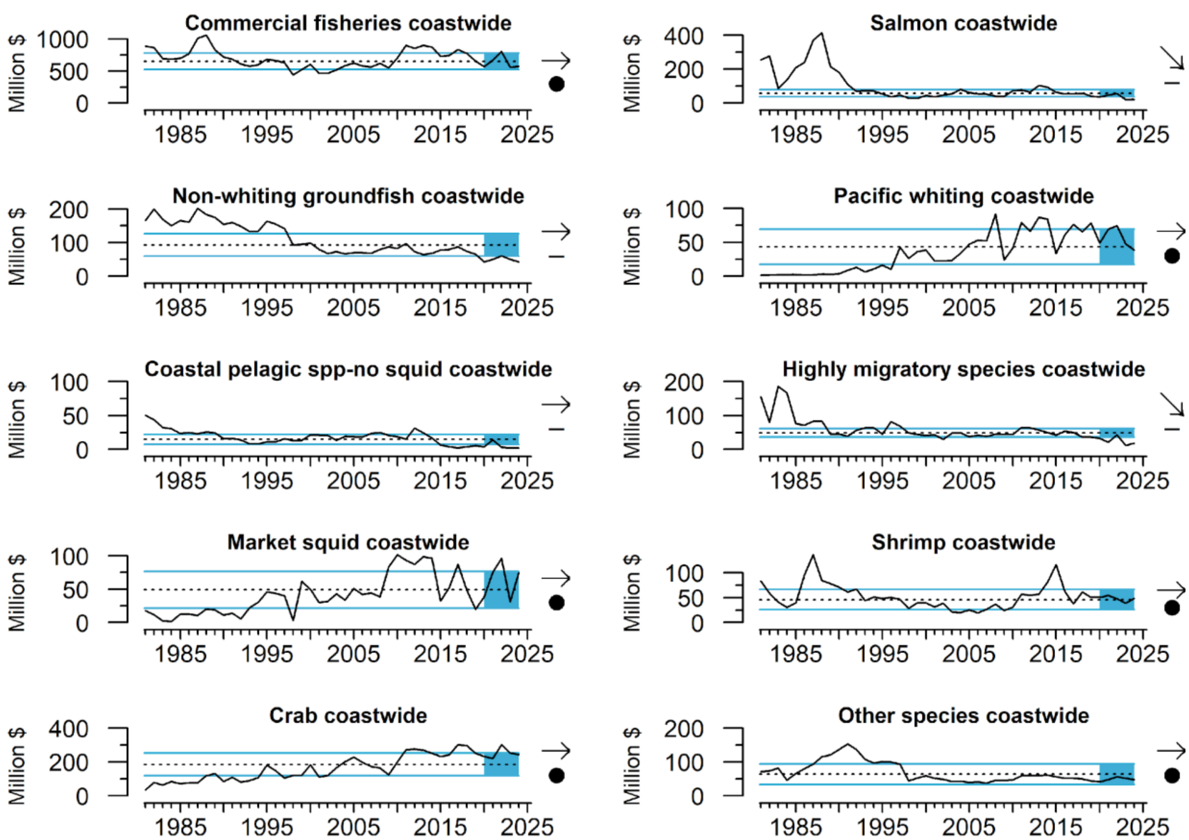

Figure T.4: Annual coastwide revenue (ex-vessel value in 2024 dollars) from West Coast commercial fisheries (data from PacFin) from 1981 - 2024. Whiting revenue includes shoreside and at-sea values from PacFIN, NORPAC

(North Pacific Groundfish Observer Program) and NMFS Office of Science & Technology. Lines, colors, and symbols are as in Fig. 2.1.

Total revenue across commercial fisheries in Washington was highly variable from 2020 to 2024, with a 10% decrease in 2024 from 2023 levels (Fig. T.5). These patterns are largely driven by variability in revenue from crab, shrimp and HMS landings over the last five years. Overall, 3 of 8 major fisheries increased in revenue in 2024 from 2023 levels: HMS (67%), shrimp (19%) and salmon (1%). In contrast, revenue from Pacific whiting (-33%), other species (-16%), non-whiting groundfish (-8%), crab (-7%) and CPS finfish (-3%) fisheries was lower in 2024 compared to 2023. Crab fisheries' revenue was >1 s.d. above long-term averages while non-whiting groundfish and salmon revenue was >1 s.d. below long-term averages. Revenue from HMS fisheries decreased by >1 s.d. of the long-term average. All other fisheries showed no trends and were within long-term averages over the last five years.

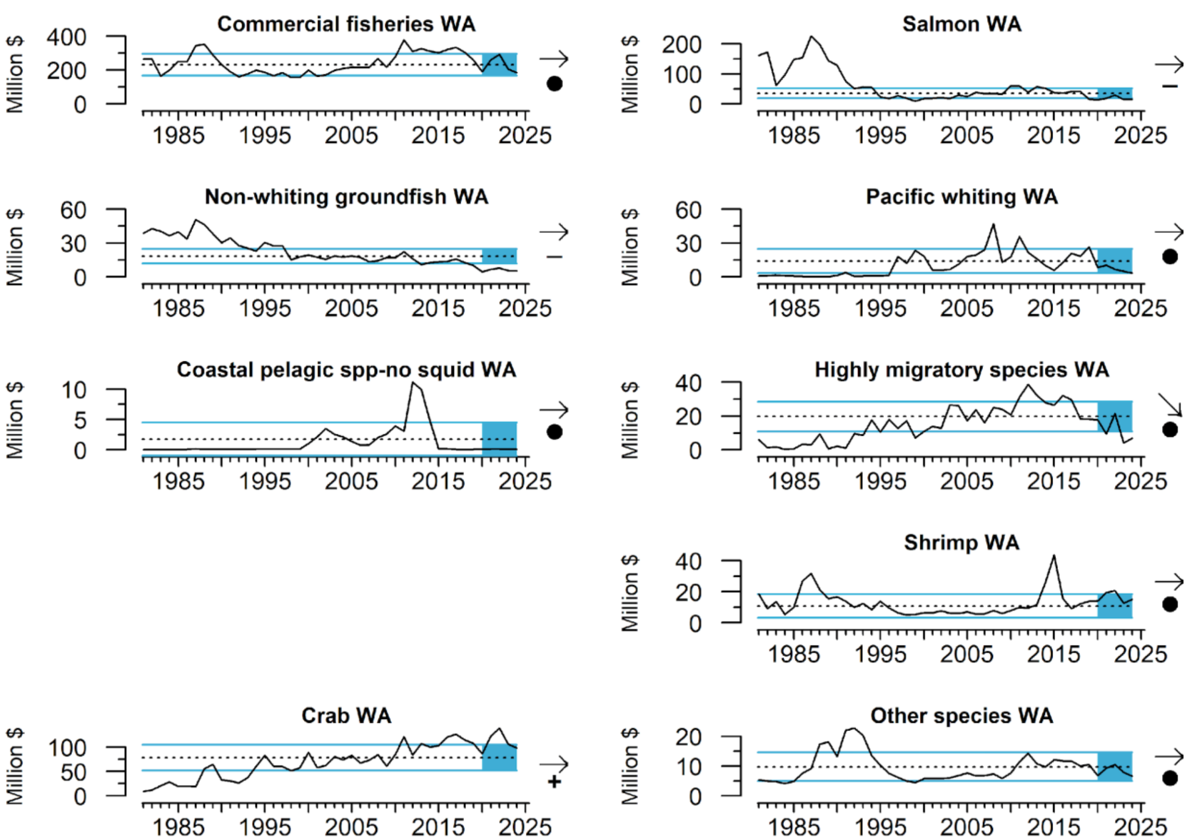

Figure T.5: Annual Washington revenue (ex-vessel value in 2024 dollars) from West Coast commercial fisheries (data from PacFin) from 1981 - 2024.

Whiting revenue includes shoreside and at-sea values from PacFIN, NORPAC (North Pacific Groundfish Observer Program) and NMFS Office of Science & Technology. Lines, colors, and symbols are as in Fig. 2.1.

Total revenue across commercial fisheries in Oregon showed no trend and was within 1 s.d. of the long-term average from 2020 to 2024, with a 3% increase in 2024 from 2023 levels (Fig. T.6). These patterns are largely driven by changes in revenue from crab and Pacific whiting fisheries over the last five years. Overall, 4 of 9 major fisheries increased in revenue in 2024 from 2023 levels: HMS (129%), shrimp (38%), salmon (35%), and crab (6%). In contrast, revenue from CPS finfish (-75%), Other species (-30%), non-whiting groundfish (-20%) and Pacific whiting (-16%) was lower in 2024 compared to 2023. Even though there was a relatively large year-to-year decrease in revenue observed in the CPS finfish fishery, revenue levels have been consistently at very low values over the last decade. Pacific whiting, market squid and crab fisheries' revenue were all >1 s.d. above long-term averages, while non-whiting groundfish was >1 s.d. below its long-term average. Revenue from other species fisheries decreased by >1 s.d. of its long-term average, while all other fisheries showed no trends over the last five years.

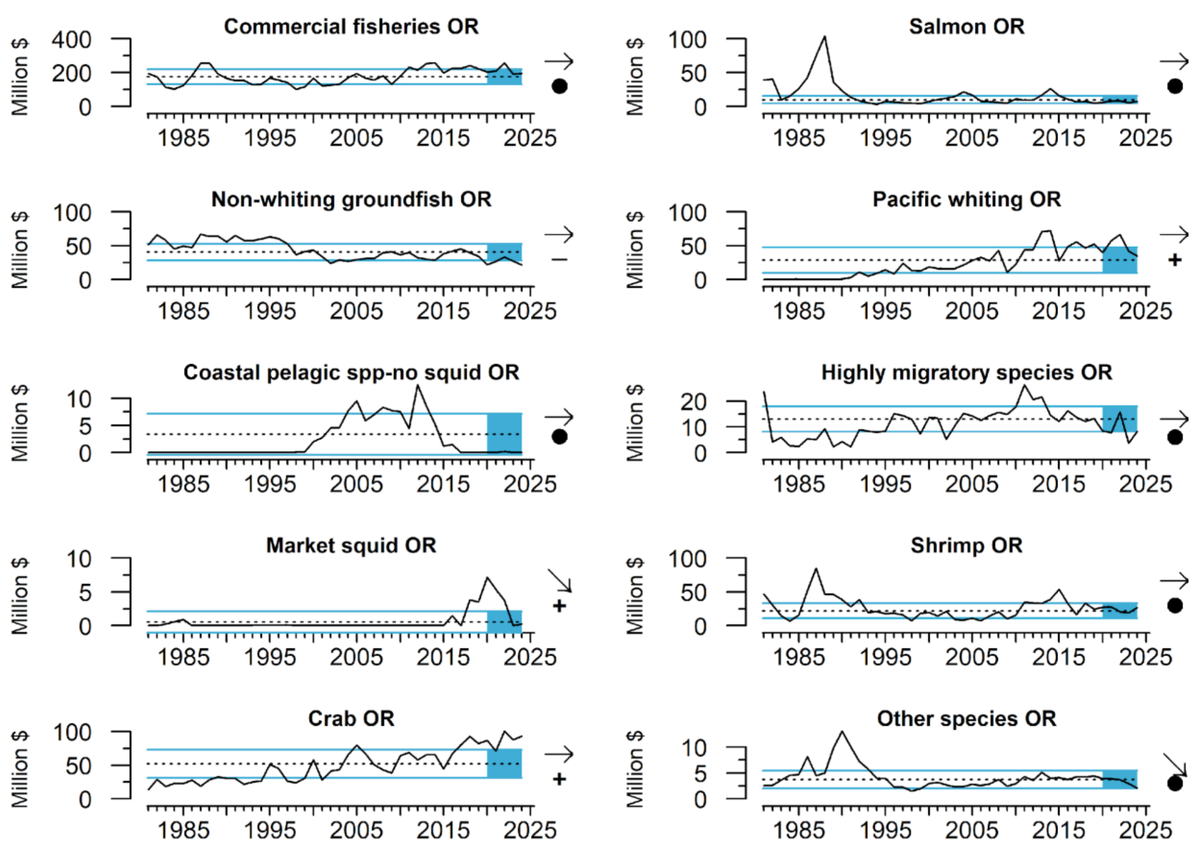

Figure T.6: Annual Oregon revenue (ex-vessel value in 2024 dollars) from West Coast commercial fisheries (data from PacFin) from 1981 - 2024. Whiting revenue includes shoreside and at-sea values from PacFIN, NORPAC (North Pacific Groundfish Observer Program) and NMFS Office of Science & Technology. Lines, colors, and symbols are as in Fig. 2.1.

Total revenue across commercial fisheries in California increased 18% from 2023 to 2024, but is still near the lower range of its long-term average (Fig. T.7). This time series is largely driven by annual variation in revenue from market squid and a decline in crab revenue since 2012. Overall, 2 of 9 major fisheries increased in revenue in 2024 from 2023 levels: market squid (136%) and CPS finfish (3%). In contrast, revenue from Pacific whiting (-91%), HMS (-31%), crab (-11%), non-whiting groundfish (-11%), other species (-5%), and shrimp (-1%) fisheries was lower in 2024 compared to 2023. Even though there was a relatively large decrease in revenue observed in the Pacific whiting fishery, revenue levels are at very low values, and this revenue comes from fishing events that occur in CA waters but processed at sea and landed outside of California. Revenue from salmon (closed in 2023 & 2024), CPS finfish, and Pacific whiting fisheries have decreased over the last five years, while all other fisheries showed no trends. Revenue from non-whiting groundfish, CPS finfish, and shrimp fisheries were >1 s.d. below their long-term average, while all other fisheries were within 1 s.d. of their long-term average over the last five years in California.

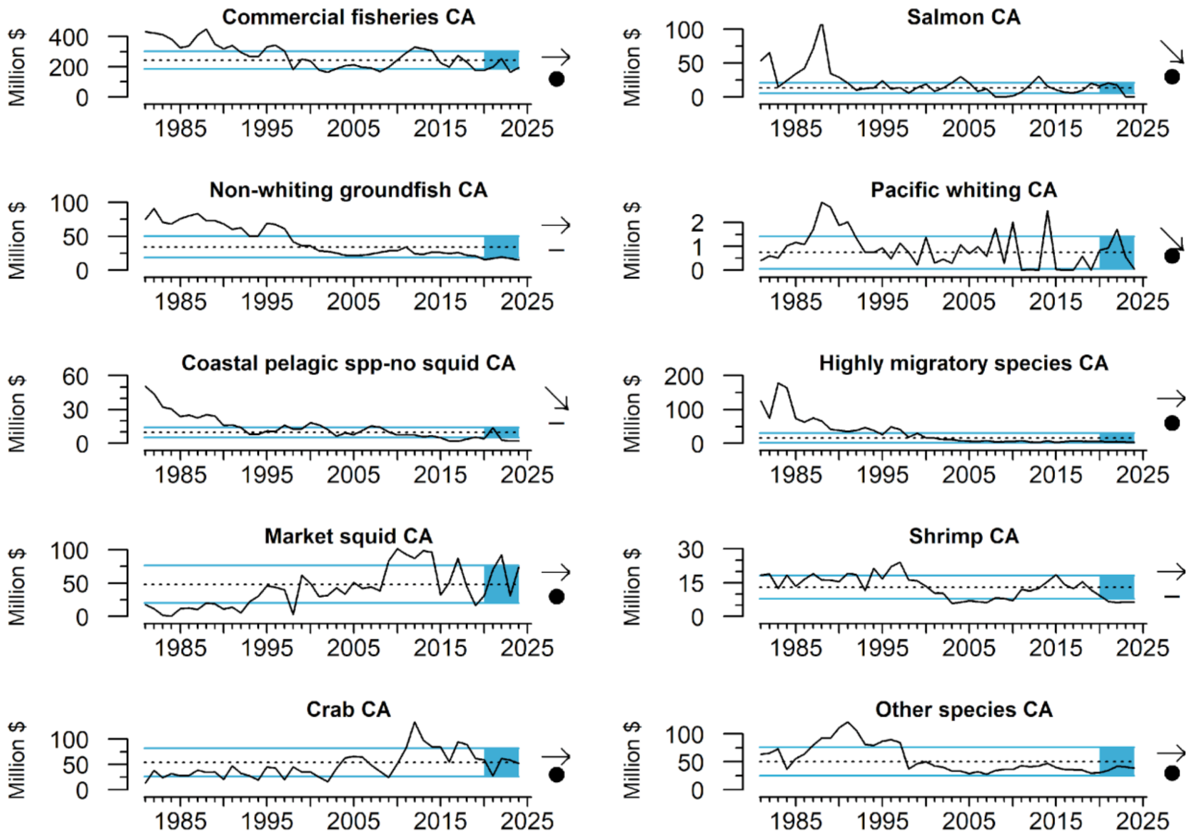

Figure T.7: Annual California revenue (ex-vessel value in 2024 dollars) from West Coast commercial fisheries (data from PacFin) from 1981 - 2024. Whiting revenue includes shoreside and at-sea values from PacFIN, NORPAC (North Pacific Groundfish Observer Program) and NMFS Office of Science & Technology. Lines, colors, and symbols are as in Fig. 2.1.

Appendix U — POTENTIAL FOR SPATIAL INTERACTIONS AMONG ECOSYSTEM INDICATORS & OCEAN-USE SECTORS

Link to main section: Potential Interactions Between Offshore Wind and Ecosystem Indicators

New ocean-use sectors of the economy (e.g., renewable energy and aquaculture) are becoming a reality off the West Coast, particularly with the Bureau of Ocean Energy Management's (BOEM) five offshore wind energy (OWE) leases off the northern and central California coast. Understanding how oceanic and atmospheric processes, protected species and their habitats, fisheries and fisheries stocks' habitat, fishing communities, and NMFS scientific surveys will be affected by new ocean-use sectors, such as OWE, is needed to inform effective marine spatial planning and adaptive management strategies, and to help minimize ocean-use conflicts across the West Coast into the future. Below, we describe two portfolios of indicators for i) oceanographic and lower-trophic level productivity and ii) fisheries activity that can help identify ocean areas important to the overall structure and function of the CCE, and that can track potential social-ecological impacts across all stages of OWE development.

U.1 Ecosystem Indicators

Here we introduce seven broad-scale indicators of long-term, spatial variation in oceanography and lower-trophic level productivity that could be used to inform spatial suitability analyses in areas off northern California being considered for OWE development. The ecosystem indicators include:

1. Average wind-driven upwelling during March-July (Fig. U.1a), calculated at 40m depth from 1988-2012 using the Regional Ocean Modeling System (Raghukumar et al. 2023).
2. Proportion of days that a front was identified during March-July, based on edge-detection analysis applied to satellite SST data from 2000-2023 (Fig. U.1b; GHRSST 2024).
3. Long-term, spatial variability and hotspots in primary productivity (Fig. U.1c), calculated from a biogeochemistry model as the average concentration of surface phytoplankton in May-July, 1995-2020 (Fiechter et al. 2018).
4. Long-term, spatial variability and hotspots in secondary productivity from May-August (Fig. U.1d), calculated as an ensemble of four different estimates of krill abundance/biomass across the West Coast (Cimino et al. 2020; Fiechter et al. 2020; Messié et al. 2022; Phillips et al. 2022).
5. Long-term, spatial variability and hotspots for young-of-year (YOY) rockfishes during their pelagic juvenile life stage in May-June from 2001-2022 (Fig. U.1e; Field et al. 2021).
6. Long-term, spatial variability and hotspots for YOY Pacific hake in May-June from 2001-2022 (Fig. U.1f; Field et al. 2021).
7. Long-term, spatial variability and hotspots of groundfish nursery habitat on the seafloor (Fig. U.1g), based on summed average densities of juveniles from 13 groundfish species in May-October from 2003-2018 (Tolimieri et al. 2020).

BOEM has been using a spatial suitability analysis developed by NOAA's National Centers for Coastal and Ocean Science (NCCOS) to identify areas for potential OWE development. In order to inform an analysis of new areas along the northern California coast, we used NCCOS's methods to calculate an overall suitability score across the seven ecosystem indicators for each grid cell (Fig. U.1h; Riley et al. 2021). Briefly, the raw data for each indicator was cropped to the area-of-interest, interpolated across a 2x2-km spatial grid, transformed using a z-membership function, and then geometrically averaged across all indicators for each grid cell. This geometric mean represents the suitability score of a grid cell for OWE development relative to the importance of these areas to the processes and taxa represented by each indicator; thus, a suitability score of '1' is most suitable for OWE, while suitability scores closer to 0 are less suitable. In addition to being applicable to siting of new areas, these indicators are being evaluated as baseline conditions that can be used to identify potential effects resulting from OWE development and to identify relevant mitigation strategies.

Wind Energy Areas (WEAs) off the coast of Oregon (e.g. "Brookings WEA" in Fig. U.1) were designated by BOEM, but leasing the areas was postponed in 2024. We include the southern coast of Oregon in our spatial domain to keep these areas in mind for possible future interactions.

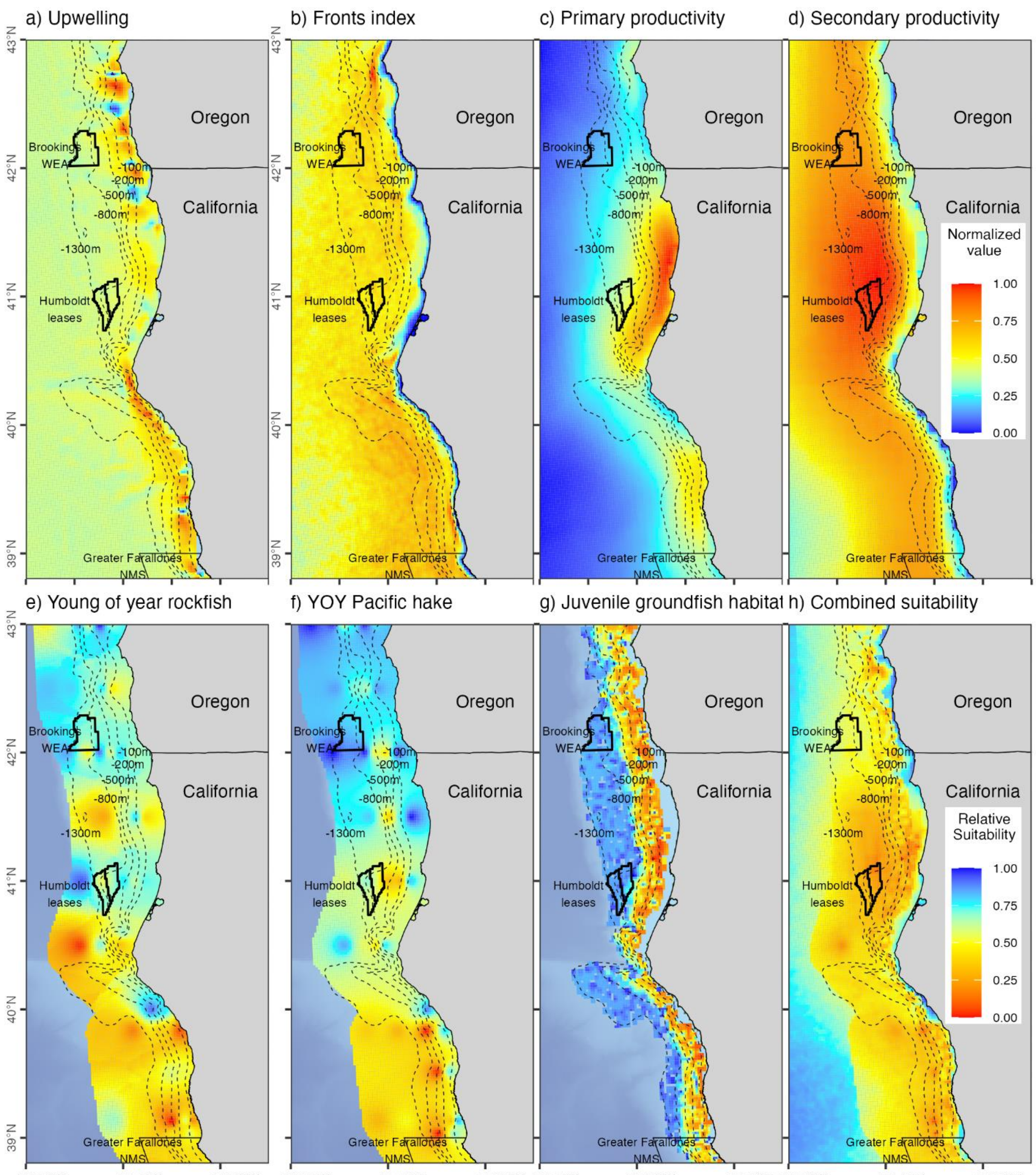
a) Upwelling
b) Fronts index
c) Primary productivity
d) Secondary productivity
e) Young of year rockfish
f) YOY Pacific hake
g) Juvenile groundfish habitat
h) Combined suitability
Oregon
California
Brookings WEA
Humboldt leases
Greater Farallones NMS
-100m
-200m
-500m
-800m
-1300m
Normalized value
Relative Suitability
1.00
0.75
0.50
0.25
0.00
43°N
42°N
41°N
40°N
39°N
125.5°W
124.5°W
123.5°W

Figure U.1: Ecosystem indicators to be considered for offshore wind energy development planning. Values for each indicator have been cropped and normalized across the area of interest and represent long-term, spatial variation during peak seasonal production. Panel h is the combined suitability index based on all 7 indicators. The WEA off the coast of Brookings, OR and the two lease areas off the coast of Humboldt Bay, CA are outlined in black. Leasing of the Brookings WEA was postponed in 2024. Panels a-g use the "Normalized value" legend shown in panel d. Data compiled by NMFS/NWFSC from sources summarized in report text. Boundaries of proposed Wind Energy and Lease Areas from BOEM (https://www.boem.gov/renewable-energy/state-activities/Oregon; https://www.boem.gov/renewable-energy/state-activities/California). Figure created by K. Andrews, NMFS/NWFSC.

U.2 Fisheries Indicators

We developed seven indicators that describe spatial and temporal variation in groundfish bottom trawling activity from 2002-2023 in the same region being considered for OWE development off the coast of northern California. These indicators were presented in the 2022 ESR (Harvey et al. 2022) and are meant to capture the spatial and temporal variation in fishing activity for the groundfish bottom trawl fishery and to be used in tandem with the ecosystem indicators to identify potential interactions across the social-ecological system. For the groundfish indicators herein, we used logbook set and retrieval coordinates from the limited-entry/catch shares groundfish bottom trawl fisheries to estimate duration trawled annually on a 2x2-km grid. These durations were then used to calculate:

1. Total duration trawled in the most recent year (2023).
2. The anomaly of the most recent year relative to the entire time series.
3. The most recent 5-year mean (2019-2023).
4. The most recent 5-year trend (2019-2023).
5. The sum of duration trawled across all years.
6. The proportion of years trawled.
7. The number of years since trawling occurred within each grid cell.

To maintain confidentiality, grid cells with <3 vessels operating within the grid cell across the years associated with the indicator have been removed. The first four indicators are consistent with measuring the 'status' and 'trends' of other ecosystem indicators presented in this report, while the last three have been developed as indicators to use within a risk analysis framework. These indicators account for only federal limited entry/catch shares groundfish bottom trawl fisheries from 2002-2023, but provide a useful framework for identifying the potential for overlap, interactions and conflict between day-to-day fisheries operations and OWE areas. Other fisheries were included in a similar framework presented in the 2022 ESR and will be added here as analyses are completed.

Across this region (Fig. U.2), groundfish bottom trawl activity was most intense inshore of the two lease areas offshore of Humboldt Bay, CA and the proposed WEA offshore of Coos

Bay, OR in 2023 (warm colors in Fig. U.2a,b). Groundfish bottom trawling activity in these areas had higher mean activity (red cells in Fig. U.2c) and an increasing trend over the last five years (red cells in Fig. U.2d) along the 200m contour. Decreasing trends of bottom trawl fishing activity occurred inshore of the proposed WEA off of Brookings, OR and within the seaward lease area off Humboldt Bay, CA (blue cells in Fig. U.2d). Across the entire time series, bottom trawling activity occurred broadly between the 200m and 1300m depth contours, with the highest levels of activity concentrated along specific depth contours (Fig. U.2e). Groundfish bottom trawl activity occurred in >50% of all years in most cells seaward of 200m depth (red and orange cells in Fig. U.2f) and there are large areas of the West Coast in which activity has occurred in the last decade (red and orange cells in Fig. U.2g). Indicators such as these for fisheries activity and the broad-scale ecosystem indicators presented above can help identify potential interactions and conflicts with new ocean-use sectors and contribute to efforts to avoid and/or minimize these conflicts across the CCE.

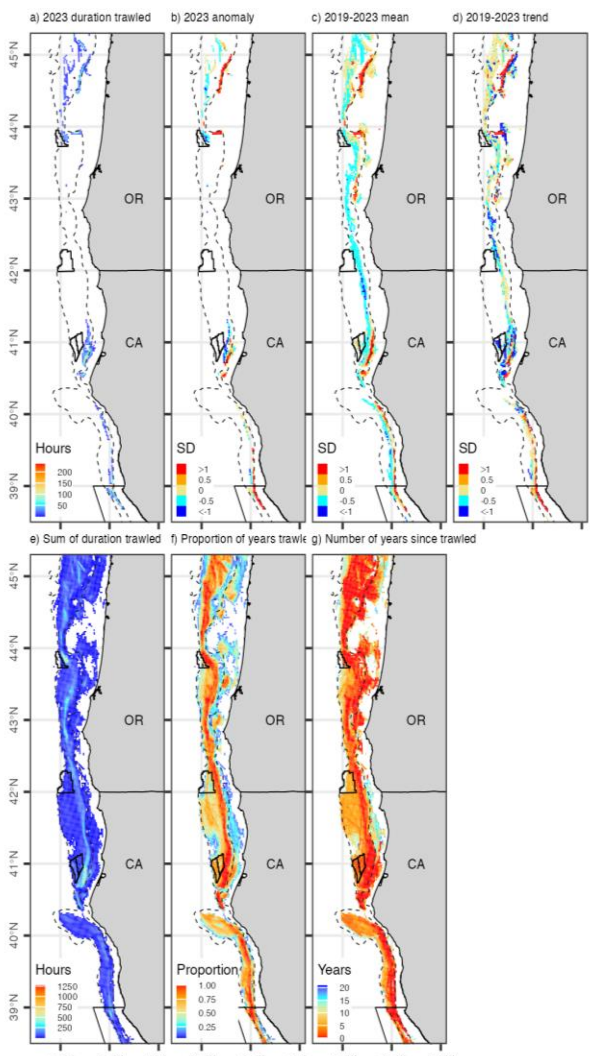

Figure U.2: Indicators of groundfish bottom trawl fisheries activity in areas under consideration for new offshore wind energy areas. Panels show (a) total duration trawled in 2023, (b) anomaly of distance trawled relative to the entire time series, (c) the most recent 5-year mean, (d) the most recent 5-year trend, (e) the sum of duration trawled across all years, (f) the proportion of years trawled (2002-2023), and (g) the number of years since trawling last occurred within each 2x2-km grid cell. Coos Bay and Brookings Wind Energy Areas and the Humboldt Wind Energy Area shown in heavy black lines from north to south, respectively. Leasing of the Coos Bay and Brookings WEAs was postponed in 2024. Grid cell values in (b-d) > 1 (red) or < -1 (blue) represent a cell in which the annual anomaly or 5-year mean was at least 1 s.d. from the long-term mean or where the 5-year trend increased or decreased by >1 s.d. of the long-term mean of that cell. The dashed lines are the 200-m and 1300-m depth contours.

Appendix V. METHODOLOGICAL OVERVIEWS

Link to online documentation: https://cciea-esr.github.io/ESR-Technical-Documentation-FY2025/

Methodological overviews will also be available in the supplemental briefing book.

Appendix W. CHANGES IN THIS YEAR'S REPORT

Below we summarize major changes in the 2024-2025 Ecosystem Status Report. As in past reports, many of these changes are in response to requests and suggestions received from the Council and advisory bodies (including those related to FEP Initiative 2, "Coordinated Ecosystem Indicator Review" (March 2015, Agenda Item E.2.b), or in response to annual reviews of indicators and analyses by the SSC-Ecosystem Subcommittee (SSC-ES). We also note items we have added and information gaps that we have filled since last year's report (Leising et al. 2024).

Request/Need/Issue	Response/Location in Document
The ESR is labor-intensive to produce, and efficiencies such as automation are needed to sustain the report and build it out to meet evolving needs of the Council and other partners. (March 2022, Agenda Item H.2.b, Supplemental EWG Report 1)	In 2024, the ESR team continued to improve automation of the report and create a more efficient and user-friendly process for updating the report annually. This year's report was produced in Quarto, an open-source package in the R programming language. Also, to reduce the length of the ESR and the redundancy among the annual reports, we have drafted an online technical documentation archive to serve as a repository for the methods used to access, collect, process, and analyze the indicators presented in the report. Until it is reviewed by the SSC and Council, this repository will be provided both as an online website and a time-stamped Methodological Overviews appendix (Appendix V) to this report; however, we propose that after review it will exist solely as an online document. In 2023, data providers were trained on uploading their metadata and data in a standard format to an online uploader, which

	significantly streamlined the 2024 data submission process.
Refinements to salmon stoplight tables and suite of indicators (*Partial response to feedback from SSC-ES from ESR topic review in September 2022*)	This year's report includes a combined stoplight table with a refined number of indicators for Sacramento River Fall Chinook, Central Valley Spring Chinook, and Klamath River Fall Chinook salmon (Fig. 3.9), as well as indicator-based outlooks of salmon returns to the California river basins two years in advance of adult returns (Appendix J)
New sources of dissolved oxygen data from the CCE (*Response to HC interest in learning more about hypoxia trend at larger spatial scale*)	We have continued to explore and summarize additional sources of DO data collected via NOAA surveys and partnerships to better describe DO levels throughout the CCE, and have added in the "Climate and Ocean Indicators" (Appendix F). This year we added additional DO maps from groundfish trawl surveys.
Stand alone appendix for short-term ecosystem predictions (*Partial response from the EWG at the March 2024 Council meeting*) *(Response to feedback from the EAS at the March 2023 Council meeting)* (*Response to the EAS recommendation to include indicators for projecting, detecting, or confirming changes or shifts in species distribution, and how such changes could affect fishery diversification and fishing communities*)	This year we present two separate climate related appendices: Climate and Ecosystem Forecasts (Appendix D) and Developing Indicators of Climate Change (Appendix E). The themes of the Climate and Ecosystem Forecasts include (1) 2025 forecasts for ENSO, marine heatwaves, and the TOTAL tool (temperature forecasts avoid Loggerheads, (2) a discussion of uncertainty in climate and ecosystem predictions, and (3) an evaluation of predicted versus observed impacts of the 2023-24 El Niño. The themes of Developing Indicators of Climate Change include (1) current state of knowledge on projected ocean and ecosystem changes under long-term climate change, (2) more holistic analyses of projected impacts of climate change on Pacific sardine, northern anchovy, and four species of groundfish, and (3) new research on how climate change affects the potential overlap of fisheries and offshore wind.

Fishermen and Scientists Roundtable (*Partial response to EAS recommendation for including observations from the fishing fleet, where appropriate*)	The CCIEA team, in partnership with Oregon Sea Grant and ODFW, held a Fishermen and Scientists Roundtable in Newport, Oregon in November 2024. The goal of the roundtable was to share new observations, build stronger collaborations and connections, and learn how to make the ESR more useful for fishermen. This roundtable also served as a pilot for how the CCIEA/ESR team and West Coast fishing communities can co-develop knowledge for future ESRs to better inform risk tables, assessments, and management decisions. This year's report includes fishermen observations in the Regional Forage sections in the main body of the report (Section 3.2.2) and the appendix (Appendix I) and in the HMS appendix (Appendix L). We are also using feedback from roundtable participants to improve analysis and communication of ESR indicators, particularly those that provide insights on human wellbeing.
Offshore wind energy and ecosystem indicators	A fronts index has been added to the suite of indicators used in a suitability analysis of potential areas for offshore wind development that reflect possible changes in the ecosystem. This new index increases the broad-scale ecosystem indicators used for this analysis from 6 to 7 (Appendix U).
Minor changes to Figures/Data/Text	**Description**
Consistent color coding among stoplight style figures	Based on multiple sources of feedback, the color coding for cluster analysis figures (Figs. 3.4, 3.5, and 3.6) has been changed from previously red = abundant and blue = rare, to blue = abundant and red = rare. The coding was done to be consistent with the thought that "red" tends to immediately signify a "warning" or "suboptimal" condition. This change enhances quick interpretation when viewing these figures and is consistent with the color coding of stoplight tables.

A new figure has been added to the main body of the report concerning the impact of harmful algal blooms on fisheries closures and whale entanglement closures	In order to better connect the timeline and spatial extent of HAB impacts on fisheries, this new figure has been developed as a way to assess overall HAB impacts both spatially and through time (Fig. 3.16).
The order of Sections 4 (Human wellbeing) and 5 (Fishing and non-fishing human activities) has been switched as compared to last years' report.	This was done to enhance the overall flow of the narrative of the main body of the report.
Social vulnerability	To enhance interpretation, Fig. 5.1. from last year's report has been split from 2 panels to 10 panels separated now by region (see Fig. 4.1 in this year's report).
Fishery diversification	To enhance readability, Fig. 4.2 has had color added to replace line shading
Fisheries participation networks	Updates to the fishery participation networks have replaced the more limited presentation from last years' report. Previous Fig. 5.3 has been replaced with new Fig. 4.3
Addition of "Key messages" text for each major section of the main report *(summarization of main text)*	To increase readability of the report and to help with easier interpretation, we have added "key messages" text at the beginning of each major section of the main report to summarize the most important take away messages for each section.
Juvenile sablefish distribution (probability of occurrence and index of abundance)	Given the heightened abundance of juvenile sablefish in recent years, an examination of their spatial distribution and abundance through time was conducted, to determine if such abundance changes were due simply to distributional shifts (new Fig. 3.11).
Coastwide abundance of krill *(data not available for this year's report)*	Biomass estimates are available every other year, starting in 2007.
Cumulative estimated biomass for CPS (*data not available for this year's report*)	Biomass estimates for 2024 were only available as preliminary estimates at the time of preparation of the report, and were therefore not included.